Investigation of the role of immunomodulators of toll-like receptor 3 (TLR3) function and associated genetic variants in the pathogenesis and progression of idiopathic pulmonary fibrosis (IPF)

Joanna Weronika Laskowska

12302808

B.Sc. (Hons) Neuroscience

M.Sc. Immunology

Trinity College Dublin
Coláiste na Tríonóide, Baile Átha Cliath
The University of Dublin

A thesis submitted to

Trinity College Dublin

for the degree of

Doctor of Philosophy

Supervisor: Dr. Michelle E. Armstrong

Co-supervisor: Prof. Seamas C. Donnelly

School of Medicine

Trinity College Dublin

May 2024

Contents

I. Declaration of Authorship

I declare that this thesis has not been submitted as an exercise for a degree at this or any other university and it is entirely my own work, with the exception of: (i) in chapter 3, in Figures 3.16 to 3.18, the live infection of primary human lung fibroblasts with *Pseudomonas aeruginosa* was performed by Dr. Andrew O'Neill, Trinity College Dublin and (ii) in chapter 5, in Table 5.1 and in Fig. 5.1, the microbiome analysis of genomic DNA from bronchoalveolar lavage samples from IPF patients was carried out by Dr. Philip Molyneaux's research group in Imperial College and the Royal Brompton Hospital, London, UK. I agree to deposit this thesis in the University's open access institutional repository or allow the library to do so on my behalf, subject to Irish Copyright Legislation and Trinity College Library conditions of use and acknowledgement.

Joanna Weronika Laskowska

II. Acknowledgments

Firstly, I would like to sincerely thank Dr. Michelle Armstrong for giving me the opportunity to join the Armstrong Lab. Throughout these four years she has been my mentor, who guided me through difficult periods in my course with plenty of patience and understanding. Towards the end of this long journey, I regard her not only as my teacher but also as my sincere friend.

I would also like to thank my co-supervisor, Prof. Seamas Donnelly, who encouraged me during every major milestone throughout my PhD.

My acknowledgments would not be complete, without thanking my dearest friend, Marie-Claire, who lifted my spirits no matter how much I struggled, who was there to listen and to offer me her invaluable advice. Her positive and cheerful outlook on life helped me through many of challenging times.

I would like to thank Dr. Andrew O'Neill, for letting me bother him with my endless questions. His aid in the lab with various experiments as well as his company made my PhD experience much more enjoyable.

Finally, I would like to thank my family. My grandmother, Zofia, who always blindly believed that I was the smartest person in the family. My grandfather, Zbigniew, who himself was a teacher and who installed in me the importance of education. My mother, Agnieszka, who gave me unwavering support and love through good and bad times. Most of all, I would like to express my gratitude towards my dad, Piotr, who stood by my side for all these years, and who never gave up on me. He made many sacrifices to get me where I am today and suffered through many difficult times for my sake. I hope to make him proud one day and I dedicate my thesis to him.

Thank you all.

III. Abstract

IPF is a fatal interstitial lung disease of unknown aetiology, with a lack of valid biomarkers and satisfactory therapeutic solutions available. Studies have shown an association between inflammation, viral and bacterial infection and the development and progression of IPF. Previous studies have suggested that almost 15% of IPF patients develop rapidly progressive disease which results in death within 12 months. In 2014, Pirfenidone and Nintedanib were FDA approved for the treatment of IPF. These agents have been shown to reduce the decline of lung function in IPF patients. Therefore, currently there is a significant and unmet clinical need in IPF to identify biomarkers which will facilitate disease stratification in IPF at diagnosis in order to identify patients most at risk of developing rapidly progressive disease, to facilitate their early referral for lung transplant.

We previously demonstrated a role for defective TLR3 function in accelerated disease progression in IPF. Specifically, we demonstrated that *TLR3* L412F, which is a TLR3 SNP associated with reduced TLR3 function, caused an acceleration, and decline in lung function and increased mortality in IPF patients. We also demonstrated that *TLR3* L412F was significantly associated with acute exacerbation (AE)-induced IPF death (AE-IPF) in patients. Furthermore, defective TLR3 function in 412F-variant primary human lung IPF fibroblasts resulted in dysregulated fibroproliferation and reduced IFN-β expression, which exacerbated fibrosis in IPF patients. The role of bacterial pathogens has been implicated in the pathology of IPF. Studies have shown that both the bacterial burden as well bacterial strain present in the BAL fluid of IPF patients were predictive of worsen clinical outcome of the disease (82-85). We previously established that 412F-heterozygous IPF lung fibroblasts have reduced anti-bacterial TLR responses to LPS (TLR4), Pam3CYSK4 (TLR1/2), flagellin (TLR5) and FSL-1 (TLR6/1) and have reduced responses to live *Pseudomonas aeruginosa* infection. Hence, we have established that *TLR3* L412F represents a candidate prognostic biomarker in IPF.

In this PhD project, we built on our previous findings which established that defective TLR3 function is pathogenic in IPF patients and drives disease progression. Specifically, in these PhD studies we hypothesised that immunomodulators, such as itaconate or IL-17A, which alter TLR3 function in IPF patients during viral or bacterial infection may accelerate IPF disease progression. In addition, we hypothesised that genetic variants of such immunomodulators, including the *IL-17A* G197A (rs2275913) promoter polymorphism, may also drive disease progression in IPF.

Itaconate is a metabolite generated during the Krebs cycle which has emerged as a potent immunomodulator with anti-bacterial and anti-viral properties. To date, the role of itaconate in viral infection in IPF is unreported. In this study, we investigated the effect of 4-octyl itaconate (4-OI), a synthetic analogue of itaconate, on TLR3 function in primary lung fibroblasts from IPF patients. Here, we demonstrated that 4-OI decreased NF-κB and IRF3 activity in IPF lung fibroblasts stimulated with TLR3 ligand. Moreover, we reported that human IPF lung fibroblasts presented with decreased Poly(I:C)-induced transcription of pro-fibrotic markers, and increased transcription of anti-oxidants, following 4-OI treatment. We predict that the dampened, IRF3-dependant anti-viral response observed in our study may be detrimental to disease progression in patients with IPF. In addition, we are the first group to confirm the expression or immune responsive gene 1 (IRG1), a gene involved in itaconate synthesis, in Poly(I:C)-stimulated human lung fibroblasts, highlighting the importance of itaconate during infection.

In this PhD project, we also investigated the effects of IL-17A on TLR3 function in terms of IPF pathology. IL-17A is a cytokine with pro-inflammatory and anti-viral properties. Increased levels of IL-17A were shown to confer protection to virally infected cells and to promote viral persistence. We and others have previously demonstrated increased levels of IL-17A in bronchoalveolar lavage (BAL) fluid and pulmonary tissue of IPF patients. Here, we demonstrated that Poly(I:C)-induced IPF lung fibroblasts treated with IL-17A presented with increased NF-κB response and decreased IRF3 response, which we predict may have pathogenic effects on IPF disease progression. Moreover, we demonstrated a significant association between the *IL-17A* G197A (rs2275913) polymorphism with development of IPF in UK patients. In addition, we demonstrated that IPF patients positive for 197A-variant had an increased risk of IPF-pneumonia death that approached statistical significance ($p=0.07$). Furthermore, IPF patients variant for 197A allele had less time to death compared to their G197-WT IPF patient counterparts. This effect was not due to a significant difference in pulmonary function in G197-WT IPF patients at diagnosis. These *IL-17A* G197A studies were carried out in an IPF cohort of modest size due to sample availability. These findings warrant further investigation into the potential use of *IL-17A* G197A SNP as a prognostic biomarker for IPF patients.

In the final chapter of this PhD thesis, we investigated the functionality of the *TLR3* L412F polymorphism *in vivo*. Firstly, we demonstrated that IPF patients who are 412F-variant exhibit a dysregulated lung microbiome, a reduction in overall pulmonary bacterial load and have

increased frequencies of the bacteria, *Streptococcus and S. aureus* compared to 413-WT IPF patients. Secondly, we investigated the functionality of the *TLR3* L412F polymorphism *in vivo* using the novel *TLR3* L413F CRISPR-Cas-9 knock-in mice which are unique to our lab. In these studies, we demonstrated that both female and male 413F-HET mice have higher constitutive lung production of RANTES and KC compared to L413-WT mice. In contrast, female L413-WT mice have increased Poly(I:C)-induced pro-inflammatory and anti-viral responses in the lung compared to 413F-HET mice. However, the lungs of male 413F-HET mice have increased levels of Poly(I:C)-induced RANTES and KC protein production compared to 413-WT female mice. These data confirm that the TLR3 L412F polymorphism is functional in our *TLR3* L413F CRISPR-Cas-9 knock-in mice. These data also suggest that there may be a sex-related difference in the function of *TLR3* L412F.

The novel findings reported in this PhD thesis warrant further investigation in order to elucidate their role in the pathogenesis and development of IPF, and their relevance in the subsequent quest for novel therapies and prognostic biomarkers.

IV. Publications and Communications

PUBLICATIONS

I. McElroy AN, Invernizzi R, **Laskowska JW**, O'Neill A, Doroudian M, Moghoofei M, Mostafaei S, Li F, Przybylski AA, O'Dwyer DN, Bowie AG, Fallon PG, Maher TM, Hogaboam CM, Molyneaux PL, Hirani N, Donnelly SC*, Armstrong ME*. Candidate Role for Toll-like Receptor 3 L412F Polymorphism and Infection in Acute Exacerbation of Idiopathic Pulmonary Fibrosis. ***Am J Respir Crit Care Med. 2022 Mar 1;205(5):550-562 (Blue Journal).*** *doi: 10.1164/rccm.202010-3880OC.*

- Featured in an associated editorial in the ***Am J Respir Crit Care Med*****. 2022; 205(5): 489-491**. *doi.org/10.1164/rccm.202110-2244ED.*

CONFERENCE PRESENTATIONS

I. **Poster presentation at the Irish Society for Immunology Annual Meeting, 19-20 September 2019, Royal College of Surgeons in Ireland (RCSI), Dublin, Ireland:** "Characterisation of the effect of interleukin-17A (IL-17A) on Toll-like receptor 3 (TLR3) function in Idiopathic Pulmonary Fibrosis (IPF): a candidate novel mechanism for disease progression."

II. **Poster presentation at the European Congress of Immunology, 1-4 September 2021 (Online): "**Itaconate attenuates anti-viral TLR3 responses in idiopathic pulmonary fibrosis patients: implications for disease progression during infection."

- Received Best Poster Award Nomination by the European Federation of Immunological Societies (EFIS) (1 of 150 selected posters from 3,000 delegates).
- Awarded EFIS Registration Bursary (1 of 7 assigned to 45 Irish Society for Immunology delegates).

V. Abbreviations

4-OI	4-octyl itaconate
6MWT	The six-minute walking test
ACE2	Angiotensin converting enzyme type 2
ACOD1	Aconitate decarboxylase 1
AE	Acute exacerbation
AEC II	Alveolar epithelial type II cells
AECs	Airway epithelial cells
AHR	Aryl hydrocarbon receptor
AIP	Acute interstitial pneumonia
AKAP13	Kinase anchor protein 13
AMs	Alveolar macrophages
AP-1	Activator protein 1
ARDS	Acute respiratory distress syndrome
ATF3	Activating transcription factor 3
ATII	Alveolar epithelial type II cells
ATP	Adenosine triphosphate
BALF	Bronchoalveolar lavage fluid
BCA	Bicinchoninic acid
Bcl-2	B cell lymphoma-2
Bcl-Xl	B cell lymphoma- extra large
BLM	Bleomycin
BMDMs	Bone-marrow-derived macrophages
C/EBP	CCAAT-enhancer-binding protein
CMV	Cytomegalovirus
Col1	Collagen type I
COP	Cryptogenic organising pneumonia
COPD	Chronic obstructive pulmonary disease
COVID	Coronavirus disease
CPA	Chronic pulmonary aspergillosis
CTGF	Connective tissue growth factor
DAMPs	Danger-associated molecular patterns
DI	Dimethyl itaconate
EAE	Experimental autoimmune encephalomyelitis
EBV	Epstein-Barr virus
ECAR	Extracellular acidification rate (ECAR)
ECM	Extracellular matrix proteins,
ELISA	Enzyme-linked immunosorbent assay
ELMO	Engulfment and cell motility
ELMOD2	Engulfment and cell motility (ELMO) domain containing 2
EMA	European Medicines Agency
ER	Endoplasmic reticulum
ERK	Extracellular signal-regulated Kinase
Erα	Estrogen receptor alpha
Erβ	Estrogen receptor beta
ESR	Electrophilic stress response
FBS	Foetal bovine serum

FDA	Food and Drug Administration
FGF	Fibroblast growth factor
Fn-1	Fibronectin-1
FVC	Forced vital capacity
GAP	Gender-age-physiology
GC-MS	Targeted gas chromatography-mass spectrometry
G-CSF	Granulocyte colony-stimulating factor
GER	Gastroesophageal reflux
GERD	Gastroesophageal reflux disease
GLUT-I	Glucose transporter 1
GPR91	G protein-coupled receptor
GSR	Glutathione-disulfide reductase
GTP	Guanosine triphosphate
GWAS	Genome-wide association study
HBLs	Human bronchial epithelial cells
HBV	Hepatitis B virus
HCV	Hepatitis C virus
HET	Heterozygous
HHV	Human Herpes Virus
HIF-1α	Hypoxia-inducible factor 1-alpha
HIV-1	Human Immunodeficiency Virus 1
HLFs	Human lung fibroblasts
HMOX-1	Heme oxygenase (decycling) 1
HOM	Homozygous
HRCT	High resolution computed tomography
HSP47	Heat shock protein 47
HSV	Herpes simplex virus
IAV	Influenza-A virus
ICL	Isocitrate lyase
IDH	Isocitrate dehydrogenase
IFN	Interferon
IIPs	Idiopathic interstitial pneumonias
IKK	I-kappa B Kinase
ILCs	Innate lymphoid cells
ILD	Interstitial lung disease
Ilk	Integrin linked kinase
IMs	Interstitial macrophages
iNOS	Inducible nitric oxide synthase
IPF	Idiopathic pulmonary fibrosis
IR	Ischaemia-reperfusion
IRAK	IL-1-receptor-associated kinase
IRF	IFN regulatory factor
IRG-1	Immunoresponsive gene 1
JAK2	Janus kinase 2
JNK	c-Jun N-terminal kinase
KDa	Kilodalton
KEAP-1	Kelch-like ECH-associated protein 1
LDH	Lactate dehydrogenase
LPA	Lysophosphatidic acid

LPS	Lipopolysaccharides
Mal	MyD88-adapter like protein
MAPK	A mitogen-activated protein kinase
MCP-1	Monocyte chemoattractant protein-1
MCs	Mesangial cells
MHC-II	Major histocompatibility complex class II
MIP-1	Macrophage inflammatory protein 1,
MMP9	Serum Matrix metalloproteinase-9
MMPs	Matrix-degrading metalloproteases
Mo-AMs	Monocyte-derived alveolar macrophages
MTB	Mycobacterium tuberculosis
MUCB5	Mucin 5B, oligomeric mucus/gel-forming
MyD88	Myeloid differentiation primary response 88
NAD	Nicotinamide adenine dinucleotide
NADPH	Nicotinamide adenine dinucleotide phosphate
NAP1	NAK-associated protein 1
NFAT	Nuclear factor of activated T-cells
NF-Kb	Nuclear factor kappa-light-chain-enhancer of activated B cells
NK cells	Natural killer cells
NLRs	Nucleotide-binding and oligomerization domain (NOD)-like receptors
NQOI	NAD(P)H quinone dehydrogenase 1
NRF2	Nuclear factor erythroid 2-related factor 2
NSIP	Non-specific interstitial pneumonia
OCR	Oxygen consumption rate
OxPhos	Oxidative phosphorylation
PAMPs	Pathogen-associated molecular patterns
PBMCs	Human peripheral blood mononuclear cells
PBS	Phosphate buffered saline
PCM	Pulmonary paracoccidioidomycosis
pDCs	Plasmacytoid dendritic cells
PDGF	Platelet-derived growth factor
PFTs	Pulmonary function tests
PHDs	Prolyl hydroxylase domain enzymes
PINK1	PTEN-induced putative kinase 1
Poly(I:C)	Polyinosinic:polycytidylic acid
PRRs	Pathogen recognition receptors
PTX-2	Pentraxin-2
qPCR	Quantitative polymerase chain reaction
RANTES	Regulated upon Activation, Normal T Cell Expressed and Presumably Secreted
RIG-I	Retinoic acid-inducible gene 1
RIPK	Receptor-interacting protein kinase
RNAseq	RNA sequencing
RORγt	Retinoic acid receptor-related orphan receptor-γt
ROS	Reactive oxygen species
SDF1	Stromal cell-derived factor 1
SDH	Succinate Dehydrogenase
SGRQ	St George Respiratory Questionnaire
SLE	Systemic lupus erythematous

SNP	Single Nucleotide Polymorphism
SPs	Surfactant proteins
STAT3	Signal transducer and activator of transcription 3
STING	Inhibit stimulator of IFN genes
TAB	TAK1- binding protein
TAK1	Transforming growth factor beta-activated kinase 1
TB	Tuberculosis
TBE	Tick-borne encephalitis
TBK1	TANK-binding kinase 1
TCA	The tricarboxylic acid
TERC	Telomerase RNA component
TERT	Telomerase reverse transcriptase
TGF-β	Transforming growth factor beta
TLR	Toll-like receptor
TMPRSS2	The transmembrane serine protease 2
TNF-α	Tumour necrosis factor alpha
TOLLIP	Toll interacting protein
TRAF	Tumour-necrosis-factor-receptor-associated factor
TRAM	TRIF-related adaptor molecule
Tr-AMs	Tissue resident macrophages
TRIF	TIR-domain-containing adapter-inducing interferon-β
TTV	Torque-Teno (Transfusion-Transmitted) (TT) virus
UIP	Usual interstitial pneumoniae
VEGF	Vascular endothelial growth factor
WT	Wild-type
α-SMA	Alpha smooth muscle actin

Chapter 1 – Introduction

1.1 Idiopathic pulmonary fibrosis (IPF)

1.1.1 Introduction

Idiopathic Pulmonary Fibrosis (IPF) is a non-neoplastic form of chronic fibrosing interstitial pneumonia [1]. The disease is hallmarked by the histological appearance of usual interstitial pneumoniae (UIP) and affects 13 to 20 in every 100,000 people worldwide [2]. IPF is inevitably fatal, and its incidence rate is on the rise. It is estimated that one in every 100 deaths in the UK occurs due to IPF [2]. The median survival rate of the patients is 3-5 years following diagnosis. The disease mostly affects older adults and is prevalent in males [2]. Although the exact mechanisms underlying IPF pathology remain elusive, the pathophysiology of IPF is hypothesised to involve aberrant wound healing of the pulmonary tissue, following an external stressor such as smoking, air pollution as well as bacterial or viral infection, in genetically susceptible individuals [3]. IPF has been associated with a heightened pro-inflammatory state, which overtime leads to epithelial cell damage, fibroproliferation, myofibroblast differentiation and increased deposition of collagens and extracellular matrix (ECM) proteins, creating imbalance between pro- and anti- fibrotic mediators. This altered state of homeostasis promotes scarring of the pulmonary tissue, which ultimately impairs gas exchange and leads to respiratory failure [3].

1.1.2 The fibrotic process

Fibrotic events constitute an essential part of the wound-healing process [4]. A prolonged state of fibrosis leads to scarring of the parenchyma, which culminates in organ dysfunction and failure [4]. A variety of diseases and factors are capable of inducing fibrosis in a wide range of organs, which suggests that fibrosis is underlined by a common biological mechanism, for example, the TGF-β molecular pathway has been associated with various forms of fibrosis in a variety of tissues up to date [4]. The fibrogenic response is associated with a number of effector cells, primarily, fibroblasts and myofibroblasts but also fibrocytes, epithelial cells, immune cells and bone marrow derived cells [4]. The process of fibrosis is initiated by an injury to the organ, often caused by acute or prolonged inflammation [4]. Tissue inflammation damages resident epithelial and endothelial cells, which results in elevated levels of pro-inflammatory mediators, and enhanced recruitment of pro-inflammatory cells including neutrophils and macrophages [4]. The fibrotic scars are a conglomerate of extracellular matrix (ECM) proteins, predominantly interstitial collagens (types I and III), cellular fibronectin, as well as basement-membrane proteins such as laminin [4]. ECM proteins

are secreted by the effector cells and following the resolution of the inflammation are degraded by matrix-degrading metalloproteases (MMPs). Under the conditions of chronic inflammation however, the consecutively activated effector cells deposit ECM proteins at a rate which cannot be degraded by the MMPs, leading to progressive scarring and tissue damage. [4]. Figure 1.1 Illustrates the common mechanism underlying the pro-fibrotic process [5].

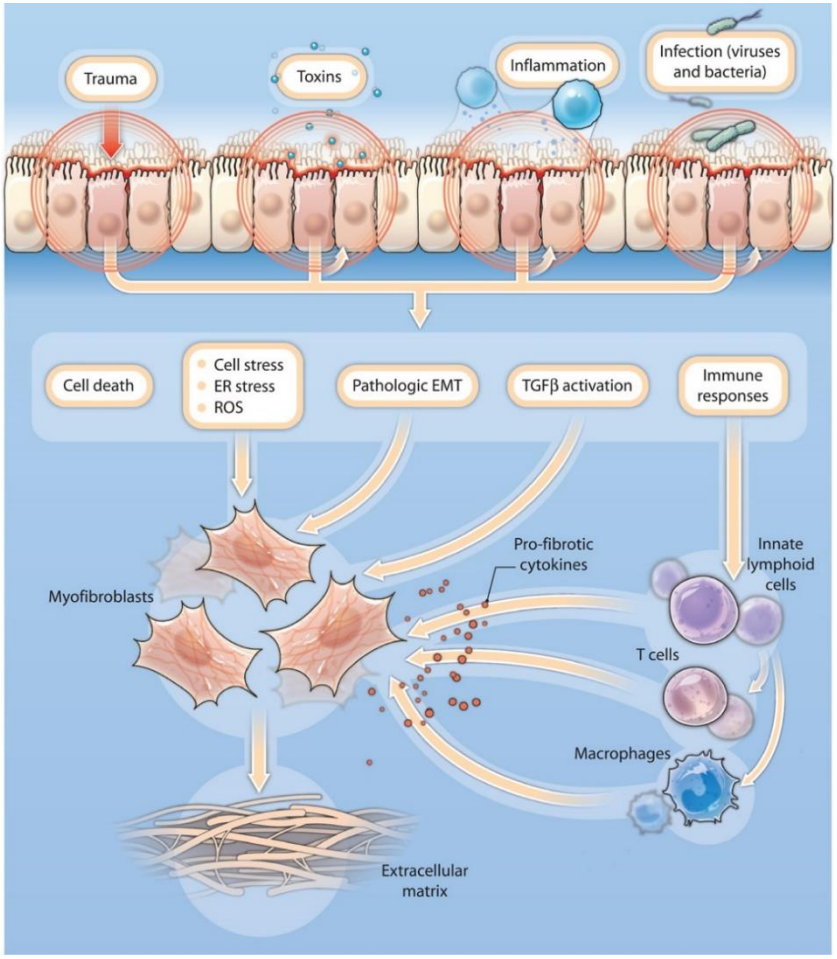

Figure 1.1 Mechanisms of fibrosis.

Stressors such as physical trauma, toxins, inflammation, and infection can induce fibroblast proliferation, activation, and differentiation into extracellular matrix-producing myofibroblasts. If uncontrolled, this process results in tissue fibrosis. *Image taken from [5].*

1.1.3 Interstitial lung disease (ILD)

IPF belongs to a family of idiopathic interstitial pneumonias (IIPs), which fall under a broader classification of interstitial lung disease (ILD) [1]. Other members of IIPs include non-specific interstitial pneumonia (NSIP), acute interstitial pneumonia (AIP) and cryptogenic organising pneumonia (COP) [1]. IIPs commonly affect the alveolar and capillary endothelia as well as the septal and bronchiovascular tissues. The fibrotic damage can be seen in the

airways, alveolar spaces and surrounding vasculature [1]. Members of the IIP family often manifest similar symptoms in patients and are challenging to diagnose. Methods used to diagnose IIPs in a clinical setting include high resolution computed tomography (HRCT), clinical presentation, surgical lung biopsy and histopathology [6]. Figure 1.2 shows the classification of the interstitial lung disease (ILD) family.

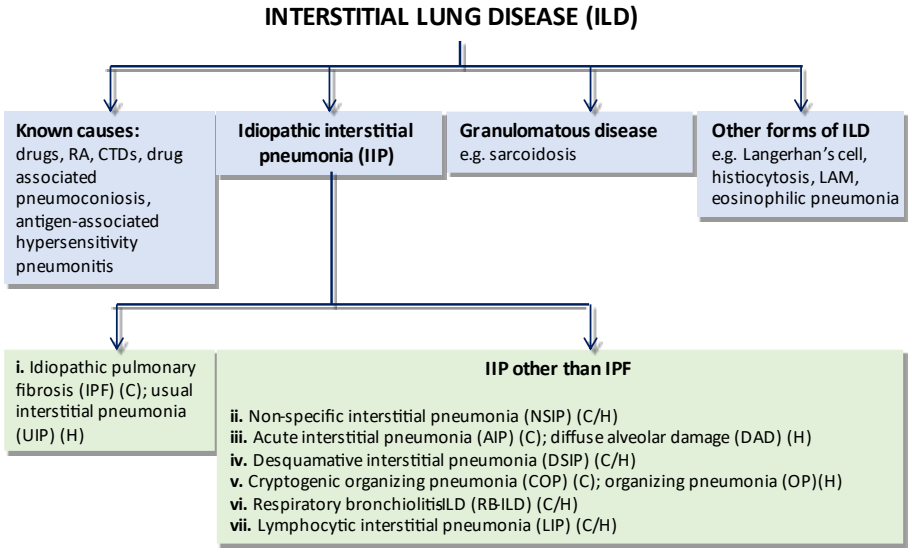

Figure 1.2 Classification of interstitial lung disease (ILD).

Idiopathic pulmonary fibrosis (IPF) falls under the classification of idiopathic interstitial pneumonia (IIP) and belongs to the family of interstitial lung disease, members of which include lung disease due to a known cause, granulomatous disease, and other forms of ILD. *Image adapted from [6].*

1.1.4 Hallmarks and clinical manifestations

The average onset of IPF is 65-67 years of age, with increased prevalence in males [1]. Clinical manifestation of the disease includes fine basal late inspiratory crackles, chronic exertional dyspnoea (shortness of breath), dry cough and finger clubbing [1]. Approximately 5% of patients are asymptomatic [1]. IPF is hallmarked by histological heterogeneity with areas of fibrotic patches in the form of collagen sheets dispersed among healthy, non-fibrotic lung tissue. This histopathological pattern creates what is commonly known as "honeycombing" and can be observed under high-resolution computed tomography (HRCT) as subpleural cystic airspaces, characterized by well-defined walls [7]. Patients with IPF experience pulmonary hypertension and right-sided heart failure which culminates in respiratory failure and death [7]. Figure 1.3 demonstrates a high-resolution computed tomography (HRCT) image, showing typical characteristics of usual interstitial pneumonia (UIP) pattern, including "honeycombing", which is a common feature in IPF patients [7].

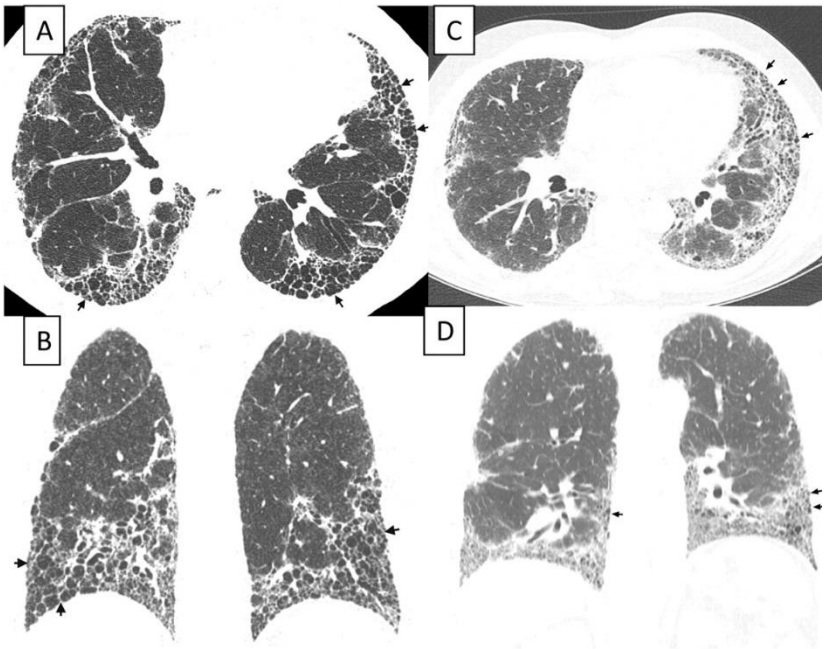

Figure 1.3 HRCT imaging of IPF lung.

High-resolution computed tomography (HRCT) images demonstrating usual interstitial pneumonia (UIP) pattern, including characteristic for IPF honeycombing. *Image adapted from [7].*

1.1.5 IPF progression pathways

IPF follows three major clinical progression pathways [7]. The majority of patients experience a slow, gradual loss of respiratory function over time. On average 15% of patients experience much more rapid disease progression and loss of lung function which leads to a life expectancy of less than 1 year [7]. Another group of patients can initially experience a slow, steady disease progression but, due to an adverse event known as an acute exacerbation (AE), will experience an accelerated decline in disease prognosis [7]. It is estimated that half of the patients who experience AE-event will die within 30 days [7]. Mucin 5B, oligomeric mucus/gel-forming (MUCB5) promoter polymorphism is a sole validated prognostic biomarker in IPF up to date. A study involving genetic screening of 492 IPF patients revealed that individuals homozygous and heterozygous for MUC5B (rs35705950) SNP were significantly more likely to develop IPF [8] Identification of prognostic markers which could be effectively measured in a timely manner is crucial for more tailored approach to patient-treatment, patient prioritisation and even early remission for lung transplantation [7]. Figure 1.4 shows known progression routes of IPF. Those include slow, stable progression of the disease, a rapid progression, as well as slow progression with an incidence of acute worsening (AE). The average lifespan of patients following the diagnosis is of 3-5 years' time [7].

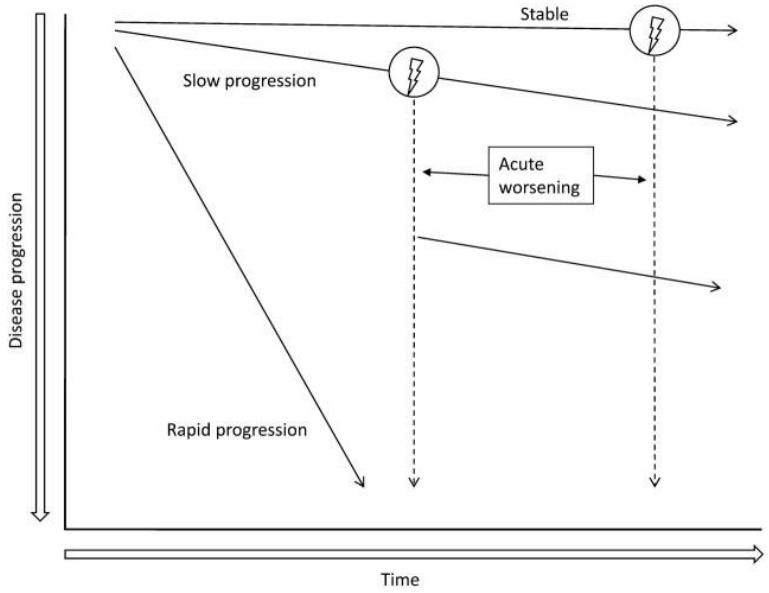

Figure 1.4 Disease progression pathways in IPF.

IPF can follow different progression pathways. In most cases, patients with IPF experience a slow and gradual loss of lung function over time. Some patients remain stable, while a smaller number of patients experience a rapid disease progression and loss of pulmonary function which leads to a life expectancy of less than 1 year. Patients may also experience an unpredictable acute worsening of the disease due to secondary complications or due to unknown reasons. *Image taken from [7].*

1.1.6 Risk factors

The exact aetiology of IPF remains elusive, however the disease is associated with several risk factors, which include cigarette smoking [9, 10], gastroesophageal reflux [11-13], environmental exposure to metal and wood dust [9, 10, 14-17], aging [18-22] as well as genetic susceptibility [23-42].

1.1.6.1 Cigarette smoking

Cigarette smoking has been heavily associated with IPF [9, 10]. In 1997, Baumgartener *et al.* conducted a multicentre case-control study on the effects of cigarette smoking in IPF. Subjects with the history of smoking were at a higher risk of developing the disease. Moreover, the risk was increased for former smokers and those with 21 to 40 pack-years [9]. Another study conducted in 2005 in Japan, confirmed the association between cigarette smoking and IPF, where a significantly increased risk of IPF was observed for smokers with 20.0–39.9 pack-years [10].

1.1.6.2 Gastroesophageal reflux

Gastroesophageal reflux disease (GERD) is a chronic illness, hallmarked by regurgitation of stomach acid which can lead to coughing, chest pain and microaspiration of stomach acid into the lungs [43]. There is a belief that introduction of acid into the pulmonary tracts can result in scarring of the lung tissue. Various studies demonstrated the link between abnormal Gastroesophageal reflux (GER) and IPF. A study conducted by Raghu *et al.* in 2011 demonstrated increased occurrence of abnormal GER in IPF patients when compared with healthy controls [11]. However, the study did not show a correlation between IPF severity and acid GER severity [11]. In their study, Patti *et al.* aimed to establish the correlation between the prevalence of GERD in patients with end-stage IPF. The group reported that two thirds of the patients suffered from GERD. The study showed no correlation between GERD severity and the severity of IPF symptoms [12]. Interestingly, IPF patients receiving anti-acid treatment showed a significantly reduced decrease in forced vital capacity (FVC) when compared to patients receiving the placebo [13].

1.1.6.3 Environmental factors

Various studies have shown the association between IPF and exposure to a range of environmental factors such as wood and metal dust [9, 10, 14, 15, 17]. In 1997 Hubbard *et al.* reported significant exposure-response effects for metal and wood dust exposure in IPF patients [14]. In 2000, the same group demonstrated increased IPF-related mortality among the employees of a major UK engineering company. In their study, Hubbard *et al.* utilised historical occupational records to establish unbiased duration of exposure to metal dust of their subjects. There was a significant correlation between the risk of death from or with IPF and the duration of metalworking [15]. A Japanese study conducted on 102 IPF patients demonstrated that the exposure to metal dust was significantly associated with an increased risk of IPF [10]. Another study, conducted in Sweden in 2007 confirmed the link between exposure to birch and hardwood dust and IPF development in men [16]. Other environmental exposures which were shown to be associated with the disease included exposure to livestock, vegetable as well as animal dust, farming, stone cutting/polishing and air pollution [9]. In agreement with these findings, an autopsy study have demonstrated increased number of inorganic particles in lymph nodes of IPF patients [17].

1.1.6.4 Aging

The average onset of IPF is between 65 and 67 years of age. Various studies have investigated age as a risk factor in the development of the disease [18-22]. Physiologically, aging is defined as cellular loss of function and ability to resolve injury and trauma [18]. Hallmarks of aging include epigenetic alterations, genomic instability, telomere attrition, cellular senescence, stem cell exhaustion, loss of proteostasis, deregulated nutrient sensing, mitochondrial dysfunction, and altered intercellular communication [18]. Many of these age-related hallmarks have been identified in patients with IPF [19]. For example, cellular senescence which has been associated both with aging and with IPF. Microarray and RNA sequencing (RNAseq) experiments have demonstrated accumulation of senescence biomarkers in IPF lung [19]. The expression of senescence markers has been associated with reduced FVC in IPF patients [19]. Moreover, in the bleomycin model of pulmonary fibrosis in mice, bleomycin injury induced cellular senescence in fibroblasts and epithelial cells [19]. Another common link between aging and IPF is dysregulated autophagy process [20]. In research done by Romero *et al.* the levels of autophagy have been decreased with age in both healthy control and IPF pulmonary fibroblasts. Lower rates of autophagy in these cells were associated with increased resistance to apoptosis [20]. In addition, shortening of telomeres is strongly associated with the aging process. Shortened telomeres have been shown to impair tissue renewal capacity which leads to senescence and decreased lifespan. Telomere shortening has been observed in patients with IPF. Alder *et al.* have reported excessive shortening of telomeres in leukocytes and alveolar epithelial cells in IPF patients compared with age-matched healthy controls [21]. Finally, PINK1 (PTEN-induced putative kinase 1) signalling has been shown to be crucial in mitochondrial homeostasis and in aging [22]. Bueno *et al.* showed the association between low expression of PINK1 and impaired mitochondria in IPF and aging lungs. Lung epithelial cells from PINK KO mice presented with mitochondrial depolarization and elevated expression of pro-fibrotic factors [22]

1.1.7 Current available treatments

Currently, the only two FDA and EMA – approved pharmacological treatments for IPF are Pirfenidone and Nintedanib. Both drugs were approved by the FDA in 2014. The EMA approved the use of Pirfenidone in 2011 and Nintedanib in 2015 [7].

1.1.7.1 Pirfenidone

Pirfenidone (5-methyl-1-phenyl-2-[1H]-pyridone) is an orally administered drug with anti-fibrotic, anti-inflammatory, and antioxidant effects. Figure 1.5 Demonstrates the chemical structure of the compound Pirefnidone [7].

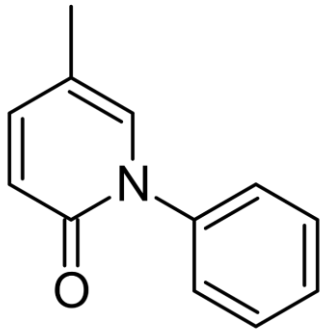

Figure 1.5 Chemical structure of Pirfenidone.

Pirfenidone is an orally active pyridinone derivative with anti-fibrotic properties, used for treatment of idiopathic pulmonary fibrosis. *Image taken from [7].*

Pre-clinical studies

In vitro studies demonstrated the ability of Pirfenidone to reduce TGF-β1-stimulated collagen synthesis in healthy pulmonary fibroblasts in a dose-dependent manner [44]. This effect was due to inhibition of HSP47 and Col1 RNA upregulation by the drug [44]. Another *in vitro* study conducted in 2014 showed that Pirfenidone decreased the rate of fibroblast proliferation, and reduced production of α-SMA induced by TGF-β, and the level of procollagen 1 in primary human lung fibroblasts [45]. In the *in vivo* studies using murine bleomycin model of pulmonary fibrosis, Pirfenidone was shown to reduce pro-inflammatory cytokines, including TNF-α, IFN-γ and IL-6. The drug was also shown to improve survival [46-48]. Iyer *et al.* reported that treatment with Pirfenidone significantly reduced influx of pro-inflammatory cells and macrophages into the lungs in a hamster bleomycin model [49]. The group has also reported decreased levels of TGF-β production in the BALF of hamsters which received the Pirfenidone treatment [49]. Fibrocytes are hematopoietic-derived cells responsible for collagen production following tissue injury. Fibrocytes are one of the main effector cells involved in the fibrotic process. Their aberrant activation promotes excessive deposition of ECM proteins which leads to fibrosis [50]. It has been shown that treatment with Pirfenidone reduced the number of circulating fibrocytes in the pulmonary tissue of mice in the murine bleomycin model of lung fibrosis [51]. Interestingly, in the context of anti-oxidant properties, free-radical scavenging ability of Pirfenidone was demonstrated in *in vitro* studies

[52]. The reaction rate between the drug and OH- was shown to be comparable to well-established anti-oxidants, including glutathione [52]. In a study conducted in sheep liver microsomes, in addition to it's free-radical scavenging properties, Pirfenidone was shown to block NADPH-dependent lipid peroxidation in a dose-dependent manner [53].

Clinical studies

Japanese trial

The first Phase III trial on Pirfenidone was carried out in Japan and published in 2009 [54]. The trial comprised of 275 IPF patients and lasted for 52 weeks. The patients were assigned to receive either a high dose of the drug (1,800 mg/day) or a low dose (1,200 mg/day). A significant reduction in the decline of FVC was reported for both cohorts. Moreover, patients receiving a higher dose of Pirfenidone showed a higher reduction in FVC decline and a significant increase in progression free survival time compared with patients receiving a low dose of the drug. The study was heavily criticised due to a change in the initial endpoint. Handling of missing values in the statistical analysis posed an additional concern. The drug was licenced in Japan follow in the study in 2008 [54].

CAPACITY trials

Another set of trials known as the CAPACITY trials were carried out in North America, Australia and Europe in 2008 and lasted for 72 weeks [55]. The trials were divided in two separate studies, referred to as study 004 and 006. (ClinicalTrials.gov identifier: NCT00287729 and NCT00287716). Study 004 comprised of 435 IPF patients with mild-to-moderate IPF. Participants were divided into two groups, assigned to receive either a high dose (2,403 mg/day) or a low dose (1,197 mg/day) of Pirfenidone. The primary end point was the change of FVC% predicted from baseline to week 72. With a mean FVC change of -8.0% vs -12.4%, participants receiving the higher dose of the drug showed a significantly reduced decline in FVC ($p=0.001$) compared with the placebo cohort. In a clinical setting, a decline over 10% FVC is a predictor of mortality in IPF patients. In this study, 2,403 mg/day Pirfenidone reduced the proportion of patients with FVC decline ≥10% compared with placebo (20% vs 35%, respectively; $P<0.001$). CAPACITY study 006 comprised of 344 patients which were assigned to receive high dose of Pirfenidone (2,403 mg/day) or placebo. Interestingly, there was no significant difference observed in the change of FVC decline between the two cohorts. Unlike in the 004 study, patients receiving the Pirfenidone treatment showed a significant reduction

in the decline in the 6-minute walks test, thereby meeting one of the secondary endpoints of the study. Pooled results from both studies showed that following 72 weeks treatment there was a significant decrease in the decline on FVC in the cohort receiving 2403 mg/day compared with the placebo. Moreover, Pirfenidone was shown to prolong progression free survival rate by 26%. The hazard ratios for overall all-cause mortality and mortality related to IPF favoured those treated with Pirfenidone. Most common adverse symptoms observed in patients receiving the treatment included nausea, dizziness, and rashes. The symptoms were mild to moderate in severity with little to no clinical significance [55]. Due to contrasting results between studies 004 and 006, the FDA requested a subsequent double-blind, randomized, placebo-controlled Phase III trial (ASCEND) to be carried out.

ASCEND trial

A Phase III trial (ClinicalTrials.gov identifier: NCT01366209) was conducted on 555 IPF patients from 9 different countries and lasted for 55 weeks [56]. The patients were divided into two cohorts, first receiving 2,403 mg of Pirfenidone per day, the second received a placebo. The primary end point of the study was the change from baseline to week 52 in the percentage of predicted FVC. The treatment was proven effective, with significant reduction in % FVC decline in patients receiving Pirfenidone compared with the placebo cohort (relative difference 45.1%; $P<0.001$). In addition, patients receiving the drug showed reduced decline of the distance walked during the 6MWT and improved progression-free survival ($P=0.04$ and $P<0.001$, respectively). A significant difference between the Pirfenidone and placebo cohorts was also seen in the reduction of patients who had a decline of ≥10% in the percentage of the predicted FVC or who died (16.5% vs 31.8% [$P<0.001$] and 22.7% vs 9.7% [$P<0.001$], respectively [56]. Pirfenidone was approved by the FDA for the treatment of IPF in 2014.

1.1.7.2 Nintedanib

A Tyrosine Kinase inhibitor, initially intended for cancer treatment, Nintedanib possesses anti-angiogenic properties mainly due to inhibition of vascular endothelial growth factor (VEGF) pathway [57, 58]. In addition, the compound was found to limit the release of pro-fibrotic mediators, such as platelet-derived growth factor, fibroblast growth factor and transforming growth factor (TGF-β) in PDGF-BB-stimulated primary human lung fibroblasts from IPF patients (58) [59]. Figure 1.6 Demonstrates the chemical structure of the compound Nintedanib [7].

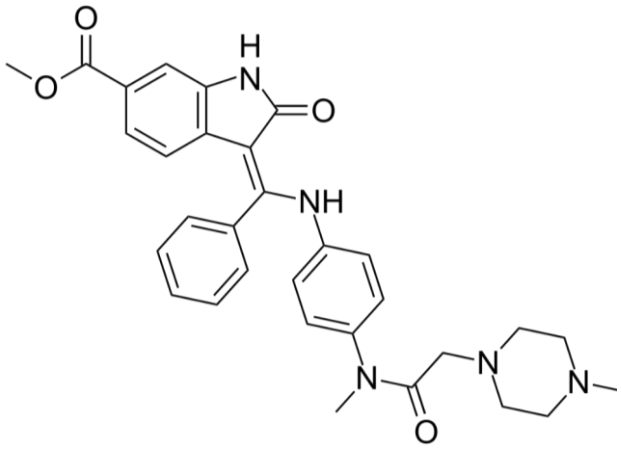

Figure 1.6 Chemical structure of Nintedanib.

A member of the class oxindoles compounds, Nintedanib is a tyrosine kinase inhibitor used for treatment of cancer and idiopathic pulmonary fibrosis. *Image taken from [7].*

Pre-clinical studies

Wollin *et al.* investigated the effects of Nintedanib in IPF using human lung fibroblasts from IPF patents and murine bleomycin models of lung fibrosis [58]. They reported that Nintedanib had inhibitory effects on PDGF-BB- stimulated PDGF activation, fibroblast proliferation, and fibroblast to myofibroblast transformation. Moreover, the drug reduced the number of circulating lymphocytes and neutrophils in the BLAF of the mice. Histologic analysis of lung extracts taken from the animal model showed a significant reduction in lung inflammation, granuloma formation, and fibrosis [58].

Clinical studies

TOMORROW trial

The first evidence of Nintedanib's efficacy in the treatment of IPF came from the Phase II TOMORROW study completed in 2010 [60]. The trial comprised of 432 participants from various countries and lasted for 52 weeks. The drug was assessed at four different doses,

50mg/day, 50 mg/ twice per day, 100 mg/ twice per day and 150 mg/ twice per day. Patients receiving the highest dose of the drug showed a reduced decline in FVC compared with the placebo, the difference however was not statistically significant. Patients receiving 150 mg of Nintedanib twice daily reached several of the secondary endpoints, including smaller number of patients suffering an FVC decline of 10%, improved quality of life, measured using the St George Respiratory Questionnaire (SGRQ) and lower number of reports of acute exacerbations [60].

INPLUSIS trials

The INPULSIS clinical trials (INPULSIS-1 and INPULSIS-2 ClinicalTrials.gov identifier: NCT01335464 and NCT01335477) were multicentre, randomized double-blind placebo-controlled Phase III studies [61]. Altogether, the trials comprised of 1066 patients, receiving either 150 mg of Nintedanib twice daily or placebo for a total of 52 weeks. In both studies, patients receiving the treatment showed reduced decline in FVC compared with the placebo cohort. Moreover, the number of patients who suffered 5% or 10% deterioration in FVC after 52 weeks in the Nintedanib group was significantly smaller. Pooled results from INPLUSIS-1 and INPLUSIS-2 trials showed no significant difference in the number of acute exacerbations, the quality of life or the mortality rate between patients receiving Nintedanib and the placebo group. Due to a reduction in the decline of FVC, Nintedanib was approved as a treatment of IPF by FDA in 2014 [61].

1.1.7.3 PBI-4050 trial

More recently, Phase II clinical trials (ClinicalTrials.gov identifier: NCT02538536) evaluated the safety and effectiveness of a small-molecule compound PBI-4050 in the treatment of IPF [62]. The study lasted for 12 weeks and recruited 25 patients. 800 mg doses of PBI-4050 were administered daily, alone and in combination with Nintedanib or Pirfenidone. The results of the study show a statistically significant reduction in FVC decline from baseline to week 12 in patients receiving a combined PBI-4050 and Pirfenidone treatment [62].

1.1.7.4 Pamrevlumab (FG-3019) trial

PRAISE (ClinicalTrials.gov identifier: NCT01890265) was a Phase II, randomised, double-blind, placebo-controlled study of the efficacy of Pamrevlumab (FG-3019) as treatment in IPF [63]. FG-3019 is a fully recombinant human monoclonal antibody against connective tissue growth factor (CTGF), a glycoprotein involved in the fibrotic process. 30mg/kg of the drug was administered to 50 IPF patients every 3 weeks via intravenous infusion. The treatment lasted for 48 weeks. FG-3019 reduced the decline in percentage of predicted FVC by 60.3% at week 48 [63].

1.1.7.5 Pentraxin-2 (PTX-2) trial

Pentraxin-2 (PTX-2) is a soluble pattern recognition receptor, involved in orchestrating monocyte/macrophage activity [64]. PTX-2 was shown to have anti-inflammatory and anti-fibrotic effects via inhibition of monocyte-derived cells. PTX-2 was studied as a possible treatment for IPF in Phase II, randomized, double-blind, placebo-controlled trial (ClinicalTrials.gov identifier: NCT02550873). 117 IPF patients received PTX-2 treatment every 4 weeks for 24 weeks. PTX-2 significantly reduced the decline in FVC % of predicted value of −2.5% compared with −4.8% placebo [64].

1.1.7.6 GLPG1690 trial

Autotaxin is an enzyme involved in the synthesis of lipid signalling molecule lysophosphatidic acid (LPA). Patients with IPF were shown to have elevated levels of autotaxin in the lung tissue and lysophosphatidic acid (LPA) in bronchoalveolar lavage fluid and exhaled condensate. FLORA (ClinicalTrials.gov identifier: NCT02738801) was a Phase 2 randomised placebo-controlled trial aimed to investigate the safety, tolerability, and therapeutic potential of GLPG1690, an autotaxin inhibitor in IPF [65]. 600 mg/day of GLPG1690 was administered to patients orally for 12 weeks. Patients receiving the drug showed a mean change from baseline in FVC of 25 mL (95% CI −75 to 124) compared with- 70mL (−208 to 68 mL) reported in the placebo cohort [65].

A subsequent Phase III, randomized, double-blind, placebo-controlled, study on the effectiveness of GLPG1690 in the treatment of IPF when used together with standard care (ISABLEA2) (ClinicalTrials.gov identifier: NCT03733444) recruits 781 participants and is set to be completed in December 2021 [66].

1.1.8 Genetic factors and susceptibility in IPF

1.1.8.1 MUC5B

MUC5B is a gene found on chromosome 11, responsible for mucous production in humans. A Single Nucleotide Polymorphism (SNP) in the promoter region of the MUC5B gene (rs35705950) which results in G>T substitution has been associated with the development of IPF [23]. A study involving genetic screening of 492 IPF patients revealed that the SNP was present at a frequency of 9% among healthy individuals, 34% among patients with familial IPF and 38% among patients with sporadic IPF. The odds ratios of developing the disease among IPF patients who were heterozygous or homozygous for the minor allele of the MUC5B SNP (rs35705950) were 9.0 and 21.8, respectively [23].

1.1.8.2 ELMO

An engulfment and cell motility (ELMO) domain containing 2 (ELMOD2) is a gene involved in anti-viral response, located on chromosome 4 in humans [24]. A genome-wide scan conduced on six multiplex families with familial IPF showed an association between over-expression of ELMO and IPF. A subsequent *in vitro* study showed that patients with IPF presented with reduced ELMOD2 mRNA expression in the pulmonary tissue compared with healthy controls. The study also highlighted the importance of ELMOD2 in anti-viral signalling via TLR3 activity. Inhibition of ELMOD2 led to abrogation of TLR3 signalling and reduced production of type I interferons in alveolar epithelial cell lines (A549) [24].

1.1.8.3 TOLLIP

Toll interacting protein (TOLLIP) gene encodes for an inhibitory adaptor protein within Toll-like receptors (TLRs). TOLLIP's involvement was shown in MyD88-dependent NF-κB activation [25]. In 2013, a genome-wide association study (GWAS) identified mutations within the TOLLIP gene to be relevant in terms of IPF pathology [26]. A SNP within the gene (rs5743890) was linked to increased morality in IPF, however was not associated with the development of the disease [26]. Interestingly, Tollip was shown to play a role in TGF-β signalling pathway via modulation of trafficking and degradation of TGF-β type I receptor (TβRI) [27].

1.1.8.4 AKAP13

A-kinase anchor protein 13 (AKAP13) is a scaffold protein involved in assembling signalling complexes downstream of G protein-coupled receptors. Allen *et al.* conducted a large, genome-wide association study in IPF patients of European ancestry across nine different centres in the UK. The study identified a novel SNP for AKAP13, rs62025270. The minor A allele of the SNP was linked to increased susceptibility to IPF and an upregulation of AKAP13 mRNA expression in lung tissue resections from IPF patients [28]. A possible explanation for the involvement of AKAP13 in IPF comes from the fact that the protein is a known activator of Rho family members, which play important roles in fibrosis via orchestrating of actin filament assembly and actomyosin contraction.

1.1.8.5 TERT/TERC

Aging, a prominent risk factors in IPF, is associated with progressive telomere shortening. Telomerase reverse transcriptase (TERT) and telomerase RNA (TERC) are both involved in restoration of telomerase length. Mutations in TERT and TERC have been found in 8-15% patients with familial IPF and were associated with abnormal telomere shortening [29, 30]. Genetic mutation within TERT and TERC have also been implicated in the pathogenesis of sporadic cases of IPF, however to a lesser extent [31, 32].

1.1.8.6 Surfactant proteins (SPs)

Secreted by alveolar epithelial type II cells (AEC II), the function of surfactant proteins (SPs) is to facilitate transport of surfactant lipids, thereby, diminishing surface tension of the alveolar cells and preventing pulmonary collapse [33, 34]. When the physiological process of SPs degradation becomes dysregulated, misfolded SPs accumulate in the Endoplasmic reticulum (ER) and cytosol. This results in chronic stress which leads to increased AEC apoptosis and pulmonary fibrosis [34-37]. Studies have shown that the levels of surfactant proteins SP-A and SP-D were elevated in the BAL and serum of patients with IPF and other ILDs [38-41]. Elevation in SPs levels was correlated with increased mortality in IPF patients [67]. Additionally, a higher concentration of SP-A and SP-D was found in patients following AE compared with those with stable disease [42]. Figure 1.7 Shows genetic polymorphisms associated with the pathology of IPF [68].

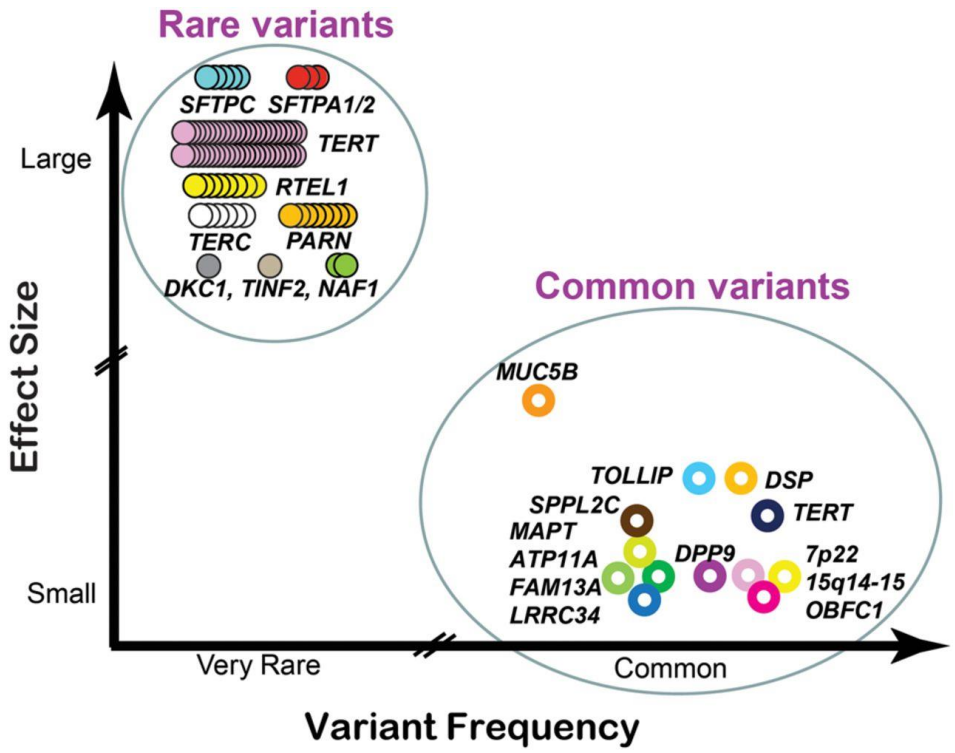

Figure 1.7 Genetic variations associated with IPF.

Common and rare polymorphisms associated with the development/ progression of interstitial pneumonia and IPF. The variants are grouped according to the frequency at which they occur and the severity of the effect that they exert in terms of the disease pathology. *Image adapted from [68].*

1.2 The role of infection in IPF

1.2.1 The role of viral infection in IPF

Viral infection was proposed to play a major role in the development and pathogenesis of IPF. Viral pathogens were identified as one of the causative factors behind acute exacerbations in IPF, moreover, many patients report having an incidence of viral infection shortly prior to the manifestation of respiratory problems [7].

1.2.1.1 Herpesviruses

Herpesviruses belong to a large family of dsDNA viruses. Members of the family include herpes simplex virus 1 and 2 (HSV), Epstein-Barr virus (EBV), cytomegalovirus (CMV) and Human Herpes Virus (HHV)-7 and -8 [69]. The role of herpesviruses infection in lung fibrosis was demonstrated using *in vivo* studies on murine bleomycin models of fibrosis [70, 71]. Moreover, clinical studies identified the presence of various herpesviruses in the pulmonary tissue of IPF patients [72-75].

In terms of *in vivo* studies, Lok *et al.* examined the effects of gammaherpes infection on fibrosis using murine, bleomycin model of fibrosis [70]. The study utilised bleomycin-resistant BALB/c mice, infected with murine gammaherpesvirus-68 (γHV68). The mice were administered bleomycin interperitoneally, 7 days following the infection. Treatment with bleomycin in conjunction with γHV68 infection, resulted in significantly increased levels of fibrosis as determined by histological examination as well as hydroxyproline estimation analysis, compared with bleomycin-only or γHV68- only mice [70].

McMillan *et al.* used *in vivo* experiments to further investigate the effects of gammaherpes infection in fibrosis [71]. The group utilised a model of fluorescein isothiocyanate-induced pulmonary fibrosis in mice. The infection with a murine gammaherpesvirus-68 was interposed on top of fully established pulmonary fibrosis. Data was recorded at the time of peak lytic viral replication. The group reported γHV68-associated exacerbations in pulmonary fibrosis as evidenced by elevated levels of total lung collagen, histologic changes of acute lung injury, and decline in lung function [71].

From a clinical approach, Yonemaru *et al.* investigated the role of a latent viral infection in the pathology of IPF [72]. The group reported significantly elevated levels of CMV IgG in serum of IPF patients when compared with healthy controls, emphysema, and sarcoidosis patients. Interestingly, the levels of CMV IgM remained unchanged, showing that the patients were not undergoing an active infection. Additionally, the levels of both of EBV viral capsid antigen and HSV IgG were significantly increased in IPF patients, compared with both healthy controls and seven collagen vascular disease-related interstitial pneumonitis, including sarcoidosis and emphysema [72].

Tang *et al.* examined lung specimens from 33 IPF patients (familial and sporadic) and 25 patients with other diseases (lobectomy for single pulmonary nodule, pulmonary hypertension, sarcoidosis, bronchiolitis obliterans, and spontaneous pneumothorax) as controls for the presence of viruses [73]. One or more members of the herpesvirus family, including CMV, EBV, HHV-7 and HHV-8 were detected in 97% of IPF patients compared with 36% in controls ($P < 0.0001$) [73].

A significantly higher prevalence of EBV in IPF compared with healthy controls has been previously reported by Stewart *et al.* who examined pulmonary tissue from 27 IPF patients for the presence of EBV [74]. Immunochemistry analysis showed that 44% of IPF patients and 10% of control subjects ($p = 0.005$) were positive for EBV. PCR data showed that 45% IPF patients and 14% controls were EBV positive ($p = 0.007$). Interestingly, 41% of IPF

patients and none of the control subjects were EBV positive by both Immunochemistry and PCR (p = < 0.001) [74].

In another study, the incidence of HSV-1 was examined in both BALF and lung tissue biopsy from IPF patients [75]. PCR analysis performed on the biopsy specimens from 11 IPF patients showed HSV-1 incident rate of 9% in the samples from IPF lung tissue, where no incidence of HSV-1 was reported in control samples. Examination of BALF from 13 IPF patients showed 10% of HSV-1 prevalence in patients and no incidence of HSV-1 in control subjects. In addition, macrophage primary cell cultures from BALF of IPF patients and healthy subjects infected with HSV-1 *in vitro* showed increased transcription of pro-fibrotic markers TGFβ1 and FGF, as well as angiogenetic markers SDF1a, SDF1b, VEGF, FGF and the regulators of tissue wound healing MMP9 and CCR7 [75].

1.2.1.2 Other viruses associated with the pathogenesis of IPF

Hepatitis C (HCV)

Hepatitis C (HCV) belongs to a family of single stranded, positive-sense RNA viruses and has been identified as a causative factor in liver cirrhosis [76]. A growing number of case series and reports is indicative for the role of HCV in the pathology of IPF. Having tested 66 IPF patients, Ueda *et al.* reported that 28.8% of patients have undergone a prior HCV infection, compared with 3.66% of control subjects [77]. Arase *et al.* approached the same question from an opposite direction, whereby 6150 HCV patients and 2050 HBV patients were examined for the incidence of IPF. The group reported 0.3% 10-year and 0.9% 20-year cumulative incidence of IPF in the HCV cohort, compared with no cases of IPF in the HBV group [78].

The Torque-Teno (Transfusion-Transmitted) (TT) virus

Another virus that has been linked to the development of IPF is the Torque-Teno (Transfusion-Transmitted) (TT) virus. It belongs to a family of single-stranded DNA viruses and was first identified in a patient with post-transfusion hepatitis. A study which examined IPF patients for the presence of the virus, reported that 35% of IPF subjects tested positive for TTV DNA. Moreover, 50% of those positive for TTV DNA died within a period of 4 years, compared with 28.6% mortality observed in TTV- negative subjects [79]. In a more recent study, TTV was identified as a virus most frequently occurring in IPF patients experiencing an acute exacerbation [80].

Influenza A virus

Studies have shown that members of the influenza A virus family have an affinity to infect epithelial type II (ATII) cells in lung tissue explants. Building on those findings, Fujino *et al.* investigated the severity of influenza virus infection of ATII cells in lungs of IPF patients and lungs of healthy subjects. In their study, ATII cells were isolated from lung, infected with A (H1N1) pdm09 and the viral titers present in the culture supernatants were analysed and compared. The data indicated a more severe infection of ATII cells derived from lungs of IPF patients compare with the cells from healthy subjects [81]. *In vivo* studies have demonstrated that infection with influenza virus promotes collagen deposition in the lungs, Moreover, it promotes αvβ6 integrin dependent TGFβ signalling in human bronchial epithelial cells *in vitro* via activation of TLR3, which leads to epithelial cell death and elevated levels of fibrosis [82].

1.2.2 Role of bacterial infection in IPF

Lower pulmonary tracts were previously believed to be sterile; this dogma has been abolished as bacterial infection began to emerge as a key factor underlying IPF pathology. 16S rRNA gene qPCR and pyrosequencing of DNA isolated from bronchoalveolar lavage (BAL) of patients with IPF as well as chronic obstructive pulmonary disease (COPD) revealed increased bacterial burden in the IPF BAL fluids compared with healthy controls and COPD subjects [83]. Moreover, bacterial load at diagnosis was higher in samples taken from IPF patients with rapidly progressing form of the disease compared with patients who experienced more stable course of the disease progression [83]. Interestingly, profiling of pulmonary microbiota indicated a correlation between elevated frequencies of distinct bacterial populations in IPF patients compared with healthy controls; *Haemophillus* sp., *Neisseria* sp., *Streptococcus* sp., *Veillonella* sp., and *Staphylococcus* sp. [83].

More recently, Molyneaux *et al.* examined the differences in the composition of lung microbiota of AE-IPF and stable IPF patients [84]. The bacterial DNA was extracted from BAL samples, amplified, quantified and pyrosequenced to reveal increased BAL bacterial burden in AE-IPF compared with stable IPF patients. The microbiota of the stable IPF subjects consisted of *Haemophilus*, *Streptococcus*, *Prevotella* and *Pseudomonas*, bacteria which are often found in patients with asthma, COPD and IPF. The group reported a change in the composition of the lung microbiota following AE, with a notable increase in *Campylobacter* sp. and *Stenotrophomonas* sp. [84].

In a retrospective study conducted by Han *et al.* bacterial DNA was isolated from 55 BAL samples from IPF patients [85]. Using pyrosequencing methods, the bacterial constitution of each patient was profiled and correlated against progression-free survival, defined as time to death, lung transplant, AE, decrease in FVC of 10% or greater or decrease in diffusion capacity of the lung (DLCO) of 15% or greater. The group reported a significant association between IPF progression and increased relative abundance of *Streptococcus* and *Staphylococcus* strains in the lungs of the patients. Moreover, microbiome profiling of the IPF BAL samples in this study has confirmed the presence of over 20 bacterial strains, previously identified in IPF patients by Molyneaux *et al.* [83, 85].

A small Japanese study in which bacterial DNA was extracted from BALF of 34 IPF patients showed increased bacterial burden of *Streptococcus* sp., *Veillonella* sp. and *Prevotella* sp. [86]. Elevated levels of bacterial DNA in the IPF subjects were correlated with higher disease progression as measured by 6MWT and the decline in FVC. Interestingly, a decrease in the diversity of the lung microbiota was associated with a relatively low FVC and higher mortality within the IPF cohort [86].

1.2.3 Role of fungal infection in IPF

Whereas viral and bacterial infection are well recognised as one of the causative factors underlying the pathology of IPF, the role of fungal infection in the disease development and progression is less known. Pulmonary aspergillosis is a term assigned to a range of conditions caused by infection with a fungus belonging to the aspergillus family. Studies show that Pulmonary aspergillosis can introduce major complications in patients with sarcoidosis, cystic fibrosis, COPD, interstitial pneumonia, and those in recovery from TB and pulmonary cancer [87, 88]. Reports from a retrospective study which reviewed analyses of autopsy findings in 52 patients with AE-IPF revealed that during the clinical course of the disease progression, 15 patients underwent bronchopneumonia, 7 of the recorded cases were of fungal origin, where patients presented with either pulmonary aspergillosis or *Candida Albican* infection [89]. Moreover, retrospective examination of patients 'records admitted to University Hospital of South Manchester with chronic pulmonary aspergillosis (CPA) revealed that a significant subset of patients developed chronic fibrosis in the lung, identified either on biopsy or radiologically, giving further evidence for the association between fungal infection and pulmonary fibrosis [90]. *In vivo* studies demonstrated that a fungal species *Paracoccidiodes brasiliensis*, responsible for the development of chronic pulmonary paracoccidioidomycosis

(PCM) can induce pulmonary fibrosis in BALB/c mice [91, 92]. The resulting fibrosis was associated with formation of granulomas as well elevation in the lung hydroxyproline, TNF-α and TGF-β levels, all prominent features observed in IPF pathology [91, 92]. Another study looked at the effects of a combined immunomodulatory (Pentoxifylline) and antifungal (Itraconazole) treatment on the development of fibrosis in a murine model of experimental PCM [93]. Administration of the drugs to mice in an advanced stage of PMC reduced granuloma formation, inflammation, and tissue fibrosis, compared with the results of classical antifungal therapy using itraconazol only treatment [93].

1.3 Immune response

1.3.1 Immune response - Overview

In response to a constant threat from invading pathogens and cellular damage, humans developed an immune system which can be divided into two separate arms: the innate and the adaptive immune system [94-96].

The innate immune system acts as the first line of defence against physical damage and infection [94-97]. The system comprises of a variety of receptors capable of sensing danger signals elicited by cellular damage and microbial invasion. Activation of these receptors leads to recruitment of innate immune cells designed to neutralise and kill invading pathogens along with infected cells. The innate immune response is carried out by a range of effector cells, including macrophages and neutrophils; mast cells including basophils and eosinophils as well as antigen presenting cells such as dendritic cells and cytotoxic natural killer cells [94-97]. These cells are not only crucial at the early stages of pathogen clearance but also play pivotal roles in activation of the adaptive immune response through antigen presentation to the components of the adaptive immune system [94-97].

In contrast to the innate immune system, the response of the adaptive immune system is specific and acquired over time. The response is initiated via presentation of fragmented antigens to T-cells, which then mature and clonally expand [98]. Two separate types of T-cells, the cytotoxic T-cells and helper T-cells are responsible for killing of the infected cells and communication with B-cells, all of which amounts to a highly specific immune response, generation of antibodies against the invading pathogens, and formation of long-term immune memory for a more efficient response in the future [98, 99]. Figure 1.8 Illustrates the relationship between the innate and the adaptive immune systems [100].

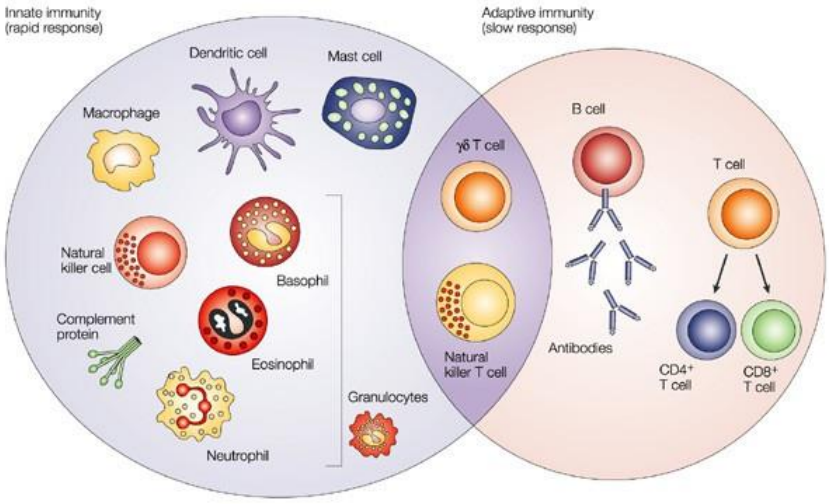

Figure 1.8 The interplay between the innate and the adaptive immune system.

The innate immune system serves as the first line of defence against invading pathogens. It comprises of soluble factors, including complement proteins as well a range of effector cells, such as mast cells, granulocytes (basophils, eosinophils and neutrophils), macrophages, dendritic cells and natural killer cells. The response of the adaptive immune system is acquired over time and slower than that of the innate system. It functions to increase antigenic specificity and immune memory. The adaptive arm of the immune system mainly comprises of antibodies, B cells, and CD4+ and CD8+ T lymphocytes, Natural killer T cells and γδ T cells. *Image taken from [100].*

1.3.2 Immunity of the lung

On average over 10,000 L of air circulates through the human lung daily. This organ is therefore exposed to a wide range of pathological agents, such as microbes and various types of irritants including dust and pollen [101]. For this reason, the airways employ a plethora of cellular and humoral host defence components, most of which belong to the innate arm of the immune system. The innate cells involved in mounting of the immune response in the lung consist of alveolar and interstitial macrophages, dendritic cells as well as resident epithelial cells [101].

1.3.2.1 Alveolar macrophages (AMs)

Alveolar macrophages (AMs) are account for 80-90% of cell population in BLAF under homeostatic conditions. They are predominant antigen-presenting and phagocytic cells in the lung which act as airway scavengers for inhaled pollutants, allergens, and microbes [102]. Alveolar macrophages respond by secretion of various pro- and anti- inflammatory agents, such as cytokines IL-1β, TNF-α, IL-6 and IL-10 [102]. In the context of IPF, alveolar macrophages have both beneficial and detrimental effects on the disease progression. Pro-inflammatory mediators secreted by macrophages contribute to the disease pathology, however, alveolar

macrophages are also known to generate MMPs which aid in breaking down of the over-proliferative ECM [103].

1.3.2.2 Interstitial macrophages (IMs)

The function of interstitial macrophages (IMs) is less defined than that of their alveolar counterparts, mainly due to technical difficulties associated with their recovery from the lung [104]. Whereas alveolar macrophages can be easily extracted from BALF, IMs require lung resection in animals and biopsy of the pulmonary tissue in humans. The extraction is then supplemented with extensive purification and isolation procedures [105-107]. Similarly, to AMs, IMs function as phagocytes for environmental and microbial particles, and are often considered as a second line of defence against pathogens evaded by AMs [106, 108-110]. Although not proven, their phagocytic ability paired with expression of MHC-II suggest a possible role for IMs as antigen presenting cells [106-112]. IMs were shown to secrete IL-6 and TNF-α in humans, their role in promotion of inflammation is yet to be established [107]. IMs are believed to predominantly carry immune-regulatory function, due to their steady secretion of IL-10 [106, 113-115]. IMs were shown to be main producers of IL-10 in a lung of CpG-treated mice[111, 112].

1.3.2.3 Airway epithelial cells (AECs)

Airway epithelial cells (AECs) positioned strategically at the interface between internal and external milieu are the first cells to encounter invading microorganisms, pollutants, and other airborne irritants [116]. AECs create a structural barrier, responsible for regulation of water and ion transport [116]. Moreover, AECs play crucial role as immune cells, due to their contribution in terms of mucociliary clearance of pathogens, both in a purely mechanical way and via secretion of antimicrobial and anti-inflammatory peptides into the respiratory epithelium [117]. In addition, AECs display a variety of pattern recognition receptors, including TLRS, retinoic acid-inducible gene I (RIG-I) receptors and NOD-like receptors (NLRs)which are responsible for sensing of bacterial, fungal and viral pathogens and initiation of the immune response [118-120].

1.3.2.4 Pulmonary fibroblasts

In contrast to the common dogma, lung fibroblasts are not solely matrix producing cells, but also carry out important function in terms of immunoregulation and control of chronic inflammation [121]. Fibroblasts have the ability to respond to chemokines, cytokines and growth factors. They are critical for maintenance of the homeostasis of adjacent cells and are responsible for regulation of inflammatory infiltrates [121, 122]. Fibroblasts play pivotal role in fibrosis as their prolonged activation, often as a result of acute or chronic inflammation, leads to their differentiation into collagen-producing myofibroblasts and generation of the fibrotic tissue [4, 121]. Therefore, elimination or regulation of inflammatory triggers is crucial for prevention of fibroblast activation, deposition of excess ECM and ultimately fibrosis.

Fibroblasts have been shown to express various Pattern Recognition Receptors (PRRs), including TLRs. PPRs are proteins capable of recognising molecules found in a variety of different pathogens. Binding of PRRs subsequently leads to direct fibroblast activation [123, 124]. Another factor which links fibroblasts to inflammation and their role in immunoregulation is their ability to orchestrate the quantity of the inflammatory infiltrate into the lungs [125]. Activated fibroblasts in the stroma were shown to recruit and permit infiltration of circulating leucocytes on endothelial cells via induction of adhesion molecules as well as release of chemokines, notably C–C and C–X–C chemokines including MCP-1, macrophage inflammatory protein (MIP)-1, RANTES, and IP-10 [125-128]. Figure 1.9 Illustrates activation of fibroblasts in pulmonary fibrosis [129].

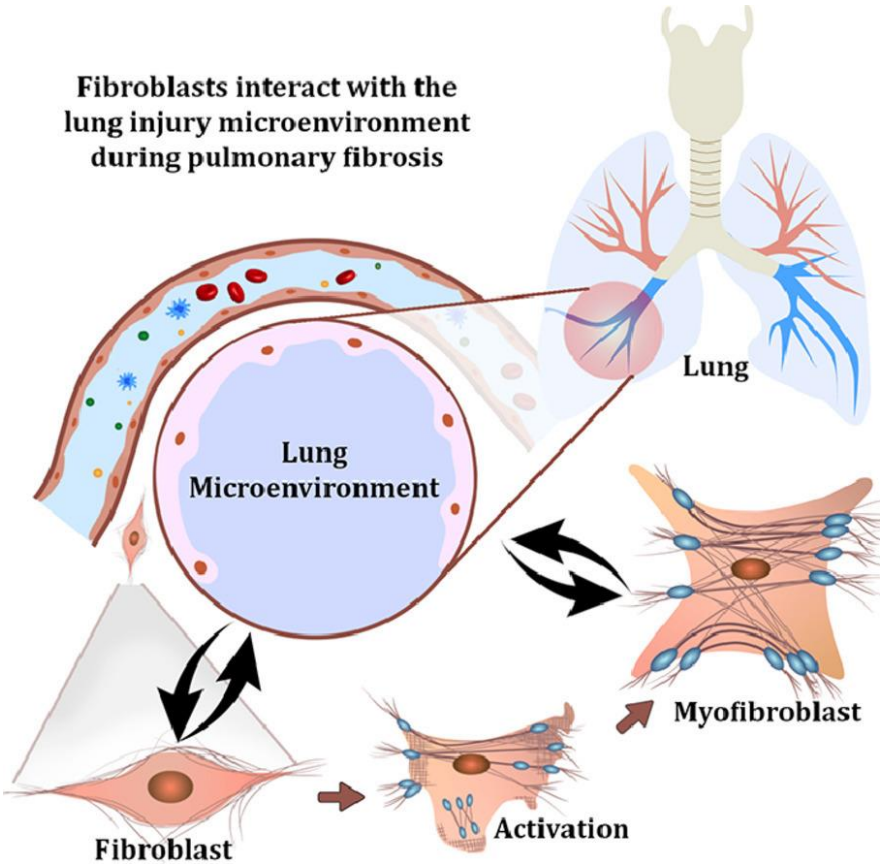

Figure 1.9 Fibroblast activation in pulmonary fibrosis.

Injury signals released by epithelial cells, endothelial cells and macrophages recruit fibroblasts from the surrounding tissue or the circulation, induce their proliferation and activation, resulting in myofibroblast differentiation. This can lead to aberrant production and deposition of ECM proteins, culminating in pulmonary fibrosis. *Image taken from [129].*

1.3.3 Pattern recognition receptors (PRRs)

Pattern recognition receptors are expressed on the surface of cell membranes, endosomal membranes and in the cytosol [130]. Having the ability to sense endogenous and exogenous pathogens as well as other dangers signals, PRRs are critical for the initiation on the immune response. PRRs were shown to recognize and bind a variety of bacterial, fungal, and viral fragments, known as pathogen-associated molecular patterns (PAMPs) as well we endogenous signals released by damaged or dying cells known as danger-associated molecular patterns (DAMPs) [130]. Figure 1.10 illustrates the classification of various PRRs according to their location [131].

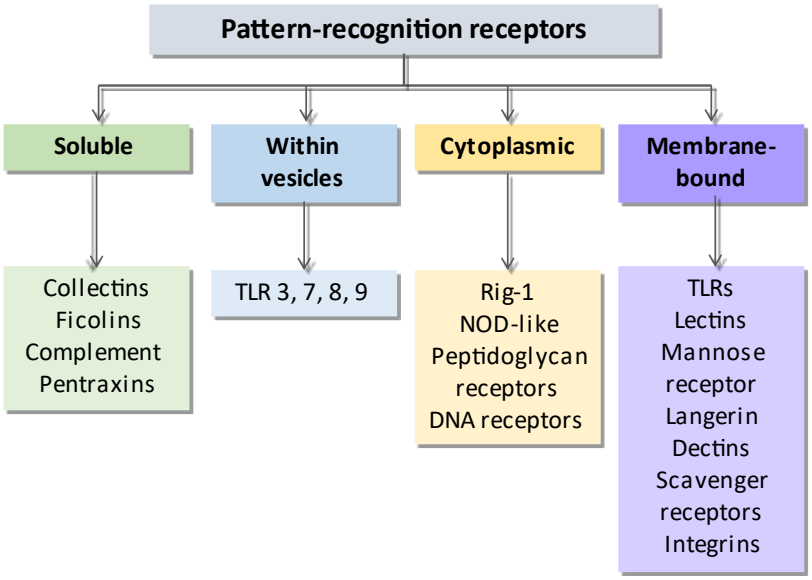

Figure 1.10 Classification of Pattern recognition receptors (PRRs).

Pattern recognition receptors sense fragments of incoming pathogens as well as other danger signals, mediating the initial step of the body's immune response. *Image adapted from [131].*

1.3.4 Toll-like receptor (TLR) superfamily

Toll-like receptors (TLRs) expressed on both cellular and endosomal membranes fall under the category of PRRs [132]. There are 10 human TLRs (TLR 1-10) and 13 murine TLRs identified up to date. Different TLRs are responsible for sensing a wide range of PAMPs and DAMPs, list of which is included in the Table 1.1 which lists Human and murine TLRs and their respective ligands.

Table 1.1 Human and murine TLRs with respective ligands

Receptor	Ligand	Location	Species
TLR1 [133]	Triacylated Lipoproteins	Cell membrane	Human & murine
TLR2 [133]	Di/triacylated Lipoproteins	Cell membrane	Human & murine
TLR3 [133]	dsRNA	Endosomes	Human & murine
TLR4 [134]	LPS	Cell membrane	Human & murine
TLR5 [133]	Flagellin	Cell membrane	Human & murine
TLR6 [135]	Triacylated lipoproteins	Cell membrane	Human & murine
TLR7 [136]	Viral single-stranded RNA (ssRNA)	Endosomes	Human & murine
TLR8 [136]	Viral ssRNA	Endosomes	Human & murine
TLR9 [136]	CpG DNA	Endosomes	Human & murine
TLR10 [137]	Unknown		Human
TLR11 [138]	Profilin, flagellin	Endosomes	Murine
TLR12 [139]	Profilin	Endosomes	Murine
TLR13 [140]	Bacterial 23s rRNA	Endosomes	Murine

1.3.5 TLR structure

The structural commonality shared amongst members of the TLR superfamily include a single transmembrane domain which connects to an extracellular domain and a cytoplasmic domain [141, 142]. The extracellular domain conserved across all the TLRs comprises of leucine-rich repeats, which are approximately 24 amino acids in length. Those leucine repeats aggregate into β-sheets and fold into a concave horse structure, responsible for binding of their respective ligands [143]. Upon binding of the ligand, the receptors' cytoplasmic domain known as the Toll/IL-1R (TIR) domain, interacts with cytosolic adapter proteins and induces downstream signalling cascades which result in production of pro-inflammatory mediators, such as cytokines, chemokines and interferons via activation of multiple inflammatory pathways [144]. Figure 1.11 illustrates a common TLR3 structure demonstrated on the example of TLR3 [145].

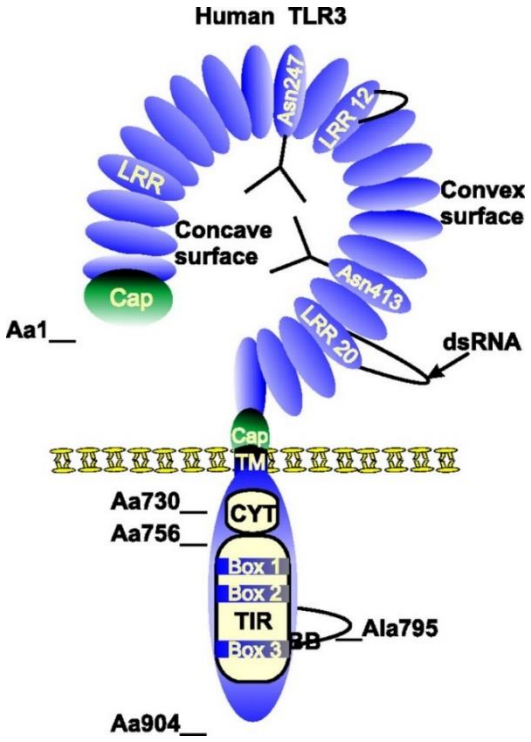

Figure 1.11 TLR Structure.

A diagram illustrating the structure of Toll-like receptor 3 (TLR3), a single transmembrane protein with leucine-rich extracellular domain and signal transducing cytoplasmic domain, shared amongst the different TLR members. *Image adapted from [145].*

1.3.6 TLR function and signalling

The localisation of TLRs can be indicative of the ligands they recognise. TLR1, TLR2, TLR4, TLR5 and TLR6 located on the plasma membrane are adapted to recognise microbial pathogens that are extracellular in nature [130]. On the other hand, TLR3, TLR7, TLR8 and TLR9 predominantly located on endosomal and lysosomal membranes are responsible for sensing RNA and DNA from intracellular pathogens, detectable following the degradation of the pathogen by the endosomes [146]. TLRs are known to oligomerize into homodimers and heterodimers in order to widen the spectrum of the different pathogens which they can recognise. For example, TLR3 and TLR4 form homodimers, whereas TLR2 is known to dimerise with TLR1 and TLR6 [142]. Binding of a ligand results in conformational shift which brings the C-termini of the two dimerised receptors into proximity and juxtaposes their intracellular TIR domains [147]. This leads to recruitment of the adapter protein to the receptors and initiates a range of intracellular signalling cascades, ultimately resulting in the induction of pro-inflammatory transcription factors, such as NF-κB, mitogen- activate protein kinases (MAPKs)

as well as members of the IRF family [95, 146]. Activation of the transcription factors causes upregulation in the production of cytokines, chemokines and IFNs which coordinate the immune response of the host [95, 146]. Adapter proteins involved in mounting of the intracellular response following TLR activation include Myeloid differentiating factor 88 (MyD88), MyD88-adapter like protein (Mal), TIR-domain-containing adaptor protein Inducing IFNβ (TRIF) and TRIF-related adaptor molecule (TRAM). Depending on a TLR induced, the signalling pathways triggered can be either MyD88-dependent or MyD88-independent [146]. Figure 1.12 demonstrates the intracellular signalling cascades triggered by biding and activation of the various TLRs in humans [95].

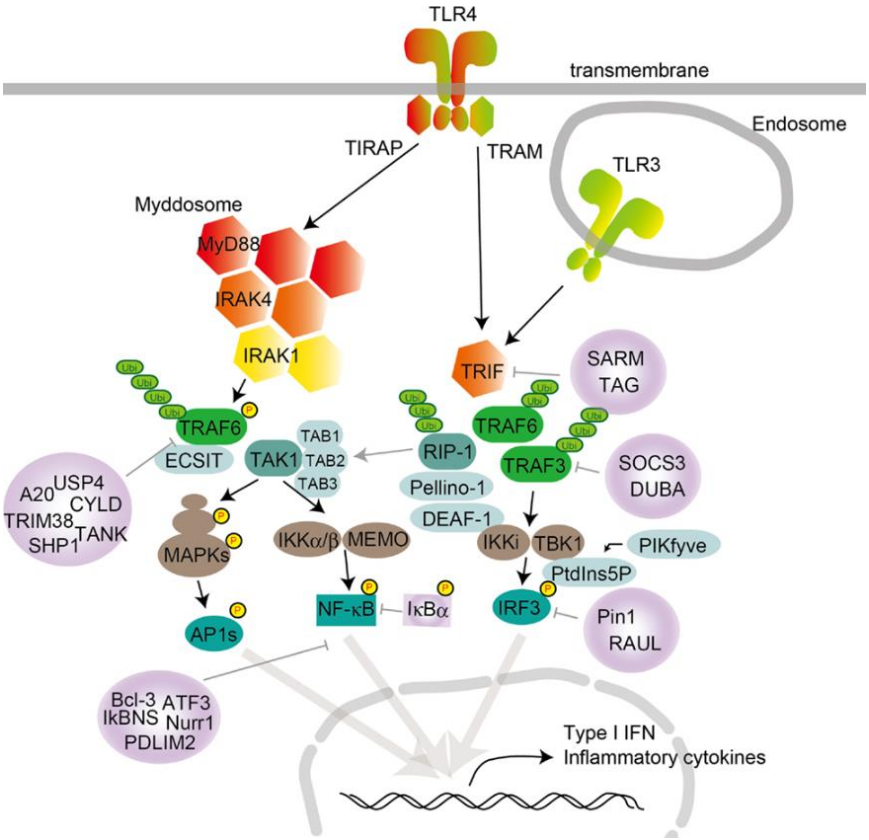

Figure 1.12 Overview of signalling cascades induced by TLR activation.

Mediated via adaptor molecules MyD88, TIRAP, TRAM and TRIF, the intracellular signal transduction induced following TLR activation leads to downstream upregulation of transcription factors NF-κB and IRF3, their subsequent nuclear translation and transcription of pro-inflammatory mediators. *Image taken from [153].*

With the exception of TLR3, TLRs utilise MyD88 as an adaptor protein which recruits IRAKs (IL-1-receptor-associated kinases) and TRAF6 (tumour-necrosis-factor-receptor-associated factor 6), in order to facilitate the signalling cascade downstream of the receptor. Signalling through TLR4 and TLR2 requires an additional adapter protein termed MyD88-adapter-like (Mal; also known as TIRAP) [95, 148]. Phosphorylation of IRAK proteins and a

subsequent recruitment of TRAF6 leads to the disassociation away from the receptor and formation of a complex with transforming-growth factor (TGF)-β activated kinase (TAK1), TAK1- binding protein 1 (TAB1) and TAB2. Following the dissolution of IRAK1 at the membrane, the remaining complex translocates into the nucleus where it phosphorylates inhibitor of nuclear factor-κB (IκB) kinase (IKK) complex and/or MAPKs. IKK complex phosphorylates IκB which leads to IκB degradation and ultimately results in translocation of NF-κB into the nucleus where it can upregulate the expression of relevant genes [95].

Signalling via TLR3 and TLR4 culminates in the induction of Interferon regulatory factor 3 (IRF3) and NF-κB, and relies on TRIF-dependent signalling pathway, which is independent of MyD88 [149]. TLR3 has the ability to recruit TRIF directly, whereas TLR4 requires an additional aid from TRAM [148]. TRIF interacts with TRAF6 and activates TAK1 in order to bring about nuclear translocation of NF-κB. In addition, TRIF recruits TRAF3 which subsequently activates TANK-binding kinase 1 (TBK1) and IKK-ε and culminates in downstream IRF3 activation. Signalling via TLR3 and TLR4 leads to production of cytokines and other IFN- inducible genes [96].

1.4 Toll-like receptor 3 (TLR3)

TLR3 is expressed on cellular and endosomal membranes in a wide range of immune cells, including endothelial cells, pulmonary epithelial cells, and fibroblasts [95, 130, 132, 141, 150-153]. It is a single transmembrane receptor, responsible for sensing of dsRNA of viruses, bacteria, and helminths [95, 130, 132, 141]. TLR3 forms homodimers and is the only member of the TLR superfamily which relies solely on TIR-domain-containing adaptor-inducing interferon-β (TRIF) for its downstream signal transduction[95, 130, 132, 141]. Activation of TLR3 leads to induction of IRF3 and NF-κB, which culminates in the transcription of cytokines, chemokines, and interferons [95, 130, 132, 141]. Figure 1.13 demonstrates the regional expression of TLR3 in the various tissues of the body as reported by the Human Protein Atlas project [152].

1.4.1 TLR3 signalling

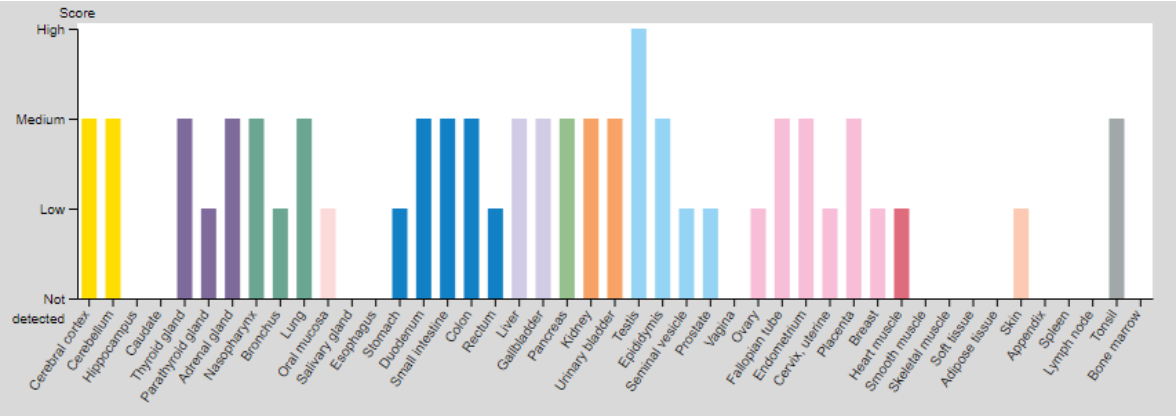

Figure 1.13 Overview of the TLR3 protein expression across different tissues in the human body.

TLR3 protein is widely expressed across various tissues of the human body, including the lung. *Image taken from [152].*

Following the binding of the PAMPs and DAMPs to the receptor, TLR3 recruits the adaptor molecule TRIF [145, 154]. DAMPS which bind the TLR3 include endogenous intracellular molecules released by necrotic cells as well as ECM molecules released upon injury and tissue damage [154]. $TRIF^{-/-}$ mice, exposed to Poly(I:C), a potent TLR3 ligand, showed defective immune responses, suggesting the vital importance of TRIF in TLR3 signalling [155, 156]. Induction of the downstream signalling cascade is due to interaction between TRIF and TRAF6 as well as TRAF3. Studies using mouse embryonic fibroblast show that both TRAF6 and RIP-1 are recruited by TRIF. This event is then followed by polyubiquitination (Ub) of RIP1, and a subsequent association of Ub RIP1 with the ubiquitin receptor protein transforming growth factor β-activating kinase (TAK) binding protein 2 (TAB2) and TAK1 [145, 154, 157]. The essential role of RIP-1 has been shown in murine embryonic fibroblasts, whereby Poly(I:C)-induced activation of NF-κB is abrogated in RIP1-deficiet mice [158]. Induction of TAK-1 results in phosphorylation of IKKα and IKKβ, which leads to degradation of NF-κB inhibitor IκB, eventually culminating into the nuclear translocation of NF-κB [145, 154]. Poly(I:C) treatment of embryonic fibroblasts from TAK1-deficient mice leads to reduced NF-κB but not IRF3 activation, suggesting the specific requirement for TAK1 in Poly(I:C)-induced NF-κB signalling. In addition to NF-κB, TAK-1 induces mitogen-activated protein kinases c-jun N-terminal kinase, p38, and extracellular signal-regulated kinase, which results in the phosphorylation and a subsequent induction of AP-1 family members [145, 154, 159]. On the other hand, TRAF3 associates with IKK-related kinases

TBK1 and IKKi through the adaptor protein NAK-associated protein 1 (NAP1). This culminates in phosphorylation and induction of IRF3. Following dimerization, IRF3 translocates from the cytoplasm into the nucleus where it induces the transcription of type I IFNs [145, 154]. Figure 1.14 illustrates the signalling cascade induced downstream of TLR3 activation [145].

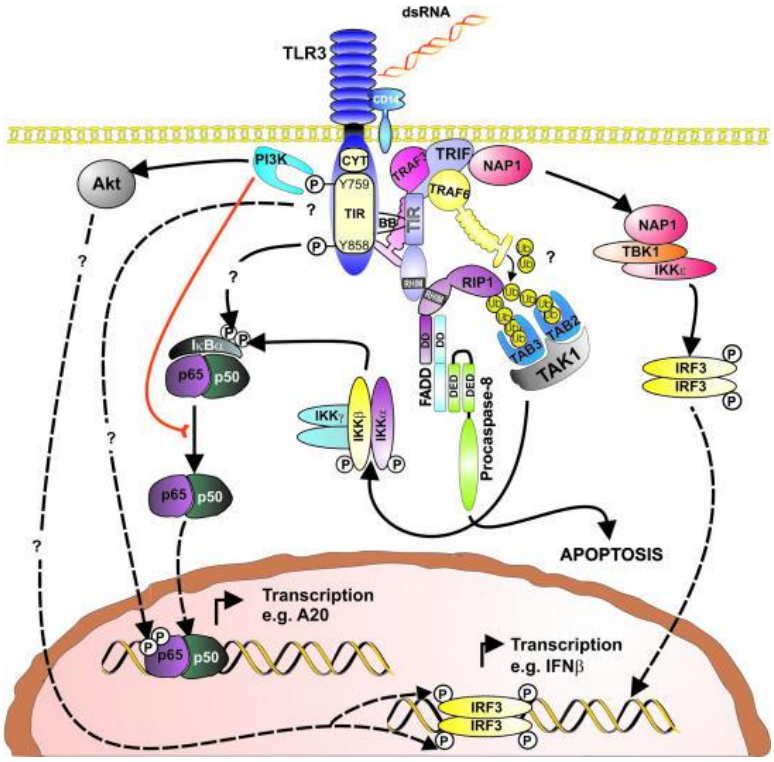

Figure 1.14 TLR3 signalling pathway.

Binding of the TLR3 leads to phosphorylation of IRF3 as well as degradation of the inhibitory subunit IKKβ by IKK. This leads to induction of IRF3-driven anti-viral response and NF-κB-driven pro-inflammatory response respectively. *Image taken from [145].*

1.4.2 Role of TLR3 in ILD

Several *in vivo* studies have demonstrated the anti-fibrotic properties of TLR3. The role of TLR3 was examined in a Schistosoma mansoni-egg induced pulmonary granuloma model by Joshi *et al.* in 2008 [160]. The group reported enlarged granulomas, as well as increased levels of collagen deposition in mice deficient in TLR3. $TLR3^{-/-}$ animals presented with increased production of Th2 cytokines and chemokines; IL-4 and CCL11 and decreased production of Th1 chemokines CXCL10 and CXCL9. Moreover, the cells derived from the lung tissue and pulmonary lymph nodes of $TLR3^{-/-}$ mice showed significantly elevated levels of a pro-inflammatory cytokines IL-17A production when compared to TLR3 WT pulmonary granuloma model [160]. Using the bleomycin model of fibrosis, our lab has previously demonstrated reduced survival and elevated levels of fibrosis in $TLR3^{-/-}$ mice when compared to their WT

counterparts. The increased levels of pulmonary fibrosis were accompanied by elevated production of pro-fibrotic mediators TGF-β, IL-4 and IL-13 as well as greater collagen deposition in the pulmonary tissue [161]. Previously, TLR4 was shown to have a protective role in fibrosis [162]. Fibrotic processes in the lung were attenuated in bleomycin-treated $TLR4^{-/-}$ mice, compared with wild-type mice, as evidenced by reduced dermal thickness as well collagen content.TLR4 deletion supressed inflammatory cell infiltration, as well as expression of pro-inflammatory cytokines. In addition, the immune profiles of the $TLR4^{-/-}$ mice were skewed towards a Th2/TH17 response against the bleomycin treatment, which demonstrated the importance of TLR4 signalling in protection against fibrosis [162]. TLR9 is another member of the TLR family implicated in the pathogenesis of pulmonary fibrosis. Studies have demonstrated TLR9 to promote myofibroblast differentiation in lung fibroblasts cultured from biopsies of IPF patients [163]. Examination of surgical lung biopsies from rapidly progressive IPF patients showed elevated expression of TLR9 [164]. Additionally, pulmonary fibroblasts from patients with worsened clinical phenotype were shown to have an exaggerated response to TLR9 agonist, CpG when compared to fibroblasts from control patients [163]. Studies on humanized SCID mice showed increased fibrotic events in mouse lungs receiving human lung fibroblasts from patients with rapidly progressive IPF, compared with mice receiving control fibroblasts. The observed fibrosis was exacerbated by intranasal CpG challenges [164].

1.4.3 *TLR3* L412F (rs3775291) in IPF

In 2007, Ranjith-Kumar *et al.* identified a single nucleotide polymorphism (SNP) within the TLR3 gene; the *TLR3* L412F (rs3775291) as a functional TLR3 polymorphism [165]. The group reported that although physiologically functional, the *TLR3* L412F resulted in a supressed TLR3 activity [165]. Our lab previously characterized the *TLR3* L412F (rs3775291) SNP in the context of IPF and pulmonary sarcoidosis [161]. O'Dwyer *et al.* published a study of two IPF cohorts in which he reported no association between *TLR3* L412F and the development of IPF. However, the presence of SNP was strongly correlated with a significantly increased hazard ratio as 412F-heterozygous and homozygous IPF patients had 5 times greater risk of mortality at 12 months and 24 months compared with *TLR3* L412 wild-type (WT) patients. Moreover, it was found that 412F-heterozygous and homozygous IPF patients experienced an accelerated rate of decline in forced vital capacity (FVC) over the period of 12 months compared with L412-WT patients [161]. Using primary human lung fibroblasts from L412-WT, 412F-heterozygote and 412F-homozygote IPF patients, we found that stimulation

of TLR3 with polyinosinicacid:polycytidylic acid (Poly(I:C)) yielded reduced pro-inflammatory cytokine and IFN-β expression responses in primary lung fibroblasts from L412F heterozygote and homozygote patients compared with L412-WT patients. Moreover, fibroblasts from patients with the L412F allele variant showed reduced lung mRNA expression of TLR3, compared with L412F wild type IPF patients [161]. Our findings led us to propose the role of defective TLR3 function in the progression of IPF. In addition to IPF and pulmonary sarcoidosis, the presence of *TLR3* L412F variant has also been associated with increased risk of development of Type I Diabetes Mellitus, Human Cytomegalovirus (CMV), Systemic lupus erythematous (SLE), Hepatitis B virus and Enteroviral myocarditis/ cardiomyopathy as well worsened disease severity in Tick-borne encephalitis (TBE) [166-173]. *TLR3* L412F polymorphism was shown to be protective in Human Immunodeficiency Virus 1 (HIV-1) and Herpes Simplex virus Type 2 (HSV-2) [174, 175]. Activation of TLR3 dictates the metabolic switch in immune cells. TLR3dependent upregulation in NF-κB and hypoxia-inducible factor-1α (HIF-1α) mRNA induce transcriptional reprogramming toward glycolytic gene expression (199). Figure 1.15 Illustrates the positioning of the L412F SNP in the extracellular domain of TLR3 [165].

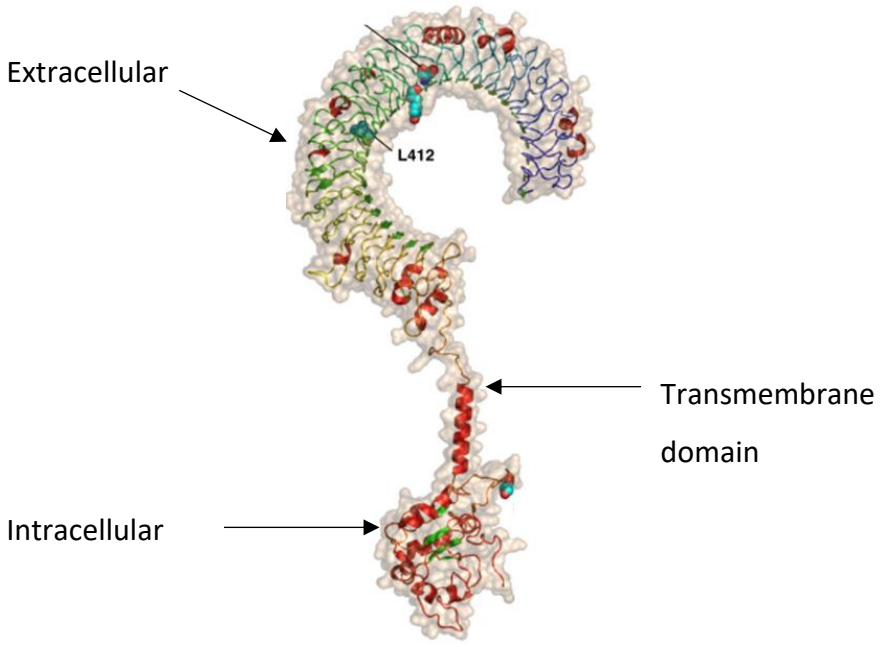

Figure 1.15 *TLR3* L412F SNP.

TLR3 L412F; a single nucleotide polymorphism encoding a leucine to phenylalanine substitution at position 412 in the extracellular domain of the TLR3 receptor. *Image taken from [165].*

1.5 Immunometabolism

1.5.1 Immunometabolism- introduction

The field of immunometabolism examines the shift in metabolic pathways in relation to the responses of the immune system in heath and disease [176]. Various metabolic processes as well as their intermediates and by-products play pivotal roles in immune cell activation and regulation of inflammatory gene expression [176, 177].

1.5.2 Overview of metabolic pathway

1.5.2.1 Glycolysis

Glycolysis is a metabolic process responsible for provision of energy, predominantly in the form of ATP, required for cellular maintenance and support of cellular homeostasis [178]. Metabolic processes involved in glycolysis are initiated following the uptake of glucose by glucose transporters into the cell. In the cytosol, glucose gets converted into pyruvate via a series of enzymatic reactions. Processing of a single glucose molecule yields a net of 2 ATP molecules and 2 NADH molecules [179, 180]. Under aerobic conditions, the pyruvate is converted into acetyl-coA by pyruvate dehydrogenase, and in this form feeds into the TCA cycle [179, 180]. Despite being a relatively inefficient way of ATP production, glycolysis results in generation of intermediates essential for synthesis of ribose, amino-acids and fatty-acids and is therefore often adapted by proliferating cells [180]. Figure 1.16 illustrates the steps involved in the glycolytic pathway [181].

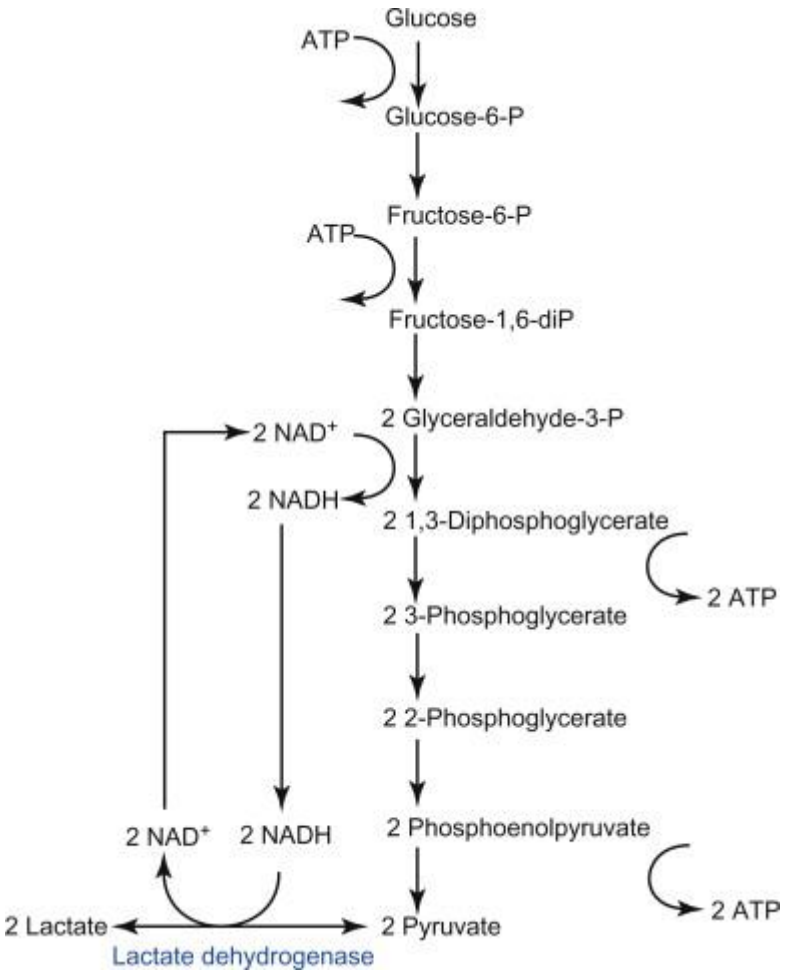

Figure 1.16 Overview of the glycolytic pathway.

Glycolysis is a metabolic process which converts glucose into ATP utilised for maintenance of cellular homeostasis. The process also generates a number of intermediates, which serve as building blocks for various cellular components, required by highly proliferative cells. *Image taken from [181].*

1.5.2.2 The tricarboxylic acid (TCA) cycle

Tricarboxylic acid cycle, (TCA cycle), also referred to as the Krebs cycle and citric acid cycle, is the second out of the 3-stage process of cellular respiration, which occurs under aerobic conditions in plants and animals [182]. It provides efficient means of harvesting of ATP from sugars (mainly glucose), fatty acids and amino acids. This catabolic process results in generation of high-energy electrons which subsequently undergo oxidative phosphorylation and prove energy needed for cellular, growth, division, and maintenance of homeostasis [182]. Before larger organic molecules can enter the TCA cycle, they are first degraded into two carbon compounds, referred to as acetyl coenzyme A (acetyl CoA), which is ultimately converted into carbon dioxide and energy. The TCA cycle commences with the reaction between acetyl CoA and the compound oxaloacetate, step which leads to generation of citrate and the release of coenzyme A (CoA-SH) [177, 182-184]. Next, re-arrangement of citrate into

isocitrate via dehydration of citrate to cis-aconitate and subsequent rehydration to isocitrate leads to the synthesis of the metabolite itaconate [177, 185]. Citrate loses a carbon dioxide molecule and following the process of oxidation, becomes converted into alpha-ketoglutarate, yielding one molecule of NADH and CO_2 [177, 186]. In a similar fashion, alpha-ketoglutarate is processed by an enzyme α-ketoglutarate dehydrogenase, subsequently becoming oxidised to the form of succinyl CoA, in a process which yields another NADH and CO_2 molecule [187]. Succinyl CoA is enzymatically converted to succinate via succinyl-CoA synthetase, in a step which generates an additional guanosine triphosphate (GTP), a molecule which functions as an energy-carrier [183, 188]. Succinate is subsequently oxidised to fumarate via succinate dehydrogenase (SDH) in a reaction that generates a metabolite FADH2 [183]. Fumarate is hydrated by fumarate hydratase into the form of malate, a compound which is oxidised by malate dehydrogenase to oxaloacetate, in a process yielding NADH molecule [189, 190]. A complete turn of the cycle is powered by the regeneration of oxaloacetate and the formation of two molecules of carbon dioxide. Each cycle yields 3 NADH molecules and FADH2 molecule, all of which enter the electron transport chain ultimately generating a net of 36 ATP molecules [177, 180, 191-195]. TCA cycle involves mitochondrial biogenesis, thus cannot be rapidly induced in a manner similar to glycolysis and therefore is mostly utilised by quiescent cells, with steady energy requirements [180]. TCA has been shown to be an important process in terms of generation of metabolites involved in regulation of immune responses [180, 182, 191]. Figure 1.17 illustrates the steps involved in the TCA cycle [182].

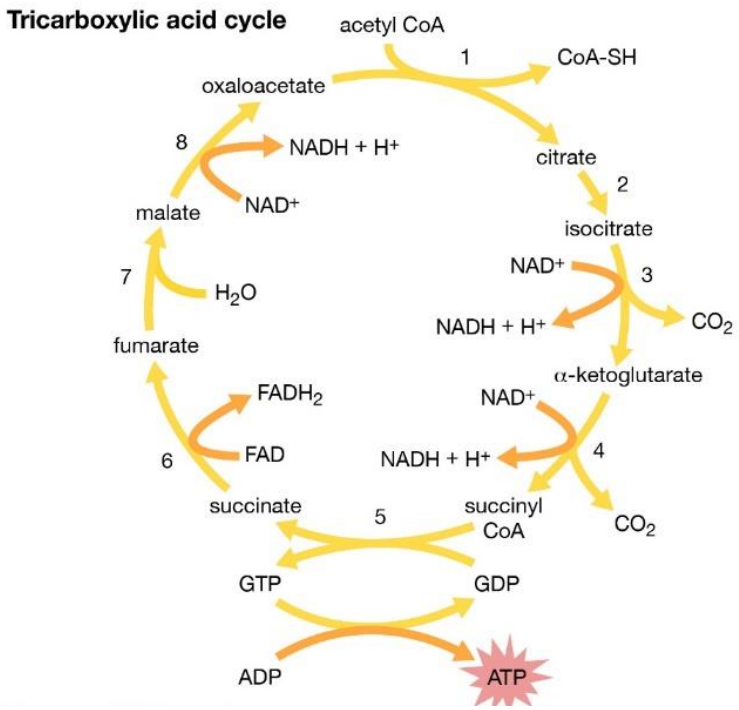

Figure 1.17 TCA cycle.

TCA cycle is an aerobic process designed to generate high yields of ATP from breaking down of nutrients such glucose and fatty acids. The process is most often used by quiescent cells for maintenance of cellular homeostasis. *Image taken from [182].*

1.5.3 Metabolic rewiring of activated macrophages

Macrophages form a heterogeneous population, and depending on the conditions, can adopt one of two main activation profiles [196]. Bacterial and viral infection associated with Th1 response are characterised by prevalence of classically activated, M1 macrophages, which present with highly pro-inflammatory phenotypes [196]. In contrast, M2 or alternatively activated macrophages, are important during parasitic infections and present with anti-parasitic and pro-regenerative phenotypes. Whereas the high pro-inflammatory signature of M1 macrophages could be associated with the onset of fibrosis, M2 macrophages are known to be involved in the matrix deposition and tissue remodelling, which if unregulated, can further drive the fibrotic processes [197]. Depending on requirements, macrophages can switch from M1 to M2 profiles and vice-versa [196]. Figure 1.18 describes phenotypes associated with classical and alternative macrophage activation [198].

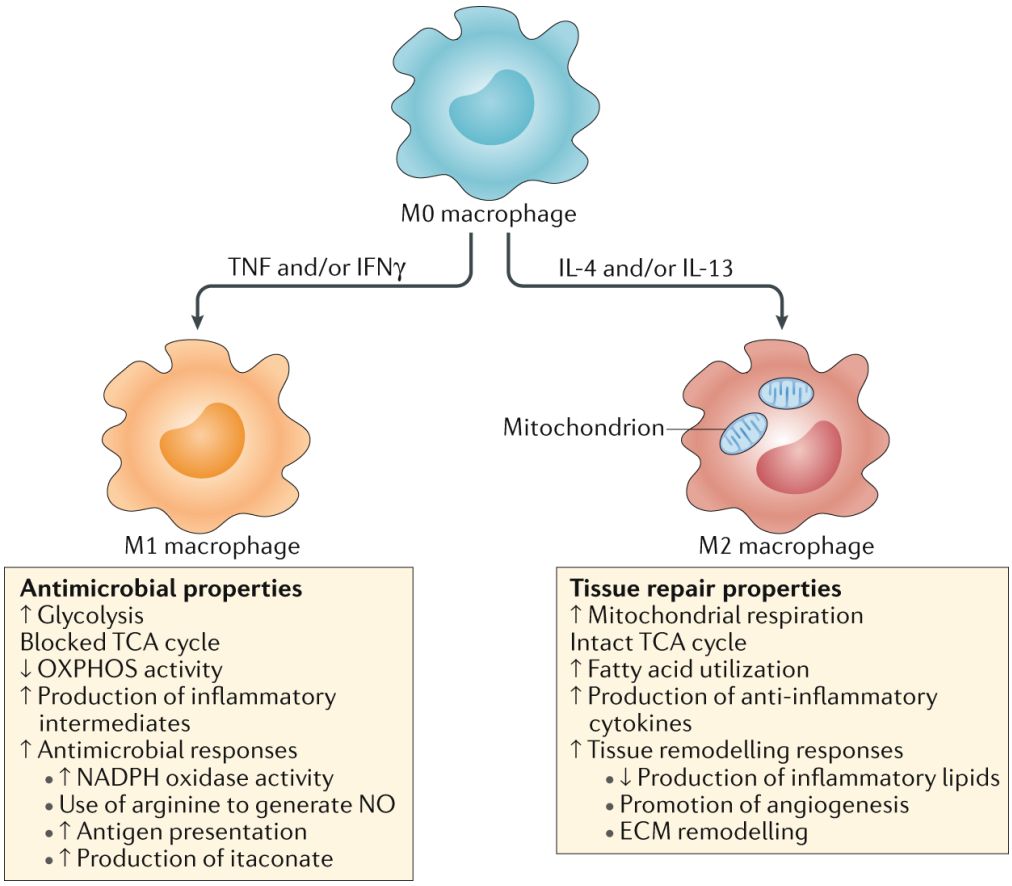

Figure 1.18 Macrophage polarisation.

M0 macrophages with a neutral signature can be polarised into either classically activated M1 macrophages, or alternatively activate M2 macrophages. Exposure to TNF, IFN or LPS leads to adaption of M1 profile and is characterised by increased rates of glycolysis and heightened pro-inflammatory activity. Polarisation of macrophages towards the M2 phenotype via exposure to Th2 cytokines such as IL-4 or IL-13 results in increased levels of mitochondrial respiration and favours tissue remodelling and regenerative responses. *Image taken from [198].*

1.5.4 The Warburg Effect

Metabolic rewiring of macrophages plays a pivotal role in tailoring of their effector function and subsequently the body's immune response to infection. Activation of immune cells such as macrophages, natural killer (NK) cells, T-cells and B-cells by LPS causes a shift from the quiescent state associated with OxPhos, the final stage of aerobic cellular respiration, towards a pro-inflammatory phenotype, accompanied by increased levels of aerobic glycolysis (Warburg effect) [199-203]. Due to a rapid turnover of ATP and generation of molecules required for biosynthetic processes, glycolysis hallmarks cellular activation and proliferation, it supports the phagocytic and anti-bacterial properties of macrophages [204].

Transcription factor hypoxia-inducible factor-1 (HIF-1), known as the master regulator of cellular response to hypoxia plays a major role in reprogramming of the metabolic response in macrophages due to its ability to induce the transcription of genes involved in angiogenesis,

apoptosis, and energy metabolism [205]. Induction of NF-κB promotes Hif-1α stabilisation in macrophages [205-208]. During macrophage activation, accumulation of succinate arising from the disturbance of the TCA cycle, leads to inhibition of the prolyl hydroxylase domain enzymes (PHDs) and prevents HIF-1α from degradation [209, 210]. LPS-treated murine HIF-$1\alpha^{-/-}$ macrophages fail to transition from OxPhos to aerobic glycolysis, this metabolic defect reduces cellular ATP pool, leads to impaired effector functions, cellular aggregation, motility, and bacterial killing [211-213]. HIF-1α has been known to promote glycolysis via induction of proteins required for the process, but also via upregulation of lactate dehydrogenase (LDH) and pyruvate dehydrogenase kinase, known to decrease available levels of pyruvate, thereby further inhibiting the TCA cycle [214].

The glycolytic shift observed in activated macrophages could be explained by an immediate requirement of the cells for increased ATP levels. Despite not being the most effective way of ATP generation, in contrary to OxPhos which involves mitochondrial biogenesis, glycolysis can be enzymatically induced in a rapid manner [204]. The process of glycolysis generates a variety of intermediates and by-products which function as building blocks for the synthesis of nucleotides, fatty acids and amino acids, all required for effective pro-inflammatory and anti-bacterial cellular response [180].

The Warburg effect and the shift towards aerobic glycolysis is a predominant feature in cancer metabolism, however the metabolic response in cancerous cells and LPS primed macrophages differs in a number of ways. The metabolic signature of classically activated macrophages is associated with increased production of various compounds necessary for effective anti-microbial activity, those include generation of reactive oxygen species (ROS), nitric oxide (NO), prostaglandins and itaconate [198].

1.5.5 TCA cycle re-programming

Inflammatory macrophage activation, observed in the classically – activated M1 macrophages is accompanied by transition towards aerobic glycolysis and away from OxPhos, a switch made possible via re-wiring of the TCA cycle. Two most prominent events hallmarking this metabolic adaptation are creation of metabolic breaks which lead to accumulation of citrate and succinate [193, 209]. Figure 1.19 summarises the events associated with TCA cycle disruption in M1 macrophages [180].

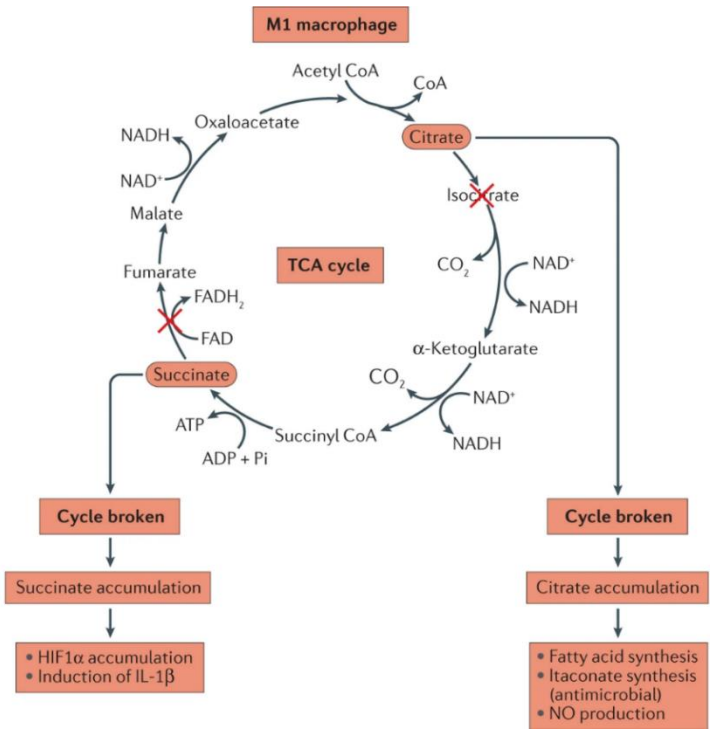

Figure 1.19 Metabolic reprogramming of the TCA cycle in M1 macrophages.

TCA cycle in classically activated macrophages presents with two breaks, which result in accumulation of the compounds citrate and succinate. The accumulated citrate is utilised for production of itaconate, or generation of fatty acids used in membrane biogenesis. Accumulation of succinate results in stabilisation of HIF-1α and induction of IL-1β. *Image taken from [180].*

1.5.5.1 Citrate accumulation

Isocitrate dehydrogenase (IDH) is enzyme that catalyses the oxidative decarboxylation of isocitrate in the TCA cycle. The enzymatic activity of IDH is repressed in LPS-activated macrophages, which leads to citrate accumulation [209]. The resulting excess citrate is processed into cis aconitate, which is subsequently converted into a metabolite, itaconate. Alternatively, citrate is used to fuel the production of fatty acids utilised in cellular biosynthesis, nitric oxide, and prostaglandins [215-217].

1.5.5.2 Succinate accumulation

Succinate dehydrogenase (SDH) is an enzyme involved in the TCA cycle, which catalyses the oxidation of succinate to fumarate. Studies have shown that classical activation of macrophages is accompanied by reduced enzymatic activity of SDH, which translates into reduced rates of succinate oxidation and leads to succinate accumulation [215].

Under normoxic conditions of homeostasis, prolyl hydroxylase (PHD) enzymes hydroxylate and destabilise HIF-1α. Succinate inhibits the enzymatic activity of PHDs which

drives inflammation and the transition towards glycolysis via stabilisation of HIF-1α. This event leads to increased HIF-1α-induced transcription of IL-1B12 [209, 218].

Moreover, succinate has been shown to signal via the G protein-coupled receptor (GPR91) GPR91 has been shown to synergize with TLR signalling which results in increased induction of TNF-α by Poly(I:C); a known ligand for TLR3 [219].

Finally, *in vivo* studies report accumulation of succinate in mouse models of ischaemia-reperfusion (IR). The studies demonstrate succinate's ability to drive mitochondrial ROS production following reperfusion. Decreased succinate levels correlate with reduced IR injury in murine models of cardiac arrest and stroke [220].

More recently, Lampropoulou *et al.* have shown that inhibition of SDH led to decreased ROS generation and mechanistically linked SDH activity to increased induction of IL-1β and IL-18 in murine BMDMs. This suggests that it is not the accumulation of succinate itself but its processing that might be responsible for driving of the pro-inflammatory response [192].
LPS stimulation of murine BMDMs with impaired SDH activity, resulted in reduced pro-IL1β and HIF-1α induction compared with BMDMs from WT mice. Moreover, SDH inhibition *in vivo* led to decreased levels of circulating IL-1β and enhanced IL-10 in a model of LPS driven sepsis [191].

1.6 Itaconate

Itaconate, encoded by immunoresponsive gene 1 (IRG-1) gene in humans, is a metabolite recently re-discovered in terms of its role as an immune-regulator. It is a product of thermal decomposition of aconitate, step which feeds into the tricarboxylic acid cycle (TCA) [221]. The initial data on the role of itaconate as an immunomodulator came from a number of studies, in which the production of itaconic acid was observed in lungs from mice infected with Mycobacterium tuberculosis(MTB), in intracellular lysates of LPS-activated RAW264.7 macrophages and the VM-M3 macrophage-like tumour cell line [222, 223]. Synthesis of itaconate was additionally recorded in LPS-activated RAW264.7 cells [224]. Although mostly restricted to active immune cells-types, such as M1 macrophages, the expression of IRG-1 was shown to be upregulated in non-immune cells, including interferon – stimulated murine lung endothelial cells [225].

1.6.1 Itaconate-mediated regulation of innate immune response

Itaconate has been shown to exert an anti-inflammatory and anti-viral effect as evidenced by the data from experiments predominantly carried out on murine macrophages [192]. In 2016 Lampropoulou *et al.* used IRG-1$^{-/-}$ mice to demonstrate increased cytokine production in macrophages treated with LPS or LPS and IFN-γ, compared with WT mice [192]. The protective role of itaconate was shown in vivo by Nair *et al.* who reported higher mortality rates of IRG-1$^{-/-}$ mice infected with MTB, compared with wild-type mice [226]. In addition, infection with influenza A virus caused a significant increase in IRG-1 levels in mouse lungs [227]. Itaconate has been proposed to mediate its anti-inflammatory activity via a number of different pathways.

1.6.1.1 Inhibition of succinate dehydrogenase

Itaconate is believed to exert its anti-inflammatory effects through various pathways, such as inhibition of succinate dehydrogenase (SDH), an enzyme which converts succinate to fumarate during the TCA cycle [192, 228]. This inhibitory event has multiple outcomes in terms of cell function, for example, disruption of the TCA cycle shifts aerobic respiration into aerobic glycolysis, a process which provides a surge of ATP to activated macrophages needed during infection [200]. Moreover, inhibition of SDH prevents stabilization of hypoxia-inducible factor 1-alpha (HIF-1α) and induction of interleukin 1 beta (IL-1β), generated upon succinate oxidation [209].

1.6.1.2 Activation of Nuclear factor erythroid 2-related factor 2 (Nrf2)

Another way in which itaconate is believed to play an anti-inflammatory role during infection comes from its ability to induce nuclear factor erythroid 2-related factor 2 (NRF2) via alkylation of Kelch-like ECH-associated protein 1 (KEAP1) [195, 229]. NRF2 responds to oxidative stress and is responsible for activation of various antioxidant genes, such as heme oxygenase (decycling) 1 (HMOX-1), glutathione-disulfide reductase (GSR) or NAD(P)H quinone dehydrogenase 1 (NQOI), all involved in synthesis of glutathione, inhibition of reactive oxygen species (ROS) and production of IL-1β. Additionally, NRF2 has been found to directly inhibit the expression of IL-1β and IL-6 encoding genes [230]. Mills *et al*. examined the effects of NRF2 activation by itaconate in terms of inflammatory response [195]. The group reported that treatment of murine BMDMs with 4-octyl itaconate (4-OI) (a cell-permeable, synthetic analogue of itaconate) decreased LPS-induced IL-1β mRNA and pro-IL-1β, HIF-1α and

interleukin 10 (IL-10) protein levels as well as ROS and inducible nitric oxide synthase (iNOS). Murine bone-marrow-derived macrophages (BMDMs) co-treated with itaconate and TLR3 agonist; Poly(I:C), had downregulated IL-1β mRNA expression. Moreover, IL-1β and tumour necrosis factor (TNF) were decreased by 4-OI in human peripheral blood mononuclear cell (PBMCs) treated with LPS [195].

1.6.1.3 Inhibition of type I IFNs

Itaconate has been shown to inhibit stimulator of IFN genes (STING) in NRF2-dependent manner. Repression of STING resulted in decreased type I IFN production in response to stimulation with herpes simplex virus in fibroblasts from patients suffering from STING-associated vasculopathy [231]. Moreover, studies have shown that 4-OI inhibits LPS and Poly(I:C) induced production of type I IFNs [195]. Interestingly, type I IFNs were found to induce IRG-1 [232], this indicates a regulatory feedback loop between IRG-1 and type 1 IFNs. Figure 1.20 illustrates the relationship between itaconate and type I interferons [233].

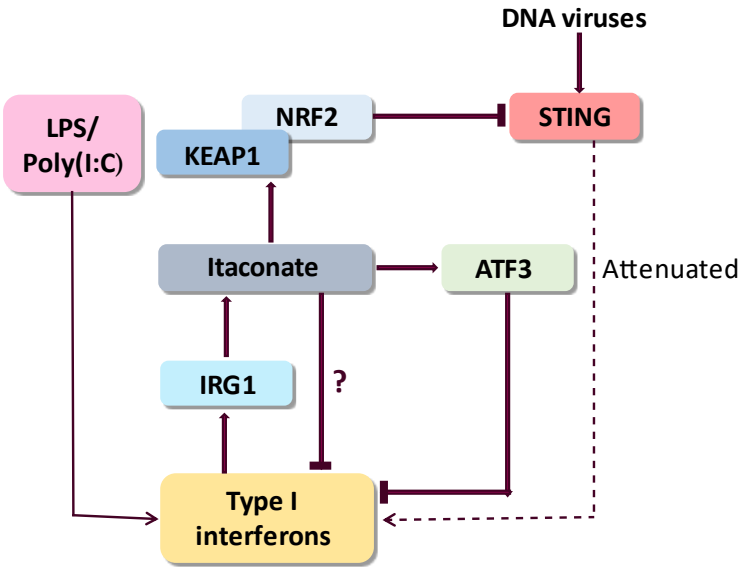

Figure 1.20 the relationship between itaconate and type I interferons.

Induction of IRG-1 expression by LPS or Poly(I:C) has been shown to be type 1 interferon-dependent. The derivatives of itaconate, such as 4-OI (yet to be evaluated in terms of endogenous itaconate) were shown to inhibit the induction of type 1 interferons, creating a self-regulatory feedback loop. This process can be both NRF2-dependent, with NRF2 blocking the stimulator of interferon genes (STING) pathway or NRF2-independent through induction of ATF3. *Image adapted from [233].*

1.6.1.4 Electrophilic stress regulation

Studies have shown that itaconate acts as a potent electrophilic stress regulator. Electrophilic stress results from excessive production of reactive electrophilic and oxygen species Itaconate targets various sulfhydryl(-SH) containing molecules, including glutathione and thereby has the ability to induce an electrophilic stress response (ESR) [229]. KEAP-1 is not the sole sensor of the ESR in the body, the ESR is regulated by various KEAP1/NRF2 independent pathways, governed by different regulators such as activating transcription factor 3 (ATF3) [234]. Studies on IRG-1$^{-/-}$ macrophages (BMDMs) demonstrated the ability of itaconate to induce ATF3, which leads to inhibition of NF-kappa-B inhibitor zeta (IκBζ) protein-induction, and by extension limits the second wave of the transcriptional response to TLR stimulation, including the production of IL-6, IL-12B, IL-10 [229]. Interestingly nuclear factor of kappa light polypeptide gene enhancer in B cells inhibitor ζ (NFKBIZ), a gene encoding for IκBζ has been identified as a major susceptibility locus for pneumococcal disease and psoriasis [231, 235], which might by of importance in terms of the effects of infection in IPF. Figure 1.21 illustrates the effects of itaconate on metabolic rewiring of macrophages [233].

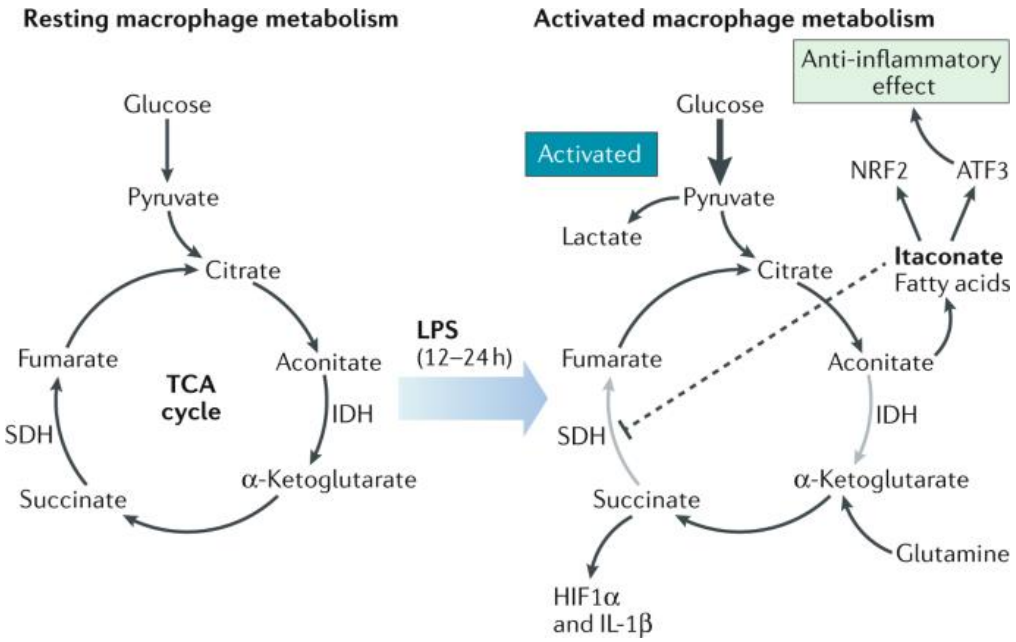

Figure 1.21 the effects of itaconate on macrophage metabolic remodelling.

Accumulation of itaconate limits succinate dehydrogenase (SDH)-associated inflammatory response and promotes the production of anti-inflammatory proteins, the nuclear factor erythroid 2-related factor 2 (NRF2) and ATF3. *Image taken from [233].*

1.6.1.5 Antibacterial properties

In terms of the antibacterial properties of itaconate, its effects are ascribed to its ability to inhibit isocitrate lyase (ICL), an essential enzyme involved in bacterial glyoxylate cycle, a process analogous to the TCA cycle in plants and microorganisms [232, 236].

Moreover, itaconate has been found to inhibit acetate assimilation via inhibition of propionyl-CoA carboxylase [237]. In accordance with these findings, studies have demonstrated the inhibitory effects of itaconate on the growth of *Salmonella enterica*, *Legionella pneumophilia*, *Staphylococcus aureus*, *Pseudomonas indigofera* in glucose-deprived environments [236, 238]. However, itaconate did not inhibit the replication of *Escherichia coli* in glucose-rich conditions [239].

Interestingly, a variety of bacteria, such as *Yersinia pestis* and *Pseudomonas aeruginosa* have retained enzymes involved in degradation of itaconate [240-242]. It has been proposed that this reflects the evolutionary development of a protective mechanism employed by the bacteria [242].

1.6.1.6 Anti-viral properties

The role of itaconate in viral infections is more ambiguous than its function during bacterial infection. Investigation into the role of itaconate in Zika virus infection showed that itaconate promotes viral clearance in mice [243]. The protein receptor-interacting protein kinase (RIPK) is involved in necroptosis required for pathogen elimination and host defence during Zika virus infection.

Ripk3$^{-/-}$ mice presented with increased viral burden and decreased survival rate compared with WT mice. A significant difference between Ripk3$^{-/-}$ mice and controls, was reduced transcription of IRG-1 in the KO animals. Interestingly, IRG-1 deletion in Zika infected mice resulted in increased mortality rates and significantly increased viral loads compared to their WT counterparts. Treatment with exogenous itaconate (4-OI) significantly decreased viral burden [243].

Furthermore, studies have shown the protective role of itaconate in West-Nile Virus infection, where it restricted viral replication in neurons [244]. Finally, IRG-1 was identified in a screen for genes whose overexpression restricted replication of several positive-stranded RNA viruses in neurons [244].

1.6.2 The role of itaconate in pulmonary fibrosis

At the commencement of my PhD project in September 2018, there were no publications addressing the role of the metabolite, itaconate, in IPF. Given the rapid development of immunometabolism at the time period, our research group commenced studies on the role of itaconate in IPF which were focused on pulmonary fibroblasts. Itaconate has been shown to have anti-viral and anti-bacterial properties, therefore, we hypothesised that it may play a role in IPF in the context of disease progression and exacerbation in infection.

At the time of submission of this PhD thesis in March 2023, there remains one published research paper addressing the role of itaconate in IPF. This publication by Ogger *et al.* is focused on examining the role of itaconate in primary alveolar macrophages in IPF [245]. Ogger *et al*. 2020 studied itaconate and its role in IPF [245]. The group examined the expression of ACOD1 (or IRG1)in primary human lung fibroblasts (HLFs), alveolar macrophages (AMs) and human bronchial epithelial cells (HBECLs) from heathy controls and IPF patients. The levels of ACOD1 transcription were significantly reduced in AMs from IPF patients compared with controls, as evident by qPCR. In addition, the total itaconate levels were decreased in BAL of IPF patients compared with heathy volunteers. However, expression of ACOD1 was not detected in HLFs or HBECs. These data indicated a significant alteration of the ACOD1-itaconate axis in IPF lung [245].

Furthermore, Ogger *et al.* utilised the murine bleomycin model of pulmonary fibrosis in order to assess the role of itaconate in the development and progression of lung fibrosis. The group reported elevated transcription of IRG1 at d7 and d21 post-bleomycin treatment in mouse lung tissue, which returned to baseline levels at d42. The maximum expression of IRG1 was reached at d21 post-bleomycin, this pattern corresponded with the levels of inflammation and peak fibrosis [245].

Targeted gas chromatography-mass spectrometry (GC-MS) was used to assess the levels of itaconate in BAL of the bleomycin mice. The levels of itaconate production were significantly increased at d7 and d21 post-bleomycin compared with PBS controls. Itaconate production returned to baseline levels a d42 [245].

The group also generated bleomycin-treated IRG1$^{-/-}$ mice in order to determine the role of IRG1 gene in the establishment of pulmonary fibrosis. Whereas the fibrosis was resolved in WT mice at d42 post-injury, IRG1$^{-/-}$ mice failed to return to baseline and presented with increased BAL cell counts. Multi-parameter flow cytometry data showed elevated

numbers of AMs and neutrophils in IRG1$^{-/-}$ mice compared with their WT counterparts at d42 post-bleomycin. Furthermore, IRG1$^{-/-}$ animals presented with worsened elastance, airway resistance and compliance compared with WT controls. Lung function, total BAL counts and pathology at d7 and d21 post-bleomycin were unaltered in IRG1-deficient mice compared with WT mice. These data suggested that itaconate was not involved in the initiation of the fibrotic events [245].

IRG1-deficient mice showed elevated Collagen-(Col)3α1 and Fibronectin-1 (Fn-1) transcription compared with WT controls at d21 but not d7 or d42 post-injury. There was no significant change in the pulmonary transcription of Col1α1 or Col4α1 at any time point assessed in the study. Finally, IRG1$^{-/-}$ mice showed increased pulmonary fibrosis compared with WT controls, as evident by elevated lung hydroxyproline levels and Ashcroft scores. These results suggested that deficiency in IRG1 was associated with enhanced pulmonary fibrosis in response to bleomycin treatment [245].

In contrast to the foetally-derived tissue resident AMs (Tr-AMs), the recruited, monocyte-derived AMs (Mo-AMs) have been previously implicated in the progression of pulmonary fibrosis in mice. Using the murine bleomycin model of pulmonary fibrosis, Ogger *et al.* demonstrated decreased proportions of Tr-AMs to Mo-AMs at d7 post-injury in WT mice compared with IRG1$^{-/-}$ mice. Mo-AMs and Tr-AMs retrieved from bleomycin-treated mice, were assessed in terms of their metabolic activity at d7 post-injury. Whereas Tr-AMs from WT mice presented with high oxygen consumption rate following bleomycin exposure, Mo-AMs presented with comparatively reduced baseline oxygen consumption rate (OCR). These data showed the distinction between metabolic phenotypes of Tr-AMs and Mo-AMs in mice. Interestingly, the expression of IRG1 was much higher in Mo-AMs compared with Tr-AMs sorted from both control and bleomycin-treated mice [245].

In order to assess the impact of itaconate on AM metabolism, Seahorse Mito Stress Test, oxygen consumption rate (OCR) and extracellular acidification rate (ECAR) measurements were taken at baseline and following sequential addition of Oligomycin, FCCP and Rotenone/Antimycin A. Mo-AMs from WT mice showed comparable levels of OxPhos and glycolysis to those from IRG1$^{-/-}$ cells. In contrast, OCR, maximal respiration and spare respiratory capacity were all reduced in IRG1$^{-/-}$ Tr-AMs compared with WT cells, while basal ECAR remained unchanged. These data demonstrated that Mo-AMs recruited to the fibrotic lungs of bleomycin-treated mice present with relatively quiescent metabolic profile, whereas

the resident Tr-AMs are characterised by high oxidative rates, indicating that itaconate deficiency results in decreased oxidative phosphorylation [245].

Next, the group investigated the mechanisms by which itaconate impacted pro-fibrotic pathways in Tr-AMs and Mo-AMs retrieved from BAL at d7 post-injury. As assessed by PCR experiments, Mo-AMs from IRG1$^{-/-}$ mice presented with a relatively high expression of genes involved in pro-fibrotic signalling, including Col1α2, Transforming growth factor β 2 (Tgfβ2) and Ccr2 compared with Tr-AMs [245].

IRG1-deficient Tr-AMs showed significantly increased transcription of fibrosis-related genes compared with WT Tr-AMs. In contrast, itaconate deficiency had a downregulating effect on the transcription of only two genes in Mo-AMs. The genetic expression of IL-1β, and Integrin linked kinase (Ilk) was significantly diminished in Mo-AMs from IRG1-deficient mice compared with cells from WT controls. IRG1$^{-/-}$ Tr-AMs showed a significant upregulation in the transcription of pro-fibrotic genes; CCAAT enhancer binding protein β (Cebpb), Tgfβr1 and Smad7 compared with WT cells. These results indicated that itaconate regulates pro-fibrotic pathways in Tr-AMs but not in Mo-AMs in mice [245].

Furthermore, the group investigated whether a transfer of Mo-AMs from WT or IRG1-deficient mice into an IRG1$^{-/-}$ fibrotic environment had an impact on disease progression [245]. Mo-AMs sorted from WT or IRG1-deficient mice were adoptively transferred into the airways of IRG1$^{-/-}$ mice at d7 post- injury. Transfer of cells sorted from WT animals but not IRG1-deficinent mice rescued the pro-fibrotic phenotype, as evidenced by reduced Ashcroft scores based on Sirius red staining and decreased transcription of pulmonary Col3α1 and Fn1. There were significant differences in BAL cell count, number of neutrophils and total AM count, as well as in the transcription of Col1α1 and Col4α1 following the adoptive AM transfer [245].

The group also investigated whether the adoptive transfer of WT Mo-AMs into IRG1-deficient mice had an impact on AM phenotype. For this purpose, the expression of macrophage activation markers CD11b and MHC II was assessed in Mo-AMs and Tr-AMs with adoptive transfer of WT or IRG1$^{-/-}$ Mo-AMs at d21 post-injury. Adoptive transfer of WT Mo-AMs into IRG1$^{-/-}$ mice resulted in Tr-AMs with increased proportion of activated cells and decreased proportion of CD11b-/MHCII- cells, a trend similar to that observed in Mo-AMs. It was concluded that the adoptive transfer of itaconate-sufficient Mo-AMs altered Tr-AM phenotype in IRG1-deficient mice exposed to bleomycin challenge [245].

The group has also assessed the direct effect of itaconate on metabolic and fibrotic activity in HLFs. Fibroblasts from IPF presented with elevated maximal respiration and spare

respiratory capacity compared with control fibroblasts, this effect was ameliorated following itaconate treatment. Proliferation and wound healing data showed that 72 hr treatment with itaconate reduced proliferative capacity of both healthy and IPF HLFs. Furthermore, itaconate downregulated the transcription of IL-1β and FN-1 in healthy HLFs. This data demonstrated that itaconate can influence metabolic phenotype, proliferation, and wound healing of lung fibroblasts in humans [245].

Finally, the group aimed to investigate the anti-fibrotic potential of exogenous, inhaled itaconate in mice. Itaconate was administered twice a week for the duration of 2 weeks during the fibrotic phase (day 10 post-bleomycin) to WT mice. Pulmonary fibrosis and function were assessed at d21 post-injury. Inhaled itaconate significantly ameliorated fibrotic hallmarks such as Ashcroft score based on Sirius red staining Col4α1 and Fn1 expression as well as pulmonary airway elastance and compliance [245].

Whereas Ogger *et al.* focused on the direct effects of itaconate on human and mouse primary alveolar macrophages in IPF, in this PhD project I investigated the role of itaconate in primary human lung fibroblasts from IPF and healthy controls. In addition, in my PhD project I specifically investigated the ability of itaconate to modulate TLR3 function in IPF lung fibroblasts.

1.7 IL-17 superfamily

In 1993, Yao Z *et al.* reported the existence of IL-17A cytokine, which became the founding member of the newly identified IL-17A superfamily [246]. This discovery has led to identification of IL-17 secreting TH17 cells, which were later differentiated as a cell line separate to Th1 and Th2 lineages [247]. Th17 differentiation is controlled by transcription factors aryl hydrocarbon receptor (AHR), signal transducer and activator of transcription 3 (STAT3) and retinoic acid receptor-related orphan receptor-γt (RORγt) [248]. This process is driven by numerous components including TGF-β as well as the cytokines IL-1, IL-6, and IL-23 [249, 250]. Almost two decades since the discovery of IL-17A, the IL-17 superfamily is known to consist of six different members IL-17A-IL-17F. With 50% homology, IL-17A and IL-17F are the most closely related. Cytokines of the IL-17 family share conserved cysteine residues, and are secreted in the form of dimers, which bind their family of receptors including IL-17RA, IL-17RB, IL-17RC, IL-17RD/SEF, and IL-17RE [249]. Figure 1.22 Shows the relationships between the receptors of the IL-17 family and their ligands [5].

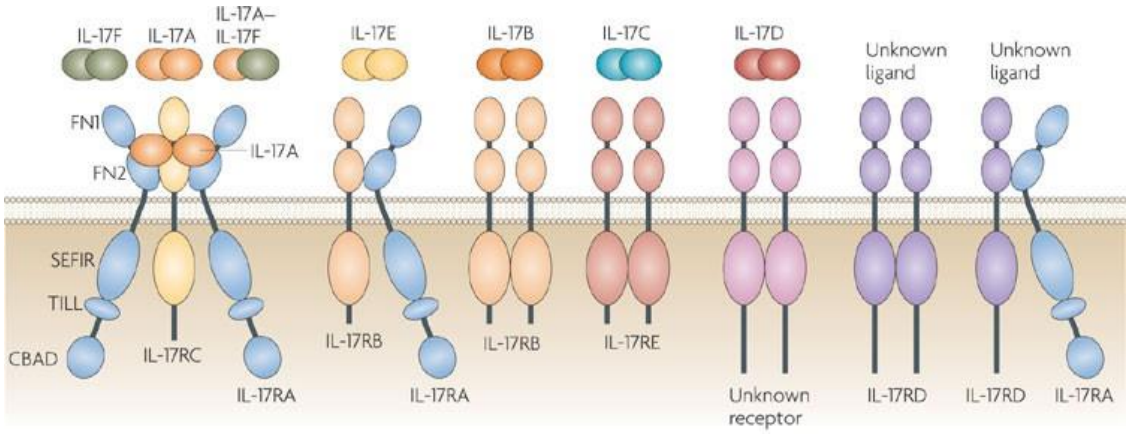

Figure 1.22 IL-17 family of receptors with their respective ligands.

Receptors of the IL-17 family dimerise and bind six different IL-17 cytokines. *Image taken from [5].*

1.7.1 IL-17A

What is currently known about the IL-17superfamily, comes from studies done predominantly on IL-17A, IL-17E (IL-25) and IL-17F. The most extensively studied member of the family, IL-17A, is expressed in human and mouse and is produced by Th17 cells, CD4+, CD8+, gamma-delta T (γδ-T), invariant NKT and innate lymphoid cells (ILCs) [251, 252]. IL-17A has been shown to heterodimerise with IL-17F. Both cytokines elicit pro-inflammatory

responses at mucosal sites such as the lung and the gut, through induction of the expression of various chemokines, such as CXCL1, CXCL10 and cytokines IL-6, IL-8 and G-CSF [253-255].

1.7.2 IL-17A receptor structure and signalling

Although the exact stoichiometry of the receptors has not been fully determined, the receptor for IL-17A and IL-17F is a single-pass transmembrane protein of approximately 130 kDa, known to exist as a heterotrimeric complex consisting of two IL-17RA subunits and one IL17RC subunit [256]. In humans, IL-17A protein is composed of 15 amino acids, with molecular weight of 15 kDa, secreted as a disulfide-bonded homodimer of 30–35 kDa glycoprotein [257]. Although IL-17A and IL-17F are primarily produced by activated T cells, a variety of cell types, including endothelial cells, epithelial cells and pulmonary fibroblasts were shown to express the IL-17R [251, 257-259]. Signalling through the receptor activates several intracellular kinases, such as TGF-beta-activated Kinase 1 (TAK1), Extracellular Signal-regulated Kinase (ERK), Glycogen Synthase Kinase 3 beta (GSK-3 beta), p38, I-kappa B Kinase (IKK) and MAPK. This leads to induction of the NF-kappa B-, C/EBP and -AP-1- and results in the expression of pro-inflammatory cytokines, chemokines, and anti-microbial peptides [260]. Figure 1.23 Illustrates signalling cascade downstream of the IL-17A/ IL-17F receptor [261].

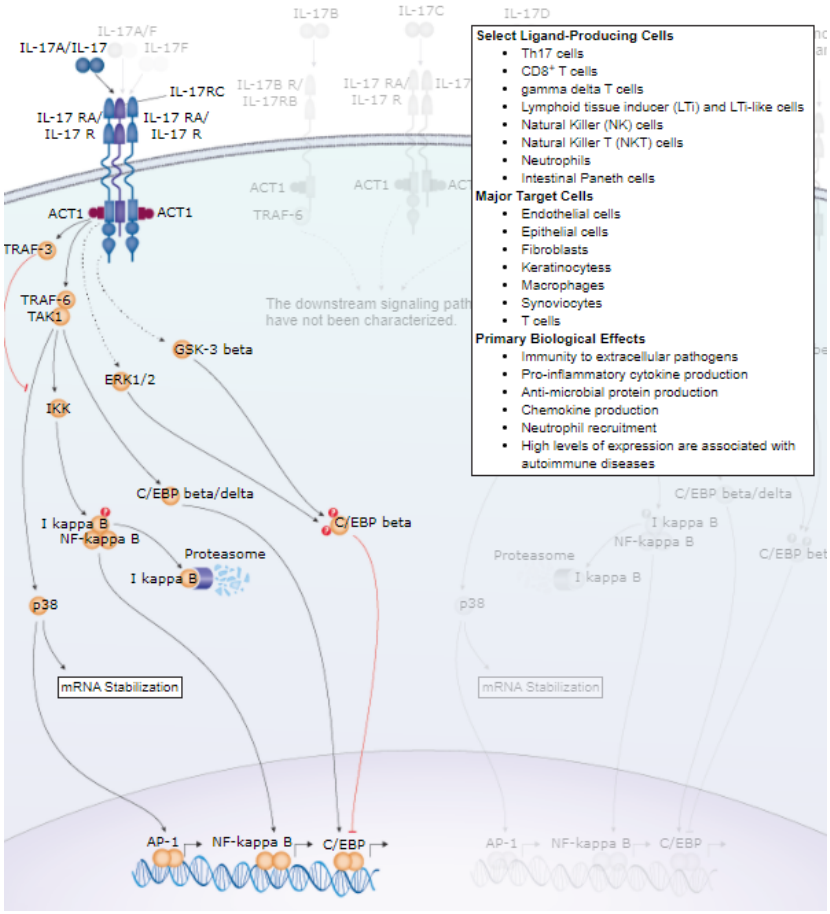

Figure 1.23 IL-17A signalling pathway.

Signalling through the IL-17R leads to the activation of a number of intracellular kinases including TGF-beta-activated Kinase 1 (TAK1), Extracellular Signal-regulated Kinase (ERK), Glycogen Synthase Kinase 3 beta (GSK-3 beta), p38, I-kappa B Kinase (IKK) and MAPK. This results in induction of the NF-kappa B-, C/EBP and -AP-1- and the expression of pro-inflammatory cytokines, chemokines, and anti-microbial peptides. Image taken from [261].

1.7.3 Role of IL-17A in disease

The chemoattractant properties of IL-17A and IL-17F were shown to play major roles in protection against gram-negative bacteria and fungal infections. Mice deficient for IL-17R showed impaired recruitment, activation and migration of neutrophils which resulted in increased susceptibility to infection with the extracellular pathogen *Klebbsiella* and the fungi *Candida* [262, 263]. Ye *et al.* demonstrated reduced ability of IL-17RA$^{-/-}$ mice to attract neutrophils to the lungs, which resulted in a greater incidence of bacterial infections, such as bacterial pneumonia [262]. In addition, IL-17A was found to be amongst cytokines preferentially secreted by T cells in mice during an infection with *Borrelia burgdoferi* and *Bacteroides fragilis* [264, 265].

Although the anti-bacterial properties of IL-17A have been well established, findings regarding the role of IL-17A during viral infection are contradictory. Studies have shown

increased expression of anti-apoptotic proteins, Bcl-2 and Bcl-xL in murine bone marrow cells, following a combined IL-6 and IL-17A treatment. The elevated expression of the proteins led to protection of virally infected cells from apoptosis and CD8+ T cell-mediated target destruction which promoted viral persistence [266]. Contrary to those findings, Acharya *et al.* showed using murine model of West Nile virus infection, that IL-17A-deficient mice had an increased viral burden and a lower survival rate compared with control animals. These results were supported by decreased CD8+ T-cell cytotoxicity characterized by a lower expression of cytotoxic-mediator genes, such as Perforin-1 and FasL [266]. Assessment of IL-17 levels in the CD4(+) T cells (Th17) of 40 HIV-seronegative volunteers compared with 40 asymptomatic HIV-infected treatment-naive patients showed association between HIV infection and a significant increase in IL-17 production in CD4(+) and CD4() T cells in peripheral blood [267]. Molesworth-Kenyon *et al.* studied IL-17A expression following HSV-1 corneal infection in mice. The ability to express IL-17R by murine corneal fibroblasts was confirmed using immunofluorescent studies. IL-17R$^{-/-}$ mice presented with a significant reduction in neutrophil infiltration and corneal opacity. However, this was a transient effect, as in terms of corneal pathology and neutrophil influx, the IL-17R-deficient mice resembled their WT counterparts 4 days post infection. Moreover, HSV-1 replication and clearance in IL-17R$^{-/-}$ was comparable to that of WT mice. Interestingly, HSV1 infection in IFN-γ$^{-/-}$ mice resulted in increased IL-17A levels and accelerated corneal opacity. These findings suggested a negative regulation of IL17-A expression by IFN-γ. The study concluded that IL-17 had a significant impact on early virus-induced corneal inflammation [268].

In addition to its role in conferring immunity against bacterial and fungal pathogens, IL-17A signalling has been heavily implicated in several autoimmune-diseases such as Crohn's disease, rheumatoid arthritis, psoriasis, or asthma [269-273]. Mice deficient in IL-17R as well those treated with IL-17R antagonist, IL-17 receptor/human IgG1 Fc fusion protein (muIL-17R: Fc) showed resistance to the development of adjuvant-induced arthritis [274, 275]. IL-17R deficiency was also protective in animal models of experimental autoimmune encephalomyelitis, whereby mice lacking the receptor exhibited delayed EAE onset and reduced disease severity [276].

1.7.4 IL-17A in lung and IPF

In terms of the role of IL-17A in the lung, Ye *et al.* 2001 reported that IL-17R-deficient mice showed reduced capability to attract neutrophils to the pulmonary tissue which resulted

in increased susceptibility to *Klebsiella pneumoniae* infection. These findings were later supported by studies conducted by Happel *et al.* in 2005 [262, 277]. IL-17R-deficient mice infected with an invasive pulmonary, pneumococcal strain (TIGR4), showed significantly increased mortality rates, compared with wild-type mice [278]. Research on mouse model of chronic pulmonary infection with Cystic Fibrosis-associated strains of P. aeruginosa showed the essential role of IL-17A signalling in survival and prevention of chronic infection [279]. In 2013, Robinson *et al.* showed that infection with Influenza A caused a significant reduction in IL-1β signalling in mice, which correlated with decreased levels of IL-17A production and was associated with more severe pulmonary *Staphylococcus aureus* infection [280]. Moreover, mice deficient in IL-22, a cytokine co- regulated by IL-17A, exhibited elevated epithelial cell damage and fibrosis following influenza challenge [281]. Additional information on the importance of IL-17A in the lung comes from two separate studies which reported increased levels of both IL-17A and IL-22 in acute respiratory distress syndrome (ARDS) patients [282, 283]. Elevated IL-17A and IL-17F mRNA expression and protein levels have been identified in the sputum of CF patients experiencing an exacerbation of their disease with evidence of colonization by *P. aeruginosa* [284]. Studies have shown increased levels of IL-17A in BALF and pulmonary tissue of IPF patients [285]. Additionally, in the bleomycin (BLM) murine model of pulmonary fibrosis, treatment with exogenous IL-17A significantly induced neutrophilia and pulmonary fibrosis [285]. Mice deficient in IL-17A challenged with BLM exhibited a significant reduction in fibrosis, compared with wild-type mice, as seen by increased collagen expression in the BAL and collagen deposition in the lung [285].

In 2001, Lee *et al.* identified another member of the IL-17 superfamily, IL-17E (IL-25) [286]. In humans, IL-17E is a protein of 20 kDA, composed of 117 amino acids [286]. The receptor for IL-17E exist as a heterodimer, composed of subunits IL-17RA and IL-17RB. Although IL-17E does not bind IL-17RA directly, this subunit is essential for its proper signalling [287, 288]. IL-17E shares 16%-20% homology with IL-17A, however, unlike IL-17A and IL-17F, IL-17E is secreted by a number of different cell types, such as T cells, dendritic cells, eosinophils, macrophages, basophils, mast cells and epithelial cells [289, 290]. Binding of IL-17E to its receptor leads to activation of numerous transcription factors, including JNK, MAPK, STAT6, NF-kB, JUNNB, NF-ATC1 and GATA3 [291]. Unlike other members of the IL-17 superfamily, IL-17E orchestrates and supports TH2-type responses. Not surprisingly dysregulated IL-17E secretion has been implicated in several chronic allergic conditions [292]. The inflammation associated with IL-17E is distinct from the one supported by IL-17A and IL-

17F, which is apparent in the composition of the immune filtrate. Where immune response induced by IL-17A and IL-17-F result in high concentration of neutrophils, inflammation induced by IL-17E is characterised by augmented eosinophils infiltration [293].

Studies have shown elevated expression of IL-17E in human pulmonary epithelial cells and murine primary type II alveolar epithelial cells following *Aspergillus oryzae* infection, as well as exposure to allergen proteases and rag weed allergens [294, 295]. Immunohistochemistry (IHC) studies have identified increased levels of IL-17E in the bronchial mucosa of asthma patients [296]. Further links between IL-17E and asthma come from a study conducted by Wang *et al.* in 2007, where the group has reported increased expression of IL-17E mRNA in asthmatics [297]. Moreover, research using murine model of asthma showed the ability of IL-17E to promote TH2 cytokine and IgE production, supported by eosinophil recruitment [298]. In terms of the role of IL-17E in fibrosis, Hams *et al.* reported a link between IL-17E and the development of pulmonary fibrosis via induction of IL-13 production. The group showed that mice deficient in IL-17E exhibited reduced pulmonary fibrosis in *S. mansoni* egg-induced pulmonary granuloma model [299]. Additionally, increased levels of IL-17E and innate lymphoid cell 2 (ILC2) were observed in BAL fluid from IPF patients [299].

1.7.5 *IL-17A* G197A (rs2275913)

Over 1600 IL-17A SNPs have been reported up to date [300]. *IL-17A* G197A (rs2275913) results from a substitution of the Guanine by an Adenosine nucleotide base in the promoter region of the IL-17A gene. It has been shown that *IL-17A* G197A promotes increased binding of Nuclear factor of activated T-cells (NFAT) to the IL-17A promoter region in humans, which results in increased production of the cytokine [301]. Currently, there are studies which associate G197A with increased risk of various cancers, elevated susceptibility to chronic periodontitis and to the development of liver cirrhosis from patients with Hepatitis B infection [248, 302, 303].

Our preliminary results demonstrated the ability of IL-17A to elevate Poly(I:C)-induced production of IL-8 and IL-6 in primary lung fibroblasts from IPF patients. Moreover, IL-17 reduced basal, and Poly(I:C)-driven production of RANTES in these cells. In addition, we have previously conducted a pilot case-control study in which we determined that the *IL-17A* 197A-homozygous genotype was significantly associated with development of IPF. The Odds Ratio of 3.167 obtained in this pilot study suggested that *IL-17A* 197A-homozygous individuals were

three times more likely to develop IPF. Table 1.2 Lists pathologies associated with the *IL-17A* G197A polymorphism.

1.7.6 The effects of IL-17A on TLR3 function

A small number of studies have investigated the effects of IL-17A on the regulation of TLR3 activity. IL-17A was shown to elevate TLR3 expression via STAT3 signalling in rheumatoid arthritis fibroblast-like synoviocytes [304]. Liu *et al.* demonstrated the ability of IL-17A to synergistically enhance Poly(I:C)-mediated IL-36γ production by human epidermal keratinocytes [305]. Our preliminary data has demonstrated that IL-17A potentiated Poly(I:C)-induced production of IL-8 and IL-6 protein from IPF primary human lung fibroblasts. We showed that IL-17A reduced Poly(I:C)-mediated increase in RANTES production, an anti-viral chemokine, in these cells. Moreover, we demonstrated that treatment of lung fibroblasts from IPF patients with IL-17A enhanced Poly(I:C)-induced IL-8 mRNA levels and decreased Poly(I:C)-induced RANTES, α-SMA and collagen transcription. In this study, we will further investigate the modulatory effects of IL-17A on TLR3 activity in IPF.

Table 1.2 *IL-17A* G197A (rs2275913) – associated pathologies

Disease	Specific role of *IL-17A* G197A	Title of Publication
Pulmonary Inflammation	Pathogenic	The relationship of polymorphisms in IL-17A Gene, IL-17F gene and the pulmonary inflammation risk in dust exposed workers in a Chinese population [306].
Asthma	Pathogenic	Association of interleukin-17a rs2275913 gene polymorphism and asthma risk: a meta-analysis [307]
Gastric Cancer	Pathogenic	Association between *IL-17A* G197A polymorphism and gastric cancer risk: an updated meta-analysis based on 6,624 cases and 7,631 controls [246].
	Pathogenic	*IL-17A* G197A and C1249T polymorphisms in gastric carcinogenesis [247].
	Pathogenic	Role of *IL-17A* rs2275913 and *IL-17F* rs763780 polymorphisms in risk of cancer development: an updated meta-analysis [248].
	Pathogenic	Polymorphism in the interleukin-17A promoter contributes to gastric cancer [249].
Colorectal Carcinoma	Pathogenic	Association between polymorphisms of *IL-17A* G197A and IL-17F A7488G and risk of colorectal cancer [250].
	Pathogenic in males	IL-17 and colorectal cancer risk in the Middle East: gene polymorphisms and expression [308].
	Pathogenic	Significant association between IL-17A polymorphism and colorectal cancer [309].
Hepatocellular Carcinoma	Pathogenic	IL-17A gene polymorphism, serum IL-17 and total IgE in Egyptian population with chronic HCV and hepatocellular carcinoma [310].
Osteoarthritis	Pathogenic	Association of IL-17A and IL-17F single nucleotide polymorphisms with susceptibility to osteoarthritis in a Korean population [311].
Coronary Artery Disease	Pathogenic	Association study between rs2275913 genetic polymorphism and serum levels of IL-17A with risk of coronary artery disease [312].
Oral Lichen Planus	Pathogenic	IL-17A polymorphism and elevated IL-17A serum levels are associated with oral lichen planus [313].
Periodontal Disease	Pathogenic	Association between polymorphisms in IL-17A and -17F genes and chronic periodontal disease [314].
	Pathogenic	The Influence of IL-17A and IL17F polymorphisms on chronic periodontitis disease in Brazilian patients [302].
HBV in Kidney Transplant	Pathogenic	Association of IL-17, IL-21, and IL-23R gene polymorphisms with HBV infection in kidney transplant patients [315].
Multibacillary Leprosy	Pathogenic	IL-8 and IL-17A polymorphisms associated with multibacillary leprosy and reaction type 1 in a mixed population from southern Brazil [316].
Chagas Disease	Pathogenic	Genetic polymorphisms of IL-17 and chagas disease in the south and southeast of Brazil [317].
Ulcerative Colitis	Pathogenic	The influence of polymorphisms of IL-17A and IL-17F genes on the susceptibility to ulcerative colitis [318].
Inflammatory Bowel Disease	Not significant	Genetic polymorphisms of IL-17A and interleukin 17F and their association with inflammatory bowel disease in a Chinese Han population [319].

1.8

Liver Cirrhosis	Pathogenic	*IL-17A* G197A gene polymorphism contributes to susceptibility for liver cirrhosis development from patients with chronic hepatitis B infection in Chinese population [320].
Liver Transplant	Pathogenic	The *IL-17A* G197A polymorphism is associated with cyclosporine metabolism and transplant rejection in liver transplant recipients [321].

The role of sex hormones in immune response

1.8.1 Sex differences in immune responses

Both auto-immune responses, and immune responses to foreign pathogens are linked to l sex of an individual. In literature, sex is described as the differential organisation of chromosomes, reproductive organs, and sex hormone levels [322].

There are significant differences in immunological responses observed between the sexes. For example, females are estimated to develop 80% of autoimmune diseases [322]. Women suffering from severe HIV infection present with 40% less viral load in blood than men [322]. Males are at an almost twofold increased risk of mortality from malignant cancer than females, in addition antibody responses to seasonal influenza are approximately twice as potent in women than they are in men [322]. In summation, women are believed to mount a more profound innate and adaptive immune responses than men, which leads to more rapid and effective pathogen clearance and greater vaccine efficacy, but also results in increased susceptibility to inflammatory and autoimmune disorders [322].

The differences in immune responses between sexes are believed to be germline encoded, for example, there are marked differences between recognition of nucleic acids by PRRs amongst male and females. In certain cases, TLR7 encoded on the X chromosome may escape X silencing which leads to increased TLR7 expression in females than in males [323]. Studies on human PBMCs demonstrated that exposure of these cells to TLR7 ligands *in vitro* resulted in higher interferon-α (IFN-α) production in women than in men [324]. Moreover, both murine and human plasmacytoid dendritic cells (pDCs) present with increased constitutive levels of IFN regulatory factor 5 (IRF5) along with increased IFN-α production following TLR7 activation [325].

Studies involving transcriptional analyses reported sex-related differences in expression of genes involved in TLR pathways and induction of type I IFN responses [326, 327]. In comparison to males, PBMCs from human adult females following anti-viral vaccination, and female adult rats challenged with various viruses presented with increased expression of

TLR-induced pro-inflammatory genes, including RIG-I, MYD88, IRF7, IFN-β, JAK2, NF-κB, IFNG, TFN and STAT3 [326, 327].

In addition, studies by other authors have shown differences in cytokine and chemokine production between the sexes. For example, activation of TLR9 in human PBMCs stimulated with viral or synthetic ligands resulted in higher IL-10 production in males than in females [328]. Moreover, human PBMCs exposed to LPS produced increased levels of TNF in males than in females [329, 330]. Due to a higher TLR4 expression on the surface of immune cells present in males than in females, LPS stimulation leads to an enhanced pro-inflammatory cytokines production in males, which can be reversed via removal of male androgens in mice [331].

1.8.2 The effects of sex hormones on TLR3 activity

A study by Leismeister *et al.* demonstrated that 17beta-estradiol supressed Poly(I:C)-induced cytokine and chemokine protein production in human endometrial epithelial cells, expressing estrogen receptor alpha Erα [332]. Svenson *et al.* reported that TLR3 activation resulted in upregulation of Erα expression on human mesangial cells, as well as Erα nuclear phosphorylation and nuclear localization [333]. The group also reported that female MCs expressed a larger number of TLR3 that male MCs, which led to an increased IL-6 protein production in the female MCs. These data indicated the presence of interaction between Poly(I:C)-driven immune responses and Erα in MCs [333].

A study by Zandieh *et al.* demonstrated that 17-B estradiol and progesterone decreased the production of IL-6 protein in the presence of TLR3 activation in the OE-E6/E7 human fallopian tube cell line [334]. The data presented in this study indicated that both estrogen and progesterone supressed TLR3 function in the human fallopian tube cells and suggested that the estrogen receptor beta (Erβ) and nuclear progesterone receptor B are the most probable mediators of hormonal regulation of TLR3 activity in human fallopian tube, as both of these receptors are main estrogen and progesterone receptors in OE-E6/E7 cell line [334]. A study by Gambara *et al.* demonstrated Poly(I:C)-driven IRF3 activation mediated apoptosis in human androgen-sensitive prostate cancer (PCa) LNCaP. In contrast, Poly(I:C)-driven IRF3 responses had a minimal effect on cell death in normal prostate epithelial cells (RWPE-1), thus demonstrating the impact of TLR3 activation on androgen-sensitive prostate cells in terms of cellular apoptosis [335].

1.8.3 Sex differences in lung pathologies

A number of studies have demonstrated that sex hormones play pivotal roles in the development, physiology and pathology of the lung [336]. The literature indicates that women are more frequently affected by various lung diseases, or demonstrate more profound severity, accelerated disease progression and higher incidence of mortality than men [337]. Differences between sexes exist in a variety of lung diseases, including IPF, chronic obstructive pulmonary disease (COPD) [338], lung cancer [339], lymphangioleiomyomatosis, and collagen vascular disease–associated interstitial lung diseases [340] as well as idiopathic pulmonary arterial hypertension [341]. The divergence in the development and progression of a variety of lung diseases observed in males and females, may be due to constitutive differences in the lung biology which manifests as early as from the sixteenth weeks of gestation period [342]. Changes in the levels of sex hormones between the two sexes continue to vary throughout the puberty and are affected by other physiological events including pregnancy and menopause [342]. Study by Silvera *et al.* have demonstrated that in contrast to androgens, female sex hormones exerted beneficial effects on the lung development and maturation in the early stages of life. However, following puberty, female hormones exacerbated various lung diseases, including severe asthma [343]. Recently there has been a publication regarding the role and impact of estrogen signalling and MicroRNAs in lung fibrosis [344, 345]. The data presented in this publication demonstrated that estrogen signalling functioned as an important factor in the development and progression of chronic lung diseases [344, 345]. Elliot *et al.* reported increased protein and mRNA expression of Erα in both lung tissue and lung fibroblasts in IPF patients compared with healthy controls [346]. The group also reported that lung fibroblasts from IPF patients were more responsive to estrogen compared with lung fibroblasts harvested from healthy individuals [345]. The increased responsiveness was diminished following estrogen blockage [345]. Moreover, inhibition of Erα and Erβ *in vivo*, reduced bleomycin-induced pulmonary fibrosis in mice [345].

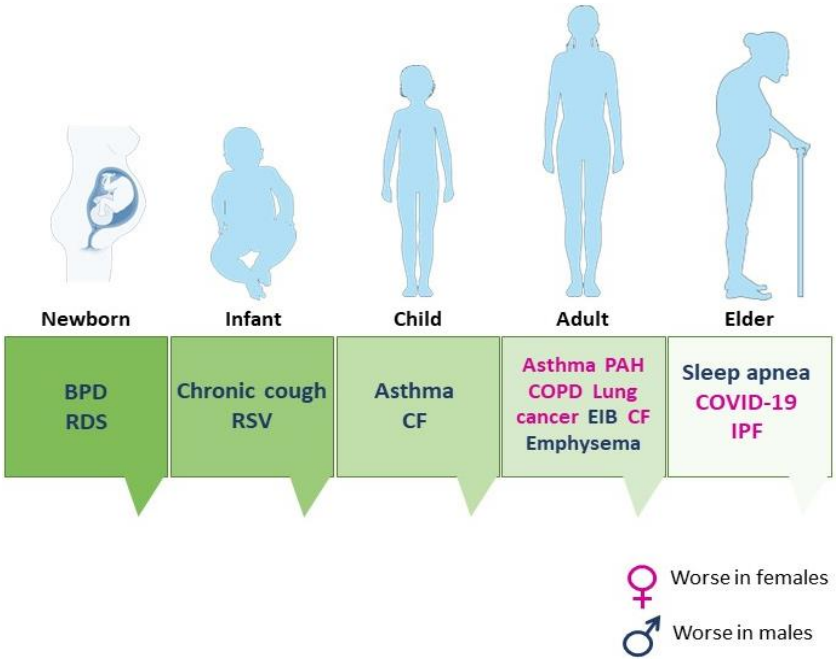

Figure 1.24 Sex and Gender Differences in Lung Disease.

Severity of different lung diseases varies among males and females at different stages of life. For example, clinical manifestation of CF and asthma are more pronounced in males than in females in childhood. This contrasts with what is observed in female patients, who experience more severe symptoms of CF and asthma in adulthood. *Image adapted from [342].*

Figure 1.24 demonstrates correlation between the severity of pulmonary diseases and gender at different life stages. *Image adapted from [342].* In terms of *in vivo* studies, Mehrnaz Gharaee-Kermani *et al.* investigated the impact of sex on pulmonary fibrosis using the bleomycin model of pulmonary fibrosis [347]. In their study, both male and female rats were administered endotracheal injections of bleomycin. The authors reported higher incidence of death rates as well as more profound levels of fibrosis among female rats compared with male rats, as demonstrated by increased lung collagen deposition and fibrogenic cytokine expression [347]. To confirm the role of female hormones in the progression of lung fibrosis, female rats were ovariectomized, then administered with either estradiol; an estrogen hormone, or endotracheal injections of bleomycin [347]. The authors reported reduced levels of fibrosis in the ovariectomized, bleomycin-treated rats without hormone replacement. In contrast, treatment with estradiol reversed the pulmonary fibrosis to the original baseline observed in the intact female rats [347]. Lung fibroblasts from rats exposed to bleomycin challenge presented with heightened responsiveness to estradiol treatment, data which is in agreement with reports by Eliot *et al.* [345]. This hyper-responsiveness to estradiol reported in the lung fibroblast of the bleomycin treated female rats resulted in increased transcription of procollagen 1 and transforming growth factor-β_1 compared with

untreated controls. In conclusion, female rats presented with an exaggerated response to pulmonary injury in the bleomycin model of pulmonary fibrosis compare with male rats due to hormonal differences between the sexes [347].

1.8.4 Sex differences in IPF pathogenesis and disease progression

Contrary to what has been reported in animal models of pulmonary fibrosis, studies in humans by have shown that IPF is more predominant in males than in females [7], however, we have limited data regarding the differences in IPF manifestation as well as the disease comorbidities between the sexes [7]. The multidimensional index and scoring system for IPF patients which includes the gender-age-physiology (GAP) score demonstrated that males are at a higher risk of mortality compared to female IPF patients [348], nevertheless, the mechanisms and pathology responsible for these differences are still poorly understood [348]. As there are data clinical confirming the differences between sexes in the prognosis and mortality in IPF between sexes, a more in depth understanding of this topic may lead not only to improved and more accurate IPF diagnosis, treatment and clinical prognosis but may also provide an insight into the disease aetiology [349].

1.8.5 Clinical studies on sex differences in IPF

A Swedish study followed the disease progression in 348 IPF patients over the span of 3 years time, where 72% of the patients were male and 28% were female, with median of 72 years in each sex [349]. The study revealed that female IPF patients present with a higher FVC% and TLC% than males at the start of the admission, this however might be correlated to the proportionally higher ratio of ex-smokers amongst the male population [349]. The study reported that male IPF patients suffered from a significantly larger incidence of cardiovascular comorbidities than female subjects. However, both the six-minute walk test and the quality-of-life measure did not show significant differences between the two sexes [349].

In another study, Zaman *et al.* examined the differences in clinical outcomes between males and female IPF patients [350]. The study involved two tertiary care canters of IPF cohorts and included 1263 patients, 71% of which were female and 29% were male, with median follow up of 3 years' time. The authors characterised the sex differences in outcomes of time to lung transplantation or death [350]. The authors reported no difference in the baseline FVC% or DLCO% between men and women at admission. The study reported that male IPF patients were at a higher mortality risk or lung transplantation than female IPF

patients [350]. Statistical estimations predicted the of difference 13 months on average in median transplant-free survival between the sexes [350].

In 2021, a French study investigated sex differences in IPF [351]. The study consisted of 236 patients with IPF, where 75% of patients were male and 22% were female, with a 5-year follow up. Authors of the study reported that women presented with a more preserved lung function at baseline, and less advanced disease at diagnosis [351]. The study showed that men were at a significantly higher risk of exposure to occupational hazards and presented with a more profound history of smoking than women patients did [351]. Regarding histopathology of the disease, CT scans revealed a more frequent occurrence of honeycombing and emphysema in male patients compared with female IPF patients [351]. These findings were consistent with previous data regarding increased demand for surgical lung biopsies in men than in women at diagnosis [351]. Contrary to what has been reported in the study conducted in Sweden (347), females were burdened with higher levels of comorbidities, due to this fact, as well as the older age of women with IPF partaking in this study, men were more likely to undergo a lung transplantation [351]. In contrast to studies by other authors [349, 350, 352], outcomes of this study did not report a significant difference in survival between women and men [351].

These data demonstrated that although most studies reported that males are at a higher risk of IPF-associated comorbidities, as well as worsened clinical prognosis and higher rates of lung transplantation, more research into the topic is needed to accurately evaluate the role of biological sex in the development and progression of the disease. One of the proposed explanations behind the worsened disease manifestation of IPF in men than in women is that men present with higher number of G>T substitution SNPs in the promoter region pf MUC5B compared with women. Regarded as the strongest and the most replicated genetic risk factor for IPF, MUC5B is the most important biomarkers for IPF development, MUC5B is a gene responsible for production of mucous in humans [28, 353]. The forementioned G<T substitution leads to increased mucus production in terminal bronchi and honeycombing cysts leading to respiratory difficulties [354].

1.8.6 Sex differences in anti-viral responses: COVID-19 infection

Most common respiratory manifestations of COVID are a reduction in the diffusing capacity of the lungs (DLCO) and the associated pulmonary interstitial damage, both pathologies are readily observed in lungs of IPF patients. Differences in the manifestation of covid-19 between males and females have been increasingly more recognised over the past 2 years. Although infection rates seem to be comparable between males and females, similarly to IPF, male COVID-19 patients present with more severe clinical symptoms of the disease and higher mortality rates [355]. Although the exact mechanism behind the reported differences in unknown, recent data demonstrated that plasma levels of pro-inflammatory cytokines IL-6, IL-8 and MCP-1 were significantly more upregulated in male covid-19 patients compared with female patients [355]. In addition, plasma samples from female covid-19 patients presented with increased expression of anti-inflammatory IL-10, 2 weeks following the infection compared with male patients [355]. Finally, male patents presented with a higher number of circulating neutrophils ad monocytes than female patients at days 7 ad 14 post infection, whereas females presented with a significantly higher number of B cells than males, indicating that males produced a more robust inflammatory response to the virus, while females developed a stronger immune response to covid-19 infection [355].

A biological explanations for the discrepancy between the severity of COVID-19 infection observed in males and females is overexpression of the angiotensin converting enzyme type 2 (*ACE2*), gene located on the x chromosome, which plays an important role in SARS-CoV-2 cellular entry [356]. The *ACE2* gene encodes a type I carboxypeptidase glycoprotein expressed on the surface of lung epithelial cells [356]. Studies have demonstrated the protective role of The ACE2 gene against edema, permeability, and lung damage, as well as hypertension and cardiovascular disease; common comorbidities in male covid-19 patients [356, 357]. Double dose of ACE2 expression in women, along with the fact that pulmonary expression of ACE2 decreases with age, a phenomenon predominantly observed in males, may account for the differences in mortality rates and severity in disease manifestation between the sexes [357, 358]. In addition, estrogen has been reported to upregulate the expression of ACE2 in human atrial tissue [359]. Other authors demonstrated that estrogen plays a protective function in SARS infection, through activation of the immune response and via direct suppression of SARS-CoV replication in mice [360]. Interestingly, a study utilizing computational analysis tools reported that lung fibroblasts from IPF patients expressed increased levels of ACE2 compared with healthy controls [361]. Data from pre-

clinical models demonstrated that chronic exposure to cigarette smoke, a widely recognized IPF developmental risk factor, was significantly associated with increased pulmonary ACE2 protein expression [361]. The transmembrane serine protease 2 (TMPRSS2) gene is a second androgen-associated gene which could explain the differences in disease progression in male and female covid-19 patients [362]. scRNA-seq analysis demonstrated a significantly increased expression of the TMPRSS2 gene in males compared with females [362]. TMPRSS2 is located on the 21st chromosome of the human genome and encodes for the transmembrane serine protease 2 capable, involved in facilitation of cellular entry of SARS-CoV-2 [363]. Studies have shown that the entrance of the SARS-CoV-2 into the cells relies on the expression of both ACE2 receptor and the cellular protease TMPRSS2 [363]. Other authors demonstrated that Italian population presented with increased presence of a polymorphism in the TMPRSS2 gene (rs35074065) responsible for over-expression of the TMPRSS2 gene, which may account for increased susceptibility to Covid-19 infection in Italians [364]. An immunochemistry analysis demonstrated a significant increase in the expression of both ACE2 and TMPRSS2 in lung fibroblasts from IPF patients compared with healthy controls [365]. Although the function of ACE2 and TMPRSS2 in both covid-19 and IPF are still poorly understood, the changes in the expression of the two genes may indicate shared mechanism behind the pathogenicity in both diseases.

1.9 Thesis hypothesis, overall aim and research objectives

Hypothesis:

We previously demonstrated that defective TLR3 function, and the *TLR3* L412F single nucleotide polymorphism (SNP), accelerate disease progression in IPF [161, 366]. Therefore, our central hypothesis is that immunomodulators, such as itaconate or IL-17A, which alter TLR3 function in IPF patients during viral or bacterial infection may accelerate IPF disease progression. In addition, genetic variants of such immunomodulators, including the *IL-17A* G197A (rs2275913) promoter polymorphism, may also drive disease progression in IPF.

Overall Aim:

To investigate the role of immunomodulators of TLR3 function, and associated genetic variants, in the pathogenesis and disease progression of IPF.

Research Objectives:

1) To evaluate the effect of the anti-viral and anti-bacterial metabolite, itaconate, on TLR3 function in primary human lung fibroblasts from IPF patients in the context of IPF pathogenesis and disease progression.

2) To characterise the effect of the anti-viral cytokine, IL-17A, on TLR3 function in primary IPF lung fibroblasts in the context of IPF pathogenesis and disease progression. To investigate the role of the promoter polymorphism *IL17A* G197A (rs2275913) in IPF development and death in a cohort of UK IPF patients.

3) To characterise the *in vivo* effect of the *TLR3* L412F (rs3775291) SNP on lung microbiome composition and bacterial load in IPF patients. To evaluate the functionality of TLR3 *in vivo* using a novel *TLR3* L413F knock-in mouse (generated by CRISPR/Cas9 gene editing) following Poly(I:C) injection.

Chapter 2 – Materials and Methods

Materials 2.1

Item	Retailer	Cat. Number
0.05% Trypsin-EDTA	Gibco®, Life Technologies	(25300-054)
10 ml pipettes	Greiner bio-one	(607180)
10 mM dNTP Mix	Invitrogen™	(18427-013)
15 ml falcon tubes	Greiner bio-one	(188261)
24 well cell culture plates	Greiner bio-one	(662168)
25 ml pipettes	Greiner bio-one	(760 180)
2-mercaptoethanol	Bio-rad	(161-0710)
2-Propanol	Sigma Aldrich, Ireland	(I9516-500ML)
2x MyTaq™ Red Mix 50 reactions	Bioline	(BIO-25043)
3.5 ml Transfer pipettes	SARSTEDT	(86.1172.001)
48 well cell culture plates	Greiner bio-one	(677-180)
4-Octyl itaconate	R&D systems, Ireland	(6662/10)
4X laemmli sample buffer	Bio- rad	(161-0737)
50 ml sterile falcon tubes	Greiner bio-one	(210270)
96 well cell culture plates	Greiner bio-one	(655-180)
Biosphere® Safe seal tube 1.5 ml	SARSTEDT	(72.706.200)
Chloroform, HPLC grade	Fischer Chemical	(C14966117)
Cryotube 1.8 ml,	ThermoScientific	(377627)
Dimethyl sulfoxide (DMSO) HybriMax®	Sigma-Aldrich, Ireland	(D2650)
Dulbecco's modified eagle medium (DMEM)	Gibco®, Life Technologies	(4196-039)
Eagle's minimal essential medium (MEM)	Gibco®, Life Technologies	(12492021)
Ethyl Alcohol	Sigma Aldrich, Ireland	(E7023-500ML)
Foetal Bovine Serum (FBS)	Gibco®, Life Technologies	(10770-106)
Heat-killed Streptococcus pneumoniae	Invivogen	(tlrl-hksp)
HphI	ThermoScientific	(ER1102)
Human IL-6 DuoSet ELISA	R&D systems, Ireland	(DY206)
Human IL-8 DuoSet ELISA	R&D systems, Ireland	(DY208)
Human RANTES DuoSet ELISA	R&D systems, Ireland	(DY278)
Hydrochloric acid S.G. 1.18 (~37%)	Fisher Chemical	(H/1150/PB17)
L-Glutamine (200 mM)	Gibco®, Life Technologies	(25030081)
Lipopolysaccharide	Invivogen, France	(tlrl—3pelps)

Microcentrifuge tubes 2.0 ml with cap	Fisherbrand®	(FB74111)
Millex-HV Syringe Filter Unit, 0.45 µm, PVDF, 33 mm, gamma sterilized	Merck Millipore Ltd.	(SLHV0033RS)
Mouse KC DuoSet ELISA	R&D systems, Ireland	(DY453)
Mouse RANTES DuoSet ELISA	R&D systems, Ireland	(DY478)
NRF2 (D1Z9C) XP® rabbit mAb	Cell Signalling Technology	(12721)
Nuclease Free water	Qiagen	(1039598)
NucleoSpin® Blood (250 preps)	Machery-Nagel	(740951.250)
Oligo (dt) 20	Invitrogen™	(18418012)
Penicillin/ Streptomycin	Gibco®, Life Technologies	(15140-122)
Petri dishes	SARSTEDT	(82.1472.001)
Platinum SYBR® Green qPCR SuperMix-UDG	Invitrogen™	(11733-038)
Polyinosinic Polycytidylic acid (PolyI:C)	Invivogen, France	(tlrl-pic)
Precision Plus Protein™ Dual Color Standards, 500 µl	Bio-rad	(161-0374)
Proteinase K	Machery-Nagel	(740506)
RIG-I (D33H10) Rabbit mAb	Cell Signalling Technology®	(4200)
RIG-I Rabbit mAb	Cell Signalling Technology	(D33H10)
RNase Out™	Invitrogen™	(10777-019)
SIGMAFAST™ OPD	Thermo Scientific	(P9187)
Sodium Chloride	Sigma Life Science	(53014-5kg)
Sodium dodecyl sulphate	Fisher Chemical	(S/5200/53)
Sterile phosphate buffered saline (PBS)	Gibco®, Life Technologies	(14190-0940)
Superscript II ™	Invitrogen™	(18064.014)
T175 tissue culture flasks	Greiner bio-one	(660175)
TaqMan ® 2X Universal PCR MasterMix,	Applied Biosystems	(4304437)
Toll-like Receptor 3 (D10F10) Rabbit mAb	Cell Signalling Technology®	(6961)
Tri-reagent®	Sigma-Aldrich, Ireland	(T9424)
Trizma® Base	Sigma Life Science	(93362-1kg)

2.2 Methods

2.2.1 Cell culture

2.2.1.1 Primary cell culture and maintenance

Primary human pulmonary fibroblast cell lines were kindly donated by Professor Cory Hogaboam, Department of Medicine, Cedars Sinai, Los Angeles, USA and Professor Seamas Donnelly, St Vincent's University Hospital, Dublin, Ireland. CCD Lu-19 pulmonary fibroblasts were purchased from the European Collection of Cell Cultures (ECACC), Wiltshire, United Kingdom. Human primary pulmonary fibroblasts were cultured in Dulbecco's Modified Eagles Medium (DMEM), supplemented with 10% foetal bovine serum (FBS) and 100 U/ml penicillin and streptomycin (pen/strep). CCD Lu-19 were cultured in Minimum Essential Medium (MEM) supplemented with 2mM L-Glutamine, 100U/ml penicillin, 100µg/ml streptomycin and 10% foetal bovine serum. Cells were maintained in a humidified environment (95% relative humidity), containing 5% CO2 at 37°C. All work with primary cell lines was undertaken in a sterile laminar flow in a purpose-built room.

2.2.1.2 Harvesting and subculture of primary cell lines

Primary human pulmonary fibroblasts were sub-cultured at 80%-90% confluency. The spent medium was decanted, and the cells were rinsed with 10 ml of pre-warmed (37°C), sterile Phosphate Buffered Saline (0.01M PBS, pH 7.4). PBS was decanted, and 5 ml of pre-warmed, sterile 0.05% Trypsin (0.53 mM EDTA) was added for 3 minutes to detach the cells from the surface of the T175 flask. 35 ml of the complete cell culture medium was added to inactivate the process of trypsinisation. The disaggregated cells were then harvested by centrifugation at 4°C, 1000 rpm for 5 minutes. For sub-culture purposes, the cell pellet was re-suspended in fresh medium and split 1:2 or 1:3 into fresh T175 tissue culture flasks. The cells were then returned to sterile incubators.

2.2.1.3 Cryo-preservation of primary cells

Primary human lung fibroblasts were cultured in T175 flasks until confluent. Cells were harvested as described in section 2.2.1.2. The cell pellet was re-suspended in pre-warmed, sterile medium and mixed gently to obtain a single-cell suspension. The cells were counted using a haemocytometer. Subsequently, the cells were frozen down in 1.5 ml cryovials at a density of 1.2x106 in 95% FBS and 5% DMSO solution. The vials were frozen at -80°C for 24 hours and then transferred to liquid nitrogen for long term storage.

2.2.1.4 Resuscitation of cryo-preserved primary pulmonary fibroblast cell lines

Pre-warmed cell medium was added to the cryovials in drop-wise fashion, using a sterile transfer pipette. When de-frosted enough, the cells were transferred into a sterile falcon tube containing 40 ml of pre-warmed medium. The solution was then transferred to a T175 tissue culture flask using a sterile, glass pipette. The flasks were incubated at 37°C in a 5% CO2 atmosphere and cultured to approximately 90% confluence, then harvested and sub-cultured as described in section 2.2.1.2

2.2.2 Treatment of primary human pulmonary fibroblasts

2.2.2.1 Preparation of experimental cell culture plates

Cells were sub-cultured in a T175 tissue culture flask. After the cell monolayer achieved 80-90% confluence, the cells were seeded at 50,000 cells/well in a 24 or 48 well culture plate and incubated at 37°C in a 5% CO2 atmosphere for 24 hours. Treatment was then initiated.

2.2.2.2 Poly(I:C) treatment

1 mg/ml stock of Poly(I:C) was made up to a concentration of 10 µg/ml -100 µg/ml in pre-warmed cell medium. Following 24 hours from seeding of the cells into cell culture plates, the spent medium was decanted, and the cells were treated with 1 ml of the treatment solution per well (24 well plate) or 500 µl of the treatment solution per well (48 well plate). Cell plates were returned to a sterile incubator and left for 24 hrs before harvesting. All steps were performed in a sterile laminar flow hood to prevent contamination.

2.2.2.3 4-Octy itaconate (4-OI) treatment

X 4-Octy itaconate (4-OI) stock was made up to a concentration of 250 µM in pre-warmed cell medium. Following 24 hours from seeding of the cells into cell culture plates, the spent medium was decanted, the cells were treated with 1 ml of the treatment solution per well (24 well plate) or 500 µl of the treatment solution per well (48 well plate). Cell plates were returned to a sterile incubator and left for 24 hrs before harvesting. All steps were performed in a sterile laminar flow hood to prevent contamination.

2.2.2.4 Lipopolysaccharide (LPS) treatment

5 x 10^6 EU of ultra-pure LPS from *E. coli* stock was made up to a concentration of 100 ng/ml in pre-warmed cell medium. Following 24 hours from seeding of the cells into cell culture plates, the spent medium was decanted, and the cells were treated with 1 ml of the treatment solution per well (24 well plate) or 500 µl of the treatment solution per well (48 well plate). Cell plates were returned to a sterile incubator and left for 24 hrs before harvesting. All steps were performed in a sterile laminar flow hood to prevent contamination.

2.2.2.5 Transforming growth factor beta (TGF-β) treatment

20 µg/mL of stock TGF-β was made up to a concentration of 10 µg/mL in pre-warmed cell medium. Following 24 hours from seeding of the cells into cell culture plates, the spent medium was decanted, and the cells were treated with 1 ml of the treatment solution per well (24 well plate) or 500 µl of the treatment solution per well (48 well plate). Cell plates were returned to a sterile incubator and left for 24 hrs before harvesting. All steps were performed in a sterile laminar flow hood to prevent contamination.

2.2.3 TLR3 function in primary pulmonary fibroblasts cell lines using live *Pseudomonas aeruginosa* infection (*P. aeruginosa)*

2.2.3.1 Culture of *P. aeruginosa*

Pseudomonas aeruginosa (*P. aeruginosa*; Lab strain: PA01) was purchased from the American Tissue Culture Collection (ATCC; Manassas, VA, USA). PAO1 was grown in LB broth at 37^{o}C with shaking for 16 hours. To generate a standard curve of OD 600 vs CFU/ml, serial dilutions of overnight cultures of PA01 were prepared, the OD 600 measured and samples subsequently plated on LB agar plates. A standard curve was generated that yielded the following formula which was then used to calculate respective MOI of experiments: Equation 1: CFU/ml = (2 x 10^9) (x)-(5 x 10^7).

2.2.3.2 Live *P. aeruginosa* infection of primary human lung fibroblasts

Fibroblasts were seeded at a density of 50,000 cells per well in a 24 well plate. Bacterial density was measured by reading the OD 600 and CFU/ml calculated using a standard curve (Equation 1). Fibroblasts were infected with live PA01 at a MOI of 30 (30 PA01: 1 fibroblast) for 1 hour at 37^{o}C in a humidified environment with 5% CO^2. Following this, all medium was removed, and fresh medium was added containing 300 µg/ml gentamicin for a further 1 hour in a humidified environment with 5% CO^2. Following this, all medium was removed and replaced with fresh antibiotic free medium for a further 6 hours at 37^{o}C in a humidified environment with 5% CO^2. IL-6, IL-8 and RANTES protein levels in cell supernatants were assessed using ELISA. *Culture and infection experiments with *Pseudomonas aeruginosa* were performed by Dr. Andrew O'Neill.

2.2.4 Quantification of cytokine production by enzyme-linked immunosorbent assays (ELISA)

Supernatants from primary human lung fibroblasts were used to quantify the levels of Interleukin 8 (IL-8; human CXCL8; Ref. DY208), RANTES (Regulated and normal T cell expressed and secreted; human CCL5; Ref. DY278), Interleukin 6 (IL-6; Ref. DY206) and human Pro-Collagen I alpha 1 (Ref. DY6220-05). 96 well plates were coated with 50 µl of capture antibody (4.0 g/ml) diluted in dPBS, wrapped in tinfoil, and left to incubate overnight at 4^{o}C. On the following day, the plates were washed 3 times in a solution of 0.05% Tween 20 and PBS, the excess washing solution was blotted onto a tissue paper. 200 µl of blocking buffer (1% BSA in PBS) was then used to block the plates for 2 hours at RT. This step was done to minimise non-specific antibody binding. Plates were washed and dried again as previously described. 25 µl of sample supernatant was added to each well along with 25 µl of reagent diluent (0.1% BSA, 0.05% Tween 20 in TBS/ 1% BSA in PBS for IL-8 and IL-6/RANTES/Col Iα1 respectively). 50 µl of IL-8, IL-6, RANTES and Col Iα1 standards in 2-fold serial dilutions were added to the plate in duplicate. The plates were wrapped in tinfoil and incubated overnight at 4^{o}C. Following the incubation period, plates were washed and dried as previously described. 50 µl of detection antibody (20.0 ng/ml) diluted in reagent diluent was added to each well and the plate was incubated for 2 hours at RT. Plates were washed and dried as previously described. 50 µl of Streptavidin-HRP diluted in reagent diluent was added to each well, the plates were incubated for 20 minutes at RT. During this step, the plates were covered under tinfoil to avoid the exposure of Streptavidin-HRP to the light, as this would provide inaccurate results. Plates were

washed and dried as previously described. 50 µl of substrate solution (One OPD gold tablet and one OPD silver tablet in 20 ml dH2O) was added to each well and the plate was incubated for 20 minutes at RT covered to protect it from the light. 25 µl of 2N H2SO4 was added to stop the reaction. The plates were read on a microplate reader at 450 nm to determine the optical density (OD). 4-parametric standard curve was generated using Software MaxPro, Molecular Devices Inc. 1999-2010 and the OD values for each sample were determined.

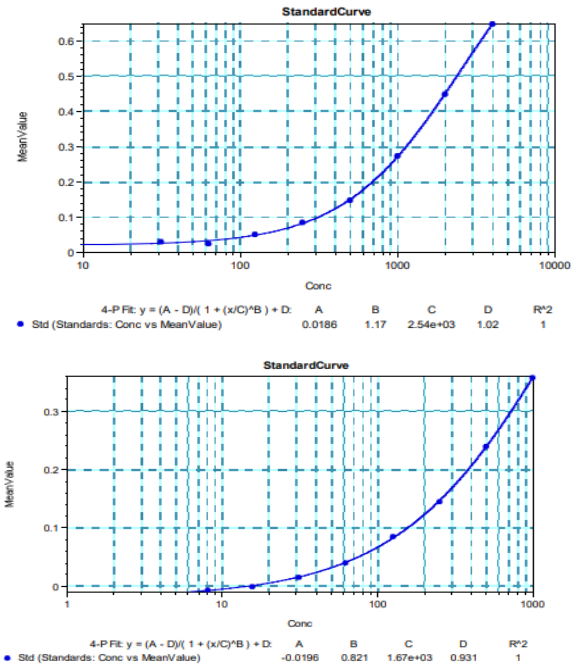

A

B

Figure 2.1 Representative standard curves for ELISA targets Software MaxPro, Molecular Devices Inc. 1999-2010.

2.2.5. Assessment of mRNA expression from cultured fibroblasts by Quantitative Real Time Polymerase Chain Reaction (qPCR) using SYBR® Green

2.2.5.1 Total RNA extraction

Fibroblasts were cultured in 24 well plates at the concentration of 50,000 cells/ml /well and treated with appropriate treatments as described in sections 2.2.1 and 2.2.2. Supernatants were harvested and stored at -20^{o}C to be analysed by ELISA. RNA was extracted using Tri Reagent© RNA isolation reagent. 1 ml of ice cold TriReagent was added to the cell monolayer in each well. To detach all cells away from the walls of the well and to obtain a homogeneous solution, the cell monolayer was disrupted using a pipette tip. The contents of each well were transferred to a sterile 1.5 ml Eppendorf tube and 200 µl of chloroform was

added to each sample. The samples were shaken vigorously for 15 seconds, vortexed then left at RT for 15 minutes. To allow phase separation to occur, the samples were then centrifuged at 13,000 rpm for 15 minutes at 4°C. Once separated into the three layers (RNA, DNA and protein), the top clear layer containing RNA was carefully pipetted out into a fresh, sterile 1.5 ml Eppendorf tube and 0.5 ml of ice-cold 2-propanol was added. The samples were mixed vigorously using a vortex and left at RT for 10 minutes. The samples were again centrifuged at 13,000 rpm for 15 minutes at 4°C. Samples were then placed on ice and the supernatant was carefully decanted, leaving the RNA pellet intact. 1ml of ice-cold 75% ethanol (Sigma Aldrich) was added to each RNA pellet. The RNA was stored in 75% ethanol at -80°C.

2.2.5.2 First-strand cDNA synthesis

First-strand cDNA synthesis was carried out using reagents from Invitrogen (see Section 2.1 Materials). RNA samples isolated according to the protocol described in section 2.2.6.1 were de-frosted on ice. The samples were centrifuged at 13,000 rpm for 15 minutes at 4°C, then washed with 1 ml of ice-cold 75% ethanol (Sigma Aldrich). The samples were centrifuged once again at 13,000 rpm for 15 min at 4°C. The ethanol was decanted until approximately 20 µL was left in each sample. The remaining ethanol was left to evaporate off in a laminar flow hood and once dry, the RNA pellet was re-suspended in 15 µl of nuclease free water. 8 µl of each RNA sample was aliquoted into the optical tubes (Agilent Technologies) along with 2 µL of master mix #1 (See Table 2.1). The samples were micro-centrifuged, then incubated in the thermocycler for 5 minutes at 65°C (lid heated to 95°C to prevent evaporation). Samples were placed on ice for 1 minute. 9 µl of Mastermix #2 (See Table 2.2) was added to each sample in a laminar flow hood. The samples were then micro-centrifuged and incubated in the thermocycler for 2 minutes at 25°C (lid heated to 95°C to prevent evaporation). Samples were placed on ice for 1 minute. 1 µl of Superscript II Reverse Transcriptase™ was added to each sample in a laminar flow hood. The contents were collected by brief micro-centrifugation. The samples were then incubated at 42°C for 50 minutes and then at 70°C for 15 minutes in a thermocycler. cDNA was then stored at -20°C.

Table 2.1: Mastermix #1 components for first strand cDNA synthesis

Mastermix #1	
Components	**Reaction volume 1X (µl)**
Oligo(dT) 20 (200 µg/ml)	1
dNTP (10 mM)	1

Table 2.2: Mastermix #2 components for first strand cDNA synthesis

Mastermix #2	
Components	**Reaction volume 1X (µl)**
5x First strand buffer	4
DTT 0.1M	2
RNase OUT™	1
Nuclease Free H2O	2

2.2.5.3 Assessment of mRNA expression by Quantitative Real Time Polymerase Chain Reaction (qPCR) using SYBR® Green

qPCR was performed using Platinum® SYBR® Green qPCR SuperMix-UDG (Invitrogen, USA). Primers for the specific target genes were either purchased from www.realtimeprimers.com in a fully validated and ready to use format or were sourced from published papers and subsequently synthesised by MWG Operon. All primers were used at a concentration of 10 µM. 2µl of cDNA sample was added to optical tubes (Agilent Technologies) with 18µl of qPCR Mastermix (See Table 2.3). Stratagene MX3000P machine was used for qPCR using the standard thermal cycling protocol (See Table 2.4). Annealing temperatures used in this protocol were primer specific (See Table 2.5). In this procedure, the copies of the target gene are bound to fluorescence intensity using the fluorescent reporter molecule SYBR Green™. A passive reference dye (ROX) was used to correct for sources of well-to-well variation during the PCR process. Reference dye normalization was achieved by division of the raw fluorescence signal of the reporter dye at any given cycle by the raw fluorescence signal of the reference dye at the same cycle and then by drawing the amplification plot based on the obtained ratio value. β-actin was used as the house-keeping gene for all experiments.

Table 2.3: Mastermix components for SYBR®-qPCR

Mastermix SYBR®-qPCR	
Components	**Reaction volume 1X (µl)**
SYBR® Green	10
Forward Primer (10 µM)	0.2
Reverse Primer (10 µM)	0.2
Nuclease Free water	7.6

Table 2.4: The SYBR®-qPCR thermal cycling protocol

Standard Thermal Cycling Protocol				
Step		**Temperature (°C)**	**Time**	**# cycles**
1		50	2 minutes	1
2	**Initial denaturation**	95	2 minutes	1
3	**Denature**	95	15 seconds	40
	Anneal	*Primer specific	30 seconds	
	Extend	72	30 seconds	
4		95	15 seconds	1
		50	30 seconds	
		95	30 seconds	

Table 2.5: Human Primers for Real Time-PCR

Gene	**5' Forward 3'**	**5' Reverse 3'**	**annealing temperature (°C)**
IL-8	TAG CAA AAT TGA GGC CAA GG	AGC AGA CTA GGG TTG CCA GA	57
RANTES	TCC TGC AGA GGA TCA AGA CA	CAA TGT AGG CAA AGC AGC AG	57
IFN-β	AGC ACT GGC TGG AAT GAG AC	TCC TTG GCC TTC AGG TAA TG	58
β-actin	GGA CTT CGA GCA AGA GAT GG	AGC ACT GTG TTG GCG TAC AG	59
RIG-I	GAG CAC CAG ACC TCC TCT TG	ACT CAC TTG GAG GAG CCA GA	59
Caspase-1	TAC AGA GCT GGA GGC ATT TG	GAT CAC CTT CGG TTT GTC CT	58
IL-1β	ATG CAC CTG TAC GAT CAC TG	ACA AAG GAC ATG GAG AAC ACC	58
HMOX-1	CTC TGG AAA GGA GGA AGG AG	TTG AGA CAG CTG CCA CAT TA	58
NQOI	AAA AGA AGC TGG AAG CCG CA	AGG ATT TGA ATT CGG GCG TC	56

GSR	CCC ACA ATA GAG GTC AGT GG	CAA TGT AAC CTG CAC CAA CA	58
IRG-1	CGT GTT ATT CAG AGG AGC AAG AG	AGC ATA TGT GGG CGG GAG	59
COL1α1	GGA CAC AGA GGT TTC AGT GG	CCA GTA GCA CCA TCA TTT CC	58
COL1α3	AGC TAC GGC AAT CCT GAA CT	GGG CCT TCT TTA CAT TTC CA	56
α-SMA	CGT TAC TAC TGC TGA GCG TAA	AAC GTT CAT TTC CGA TGG TG	57
TGF-β	CGT GGA GCT GTA CCA GAA ATA	TCC GGT GAC ATC AAA AGA TAA	56

Table 2.6 Murine primers for Real Time-PCR

Gene	**5' Forward 3'**	**5' Reverse 3'**	**annealing temperature (°C)**
IL-1β	AAC CTG CTG GTG TGT GAC GTT C	CAG CAC GAG GCT TTT TTG TTG T	60
IL-6	GAG GAT ACC ACT CCC AAC AGA CC	AAG TGC ATC ATC GTT GTT CAT ACA	61
Caspase-1	AGG AAT TCT GGA GCT TCA ATC AG	TGG AAA TGT GCC ATC TTC TTT	59
β-actin	AAG AGC TAT GAG CTG CCT GA	TAC GGA TGT CAA CGT CAC AC	58
TNF-α	GAT CTC AAA GAC AAC CAA CAT GTG	CTC CAG CTG GAA GAC TCC TCC CAG	63
RANTES	CAA TCT TGC AGT CGT GTT TG	GGA GTG GGA GTA GGG GAT TA	58
IFN-β	AGC TCC AAG AAA GGA CGA ACA T	GCC CTG TAG GTG AGG TTG ATC T	60
RIG-I	CCA CCT ACA TCC TCA GCT ACA TGA	TGG GCC CTT GTT GTT CTT CT	60
TLR3	CTG GGT CTG GGA ACA TTT CT	TTG CTG AAC TGC GTG ATG TA	58
IRF3	GGC TTG TGA TGG TCA AGG TT	CAT GTC CTC CAC CAA GTC CT	58
IRG-1	GCG AAC GCT GCC ACT CA	ATC CCA GGC TTG GAA GGT C	58
HMOX-1	TCA GGC AGA GGG TGA TAG AA	GCT CCT GCA ACT CCT CAA A	57
GLUT-1	TCA ACA CGG CCT TCA CTG	CAC GAT GCT CAG ATA GGA CAT C	59

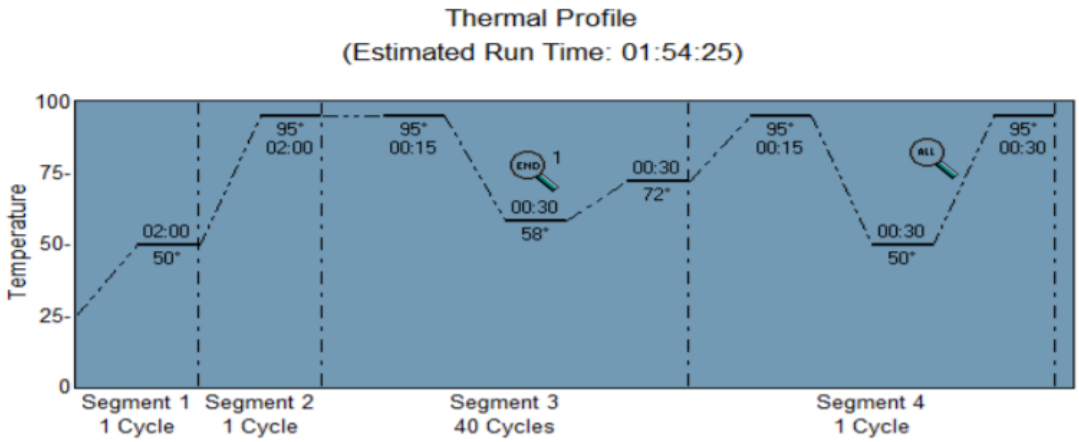

Figure 2.2 Representative illustration of thermal cycling protocol for QPCR.

2.2.6 Genomic DNA extraction from whole blood from IPF patients

Whole blood samples were stored at -80°C in EDTA blood tubes. Genomic DNA was extracted using the Nucleospin© Tissue kit (Macherey-Nagel) according to manufacturer's instructions. Once the samples were completely thawed, 400 µl of blood was decanted and 50 µl of Proteinase K was added to each sample. Next, 400 µl of Buffer B3 was added and the samples were vigorously mixed mechanically, after which they were incubated at RT for 5 minutes. The samples were then incubated at 70°C for 15 – 30 minutes. 420 µl of Ethanol (Sigma Aldrich) was the added to each sample and the solution was mechanically mixed for 10 seconds. 400 µl of each sample was added to a Nucleospin© tissue column and collection tube. The samples were centrifuged at 11,000 x g for 1 minute and the flow-through in the collection tube was discarded. 500 µl of Buffer BW was used to wash the silica membrane in the tissue column and centrifuged for 1 minute at 11,000 x g. The flow-through was discarded again. The membrane was washed with 600 µl of Buffer B5 and centrifuged for 1 minute at 11,000 x g. The silica membrane was then dried by centrifugation at 11,000 x g for 1 minute. 50 µl of previously pre-heated (70°C) elution buffer was added to the tissue column and allowed to stand for 3 minutes. The samples were then centrifuged at 11,000 x g for 1 minute. The step was repeated to obtain the final flow through containing a high concentration of genomic DNA. This concentration was quantified using a Nanodrop™ UV Spectrophotometer (Thermo Scientific). A solution of genomic DNA at 10 ng/µl was equilibrated for further downstream applications and stored at -20°C.

2.2.7 *IL-17A* G197A (rs2275913) single nucleotide polymorphism genotyping assay

The genomic DNA was extracted and quantified as described in section6. 10 ng/µl of genomic DNA sample was used to genotype IPD samples for the *IL-17A* rs2275913 SNP using a made-to-order Taqman Genotyping Assay (Applied Biosciences, Foster City, USA). 1.5 µl of genomic DNA was added to PCR tubes along with the other required reaction components (See Table 2.7). Genotyping runs were carried out using a Stratagene MX3000P RT-qPCR machine using a thermal programme shown in Table 2.8. In this protocol, ROX dye was used as the reference dye, HEX dye identified the variant allele (A) and FAM dye identified wild-type allele (G).

Table 2.7: Reaction components for qPCR

Component	Reaction Volume (µl)
TaqMan® Universal Master Mix (MM)	6.875
40X SNP genotyping assay	0.343
Nuclease-free H2O	5.032
gDNA	1.5
Total Volume	13.75

Table 2.8: Thermal cycling protocol for qPCR

Standard Thermal Cycling Protocol				
Steps		**Temperature (°C)**	**Time**	**# cycles**
1	Taq Activation	95	10 minutes	
2	Denature	92	15 seconds	40
3	Anneal/Extend	60	1 minute	

2.2.8 Assessment of protein expression by western blot analysis

2.2.8.1 Sample harvesting for western blot

Cells were cultured and seeded at 50,000 cells/well in a 24 well plate, as per protocol described in section 2.2.1. Following 24 hr of incubation with relevant treatments, the supernatants were transferred to a fresh 24 well plate and stored at -20 °C for future experimental procedures. The remaining cell monolayer was harvested using RIPA lysis buffer containing protease inhibitors (See Table 2.9). Cells were washed with 1ml of ice cold dPBS. 5 µl of RIPA lysis buffer containing protease inhibitors was added to each well and left to incubate for 30 minutes. To detach the cells from the surface of the well, the sides and the bottom of each well were scratched using a pipette tip and the contents were transferred to

1.5 ml Eppendorf tube, then centrifuged at 14,000 rpm for 30 minutes at 4°C. Samples were stored at -20°C. Samples were kept on ice all throughout the harvesting protocol.

Table 2.9: RIPA lysis buffer

RIPA lysis buffer solution		
Volume	Reagent	Desired concentration
0.88 g	NaCl	150 mM
1 ml	Triton x-100	1%
0.1g	SDS	0.1%
0.6 g	Tris	50 mM
Make up to 100 ml with distilled H2O		
Add 1X solution of Protease Inhibitors to RIPA buffer before use		
Store at 4°C		

2.2.8.2 Bicinchoninic acid Assay (BCA) assay

Samples were defrosted on ice and centrifuged at 14,000 rpm for 30 minutes at 4°C. The supernatants containing protein samples were transferred into fresh, labelled Eppendorf tubes. The pellet was discarded. 5 µl of previously prepared BSA standard solution and 5 µl of each sample was added to a 96 well plate in duplicate. 5 µl of RIPA lysis buffer was added to each sample well. The BCA reagent mix was prepared using BCA reagent A and BCA reagent B in a ratio 50:1. 200 µl of the BCA reagent mix was added to each well. The 96 well plate was incubated for 30 minutes at 37°C. The plate was read on a microplate reader at 562 nm. The resulting readings were multiplied by the factor of 2, to account for 50% dilution of the samples with RIPA lysis buffer. Using the generated standard curve, the protein concentration was calculated for each sample.

2.2.8.3 Sample preparation for western blot

Loading buffer was made up using 900 µl 4X Laemmli sample buffer and 100 µl β-mercaptoethanol. The protein samples were equilibrated to the desired concentration of 10 µg and 25 µg protein/ sample in the loading buffer. Diluted samples were boiled at 90°C for 5 minutes. The samples were spun down in a microcentrifuge and stored at -20°C.

2.2.8.4 Quantification of NRF2, RIG-I and TLR3 protein expression in primary human lung fibroblasts

The protein samples were run on a 4-12% gradient gel in the running buffer, along with a molecular weight ladder (Bio-Rad, Ref. 1610394) used as protein size reference. The gel was run at 100 V for 15 minutes and 150-200 V for 45-60 minutes. The wet transfer method was used to transfer the proteins to a PVDF membrane at 200 mA for 90 minutes at RT. The transfer tank was placed on ice in a Styrofoam box to prevent overheating. After 90 minutes the PVDF membrane was blocked in a solution of 5% non-fat dried (marvel) milk in TBS-0.1% Tween 20 for 1 hour. The membranes were incubated in the primary antibody at 4^{o}C overnight, followed by the secondary antibody for 1 hour at RT. Primary antibodies were diluted in a solution of 5% BSA in TBS-0.1% Tween 20. The secondary antibodies were diluted in a solution of 5% non-fat dried (marvel) milk in TBS- 0.1% Tween 20. The membranes were then washed in 1X TBS with 0.1% Tween 20 for 15 minutes 3 times. The bands were visualised using chemiluminescent HRP substrate (Millipore Immobilon™ Western).

Table 2.10: Buffers used in Western blotting protocol

Western blot buffers		
Running Buffer – 10X	**Transfer Buffer – 10X**	**Transfer Buffer – 1X**
60.4 g Trizma Base	60.4 g Trizma Base	100 ml Transfer Buffer 10X
288 g Glycine	288 g Glycine	100 ml Methanol
20 g SDS	Make up to 2 litres with distilled H2O	800 ml distilled H2O
Make up to 2 litres with distilled H2O		

Table 2.11: Antibody Dilutions

Antibody Dilutions	
Primary Antibody Dilutions	
RIG-I	1:2000
TLR3	1:1000
NRF2	1:1000
B-actin	1:5000
Secondary Antibody Dilutions	
Anti-Rabbit IgG – HRP linked antibody	1:5000

Table 2.11: Gel preparations

Gel composition		
Reagents	**4% gel**	**12% gel**
dH2O	3.05 ml	3.35 ml
Bis Acrylamide	0.65 ml	4 ml
*Tris-HCL	1.25 ml	2.5 ml
10 % SDS	50 µl	100 µl
10 % APS	25 µl	50 µl
TEMED	8 µl	10 µl
* 4% stacking gel requires 0.5M Tris-HCL and 1.5M Tris-HCL were used to prepare 4% stacking gel and 12% resolving gel respectively		

2.2.8.5 PVDF membrane stripping

The stripping solution up was made up as per Table 2.13. The PVDF membrane was submerged in 10 ml of the stripping solution and placed on a rocker for 7-8 minutes. The membrane was then washed in 1X TBS with 1% Tween 20 for 10 minutes 3 times. The membrane was blocked in 5% non-fat dried (marvel) milk in TBS-0.1% Tween 20 for 1 hour and incubated in the primary antibody at 4^{o}C overnight.

Table 2.13: Stripping Solution

Western blot stripping solution	
7.5 g Glycine	*Make up to 500 ml with dH2O
0.5 g SDS	*Adjust the pH to pH2
5 ml Tween 20	

2.2.9 *TLR3* L413F – CRISPR/Cas9 Knock-in mice

We commissioned the generation of the TLR3 L413F knock in mouse by CRISPR/Cas9 mediated gene editing. Mice were generated on a C57BL/6NTac background. The target gene was located on chromosome 8. The human Leu412Phe amino acid substitution corresponds to Leu413Phe in mice (TLR3 L413F knock-in mouse). Fig 2.2 below illustrates the position of the SNP in human and mouse TLR3 gene. Validation studies were carried out by Taconic Biosciences. The mice were genotyped as per protocol in Section 2.9.1.

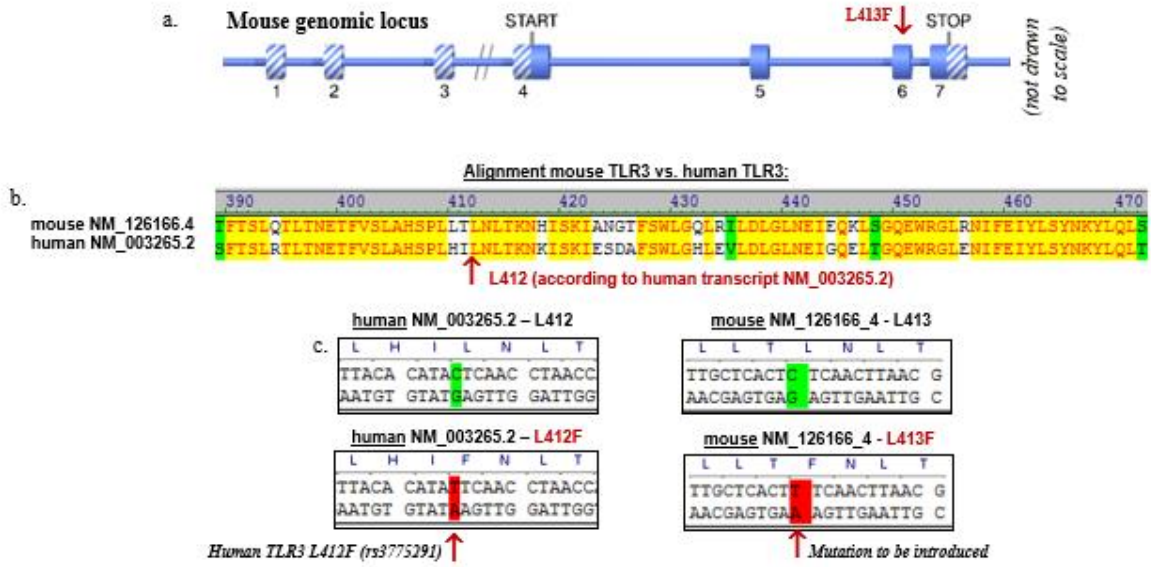

Fig. 2.3. Alignment of human and mouse TLR3 gene with introduction of the TLR3 L413F SNP in mice
The TLR3 L412F SNP (L413F in mice) was introduced into the murine TLR3 gene by CRISPR/Cas9 gene editing. It involved a single base pair change in C > T. The above diagram illustrates the position at which the mutation was introduced and alignment of both murine and human TLR3 genes. Image generated by Taconic Biosciences.

2.2.9.1 Day 1: Ear Punch Lysis:

Ear punches from *TLR3* L413F – CRISP/Cas9 Knock-in-mice were lysed overnight for 16-18 hours (max). Fresh Master Mix Proteinase K and DNA lysis buffer were prepared on the day of the experiment. 20 µl of Proteinase K is needed per 1ml of DNA lysis buffer. For each rection, 500 µl of Proteinase K/DNA lysis buffer as added to separate 1.5 l Eppendorf tube containing individual ear punch, ensuring that the ear punches were entirely submerged in the lysis buffer. The Eppendorf tubes containing ear punches in lysis buffer were left at 55^{o}C shaking overnight (350 – 400 rpm) on the Thermomixer.

2.2.9.2 Day 2: Wash, PCR & Digest:

Stage 1: Wash

On Day 2 (after 16-18 hours), sample tubes were taken off the shaker. 1 ml of molecular grade 100% ethanol was added to each tube. The contents of the tube were mixed gently by inverting the tube multiple times until the DNA had become visible. The tubes were centrifuged for 10 minutes at room temperature at 14, 000 rpm. The supernatant was carefully discarded from each tube with a pipette not to disturb the pellet. 500 µl of 70% molecular grade ethanol (made up in in DEPC H_2O) was wadded to each tub containing the pellet and inverted gently a number of times. Each tube was centrifuged for 5 minutes at room

temperature at 14, 000 rpm. The supernatant was carefully discarded from each tube with a pipette not to disturb the pellet. The tubes were inverted and blotted on tissue paper. Each tube was centrifuged for 1 minute at room temperature at 14, 000 rpm. Any remaining ethanol as carefully discarded using a 10 µl pipette. The tubes were air-dried fro 2 minutes at room temperature. 60 µl of DEPC H_2O was added to each tube to dissolve DNA and flicked to re-suspend the pellet. The tubes were left at 55^oC for 2 hours, shaking on the Thermomixer, then centrifuged for 2 minutes at room temperature at 14, 000 rpm. Samples were then ready to undergo the PCR reaction on the same day or placed at -20^oC for use at a later stage.

Stage 2: PCR

PCR Master Mix was made up on the day of the experiment according to Table 2.14. 48 µl of Master Mix was added into each 8-tube PCR strip. 2 µl of DNA was added into each PCR tube. PCR tubes were vortexed and spun to collect the solution in the base of the PCR tube.

Table 2.14 MyTaq Red Mix

Master-Mix Ingredients	**1X (µl)**	**20X (µl)**
My Taq Red mix, 2X	25	500
Forward Primer (5 µM)	1	20
Reverse Primer (5 µM)	1	20
ddH_2O	21	420
Total	**48**	**960**

PCR protocol:

Table 2.15: PCR protocol for Murine Genotyping Protocol. *TLR3* L413F – CRISPR/Cas9 Knock-in mice

	Program Steps	**Temperature**	**Time**
	1	95 ^oC	5 min
35 times	**2**	95 ^oC	30 secs
	3	60 ^oC	30 secs
	4	72 ^oC	1 min
	5	72 ^oC	10 min
	6	4 ^oC	Pause

Stage 3: Digestion

Following the PCR protocol (1 hour 56 min), the samples were ready to digest.

Digestion Master Mix was made up in DEPC H2O, 10x Buffer and Hphl restriction enzyme (Thermo Scientific), according to the Table 2.16. Fresh set of PCR tubes were labelled for overnight digest-reaction (See Table 2.17). 40 µl of the Digestion Master Mix (See table 2.16) was added to each PCR tube. 20 µl of the PCR reaction mixture to the PCR tubes. Tubes were flicked, mixed and vortexed.

Table 2.16: Master Mix for sample digestion

Master-Mix Ingredients	**1X reaction (µl)**	****USE**Double reaction volume (µl)**
ddH_2O	16	32
10x Buffer	3	6
HphI	1	2
PCR reaction	10	20
Total	30 µl	60 µl (Can run gel twice)

Digestion Protocol:

Table 2.17: Digestion Protocol

Program Steps	**Temperature**	**Time**
1	37^oC	16 hours
2	65 ^oC	20 min
3	4 ^oC	Pause

2.2.9.3 Day 3: Running the gel

The gel was ran directly following the restriction-digestion step of the experiment. 2% of agarose gel was made up in 120 ml of 1x TAE.

- Weigh out 2.4 g agarose.
- Add to a glass jar/ conical flask with 120 ml of 1X TAE
- Heat in the microwave (lid off) until all agarose has dissolved, clear and bubbling. (Stop the microwave and swirl occasionally to help dissolve).
- Add 13.33 µl of SYBR Safe DNA stain to the conical flask when slightly cooled.

15 well combs along with the previously prepared 2% agarose gel were added to the grey plastic tray and allowed to set for 20-30 minutes. The gel was placed in the rig, ensuring that the level of the 1X TAE is above the gel. The 15 well combs were carefully removed. 20 µl of each sample was added to each well along with 2 µl of 6x loading dye and 10 µl ladder. The gels were run at 90-100V until the dye has run 3/4s of the way down the gel. MP Imaging software was sued to image the gel.

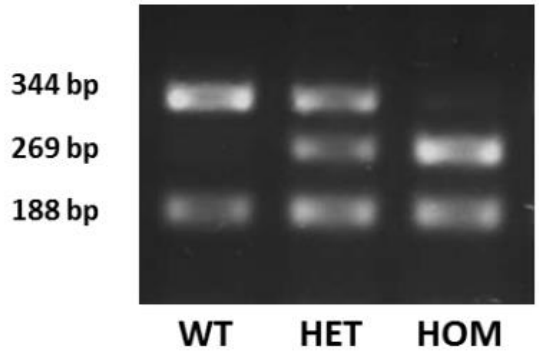

Figure 2.3 Representative image of *TLR3* L413F genotyping DN gel.

Following digestion, PCR product was separated into distinct DNA bands. The *TLR3* L413F wild-type genotype presents itself as two separates at 344 bp and 188 bp. The *TLR3* L413F heterozygote genotype presents itself as three separate bands at 344 bp, 269 bp and 188 bp. The *TLR3* L413F homozygote genotype presents as two separate bands at 269 bp and 188 bp.

2.2.10 Preparation of murine tissue homogenates for mRNA and ELISA.

The novel *TLR3* L413F knock-in, CRISPR/Cas 9 mice (C57BL/6 background) were generated by Taconic Biosciences Inc., Köln, Germany. Mice were 8–10 weeks old at the initiation of experiments and were housed individually in ventilated cages. All experiments were performed in accordance with regulations of the Irish Department of Health, the European Union, and the Ethics Committee of Trinity College Dublin.

2.2.10.1 Injection of mice with PBS and Poly(I:C).

Each mouse received an I.P injection of 200 µl of sterile **(i)** PBS or **(ii)** Poly(I:C) using 25-gauge needle. Each mouse was humanely killed 6 hours post I.P injection via cervical dislocation.

i) I.P injection of PBS is practiced as the standard procedure, necessary to establish a physiological baseline, which serves as a control and is used for comparison to the Poly(I:C) treatment used in this experiment.

ii) Poly(I:C) is a synthetic analogue of viral dsRNA which binds TLR3. I.P injection of Poly(I:C) is a well-established method of TLR3 activation *in vivo* in mice. The Poly(I:C) solution is sterile and non-infectious. The concentration of Poly(I:C) used for the I.P. administration has referenced from Alexopoulou *et al.* 2001 [367]. Specifically, mice will be given a single I.P. injection with sterile Poly(I:C) at 2.5 mg/kg per mouse (i.e., 50 µg per 20 g mouse)

2.2.10.2 Dissection and tissue homogenisation

Sections of individual organs (lungs, liver, brain, and spleen) were carefully dissected from each mouse, homogenised in 1 mL of TRI Reagent (Sigma) and frozen at -80oC for subsequent mRNA analysis.

Sections of each organ were also homogenised in Tris-HCL buffer (0.25 mol/L [pH 7.4]) with 2% foetal calf serum. BCA assay was used to quantitate protein concentration in each sample, as described in section 2.2.8.2. The homogenates were used for subsequent estimation of various target proteins by ELISA (Duo-Set; R&D Systems) as described in section 2.2.4.

2.2.11 Methodology for microbiome analysis of IPF BAL genomic DNA

2.2.11.1 Bacterial DNA isolation and quantification for IPF lung microbiome analysis

Genomic DNA was extracted from BAL as previously described (7). Aliquots of 2 ml of the BAL samples were centrifuged (21,000 x *g*; 30 minutes) to pellet cell debris and bacteria. Pellets were resuspended in 100 µl of supernatant and transferred to lysing matrix E (LME) tubes (MP Biomedicals, USA), to which 500 µl cetyl trimethylammonium bromide (CTAB) buffer (10% w/v CTAB in 0.5 M phosphate buffered NaCl) and 500 µl phenol:chloroform:isoamyl alcohol (25:24:1) were added, and shaken (5.5 m s^{-1}; 60 seconds) in a FastPrep Instrument (MP Biomedicals, USA). Samples were then extracted with an equal volume of chloroform:isoamyl alcohol (24:1), and DNA precipitated with 2 volumes of precipitation solution (30% w/v PEG6000 in NaCl). Following ethanol washing, pellets were resuspended in 100 µl Tris-EDTA. A NanoDrop™ 1000 Spectrophotometer (Thermo Fisher Scientific, UK) was used to measure the quality and quantity of the extracted DNA and the DNA was stored at -80 °C until further analysis.

2.2.11.2 16S rRNA sequencing and bioinformatics analysis

Paired-end sequencing of the hypervariable V4 region of the 16S rRNA gene was performed with the 515 forward and 806 reverse primers using an Illumina MiSeq instrument (Illumina, San Diego, CA) to produce 150 base-paired reads. Bioinformatics analysis of bacterial 16S rRNA amplicon data was conducted using the Quantitative Insights into Microbial Ecology (QIIME2, version 2019.10) pipeline (8). Initial demultiplexing and denoising was performed to remove sequencing errors and chimeric reads. Sequences were clustered

into amplicon sequence variants (ASV) using DADA2 (9) and assigned a taxonomic identity with the Greengenes database (10). Phylogenetic tree construction was conducted using FastTree 2 (11). Downstream pre-processing was performed in R (version 3.4.3) to obtain the relative abundances of the microbiota in each sample.

2.2.11.3 16S rRNA gene qPCR

Triplicate 10 µl quantitative polymerase chain reactions (qPCR) were set up containing 1 µl of bacterial DNA and 9 µl of Femto™ bacterial qPCR premix (Cambridge bioscience, UK) as previously described (7).

2.2.12 Statistical Analyses

All statistical analyses were carried out using GraphPad InStat Software (GraphPad Software Inc. CA, USA). All data was tested initially for normality using the Kolmogorov and Smirnov test. In addition, significant differences in standard deviation between experimental groups were examined using the Bartlett test (ANOVA). A non-parametric ANOVA must be employed where significant differences in standard deviation between experimental groups is present, even is the data itself is normally distributed. Therefore, in some cases, the data will be presented as the mean ± SEM (normally distributed) but where a non-parametric assay was employed (as prompted by the GraphPad InStat Software) because the standard deviation between the experimental groups is significantly different.

In ELISA and qPCR analyses, One-way ANOVA (parametric) or the Kruskal-Wallis Test (non-parametric ANOVA) were used to test for statistical significance (two-tailed analysis) between experimental groups of three or more. Multiple comparisons between groups were then assessed using the Tukey-Kramer Multiple Comparison Test post-hoc test (for parametric analysis) or Dunn's Multiple Comparison Test post-hoc test (for non-parametric analysis).

For data sets with only two experimental groups with equal standard deviations (SDs), unpaired Students T tests were used to compare data sets. Unpaired T tests with Welch's correction were used for analysis if the data sets did not have equal SDs (two tailed analysis). Non-parametric data was analysed using a Mann-Whitney U test for statistical significance (two tailed analysis). Statistical analyses of genotype frequencies were carried out using two-tailed Fisher exact tests. Statistical significance was recorded at $p<0.05$.

In chapters 3 and 4 of this PhD thesis, cell lines from 3 individual healthy donors and 3 individual IPF patients, respectively, were used. In these chapters, in each experiment carried

out, 6 experimental replicates were used, and the results were averaged. Each separate experiment was repeated twice. Therefore, each graph from the cellular studies in chapters 3 and 4 represents n=6 data points from healthy donors and IPF patients, respectively. In chapter 5, the *TLR3* L431F knock-in mouse model study, n=6 mice were used per mouse group and the pilot *in vivo* study was performed once.

Chapter 3 – Characterisation of the immunomodulatory effects of the metabolite, itaconate, on TLR3 function in primary human lung fibroblasts from IPF patients.

3.1 Introduction

Toll-like receptor 3 (TLR3) is expressed on cellular and endosomal membranes in a wide range of immune cells, including pulmonary epithelial cells and fibroblasts. The receptor plays a critical role in host immune defence and is known to bind double-stranded ribonucleic acid (dsRNA) from viruses, bacteria, helminths, and messenger ribonucleic acid (mRNA) released from necrotic cells [1, 367-369]. Activation of TLR3 triggers a signalling cascade leading to induction of nuclear factor kappa B (NF-κB) and interferon regulatory factor 3 (IRF3) which ultimately results in upregulation in mRNA expression of pro-inflammatory cytokines and type I IFNs [95, 130].

Research data implicate the role of TLR3 in the pathology of IPF. Anti-fibrotic properties of TLR3 were investigated *in vivo* using *Schistosoma mansoni* egg induced pulmonary granuloma model, whereby $TLR3^{-/-}$ presented with enlarged granulomas, as well as increased levels of collagen deposition compared with their wild-type (WT) counterparts [160]. Another *in vivo* study investigating the role of TLR3 on fibrotic processes came from our own lab, whereby we utilised the murine bleomycin model of pulmonary fibrosis to demonstrate reduced survival and elevated levels of fibrosis in $TLR3^{-/-}$ mice, compared with WT mice [161]. In addition, the reported increased levels of pulmonary fibrosis were accompanied by elevated production of pro-fibrotic mediators TGF-β, IL-4 and IL-13 as well as greater collagen deposition in the pulmonary tissue [161]. In terms of clinical studies, our group has characterised the *TLR3* SNP L412F (rs3775291), previously shown to result in supressed TLR3 activity, in the context of IPF and pulmonary sarcoidosis [161, 165]. We published a study featuring two IPF cohorts in which we reported a significantly increased risk of mortality as well as an accelerated decline in FVC in IPF patients who were 412F-variant [161]. Stimulation of TLR3 in primary pulmonary fibroblasts from L412F IPF patients led to dysregulated cytokine, type I IFN and fibroproliferative responses [161]. Moreover, treatment of lung fibroblasts with Poly(I:C) from 412F-variant IPF patients had reduced mRNA expression of TLR3, compared with L412-wild type patients [161]. In our most recent study, we demonstrated a significantly higher incidence of AE-related death in IPF patients heterozygous for 412F-variant compared to L412-wild type patients [366]. In addition, we reported dysregulated anti-bacterial responses to LPS, Pam3CYSK4, flagellin, FSL-1 and live *Pseudomonas aeruginosa* infection in 412F-heterozygous IPF patients [366]. The previous studies from our laboratory support a role for defective TLR3 function in the progression of IPF [161, 366].

Itaconate, encoded by immunoresponsive gene 1 (IRG-1) gene in humans, is a metabolic by-product of the citric acid (TCA) cycle, recently re-discovered as a potent immunomodulator with anti-bacterial, anti-viral and anti-inflammatory properties [221, 238]. The initial data investigating the modulatory effects of itaconate came from a number of studies which reported synthesis of itaconic acid in the lungs from mice infected with MTB, as well as in intracellular lysates of LPS-activated RAW264.7 macrophages and the VM-M3 macrophage-like cell line [222, 223]. Production of itaconate was additionally recorded in supernatants of the LPS-activated RAW264.7 cells [224]. Although most data characterising the role of itaconate in terms of immune response modulation was derived from observations on active immune cells-types, such as M1 macrophages, interestingly, the expression of IRG-1 was also shown to be upregulated in non-immune cells, including interferon – stimulated murine lung endothelial cells [225, 278]. Generation of IRG-1 $^{-/-}$ mice allowed for more in-depth investigation into the modulatory effects of itaconate and revealed the anti-inflammatory and anti-viral properties of the metabolite. Lampropoulou *et al.* demonstrated elevated production of pro-inflammatory cytokines in IRG-1 $^{-/-}$ macrophages treated with LPS or LPS and IFN-γ, compared with macrophages derived from WT mice [192]. Further data supporting anti-inflammatory properties of the metabolite came from Mills *et al.* who reported that 4-OI; a synthetic analogue of itaconate, reduced Poly(I:C)-driven IFN-β production in human PBMCs, and decreased Poly(I:C)-driven IL-1β transcription in mouse macrophages [195]. The anti-bacterial role of itaconate was shown in a consequent study conducted by Nair *et al*. in which IRG-1 deletion in MTB infected mice correlated with higher mortality rates compared with WT mice [226]. Moreover, itaconate inhibited the growth of Salmonella *enterica*, Legionella *pneumophilia*, Staphylococcus *aureus* and Pseudomonas *indigofera* in glucose-deprived environments [236, 238]. Itaconate has also been shown to carry anti-viral effects. IRG-1 levels were significantly elevated in murine lungs in response to influenza A virus infection [227, 370]. Treatment with DI; a synthetic analogue of itaconate reduced pulmonary inflammation and mortality in these animals [370]. Both 4-OI and DI decreased the transcription of IFN-regulated genes in human macrophages infected with influenza A virus [370]. Treatment of SARS-CoV-2-infected Vero cells with 4-OI supressed viral replication in NRF2-dependent manner [370]. Studies on Zika virus infection revealed that the metabolite promotes viral clearance in mice [335]. Animals lacking the kinase required for pathogen elimination during Zika virus infection presented with a significantly reduced transcription in IRG-1 gene compared with their WT counterparts. Moreover, deletion of IRG-

1 in mice infected with Zika virus resulted in higher rates of mortality [335]. Treatment with exogenous itaconate (4-OI) significantly decreased viral burden in these animals [335]. The anti-viral properties of itaconate have also been shown using the animal model of the West-Nile virus infection, in which itaconate restricted viral replication in neurons [371].

Itaconate has been proposed to mediate its anti-inflammatory effects via several different pathways. Amongst which is its ability to inhibit the activity of succinate dehydrogenase (SDH), an enzyme involved in the processing of succinate during the tricarboxylic acid (TCA) cycle [192]. Increased levels of succinate oxidation by SDH have been linked to mitochondrial generation of ROS, as well as hypoxia-inducible factor 1-alpha (HIF-1α) – dependent production of IL-1β [191, 192, 209]. In addition, itaconate exerts its anti-inflammatory effects via activation of nuclear factor-erythroid factor 2-related factor 2 (NRF2), which acts an inducer of several antioxidant genes, including heme oxygenase (decycling) 1 (HMOX-1), glutathione-disulfide reductase (GSR) or NAD(P)H quinone dehydrogenase 1 (NQOI), all involved in inhibition of ROS and HIF-1α-dependent production of IL-1β[195, 229, 230]. In terms of the anti-inflammatory properties, itaconate exerted inhibitory activity on the stimulator of IFN genes (STING) in NRF2-dependant manner [195]. Itaconate inhibited Poly(I:C) and LPS driven production of type I IFNs [195]. Interestingly transcription of IRG-1 has shown to be type I IFN-dependent, indicating the existence of a regulatory feedback loop between IRG-1 and type I IFNs [232].

A heightened state of inflammation, associated with both viral and bacterial infection, has been identified as key a driver underlying IPF pathology. Our previous findings highlighted the importance of defective TLR3 function in the progression of the disease. Considering the emerging evidence on the immunomodulatory properties of itaconate, and its ability to modulate Poly(I:C)-driven responses in human and mouse macrophages, in this chapter we investigated the effects of 4-OI (a synthetic analogue of itaconate) on modulation of TLR3 function in terms of: (i) pro-fibrotic, (ii) pro-inflammatory, (iii) anti-viral and (iv) anti-oxidative responses in primary pulmonary fibroblasts from IPF patients and healthy controls. When this PhD project was commenced in September 2018, there was no published literature on the role of itaconate in IPF. Furthermore, 4-OI, the synthetic analogue of itaconate, was not commercially available. Therefore, we were given a kind donation of 4-OI to complete the enclosed experiments by Professor Luke O'Neill, School of Biochemistry and Immunology, Trinity College, Dublin, Ireland.

Additionally, in this project we investigated whether the effects of 4-OI were limited to TLR3 regulation, by studying the effects of 4-OI on LPS and TGF-β-driven responses in healthy and IPF lung fibroblasts, as well as live *P. aeruginosa* infection. **Figure 3.1**. below illustrates the experimental design for research in this chapter.

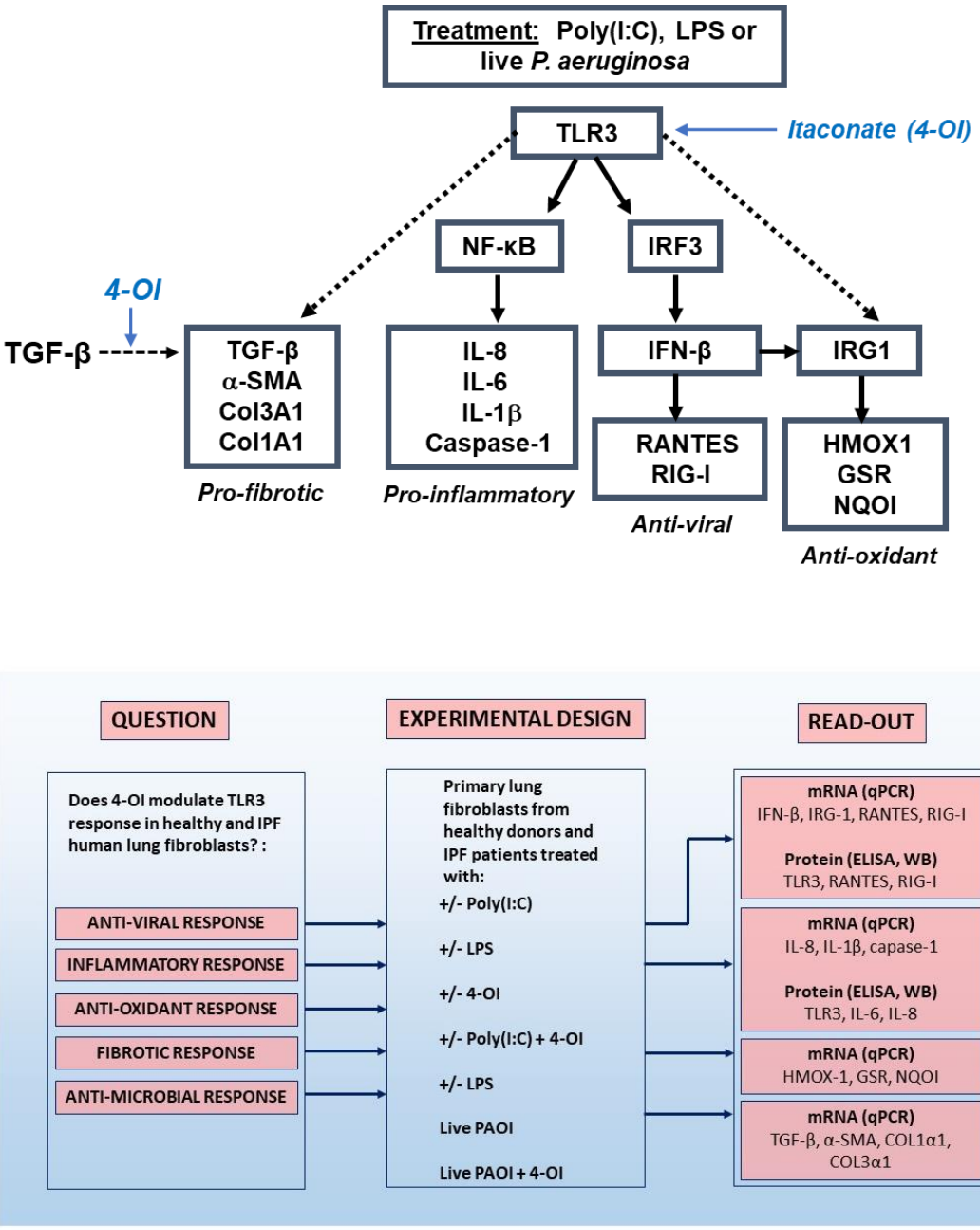

Figure 3.1. **Overview of the experimental design for chapter 3.** In this chapter, we investigated the effects of itaconate (4-OI) on TLR3 function (Poly(I:C) treatment) in primary human lung fibroblasts from IPF patients (n=3) and healthy donors (n=3). We also investigated the ability of 4-OI to modulate LPS/TLR4- and TGF-β responses, in addition to modulation of lung fibroblast responses to live *P. aeruginosa*, respectively, in IPF patients and healthy donors.

3.2. Effects of 4-OI on Poly(I:C)-induced IL-8 protein production in primary human lung fibroblasts from healthy donors and IPF patients.

TLR3 is a highly specialized sensor of damage–associated molecular patterns (DAMPs), endogenous mRNA and viral dsRNA as well as tissue necrosis [130, 367-369, 372]. Upon its activation TLR3 employs the proinflammatory arm of signalling (NF-κB) and its anti-viral counterpart (IRF3) [130, 373, 374]. In this experiment, primary human lung fibroblasts from healthy donors and IPF patients were stimulated with TLR3 agonist, Poly(I:C), a synthetic itaconate analogue, 4-OI or co-treated with Poly(I:C) and 4-OI for 24 hours. IL-8 protein production was quantitated and subsequently used as a read-out for NF-κB activity. Poly(I:C) treatment significantly increased IL-8 protein production from primary human lung fibroblasts from healthy donors and IPF patients in a dose-dependent manner (**Fig. 3.2A, B; **p<0.01, ***p<0.001)**. In agreement with previous findings, lung fibroblasts from IPF patients produced higher levels of IL-8 protein in response to Poly(I:C) treatment, relative to fibroblasts from healthy donors [375, 376]. 4-OI treatment had no significant effect on the production of IL-8 protein in healthy donors and IPF fibroblasts (**Fig. 3.2A-D)**. The presence of 4-OI (250 μM) had no significant effect on Poly(I:C)-induced protein production of IL-8 compared with Poly(I:C) treatment alone in healthy and IPF fibroblasts (**Fig. 3.2A, B)**.

3.3. Dose-dependent effects of 4-OI on Poly(I:C)-induced production of RANTES protein in primary human lung fibroblasts from healthy donors and IPF patients.

RANTES is an anti-viral chemokine, production of which is induced through Poly(I:C)-driven IRF3 signalling [377]. Here, primary human lung fibroblasts from healthy donors and IPF patients were stimulated with Poly(I:C), 4-OI or co-treated with Poly(I:C) and 4-OI. RANTES protein production was quantitated and subsequently used as a read-out for IRF3 activity. Poly(I:C) treatment significantly increased RANTES protein production from primary human lung fibroblasts from healthy donors and IPF patients in a dose-dependent manner (**Fig. 3.3A, B; **p<0.01, ***p<0.001)**. 4-OI treatment had no significant effect on the production of RANTES protein in healthy and IPF fibroblasts (**Fig. 3.3A-D)**. In the presence of 4-OI (250 μM), Poly(I:C)-induced protein production of RANTES was significantly decreased compared with Poly(I:C) treatment alone in healthy and IPF lung fibroblasts (**Fig. 3.3D; †††p<0.001)**.

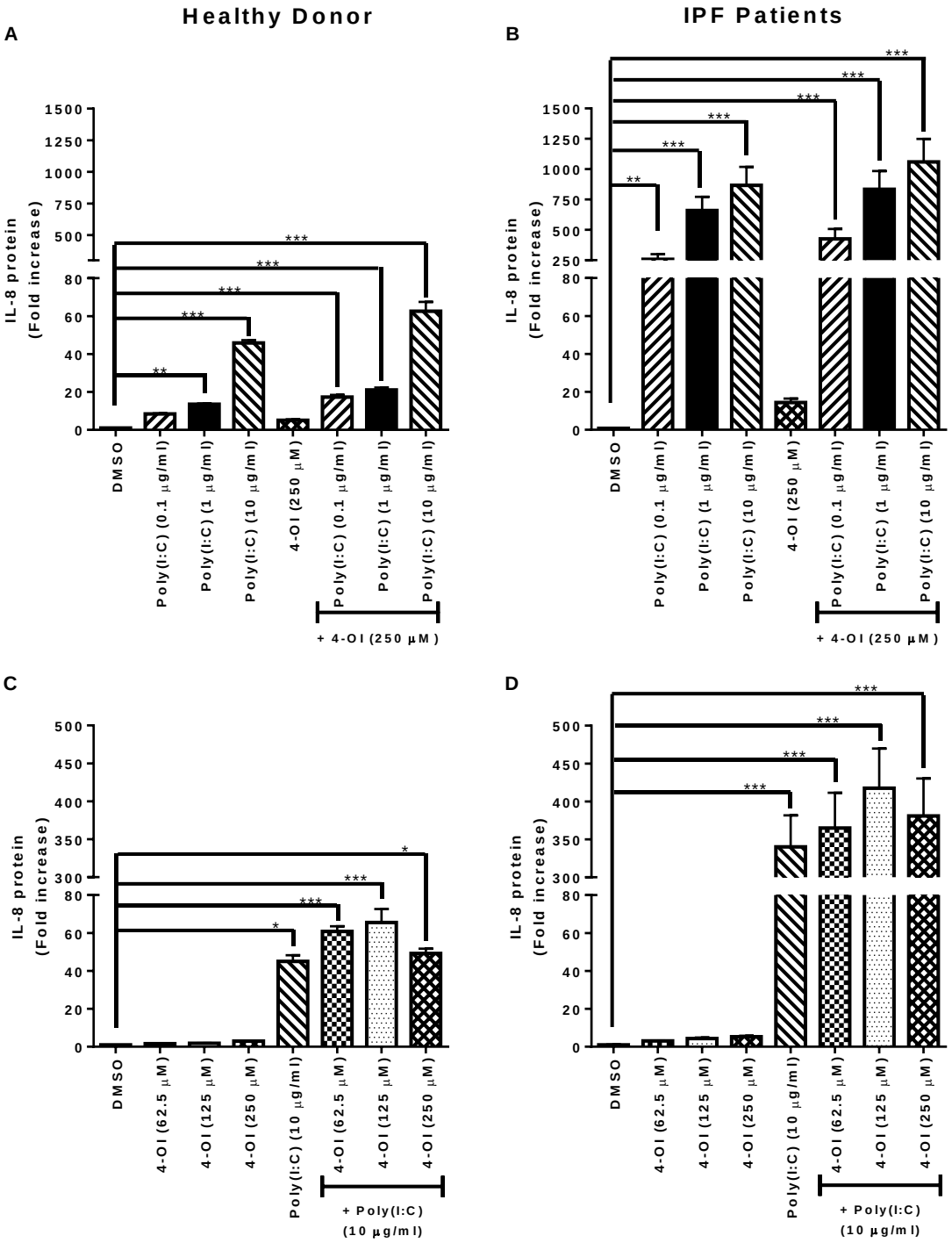

Figure 3.2. Effects of 4-OI on Poly(I:C)-induced IL-8 protein production in primary human lung fibroblasts from healthy donors and IPF patients. Poly(I:C) treatment significantly increased levels of IL-8 protein production in primary human lung fibroblasts from healthy donors (**A**) and IPF patents (**B**) in a dose-dependent manner. 4-OI treatment had no effect on protein production of IL-8 in both control (**A, C**) and IPF fibroblasts (**B, D**). 4-OI had no significant effect on Poly(I:C)-induced IL-8 in primary human lung fibroblasts from healthy donors (**A**) and IPF patients (**B**). IL-8 protein production was quantitated by ELISA at 24 h post-treatment. A Kruskal-Wallis Test with a Dunn's multiple comparison post-hoc test was used to test for statistical differences. *p<0.05, **p<0.01, ***p<0.001: DMSO compared with Poly(I:C) or Poly(I:C) & 4-OI treatment, respectively. Each graph represents data from primary lung fibroblasts from 3 healthy donors and 3 IPF patients, respectively, performed twice (n=6). Results shown represent the mean +/- S.E.M. [Poly(I:C), 0.1, 1, 10 µg/ml; 4-OI, 62.5, 125, 250 µM].

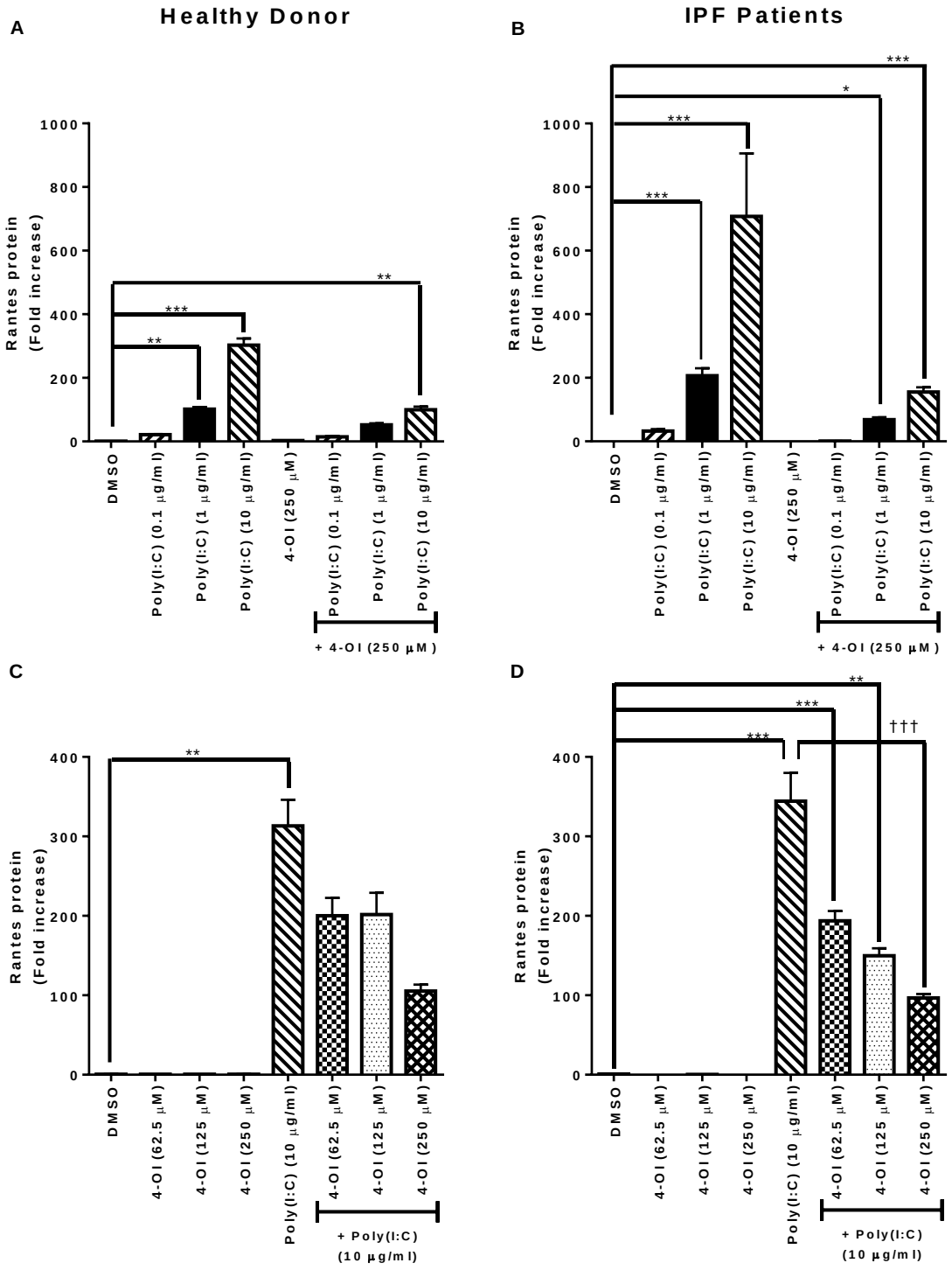

Figure 3.3. Effects of 4-OI on Poly(I:C)-induced RANTES protein production in primary human lung fibroblasts from healthy donors and IPF patients. Poly(I:C) treatment increased levels of RANTES protein production in primary human lung fibroblasts from healthy donors (**A**) and IPF patients (**B**) in a dose-dependent manner. 4-OI treatment had no effect on protein production of RANTES in both control (**A, C**) and IPF fibroblasts (**B, D**). In the presence of 4-OI (250 µM), Poly(I:C)-induced protein production of RANTES was significantly decreased in IPF fibroblasts compared with Poly(I:C) treatment alone **(B).** RANTES protein production was quantitated by ELISA at 24 h post-treatment. A Kruskal-Wallis Test with a Dunn's multiple comparison post-hoc test was used to test for statistical differences. *p<0.05, **p<0.01, ***p<0.001: DMSO compared with Poly(I:C) or Poly(I:C) & 4-OI treatment, respectively. †††p<0.001: Poly(I:C) & 4-OI treatment compared with Poly(I:C) treatment only. Each graph represents data from primary lung fibroblasts from 3 healthy donors and 3 IPF patients, respectively, performed twice (n=6). Results shown represent the mean +/- S.E.M. [Poly(I:C), 0.1, 1, 10 µg/ml; 4-OI, 62.5, 125, 250 µM].

3.4. Effects of 4-OI on Poly(I:C)-mediated protein production of IL-8, IL-6 and RANTES in primary human lung fibroblasts from healthy donors and IPF patients.

In this experiment, primary human lung fibroblasts from healthy donors and IPF patients were stimulated with Poly(I:C), 4-OI or co-treated with Poly(I:C) and 4-OI. Corresponding protein production of IL-8, IL-6 and RANTES was quantitated. Lung fibroblasts from IPF patients exhibited an exaggerated IL-8, IL-6 and RANTES response (**Fig. 3.4B, D, F)** to Poly(I:C) treatment compared with healthy controls (**Fig. 3.4A, C, E)**. Treatment of fibroblasts from healthy donors and IPF patients with 4-OI had no significant effect on the production of IL-8, IL-6 and RANTES protein, compared with DMSO **(Fig. 3.4A-F).** Treatment with 4-OI had no significant effect Poly(I:C)-induced IL-8 or IL-6 protein production in lung fibroblasts from healthy donors and IPF patients (**Fig. 3.4A-D)**. Treatment with 4-OI significantly reduced Poly(I:C)-induced RANTES production in compared with Poly(I:C) only treated IPF fibroblasts (**Fig. 3.4F; †††p<0.001**).

3.5. Effects of 4-OI on Poly(I:C)-induced transcription of pro-inflammatory genes IL-8, IL-1β and caspase-1 in primary human lung fibroblasts from healthy donors and IPF patients.

TLR3 activates pro-inflammatory responses in targeted cells [367]. Increased levels of IL-8, IL-1β and caspase-1, have been associated with fibrosis and tissue remodelling in diseases such as IPF, asthma, liver cirrhosis, and renal fibrosis [375, 378]. In this experiment, primary human lung fibroblasts from healthy donors and IPF patients were stimulated with Poly(I:C), 4-OI or co-treated with Poly(I:C) and 4-OI. Transcription of pro-inflammatory IL-8, IL-1β and caspase-1 was quantitated. Treatment with Poly(I:C) significantly upregulated IL-8, IL-1β and caspase-1 transcription in fibroblasts from IPF patients compared with DMSO (**Fig. 3.5B, D, F; ***p<0.001**). Poly(I:C) significantly upregulated IL-8 and caspase-1 transcription in fibroblasts from healthy donors compared with DMSO (**Fig. 3.5A, E; ***p<0.001**). IPF fibroblasts (**Fig. 3.5B, D, F)** expressed an exaggerated IL-8, IL-1β and caspase-1 response to Poly(I:C) treatment relative to healthy controls (**Fig. 3.5A, C, E)**. 4-OI treatment had no significant effect on the transcription of IL-8, IL-1β and caspase-1 in lung fibroblasts from healthy donors or IPF patients, compared with DMSO. Treatment with 4-OI significantly decreased Poly(I:C)-induced caspase-1 transcription in fibroblasts from healthy donors (**Fig.3.5E; †p<0.05)** and IPF fibroblasts (**Fig. 3.5F; †††p<0.001)**, respectively, compared with Poly(I:C) only treated fibroblasts.

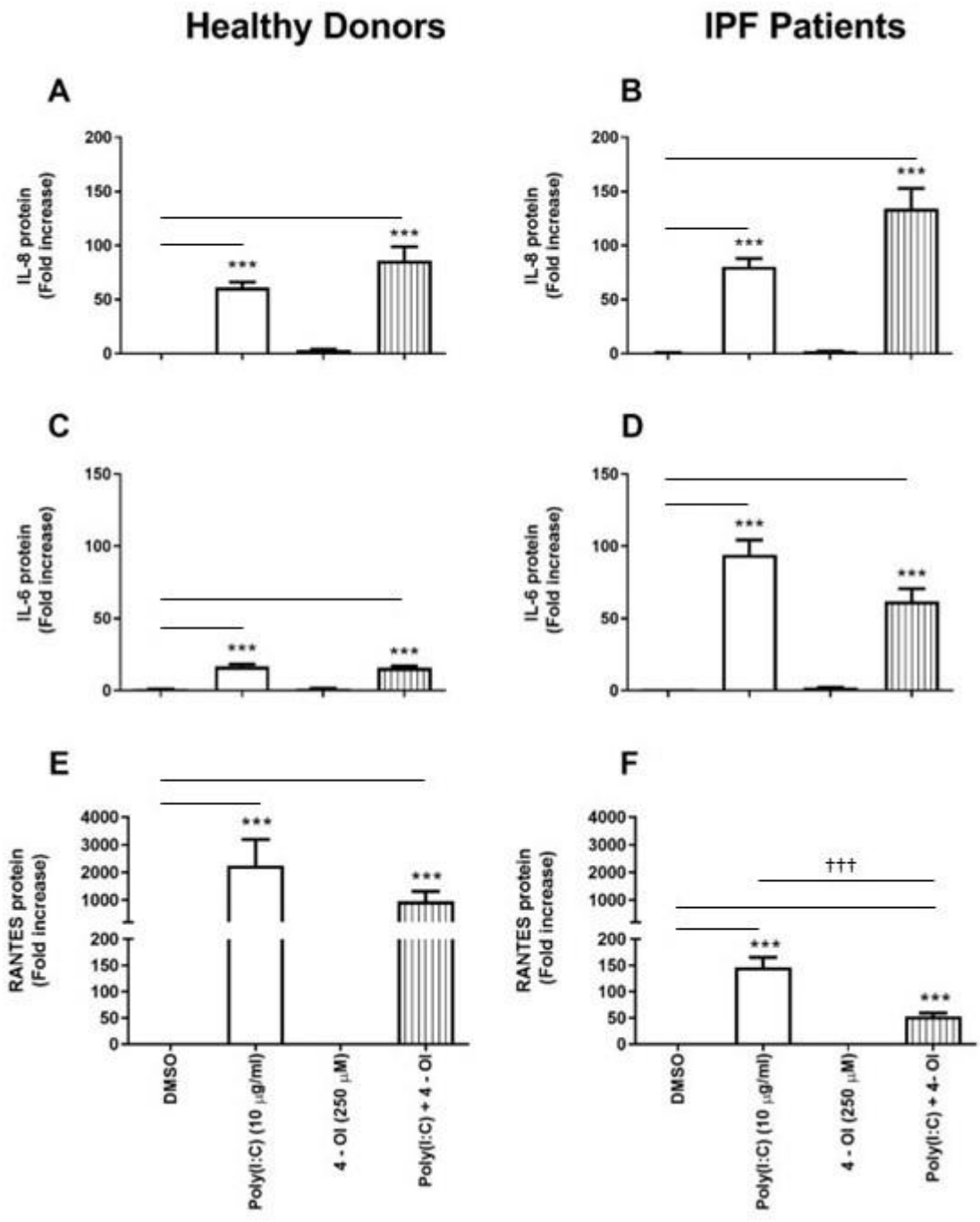

Figure 3.4. Effects of 4-OI on Poly(I:C)-mediated protein production of IL-8, IL-6 and RANTES in primary human lung fibroblasts from healthy donors and IPF patients. Poly(I:C) treatment significantly increased levels of IL-8, IL-6 and RANTES protein production in primary lung fibroblasts from healthy donors (**A, C, E**) and IPF patients (**B, D, F**). 4-OI treatment had no effect on Poly(I:C)-induced IL-6, IL-8 or RANTES protein production in healthy or IPF lung fibroblasts, respectively **(A-F).** In the presence of 4-OI (250 μM), Poly(I:C)-induced protein production of RANTES was significantly decreased in IPF fibroblasts compared with Poly(I:C) treatment alone **(B).** IL-8, IL-6 and RANTES protein production was quantitated by ELISA at 24 h post-treatment. A Kruskal-Wallis Test with a Dunn's multiple comparison post-hoc test was used to test for statistical differences. ***p<0.001: DMSO compared with Poly(I:C) or Poly(I:C) & 4-OI treatment, respectively. †††p<0.001: Poly(I:C) & 4-OI treatment compared with Poly(I:C) treatment only. Each graph represents data from primary lung fibroblasts from 3 healthy donors and 3 IPF patients, respectively, performed twice (n=6). Results shown represent the mean +/- S.E.M. [Poly(I:C), 10 μg/ml; 4-OI, 125 μM].

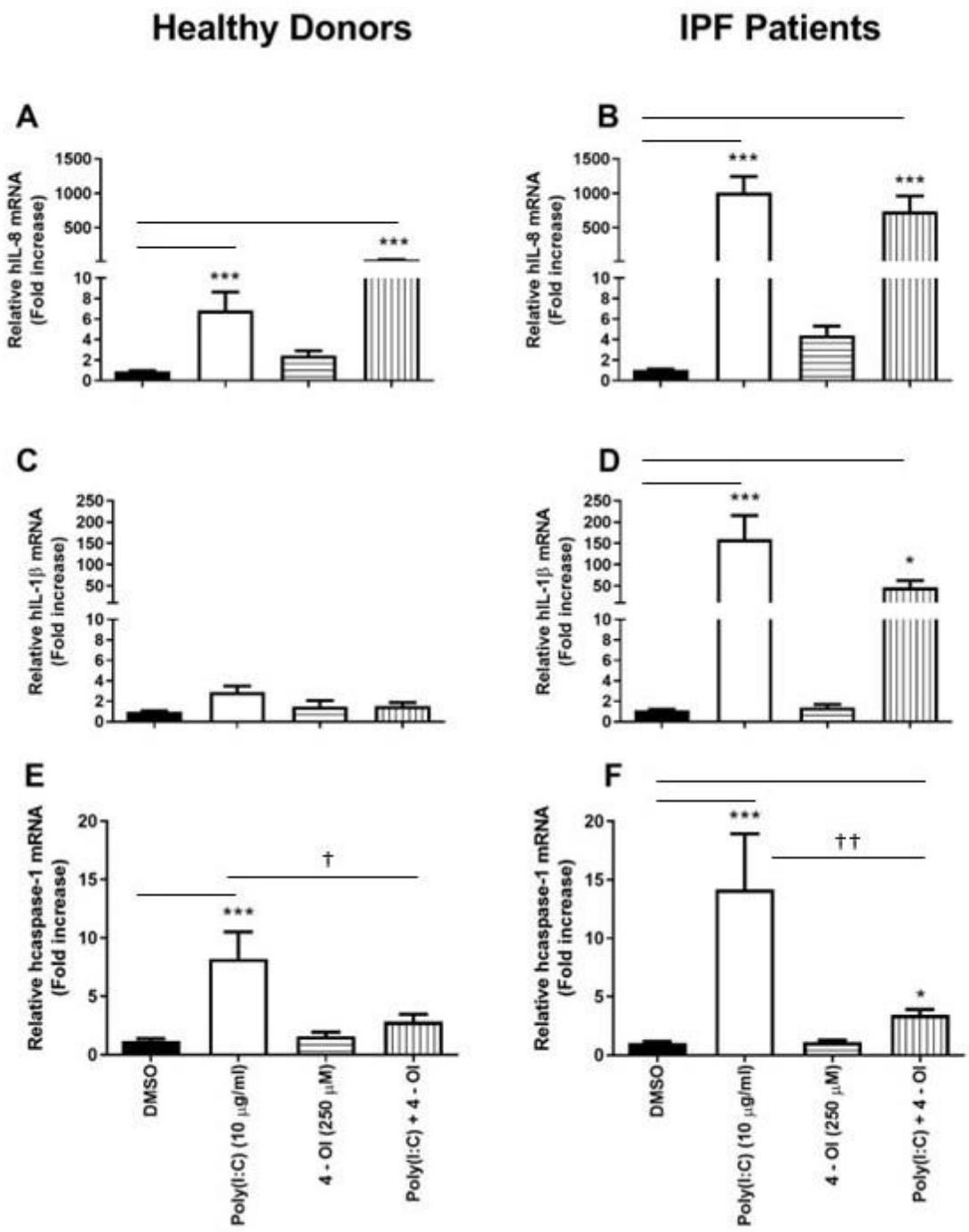

Figure 3.5. Effects of 4-OI on Poly(I:C)-induced, NF-κB-dependent transcription of pro-inflammatory agents, IL-8, IL-1β and caspase-1 in primary human lung fibroblasts from healthy donors and IPF patients. Poly(I:C) treatment significantly increased levels of IL-8 and caspase-1 transcription in lung fibroblasts from healthy donors (**A, E**). Poly(I:C) treatment significantly increased levels IL-8, IL-1β and caspase-1 mRNA in IPF patients (**B, D, F**). 4-OI had no effect on IL-8, IL-1b and caspase-1 mRNA in healthy donor or IPF fibroblasts (**A-F).** In the presence of 4-OI (250 μM), Poly(I:C)-induced caspase-1 transcription was significantly reduced decreased in healthy donor and IPF fibroblasts compared with Poly(I:C) treatment alone **(D, E).** IL-8, IL-1β and caspase-1 mRNA expression was quantitated by qPCR at 24 h post-treatment. A Kruskal-Wallis Test with a Dunn's multiple comparison post-hoc test was used to test for statistical differences. *p<0.05, ***p<0.001: DMSO compared with Poly(I:C) or Poly(I:C) & 4-OI treatment, respectively. †p<0.05, ††p<0.01: Poly(I:C) & 4-OI treatment compared with Poly(I:C) treatment only. Each graph represents data from primary lung fibroblasts from 3 healthy donors and 3 IPF patients, respectively, performed twice (n=6). Results shown represent the mean +/- S.E.M. [Poly(I:C), 10 μg/ml; 4-OI, 250 μM].

3.6. Effects of 4-OI on Poly(I:C)-induced, IRF3-dependent transcription IFN-β, RANTES and RIG-I in primary human lung fibroblasts from healthy donors and IPF patients.

The IRF3 pathway act as the anti-viral arm of Poly(I:C)-induced response in target cells. Activation of IRF3 leads to the induction of a number of anti-viral mediators, such as IFN-β, RANTES and RIG-I [379-381]. Our previous data links defective Poly(I:C)-dependant type 1 IFN response in IPF patients with a worsened clinical prognosis [161]. In this experiment, primary human lung fibroblasts from healthy donors and IPF patients were stimulated with Poly(I:C), 4-OI or co-treated with Poly(I:C) and 4-OI. Transcription of IFN-β, RANTES and RIG-I was used as a readout of Poly(I:C)-induced anti-viral activity. Poly(I:C) treatment significantly upregulated IFN-β, RANTES and RIG-I transcription in both control and IPF lung fibroblasts (**Fig. 3.6A-F; ***p<0.001**). Poly(I:C)-induced IFN-β and RIG-I response was more pronounced in IPF fibroblasts **(Fig. 3.6B, F)** relative to the controls (**Fig. 3.6A, E)**. 4-OI treatment had no significant effect on the transcription of IFN-β, RANTES and RIG-I in fibroblasts from healthy donors and IPF patients **(Fig. 3.6A-F)**. Treatment with 4-OI significantly reduced Poly(I:C)-induced transcription of IFN-β in healthy lung fibroblasts (**Fig. 3.6A; †p<0.05)**.

3.7. Effects of 4-OI on Poly(I:C)-induced IRG-1 mRNA expression and NRF2-dependent transcription of antioxidant genes, HMOX-1, GSR and NQOI in primary human lung fibroblasts from healthy donors and IPF patients.

Damage caused by oxidative stress has been implicated in the pathology of IPF [382-385]. The IRG-1 gene has been shown to encode cis-aconitate decarboxylase, an enzyme which catalyses the synthesis of itaconate from the tricarboxylic acid (TCA) cycle [238]. IRG-1 drives the production of itaconate and subsequently induces the signalling of NRF2, a master regulator of antioxidant gene expression. NRF2 has been shown to play a vital role in protection against oxidative damage in a variety of organs, including lungs [195, 386, 387]. In this experiment, primary human lung fibroblasts from healthy donors and IPF patients were stimulated with Poly(I:C), 4-OI or co-treated with Poly(I:C) and 4-OI. Transcription of IRG-1 as well as transcription of the NRF2-induced antioxidants, HMOX-1, GSR and NQOI was quantitated. Treatment of healthy lung fibroblasts with Poly(I:C) produced no significant change in HMOX-1, GSR, NQOI and IRG-1 response, compared with DMSO (**Fig. 3.7A, C, E, G)**. Poly(I:C) treatment significantly induced IRG-1 transcription in IPF fibroblasts (**Fig. 3.7H; ***p<0.001**). 4-OI treatment produced a significant induction in HMOX-1 transcription in healthy fibroblasts compared with DMSO (**Fig. 3.7A ***p<0.001**); as well as in HMOX-1 and

GSR transcription in IPF fibroblasts compared with DMSO (**Fig. 3.7B, D; ***p<0.001**). 4-OI treatment significantly increased Poly(I:C)-induced HMOX-1 transcription in healthy lung fibroblasts (**Fig. 3.7A; †††p<0.001)**; and significantly increased HMOX-1 and GSR transcription in IPF lung fibroblasts **(Fig. 3.7B, D; †††p<0.001)**, respectively, compared with Poly(I:C) treatment alone. Poly(I:C) treatment significantly increased IRG-1 transcription in IPF lung fibroblasts compared with DMSO only treatment (**Fig. 3.7H; ***p<0.001**). These data demonstrated, for the first time, that Poly(I:C) treatment significantly increased IRG-1 transcription, demonstrating that lung fibroblasts had the potential to synthesize itaconate.

3.8. Effects of 4-OI on Poly(I:C)-induced TGF-β, α-SMA, COL3α1 and COL1α1 transcription in primary human lung fibroblasts from healthy donors and IPF patients.

IPF lung fibroblasts generate excessive contractile force to stimulate the production of various pro-fibrotic agents, such as collagens, α-SMA and TGF-β. When activated, TGF-β has been shown to act as a pleiotropic growth factor with chemotactic and proliferative properties [388-391]. Recent studies have revealed that using the bleomycin model of murine pulmonary fibrosis, IRG-$1^{-/-}$ mice show decreased rates of survival, increased collagen deposition and worsened lung function compared with WT mice [245]. In this study, primary human lung fibroblasts from healthy donors and IPF patients were stimulated with Poly(I:C), 4-OI or co-treated with Poly(I:C) and 4-OI. Transcription of pro-fibrotic mediators, TGF-β, α-SMA, COL3α1 and COL1α1 was quantitated. Treatment with Poly(I:C) significantly induced the transcription of α-SMA (**Fig. 3.8D; ***p<0.001**) and COL1α1 in IPF lung fibroblasts compared with DMSO treatment (**Fig. 3.8H; ***p<0.001**); and had no effects in fibroblasts from healthy donors (**Fig. 3.8A, C, E, G)**. Control and IPF fibroblasts treated with 4-OI showed no change in the transcription of TGF-β, α-SMA, COL3α1 and COL1α1 compared with DMSO (**Fig. 3.8A-H)**. 4-OI treatment significantly decreased Poly(I:C)-induced transcription of α-SMA (**Fig. 3.8D; †††p<0.001**), COL3α1 (**Fig. 3.8F; †p<0.05**) and COL1α1 (**Fig. 3.8H; †p<0.05**) in IPF lung fibroblasts compared with Poly(I:C) only treatment.

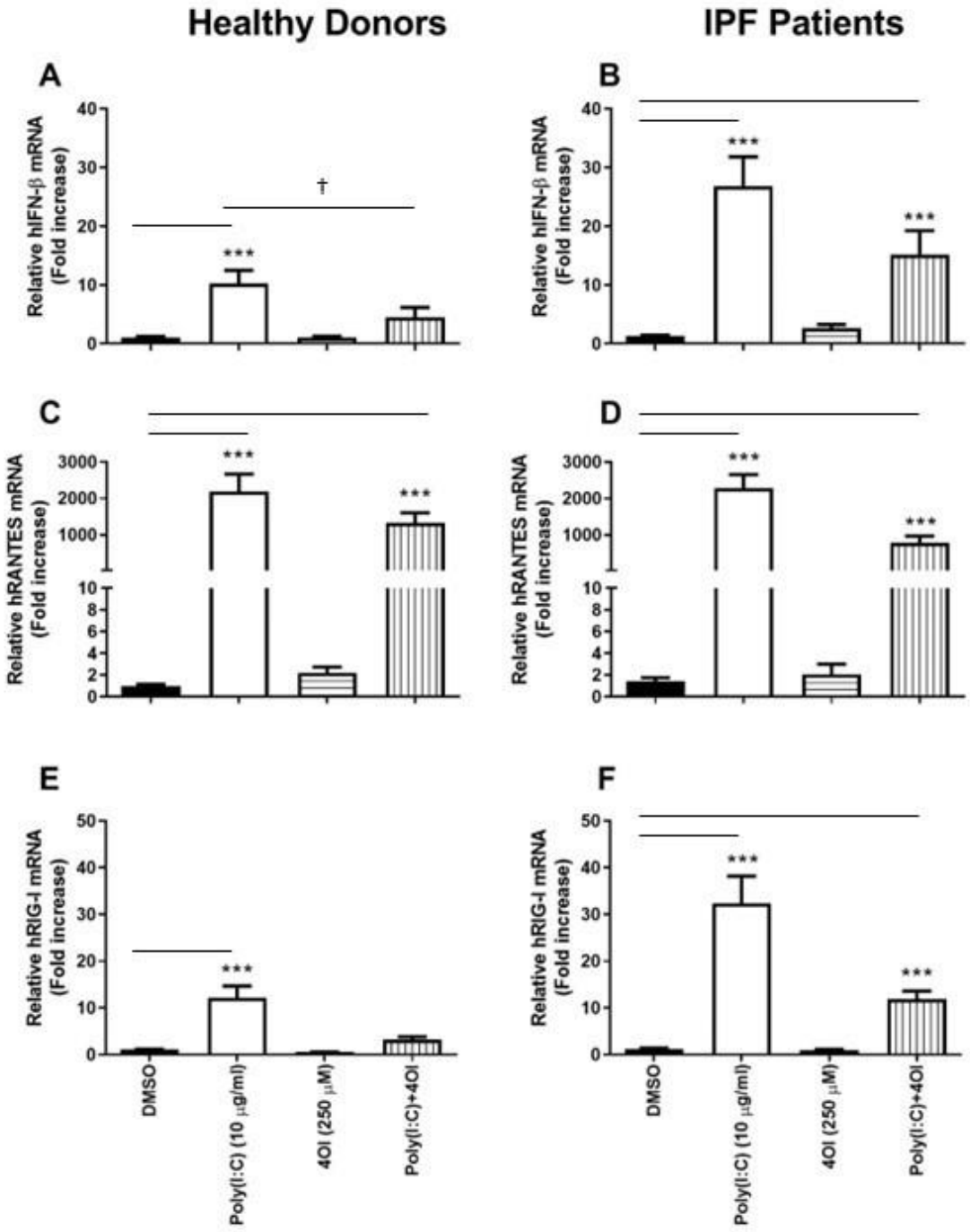

Figure 3.6. Effects of 4-OI on Poly(I:C)-induced, IRF3-dependent transcription of IFN-β, RANTES, RIG-I in primary human lung fibroblasts from healthy donors and IPF patients. Poly(I:C) treatment significantly increased levels of IFN-β, RANTES and RIG-I transcription in healthy controls (**A, C, E**) and primary human lung fibroblasts from IPF patients (**B, D, F**). 4-OI treatment had no significant effect on healthy donor or IPF fibroblasts. In the presence of 4-OI (250 μM), Poly(I:C)-induced IFN-β transcription healthy lung fibroblasts compared with Poly(I:C) treatment only **(A).** IFN-β, RANTES and RIG-I mRNA expression was quantitated by qPCR at 24 h post-treatment. A Kruskal-Wallis Test with a Dunn's multiple comparison post-hoc test was used to test for statistical differences. ***p<0.001: DMSO compared with Poly(I:C) or Poly(I:C) & 4-OI treatment, respectively. †p<0.001: Poly(I:C) & 4-OI treatment compared with Poly(I:C) treatment only.. Each graph represents data from primary lung fibroblasts from 3 healthy donors and 3 IPF patients, respectively, performed twice (n=6). Results shown represent the mean +/- S.E.M. [Poly(I:C), 10 μg/ml; 4-OI, 250 μM].

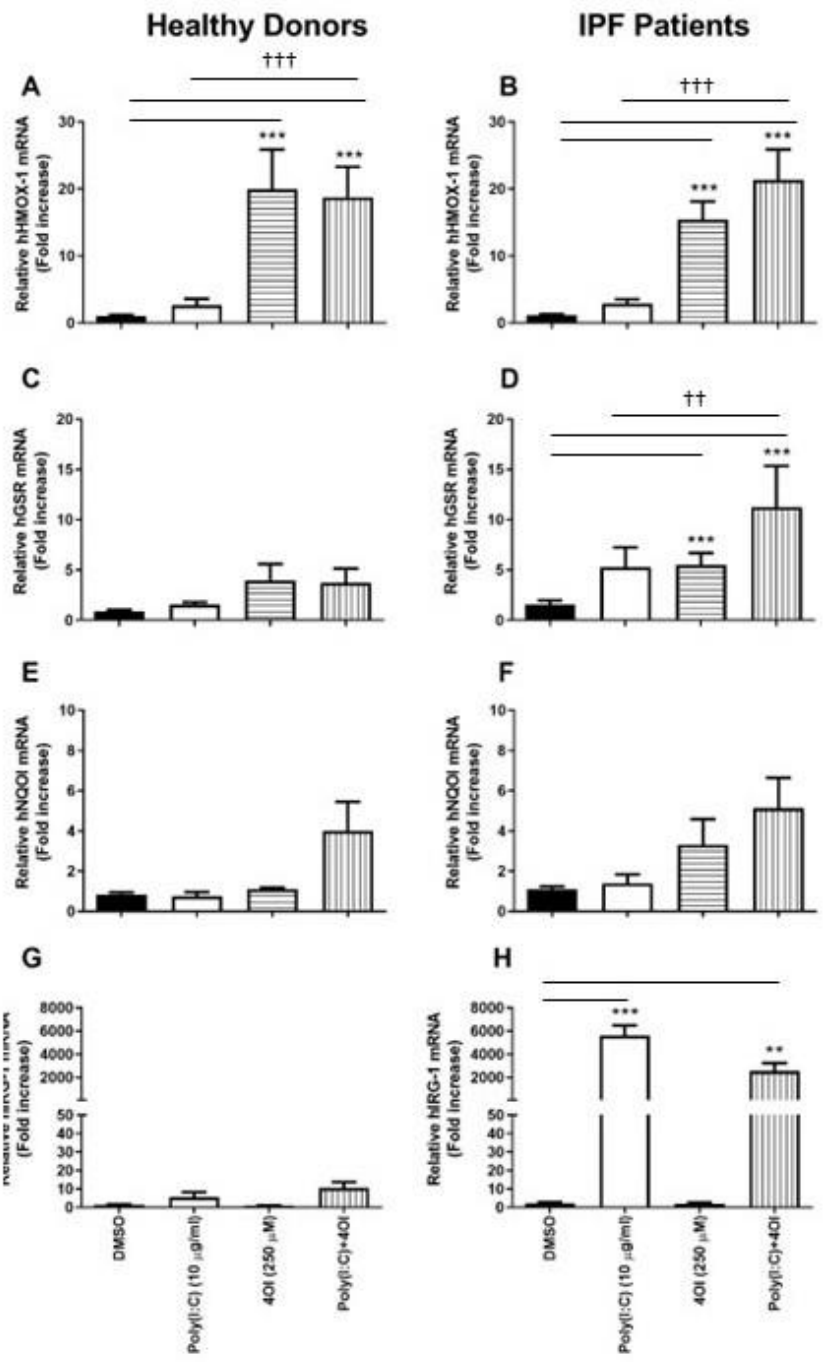

Figure 3.7. Effects of 4-OI on Poly(I:C)-induced IRG-1 mRNA expression and NRF2-dependent transcription of antioxidant genes, HMOX-1, GSR and NQOI in primary human fibroblasts from healthy donors and IPF patients. Poly(I:C) treatment had no significant effect on the transcription of HMOX-1, GSR, NQOI and IRG-1 in lung fibroblasts from healthy donors (**A, C, E, G**) and IPF patients (**B, D, F**); with the exception of IRG-1 transcription, which was significantly increased in IPF lung fibroblasts (**G**). Treatment with 4-OI significantly increased transcription of HMOX-1 in healthy fibroblasts (**A**), as well as in HMOX-1 and GSR transcription in IPF fibroblasts (**B, D**). In the presence of 4-OI (250 µM), Poly(I:C)-induced HMOX-1 transcription was significantly increased in healthy donor and IPF fibroblasts compared with Poly(I:C) treatment alone **(A, B);** and GSR transcription was significantly increased in IPF kung fibroblasts following this co-treatment **(D).** HMOX-1, NQOI, GSR and IRG-1 mRNA expression was quantitated by qPCR at 24 h post-treatment. A Kruskal-Wallis Test with a Dunn's multiple comparison post-hoc test was used to test for statistical differences. **p<0.01, ***p<0.001: DMSO compared with Poly(I:C) or Poly(I:C) & 4-OI treatment, respectively. ††p<0.01, †††p<0.001: Poly(I:C) & 4-OI treatment compared with Poly(I:C) treatment only. Each graph represents data from primary lung fibroblasts from 3 healthy donors and 3 IPF patients, respectively, performed twice (n=6). Results shown represent the mean +/- S.E.M. [Poly(I:C), 10 µg/ml; 4-OI, 250 µM].

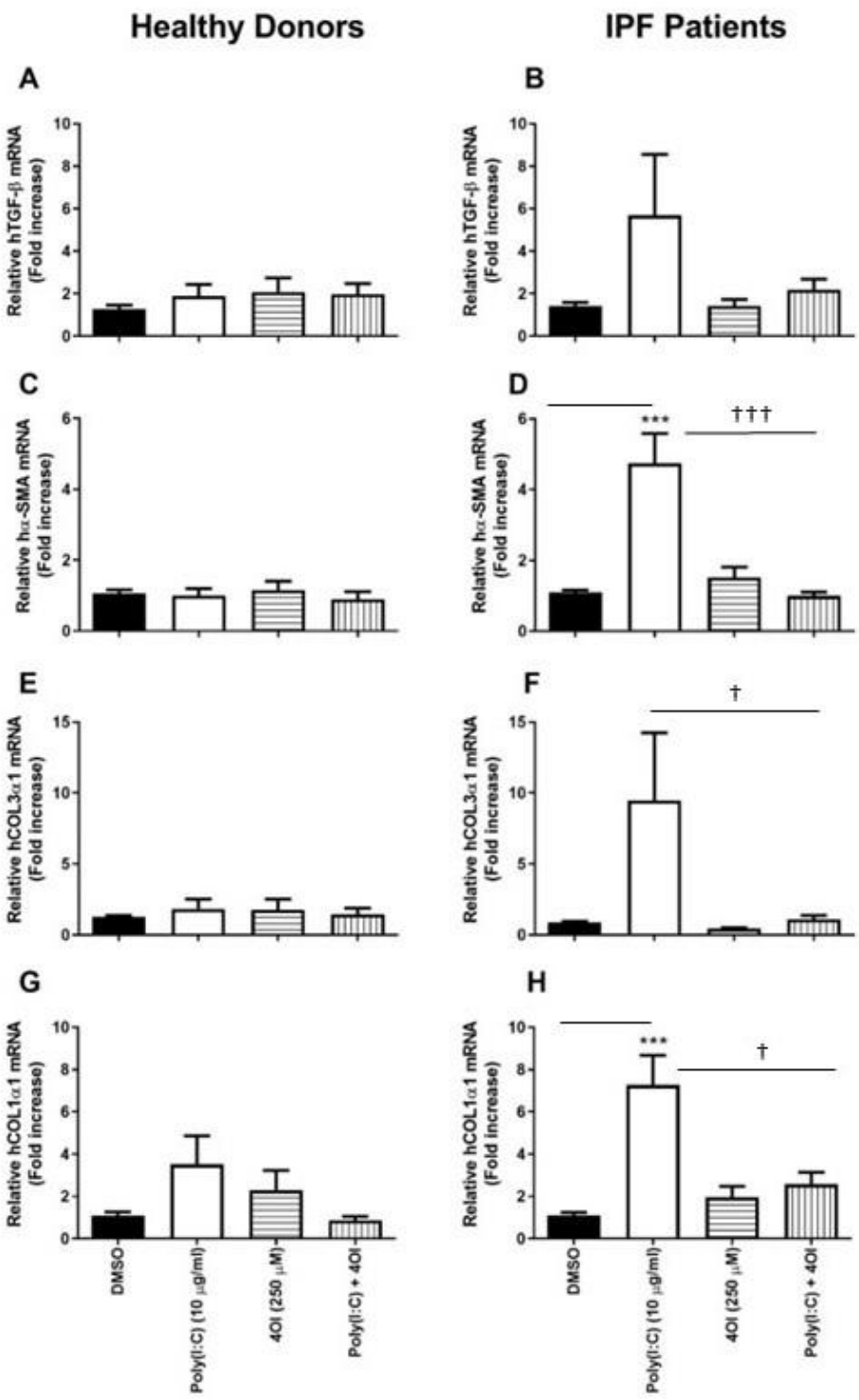

Figure 3.8. Effects of 4-OI on Poly(I:C)-induced TGF-β, α-SMA, COL3α1 and COL1α1 transcription in primary human lung fibroblasts from healthy donors and IPF patients. Poly(I:C) treatment significantly increased transcription on α-SMA and COL1α1 compared with DSMO treatment in IPF fibroblasts (**B, H**). Treatment with 4-OI had no effect on the transcription of TGF-β, α-SMA, COL3α1 and COL1α1 in healthy and IPF lung fibroblasts (**A-H**). In the presence of 4-OI (250 μM), Poly(I:C)-induced α-SMA (**D**), COL3α1 (**F**) and COL1α1 (**H**) transcription was significantly reduced in IPF fibroblasts at 24 h post-treatment, as quantitated by qPCR analysis. A Kruskal-Wallis Test with a Dunn's multiple comparison post-hoc test was used to test for statistical differences. ***p<0.001: compared with DMSO treatment only. †p<0.05, †††p<0.001: compared with Poly (I: C) treatment. Each graph represents data from primary lung fibroblasts from 3 healthy donors and 3 IPF patients, respectively, performed twice (n=6). Results shown represent the mean +/- S.E.M. [Poly(I:C), 10 μg/ml; 4-OI, 250 μM].

3.9. Effects of Poly(I:C) and LPS treatment on IL-6, IL-8 and RANTES protein production in primary human lung fibroblasts from healthy donors and IPF patients.

Activation of TLR4 by LPS has been shown to induce production of pro-inflammatory, IL-8, IL-6 and the anti-viral RANTES protein in various cell types, including nasal polyp-derived fibroblasts, skin fibroblasts and airway smooth muscle cells [392-395]. In this experiment, primary human lung fibroblasts from healthy donors and IPF patients were stimulated with Poly(I:C) and LPS. Protein production of IL-6, IL-8 and RANTES was quantitated. Poly(I:C) treatment significantly induced IL-6, IL-8 and RANTES response in fibroblasts from healthy donors and IPF patients (**Fig. 3.9A-F; ***p<0.001**). Treatment with LPS significantly increased IL-6, IL-8 and RANTES protein production IPF lung fibroblasts compared with medium only treatment (**Fig. 3.9B, D, F; ***p<0.001**).

3.10. Effects of 4-OI on LPS-induced IL-8 and RANTES production in primary human lung fibroblasts from healthy donors and IPF patients.

We showed that TLR3- and TLR4-activation induced IL-8 and RANTES signalling in IPF lung fibroblasts, respectively, which is associated with the pathology of IPF (**Fig. 3.9**). In order to investigate the effects of 4-OI on TLR3 and TLR4-driven protein production of pro-inflammatory agents, primary human lung fibroblasts from healthy donors and IPF patients were stimulated with Poly(I:C), LPS, 4-OI, co-treated with Poly(I:C) and 4-OI or LPS and 4-OI. Protein production of IL-8 and RANTES was quantitated. Poly(I:C) treatment significantly induced protein production of IL-8 and RANTES compared with DMSO in healthy and IPF fibroblasts (**Fig. 3.10A-D; ***p<0.001**). Treatment with LPS significantly increased IL-8 protein production in IPF lung fibroblasts compared with DMSO treatment (**Fig.3.10B)**. 4-OI had no significant effect on the production of IL-8 and RANTES (**Fig. 3.10A-D)**. Poly(I:C)-induced protein production of RANTES was significantly downregulated following co-treatment with 4-OI in healthy lung fibroblasts (**Fig. 3.10C; †††p<0.001**). 4-OI treatment had no significant effect on LPS-induced IL-8 in IPF fibroblasts compared with LPS treatment only (**Fig.3.10B)**.

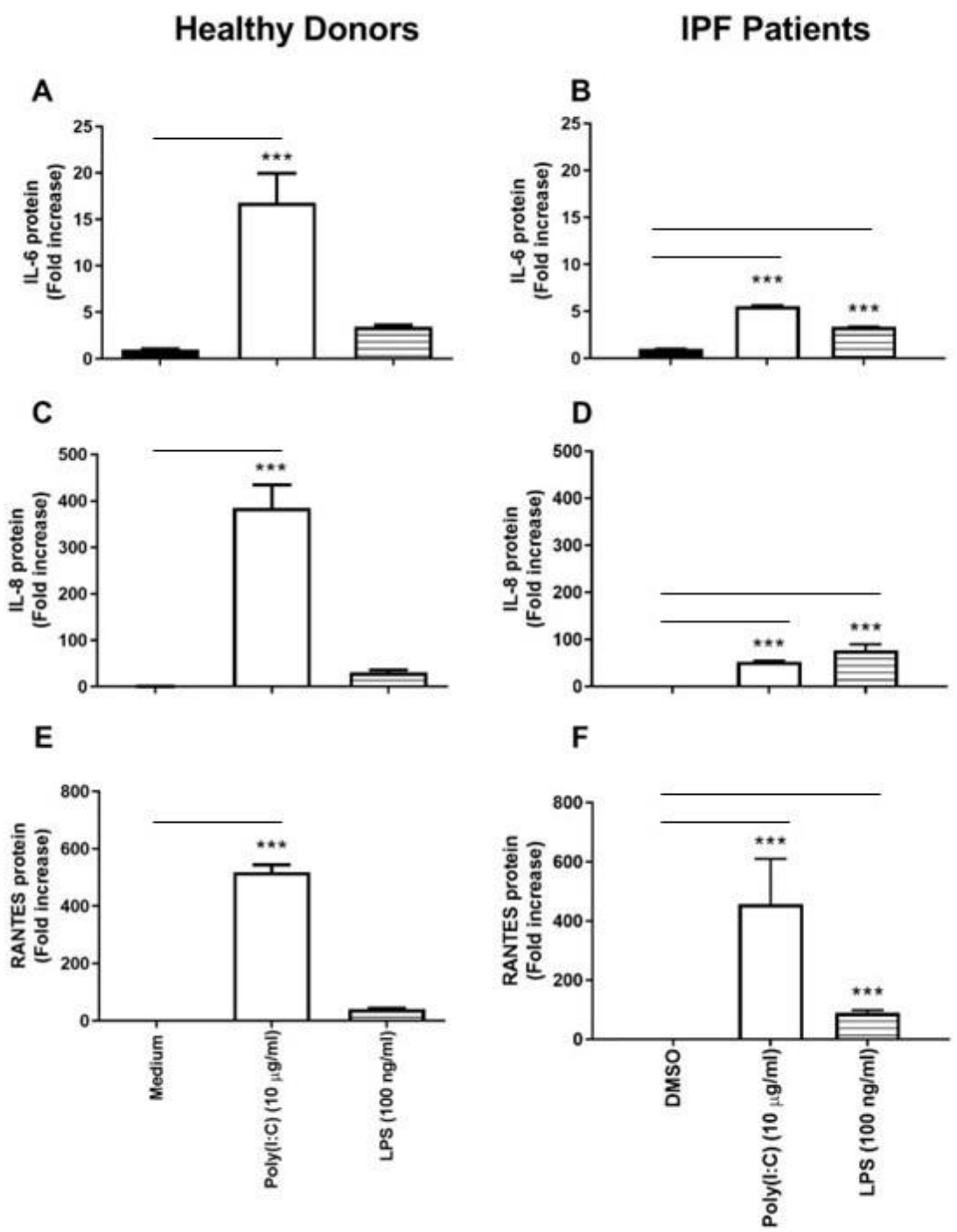

Figure 3.9. Effects of Poly(I:C) and LPS treatment on IL-6, IL-8 and RANTES protein production in primary human lung fibroblasts from healthy donors and IPF patients. Poly(I:C) treatment of IPF lung fibroblasts significantly increased protein production of IL-6, IL-8 and RANTES in healthy (**A, C, E**) and IPF fibroblasts (**B, D, F**). Treatment with LPS significantly upregulated protein production of IL-6, IL-8 and RANTES from IPF lung fibroblasts (**B, D, F**) at 24 h post-treatment, as quantitated by ELISA. A Kruskal-Wallis Test with a Dunn's multiple comparison post-hoc test was used to test for statistical differences. ***p<0.001: Medium-only compared with Poly(I:C) or LPS treatment, respectively. Each graph represents data from primary lung fibroblasts from 3 healthy donors and 3 IPF patients, respectively, performed twice (n=6). Results shown represent the mean +/- S.E.M. [Poly(I:C), 10 μg/ml; LPS, 100 ng/ml].

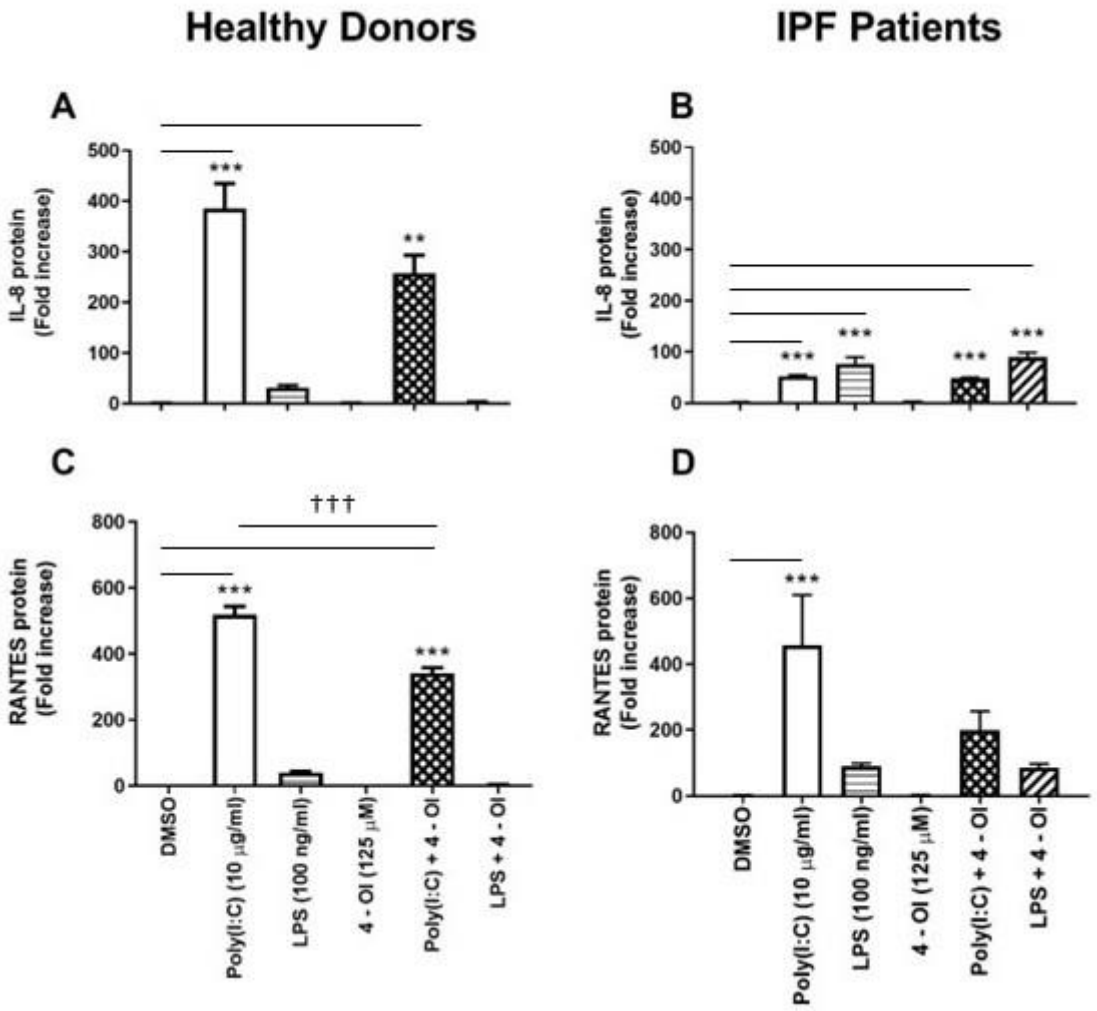

Figure 3.10. Effects of 4-OI on LPS-induced TLR4-driven protein production of IL-8 and RANTES production in primary human lung fibroblasts from healthy donors and IPF patients. Poly(I:C) treatment significantly increased protein production of IL-8 and RANTES, compared with DMSO in primary human lung fibroblasts from healthy donors (**A, C**) and IPF patients (**B, D**). LPS significantly increased IL-8 protein production, compared with DMSO in IPF fibroblasts (**B**). 4-OI had no effect on protein production of IL-8 and RANTES (**A-D**). In the presence of 4-OI (125 μM), Poly(I:C)-induced protein production of RANTES was significantly decreased in healthy lung fibroblasts compared with Poly(I:C) treatment alone **(C).** IL-8 and RANTES protein production was quantitated by ELISA at 24 h post-treatment. A Kruskal-Wallis Test with a Dunn's multiple comparison post-hoc test was used to test for statistical differences. ***p<0.001: compared with DMSO treatment only. **p<0.01, ***p<0.001: DMSO compared with Poly(I:C), LPS, Poly(I:C) & 4-OI or LPS & 4-OI treatment, respectively. †††p<0.001: Poly(I:C) & 4-OI treatment compared with Poly(I:C), treatment only.

Each graph represents data from primary lung fibroblasts from 3 healthy donors and 3 IPF patients, respectively, performed twice (n=6). Results shown represent the mean +/- S.E.M.. [Poly(I:C), 10 μg/ml; LPS, 100 ng/ml; 4-OI, 125 μM].

3.11. Effects of 4-OI on LPS-induced transcription of pro-inflammatory IL-8, IL-1β and caspase-1 in primary human lung fibroblasts from healthy donors and IPF patients.

Primary human lung fibroblasts from healthy donors and IPF patients were stimulated with Poly(I:C), LPS, 4-OI, co-treated with Poly(I:C) and 4-OI or LPS and 4-OI. Transcription of IL-8, IL-1β and caspase-1 was quantitated and used as read-out for Poly(I:C)-induced TLR3 activation as well as LPS-induced TLR4 activation. Treatment with LPS significantly increased IL-8 and IL-1β transcription in IPF lung fibroblasts compared with DMSO treatment only (**Fig. 3.11B, D, F)**. Treatment with 4-OI had no significant effect on IL-8, IL-1β or caspase-1 transcription in healthy or IPF lung fibroblasts. 4-OI treatment had no significant effect on Poly(I:C)- or LPS-induced IL-8, IL-1β and caspase-1 transcription, respectively.

3.12. Effects of 4-OI on LPS-induced transcription of anti-viral IFN-β, RANTES and RIG-I in primary human lung fibroblasts from healthy donors and IPF patients.

In this experiment, primary human lung fibroblasts from healthy donors and IPF patients were stimulated with Poly(I:C), LPS, 4-OI, co-treated with Poly(I:C) and 4-OI or LPS and 4-OI. Transcription of IFN-β, RANTES and RIG-I was quantitated and used as a read-out for TLR3 and TLR4-driven anti-viral response. Poly(I:C) treatment significantly induced RANTES transcription in healthy lung fibroblasts (**Fig. 3.12A; **p<0.01).** Poly(I:C) treatment significantly induced IFN-β, RANTES and RIG-I transcription in IPF fibroblasts (**Fig. 3.12B, D, F; *p<0.05, **p<0.01).** Treatment of IPF fibroblasts with LPS significantly increased RANTES transcription compared with DMSO (**Fig. 3.12D; *p<0.05).** Treatment with 4-OI had no significant effect on IFN-β, RANTES and RIG-I transcription in healthy or IPF lung fibroblasts. 4-OI treatment had no significant effect on Poly(I:C)- or LPS-induced IFN-β, RANTES and RIG-I transcription, respectively.

3.13. Effects of 4-OI on LPS-induced transcription of GSR, NQOI and HMOX-1 in primary human lung fibroblasts from healthy donors IPF patients.

Data regarding the function of oxidative damage in IPF is controversial. Increased expression of HMOX-1 has been associated with various pulmonary diseases, such as hyperoxia, asthma and obstructive pulmonary disease [396-398]. Conversely, the majority of studies report that increased levels of ROS as well as impaired antioxidative mechanisms are toxic and promote fibrotic events in IPF. Protective properties of NRF2-mediated antioxidant activity have been reported in a variety of organs including lungs [195, 382-387, 399]. In this

experiment, primary human lung fibroblasts from healthy donors and IPF patients were stimulated with Poly(I:C), LPS, 4-OI, co-treated with Poly(I:C) and 4-OI or LPS and 4-OI. Transcription of NRF2-induced antioxidants, GSR, NQOI and HMOX-1 was quantitated in order to investigate the effects of 4-OI on modulation of TLR3 and TLR4-associated transcription of antioxidant genes. Poly(I:C)- or LPS-treatment, respectively did not induce a significant change in GSR, NQOI and HMOX-1 transcription in healthy and IPF fibroblasts (**Fig. 3.13A-D)**. Treatment with 4-OI had no significant effect on GSR, NQOI and HMOX-1 I transcription in healthy or IPF lung fibroblasts. 4-OI treatment had no significant effect on LPS-induced IFN-β, RANTES and RIG-I transcription, respectively. 4-OI significantly increased Poly(I:C)-induced HMOX-1 in IPF lung fibroblasts (**Fig.13D; †p<0.05).**

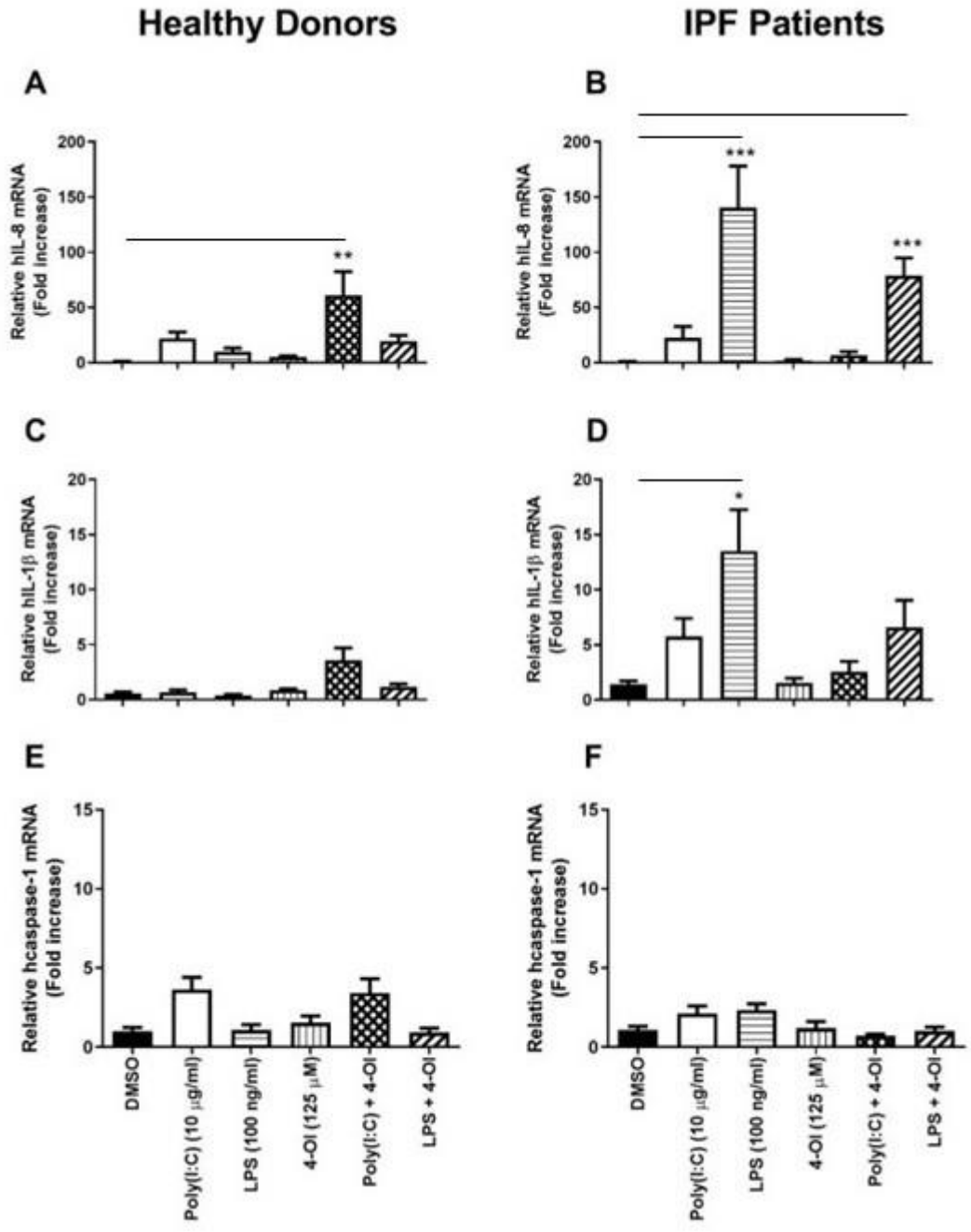

Figure 3.11. Effects of 4-OI on LPS-induced transcription of pro-inflammatory IL-8, IL-1β and caspase-1 in primary human lung fibroblasts from healthy donors and IPF patients. LPS treatment significantly increased IL-8 (**B**) and IL-1β (**D**) transcription in fibroblasts from IPF patients. 4-OI had no effect on IL-8, IL-1β and caspase-1 mRNA in healthy or IPF lung fibroblasts (**A-F).** IL-8, IL-1β and caspase-1 transcription was quantitated at 24 h post-treatment by qPCR analysis. A Kruskal-Wallis Test with a Dunn's multiple comparison post-hoc test was used to test for statistical differences. *p<0.05, **p<0.01, ***p<0.001: DMSO compared with LPS, Poly(I:C) & 4-OI treatment or LPS & 4-OI treatment, respectively. Each graph represents data from primary lung fibroblasts from 3 healthy donors and 3 IPF patients, respectively, performed twice (n=6). Results shown represent the mean +/- S.E.M. Poly(I:C), 10 μg/ml; LPS, 100 ng/ml; 4-OI, 125 μM].

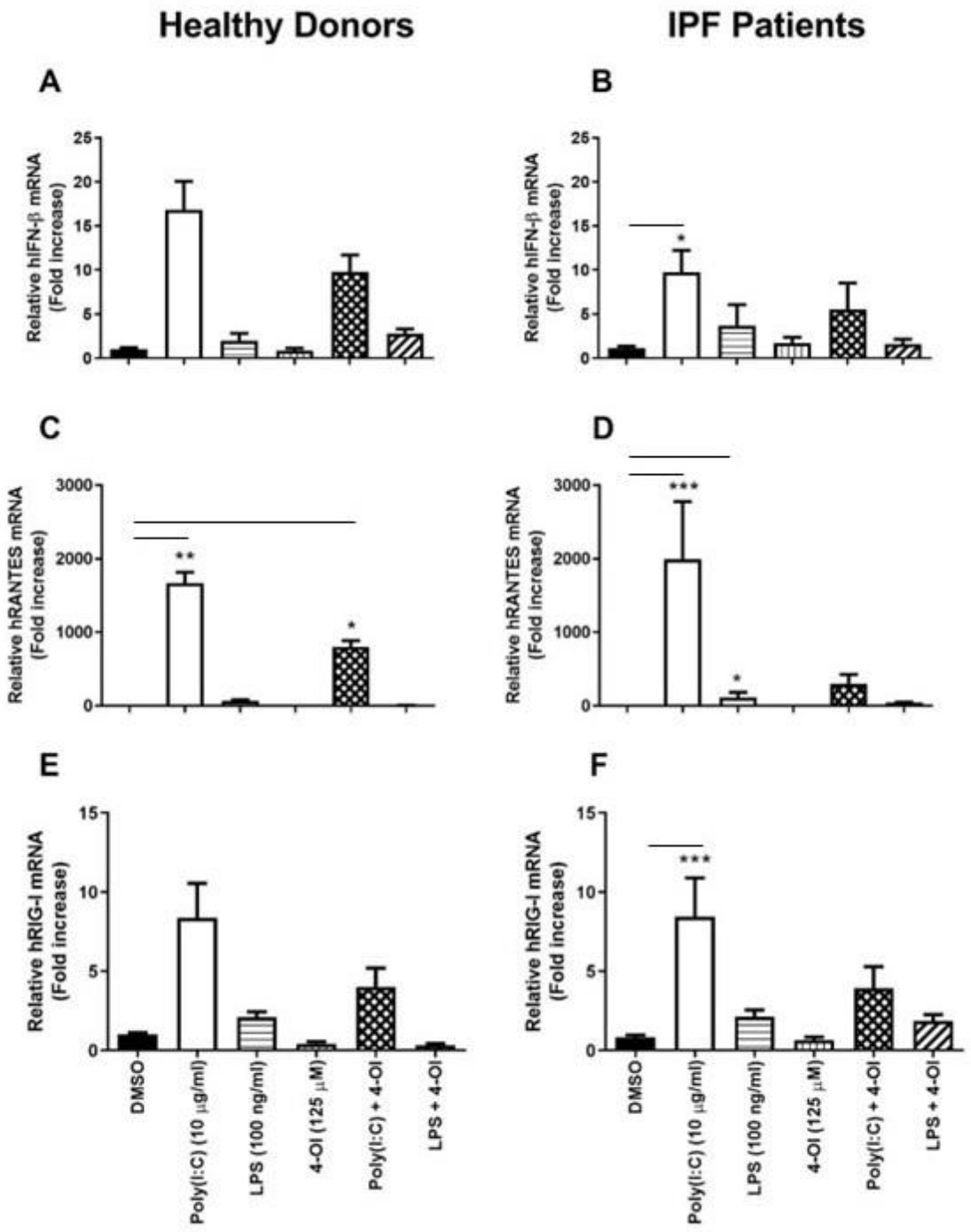

Figure 3.12. Effects of 4-OI on LPS-induced transcription of anti-viral IFN-β, RANTES and RIG-I in primary human lung fibroblasts from healthy donors and IPF patients. Transcription of IFN-β, RANTES and RIG-I was significantly induced following Poly(I:C) treatment in IPF lung fibroblasts (**B, D, F**). Poly(I:C) treatment significantly induced RANTES transcription in healthy lung fibroblasts (**C**). LPS treatment significantly induced RANTES transcription in IPF lung fibroblasts (**D**). 4-OI had no effect on IFN-β, RANTES and RIG-I transcription in healthy or IPF lung fibroblasts (**A-F),** as quantitated at 24 h post-treatment by qPCR analysis. A Kruskal-Wallis Test with a Dunn's multiple comparison post-hoc test was used to test for statistical differences. *p<0.05, **p<0.01, ***p<0.001: DMSO compared with Poly(I:C), LPS and Poly(I:C) & 4-OI treatment, respectively. Each graph represents data from primary lung fibroblasts from 3 healthy donors and 3 IPF patients, respectively, performed twice (n=6). Results shown represent the mean +/- S.E.M.. Poly(I:C), 10 μg/ml; LPS, 100 ng/ml; 4-OI, 125 μM].

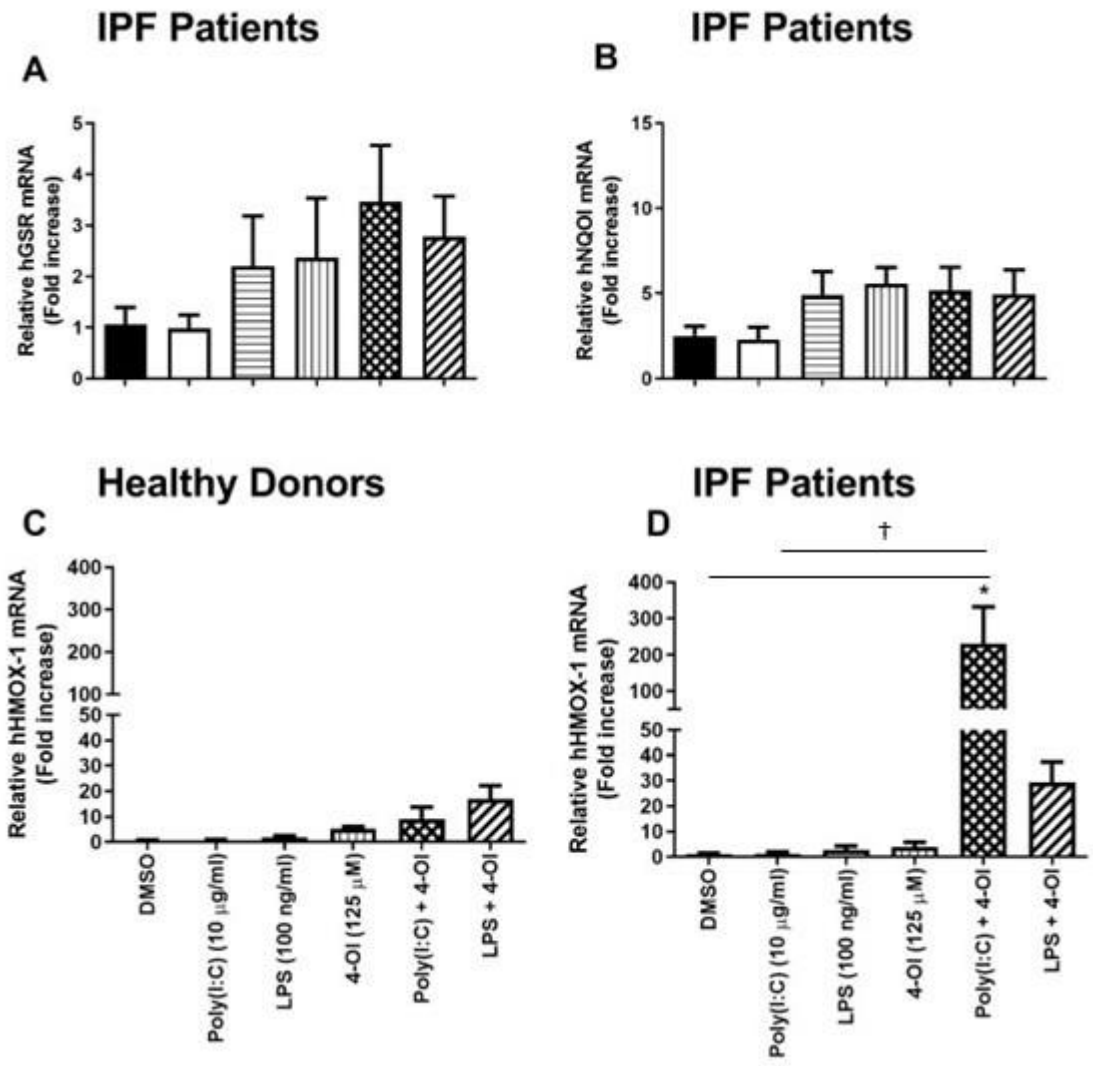

Figure 3.13. Effects of 4-OI on LPS-induced TLR4-driven transcription of GSR, NQOI and HMOX-1 in primary human lung fibroblasts from healthy donors and IPF patients. Poly(I:C), LPS or 4-OI treatment had no significant effect on the transcription of GSR, NQOI, and HMOX-1 in healthy and IPF fibroblasts, compared with DMSO treatment only (**A-D**). In the presence of 4-OI (125 µM), Poly(I:C)-induced HMOX-1 transcription was significantly increased in IPF fibroblasts compared with Poly(I:C) treatment alone **(B)** at 24 h post-treatment, as quantitated by qPCR analysis. A Kruskal-Wallis Test with a Dunn's multiple comparison post-hoc test was used to test for statistical differences. *p<0.05: DMSO compared with Poly(I:C) & 4-OI treatment. †p<0.05: Poly(I:C) & 4-OI treatment compared with Poly(I:C), treatment only. Each graph represents data from primary lung fibroblasts from 3 healthy donors and 3 IPF patients, respectively, performed twice (n=6). Results shown represent the mean +/- S.E.M. [Poly(I:C), 10 µg/ml; LPS, 100 ng/m; 4-OI, 125 µM].

3.14 Effects of 4-OI on TGF-β-induced transcription of antioxidants, HMOX-1 and NQOI in primary human lung fibroblasts from IPF patients.

TGF-β activation has been implicated in the pathogenesis of IPF [195, 229, 230, 400]. TGF-β is known to decrease levels of antioxidants such as glutathione (GSH) and to increase the production of reactive oxygen species, which are associated with the development and progression of IPF [195, 229, 230, 234]. In order to characterise the effects of 4-OI on TGF-β-induced mRNA expression of antioxidants, HMOX-1 and NQOI, primary human lung fibroblasts IPF patients were stimulated with TGF-β, 4-OI or co-treated with TGF-β and 4-OI. Fibroblasts treated with TGF-β exhibited no significant change in HMOX-1 (**Fig. 3.14A)** or NQOI transcription (**Fig. 3.14B)** when compared with DMSO. 4-OI treatment significantly increased HMOX-1 (**Fig. 3.14A; *** p<0.001**) and NQOI (**Fig. 3.14B; * p<0.05**) transcription IPF lung fibroblasts compared with DMSO treatment only. In the presence of TGF-β, 4-OI significantly increased HMOX-1 transcription (**Fig. 3.14A; † p<0.05**) in IPF fibroblasts compared with TGF-β treatment.

3.15. Effects of 4-OI on TGF-β-driven transcription of pro-fibrotic markers TGF-β, α-SMA, COL1A1 and COL3A1 in primary human lung fibroblasts from IPF patients.

Elevated levels of TGF-β, α-SMA, COL1A1 and COL3A1 are all indicative of tissue fibrosis [195, 229, 230, 400]. In this experiment, primary human lung fibroblasts from IPF patients were stimulated with TGF-β, 4-OI or co-treated with TGF-β and 4-OI, in order to characterise the effects of 4-OI on TGF-β-induced transcription of pro-fibrotic markers TGF-β, α-SMA, COL1A1 and COL3A1. TGF-β treatment had no significant effect on transcription of TGF-β (**Fig. 3.15A**), α-SMA (**Fig. 3.15B**), COL1A1 (**Fig. 3.15C)** and COL3A1 (**Fig. 3.15D)** in IPF fibroblasts compared with DMSO. 4-OI treatment had no significant effect on the transcription of TGF-β, α-SMA, COL1A1 and COL3A1 in IPF lung fibroblasts, respectively.

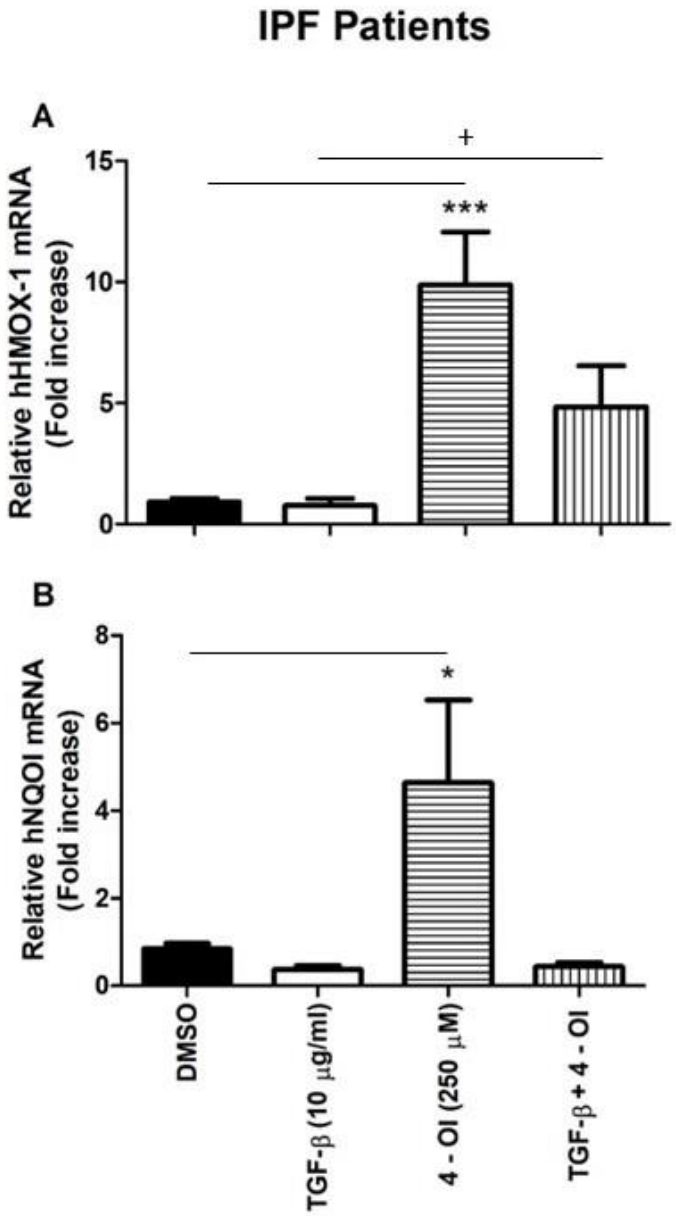

Figure 3.14. Effects of 4-OI on TGF-β-driven transcription of antioxidants, HMOX-1 and NQOI in primary human lung fibroblasts from IPF patients. Treatment of lung fibroblasts from IPF patients with TGF-β had no effect on the transcription of HMOX-1 (**A**) and NQOI (**B**), compared with DMSO. 4-OI treatment significantly increased HMOX-1 (**A**) and NQOI (**B**) transcription in IPF fibroblasts. In the presence TGF-β, 4-OI treatment significantly increased TGF-β-induced transcription of HMOX-1 (**A**) in fibroblasts from IPF patients at 24 h post-treatment, as quantitated by qPCR analysis. A Kruskal-Wallis Test with a Dunn's multiple comparison post-hoc test was used to test for statistical differences. ***p<0.001: DMSO compared with TGF-β treatment. $_{k}$p<0.05: TGF-β compared with TGF-β & 4-OI treatment. Each graph represents data from primary lung fibroblasts from 3 IPF patients performed twice (n=6). Results shown represent the mean +/- S.E.M. [TGF-β, 10 ng/ml; 4-OI, 250 μM].

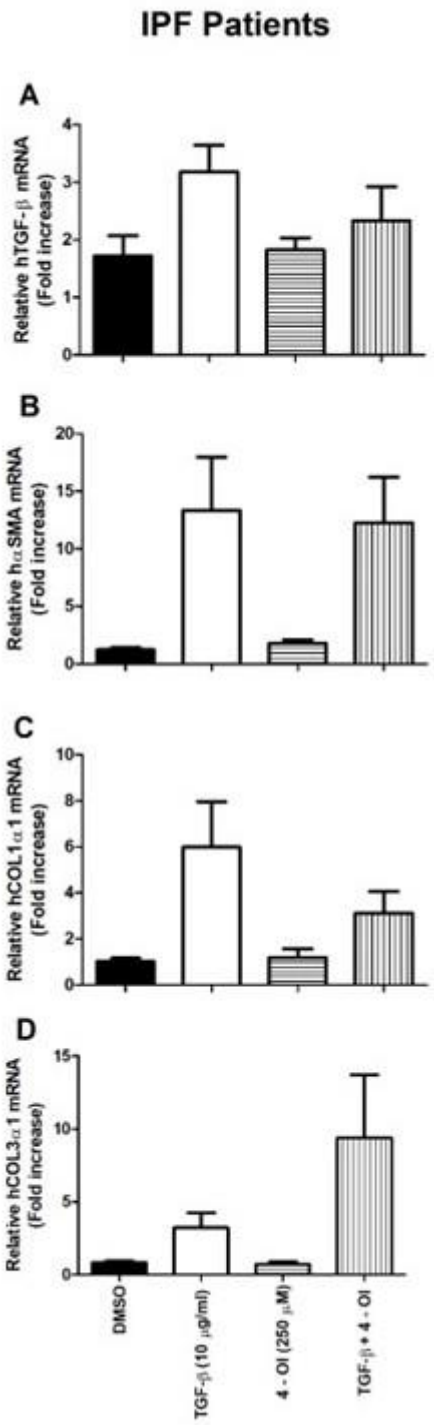

Figure 3.15. Effects of 4-OI on TGF-β-driven transcription of pro-fibrotic markers, TGF-β, α-SMA, COL1α1 and COL3α1 in primary human lung fibroblasts from IPF patients. Treatment of IPF lung fibroblasts for 24 h with DMSO, TGF-β, 4-OI or TGF-β & 4-OI, respectively, had no significant effect on transcription of TGF-β (**A**), α-SMA (**B**), COL1α1 (**C**) and COL3α1 (**D**), compared with DMSO treatment only, as quantitated by qPCR analysis. A Kruskal-Wallis Test with a Dunn's multiple comparison post-hoc test was used to test for statistical differences. Each graph represents data from primary lung fibroblasts from 3 IPF patients performed twice (n=6). Results shown represent the mean +/- S.E.M. [TGF-β, 10 ng/ml; 4-OI, 250 μM].

3.16. Effects of 4-OI on IL-6, IL-8 and RANTES protein production from primary human lung fibroblasts from healthy donors and IPF patients following live *Pseudomonas aeruginosa* infection for 8 h.

Historically, the human lower respiratory tract was believed to be sterile [401]. This was due to an inadequacy of culture-dependent techniques which were less sensitive than the PCR-based methodologies currently in use. Bacteria have been shown to cause injury to alveolar epithelial cells, which dysregulates the function of underlying pulmonary fibroblasts and promotes the development of IPF [402, 403]. Transcription of genes responsible for antibacterial defence, including alpha-defensin (AD) are elevated in patients with IPF compared with healthy individuals [354]. Moreover, bronchoalveolar lavage fluid (BALF) samples from IPF patients were found to contain a higher load of bacteria and increased frequencies of bacterial species such as *Prevotella, Neisseria,, Veillonella*, *Streptococcus* and *Staphylococcus* compared with healthy controls [83]. Increased bacterial load in IPF patients has been shown to be associated with accelerated disease progression and increased mortality rates [83, 85]. Studies have demonstrated the ability of itaconate to inhibit the growth of *Salmonella enterica*, *Legionella pneumophilia* and *Staphylococcus aureus* [232, 238]. The metabolite has been shown to exerts its antibacterial properties by inhibition of the enzyme isocitrate lysase (ICL). This enzyme is involved in the glyoxylate cycle, which is a bacterial process analogous to the TCA cycle [236]. The glyoxylate pathway is utilised by bacteria as a survival mechanism in low glucose-environments, including host phagolysosomes [232, 236, 238, 404]. In this experiment, primary human lung fibroblasts from healthy donors and IPF patients were infected with live *Pseudomonas aeruginosa* (*P. aeruginosa,* PAO1) for 8 h. Protein production of IL-6, IL-8 and RANTES was quantitated. Furthermore, we investigated the ability of 4-OI to modulate the effects of PAO1 on IL-6, IL-8 and RANTES production from these cells.

Live PAO1 infection significantly increased IL-8 production in healthy (**Fig. 3.16A; **p<0.01**) and IPF fibroblasts (**Fig. 3.16B; **p<0.01**), respectively, compared with DMSO. Live PAO1 infection significantly increased IL-6 production in healthy (**Fig. 3.16C; *p<0.05**) and IPF fibroblasts (**Fig. 3.16D; ***p<0.001**), respectively, compared with DMSO. Live PAO1 infection failed to induce RANTES response in healthy (**Fig. 3.16E)** and IPF fibroblasts (**Fig. 3.16F)**. 4-OI treatment had no significant effect on PAO1-induced IL-6, IL-8 or RANTES protein production **(Fig. 3.16A-F).** These results demonstrated that live infection with the Gram-negative bacteria, *P. aeruginosa*, increased production of the pro-inflammatory agents IL-6 and IL-8 in lung

fibroblasts from heathy donors and IPF patients. In this experiment, 4-OI had no effect on PAO1-induced cytokine production. The 8 h infection time used in the experiment may have been too early to have seen production of RANTES from these cells. The 8 h PAO1 infection duration is routinely used in order to prevent significant cell death during the experiment.

3.17. Effects of 4-OI on IL-8, IL-1β and caspase-1 transcription in primary human lung fibroblasts from healthy donors following live *P. aeruginosa* infection for 8 h.

As previously mentioned, increased bacterial load at diagnosis is associated with accelerated disease progression and increased mortality in IPF patients [83, 85]. Moreover, itaconate has been previously shown to exert its antibacterial properties through inhibition of the enzyme isocitrate lyase (ICL) [232, 236, 238, 404]. In this experiment, primary human lung fibroblasts from healthy donors were infected with live *P. aeruginosa* (PAO1) for 8 h.

Transcription of IL-8, IL-1β and caspase-1 was quantitated. Furthermore, we investigated the ability of 4-OI to modulate the effects of PAO1 on IL-8, IL-1β and caspase-1 transcription in these cells. Healthy lung fibroblasts infected with PAO1 had significantly increased levels of IL-8 (**Fig. 3.17A; ***p<0.001**) and IL-1β transcription (**Fig. 3.17B; *p<0.05**) compared with DMSO treated fibroblasts. Treatment of healthy donors' fibroblasts with 4-OI had no significant effect on the transcription of IL-8, IL-1β and caspase-1. 4-OI treatment significantly reduced PAO1-induced caspase-1 transcription in healthy lung fibroblasts compared with PAO1 infection only.

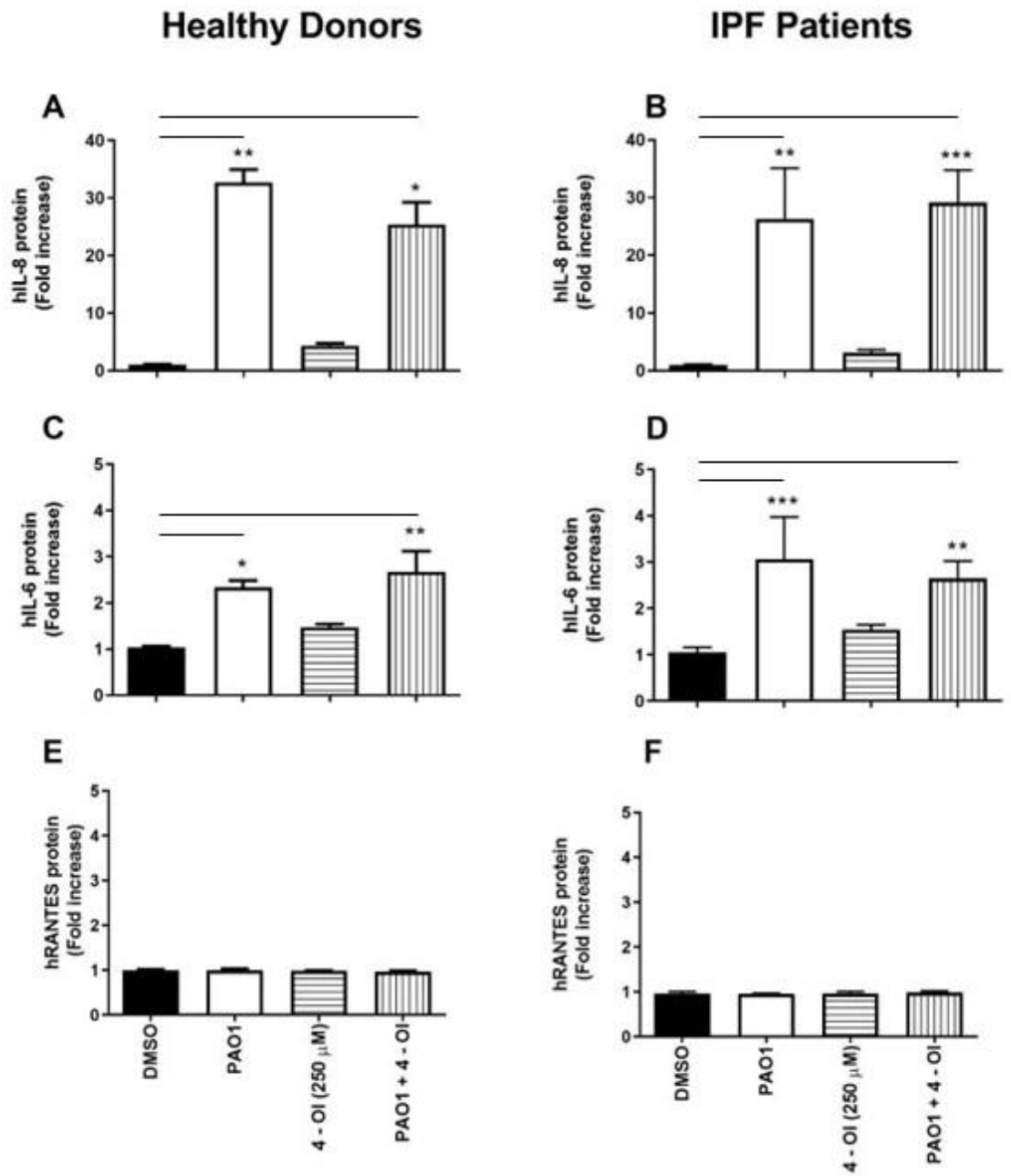

Figure 3.16. Effects of 4-OI on protein production of IL-6, IL-8 and RANTES in primary human lung fibroblasts from healthy donors and IPF patients, live infected with *P. aeruginosa.* PAO1 infection significantly increased IL-8 and IL-6 protein production in heathy donor (**A, C**), and IPF fibroblasts (**B, D**), compared with DMSO treatment only. Fibroblasts from healthy donors and IPF patients showed no change in protein production of RANTES upon PAO1 infection (**E, F**). 4-OI treatment resulted in no significant change in protein production of IL-6, IL-8 and RANTES in control and IPF fibroblasts (**A-F**). 4-OI treatment produced no significant change in PAO1-induced IL-8, IL-6 and RANTES response in healthy and IPF fibroblasts relative to PAO1 infection at 8 h post-treatment, as quantitated by ELISA analysis. A Kruskal-Wallis Test with a Dunn's multiple comparison post-hoc test was used to test for statistical differences. *p<0.05, **p<0.01, ***p<0.001: DMSO compared with PAO1 or PAO1 & 4-OI treatment, respectively. Each graph represents data from primary lung fibroblasts from 3 healthy donors and 3 IPF patients, respectively, performed twice (n=6). Results shown represent the mean +/- S.E.M. [MOI of 30 (30 PA01: 1 fibroblast); 4-OI, 250 μM].

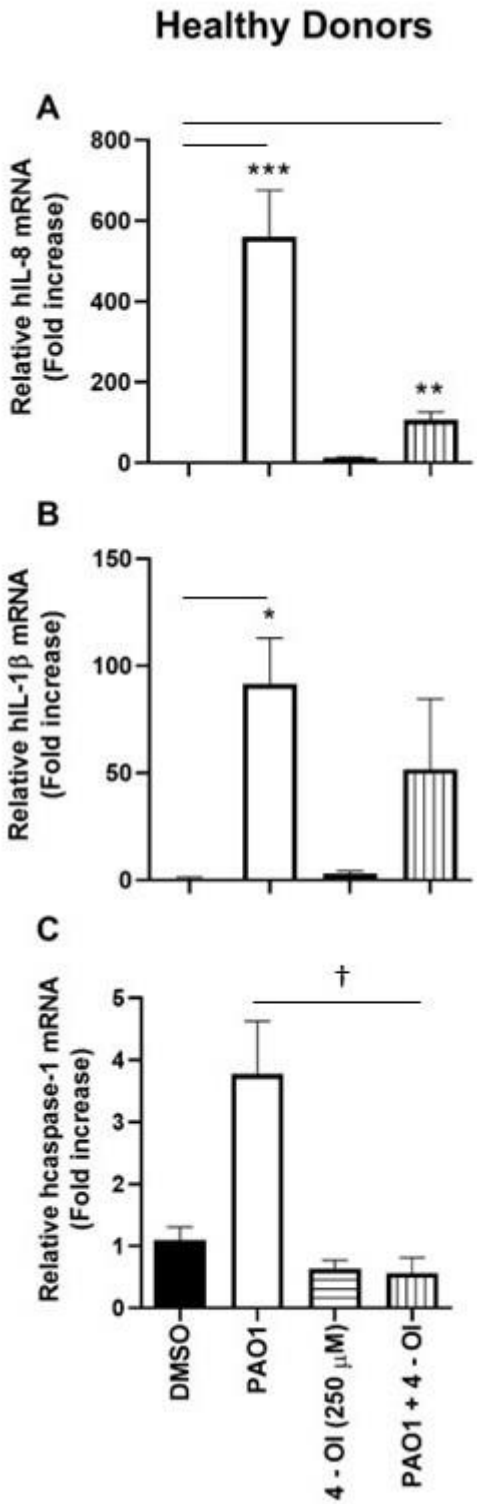

Figure 3.17. Effects of 4-OI on IL-8, IL-1β and caspase-1 transcription in primary human lung fibroblasts from healthy donors following live *P. aeruginosa* infection for 8 h. Healthy lung fibroblasts infected with PAO1 exhibited an increase in transcription of IL-8 (**A**) and IL-1-β (**B**) compared with DMSO treatment. Treatment of healthy donors' fibroblasts with 4-OI caused no change in the transcription of IL-8, IL-1β and caspase-1. 4-OI had no significant effect on IL-8, IL-1β and caspase-1 transcription **(A-C).** 4-OI treatment decreased PAO1-induced transcription of caspase-1 (**C**) compared with PAO1 infection only at 8 h post-treatment, as quantitated by qPCR analysis. A Kruskal-Wallis Test with a Dunn's multiple comparison post-hoc test was used to test for statistical differences. *p<0.05, **p<0.01, ***p<0.001: DMSO compared with PAO1 or PAO1 & 4-OI treatment, respectively. +p<0.05: PAO1 only compared with PAO1-β & 4-OI treatment. Each graph represents data from primary lung fibroblasts from healthy donors performed twice (n=6). Results shown represent the mean +/- S.E.M. [MOI of 30 (30 PA01: 1 fibroblast); 4-OI, 250 μM].

3.18. Effects of 4-OI on IFN-β, RANTES, RIG-I and IRG-1 transcription in primary human lung fibroblasts from healthy donors following live *P. aeruginosa* infection for 8 h.

In this experiment, primary human lung fibroblasts from healthy donors were infected with live *P. aeruginosa* (PAO1) for 8 h. Transcription of IFN-β, RANTES and RIG-I was quantitated. Furthermore, we investigated the effects of 4-OI treatment on live *P. aeruginosa* infection in the context of itaconate–encoding gene, *IRG-1* in lung fibroblasts from healthy donors. Healthy lung fibroblasts infected with PAO1 had significantly increased levels of RIG-I transcription (**Fig. 3.17C; **p<0.01**) compared with DMSO treated fibroblasts. Treatment of healthy donors' fibroblasts with 4-OI had no significant effect on the transcription of IFN-β, RANTES and RIG-I. 4-OI treatment had no significantly effect on PAO1-induced IFN-β, RANTES or RIG-I transcription in healthy lung fibroblasts compared with PAO1 infection only.

3.19. Investigation of the TLR3 and RIG-I protein expression in primary human lung fibroblasts from healthy donors and IPF patients following using western blot.

Our lab has previously shown that defective TLR3 plays an essential role in IPF progression. Specifically, we have demonstrated that the TLR3 SNP (*TLR3* L412F, rs3775291) responsible for aberrant TLR3 signalling is associated with a significantly greater risk of mortality and an accelerated decline in FVC in IPF patients [161]. Our previous qPCR data demonstrated that 4-OI downregulated Poly(I:C)-induced RIG-I transcription. RIG-I acts as cytoplasmic sensor of viral RNA. Its downstream signalling induces type 1 IFN production and anti-viral gene expression, making it a crucial mediator of inflammatory response. In this experiment, primary human lung fibroblasts form healthy donors and IPF patients were stimulated with Poly(I:C), 4-OI or co-treated with Poly(I:C) and 4-OI. The protein expression of TLR3 and RIG-I was measured. Treatment with Poly(I:C) induced TLR3 and RIG-I protein expression in both healthy and IPF fibroblasts. 4-OI had no effect on the expression of TLR3 and RIG-I protein. Lung fibroblasts from healthy donors and IPF patients showed a decrease in Poly(I:C)-induced TLR3 and RIG-I protein expression following 4-OI treatment. These results suggest that 4-OI can modulate Poly(I:C)-induced, Poly(I:C)-driven protein expression of TLR3 and RIG-I in healthy and IPF lung fibroblasts.

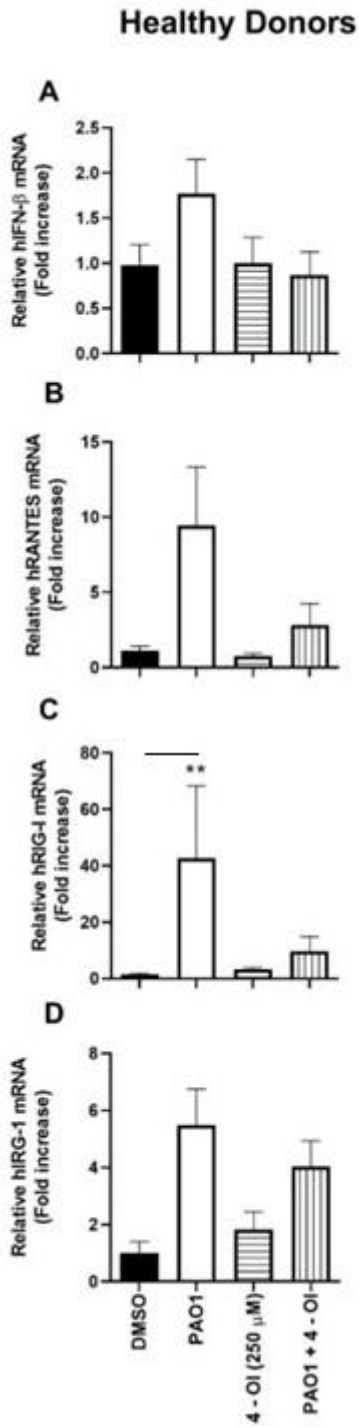

Figure 3.18. Effects of 4-OI on IFN-β, RANTES, RIG-I and IRG-1 transcription in primary human lung fibroblasts from healthy donors following live *P. aeruginosa* infection for 8 h. Healthy lung fibroblasts infected with PAO1 exhibited an increase in RIG-I transcription (**C**) compared with DMSO treatment. Treatment with 4-OI had no significant effect on IL-8, IL-1β and caspase-1 transcription **(A-C)**, at 8 h post-treatment, as quantitated by qPCR analysis. Kruskal-Wallis Test with a Dunn's multiple comparison post-hoc test was used to test for statistical differences. **p<0.01: DMSO compared with PAO1 infection. Each graph represents data from primary lung fibroblasts from healthy donors performed twice (n=6). Results shown represent the mean +/- S.E.M. [MOI of 30 (30 PA01: 1 fibroblast); 4-OI, 250 μM].

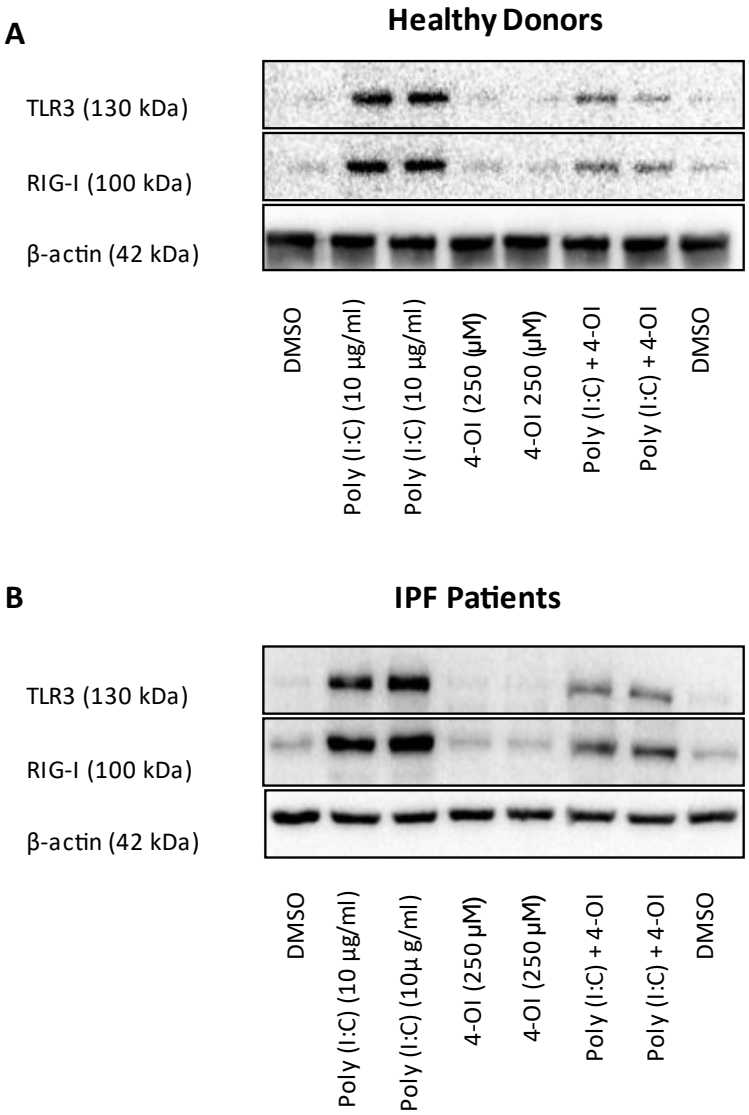

Figure 3.19. Investigation of the TLR3 and RIG-I protein expression in primary human lung fibroblasts from healthy donors and IPF patients using western blot. Protein expression of TLR3 and RIG-I was upregulated following Poly(I:C) treatment in primary human lung fibroblasts from healthy donors (A) and IPF patients (B). Treatment with 4-OI reduced Poly(I:C)-induced protein expression of TLR3 and RIG-I in healthy (A) and IPF fibroblasts (B) at 24 h treatment with Poly(I:C) (10 µg/ml), 4-OI (250 µM), Poly(I:C) (10 µg/ml) and 4-OI (250 µM). β-actin was used as a loading control. Each western blot represents data from primary lung fibroblasts from 3 healthy donors and 3 IPF patients, respectively, performed twice (n=6).

3.20 Discussion

Idiopathic pulmonary fibrosis is a fatal disorder, characterised by formation of fibrotic patches within the lung [1]. Although its exact causes are unknown, inflammation associated with viral and bacterial infection is believed to play a key role in the development and progression of the disease [405]. Our lab has previously identified a TLR3 SNP (*TLR3* L412F, rs3775291) which confers aberrant TLR3 function, fibroblast proliferation, cytokine, and interferon response in 412F-variant IPF patients [161, 366]. We reported a greater risk of mortality and an accelerated FVC in IPF patients heterozygous and homozygous for *TLR3* L412F, compared with L412F WT patients, thereby demonstrating the importance of TLR3 function in the progression of IPF [161, 366].

Itaconate is a metabolite generated during the Krebs cycle which has recently been re-discovered in terms of its anti-inflammatory, anti-viral and anti-microbial roles [406]. In 2020, Ogger *et al.* published the first research article which demonstrated a role for itaconate in IPF in primary alveolar macrophages and in the bleomycin model of pulmonary fibrosis [245]. These authors demonstrated that itaconate levels were reduced in BAL fluid from IPF patients and that itaconate was protective in the bleomycin model of IPF [245].

In an earlier study, Mills *et al*. reported that 4-OI; a synthetic analogue of itaconate, downregulated Poly(I:C)-driven IFN-β production in human PBMCs, and decreased Poly(I:C)-driven IL-1β transcription in mouse BMDMs [195]. These data suggested that 4-OI downregulated Poly(I:C)-induced anti-viral and pro-inflammatory responses in macrophages. To date, the effects 4-OI on Poly(I:C)-driven function in IPF has not been previously reported.

In this chapter, we investigated the role of 4-OI in primary human lung fibroblasts from healthy donors and IPF patients. Specifically, we examined the ability of itaconate/4-OI to modulate TLR3 function in these lung fibroblasts in the context of Poly(I:C)-induced NF-κB and IRF3-induced pro-inflammatory and anti-viral mediators, as well as the transcription of pro-fibrotic markers, and NRF2-induced anti-oxidant activity.

Firstly, we characterised the effects of 4-OI on Poly(I:C)–induced, Poly(I:C)-mediated production of IL-8, IL-6 and RANTES protein in lung fibroblasts from healthy controls and IPF patients **(Fig. 3.4A-F).** We reported that production of IL-8, IL-6 and RANTES protein was significantly induced following Poly(I:C) treatment, compared with DMSO treatment, in lung fibroblasts from healthy donors and IPF patients. This is in agreement with findings by other authors which demonstrated that activation of TLR3 readily induced NF-κB and IRF3 signalling pathways [3, 95, 130, 132, 141, 231, 407].

We demonstrated that on its own, 4-OI treatment had no effect on protein production of IL-8, IL-6 and RANTES in lung fibroblasts from healthy donors and IPF patients (Fig. 3.4A-F). Other studies carried out in human monocytes, infected with influenza A, showed an increase in IL-8 protein production following treatment with DI; a synthetic analogue of itaconate, in both infected and uninfected cells [370]. Numerous studies have demonstrated that signalling of NF-κB induced overproduction of IL-8, and drives the pro-inflammatory response, detrimental to the development and progression of IPF [3, 408-410]. Moreover, other authors reported elevated levels of IL-8 protein in the BALF serum, plasma, and sputum of IPF patients compared with healthy controls [376, 411-414]. We predict that increased presence of 4-OI would not be beneficial in relation to Poly(I:C)-induced IL-8 production in the context of IPF.

In this study, we reported that the 4-OI-mediated reduction in Poly(I:C)-induced production of IL-6 protein in lung fibroblasts from IPF patients was not significant (Fig. 3.4D) . Other studies have shown that itaconate reduced IL-6 protein production in LPS-stimulated murine BMDMs, human chondrocytes and human lung fibroblasts [192, 229, 415, 416]. 4-OI's ability to downregulate IL-6 response may be explained by its NRF2-inducing properties, as NRF2 has been shown to directly inhibit IL-6 transcription [195, 230]. Bambouskova *et al.* reported that itaconate inhibited IL-6 response independently of NRF2 activation, via induction of ATF3 [229]. Increased ATF3 expression led to inhibition of NF-κB inhibitor zeta (IκBζ) protein-induction, which limits IL-6 transcription [229]. Other studies have demonstrated increased levels of IL-6 in serum from IPF patients [376, 417, 418].

In this study, protein production of RANTES was used as a read-out for anti-viral chemokine activity. We demonstrated that 4-OI significantly decreased Poly(I:C)-induced RANTES in IPF lung fibroblasts **(Fig. 3.4E).** Other authors demonstrated anti-viral properties of itaconate using the murine model of influenza A virus, whereby IRG-1 was highly upregulated in the pulmonary tissue of infected mice [227]. In a more recent study by Sohail *et al.* induction in IRG-1 transcription has been demonstrated in human PBMCs and macrophages infected with IAV [370]. The same study reported downregulation of IFN responses in IAV infected human macrophages by 4-OI [370]. 4-OI was shown to inhibit viral transcription in peripheral blood mononuclear cells [370]. Other studies demonstrated that itaconate inhibited stimulator of interferon genes (STING), which led to a decrease in type I interferon response [195, 231]. Our previous data showed a correlation between worsened IPF prognosis, increased rate of AE-related mortality and dysregulated type I IFN response, including attenuated production of Poly(I:C)-induced RANTES protein by primary human lung fibroblasts

[161, 366]. The reduction in Poly(I:C)-driven RANTES protein production in IPF lung fibroblasts reported in our study may be pathogenic in the context of IPF.

IL-8, IL-1β and caspase-1 are markers of NF-κB activation, associated with enhanced levels of inflammation, which has shown to be detrimental in IPF [3]. Other authors demonstrated that 4-OI downregulated IL-1β transcription in murine BMDMs co-treated with itaconate and Poly(I:C) [192, 195]. In this chapter, we examined the effects of 4-OI on transcription of proinflammatory genes, IL-8, IL-1β and caspase-1 in primary human lung fibroblasts from healthy donors and IPF patients. We report that although overall, 4-OI increased Poly(I:C)-induced production of IL-8 protein **(Fig. 3.4B),** Poly(I:C)-induced transcription of IL-8 was decreased, respectively, non-significantly **(Fig. 3.5B).** 4-OI reduced IL-1β transcription in IPF lung fibroblasts and significantly decreased caspase-1 transcription in lung fibroblasts from healthy donors and IPF patients **(Fig. 3.5C, D).** This repression may be explained by inhibition of IκBζ production by itaconate, via induction of ATF3, which impedes NF-κB signalling and decreases the expression of NF-κB-activated genes, such as IL-8, IL-1β and capsase-1 [229]. Other authors reported that 4-OI alkylated cysteine residues on GAPDH, which led to attenuation in the enzyme activity, production of lactate and extra cellular acidification rate (ECAR). As a result, 4-OI reduced nuclear translocation of NF-κB as well the expression of IL-1β, TNF, and iNOS in LPS-activated, murine macrophages [400]. Moreover, itaconate has been shown to induce NRF2, resulting in reduced IL-1β expression, both indirectly through inhibition of ROS and iNOS production, and directly via inhibition of the transcriptional initiation of IL-1β gene [195, 230]. Additionally, Tannahill *et al.* showed that inhibition of SDH by itaconate reduced the production of IL-1β, generated upon succinate oxidation [209]. In terms of IPF, other studies drew association between increased transcription of IL-1β and exacerbation of fibrotic events using bleomycin model of pulmonary fibrosis [285, 419]. Upregulated transcription of IL-8 has been linked to a more adverse disease prognosis and higher mortality in patients [376, 414, 420]. Therefore, our data indicates a potential beneficial effect of 4-OI in terms of reduction of IL-8, IL-1β and caspase-1 transcription in IPF lung fibroblasts.

It has been proposed that viral infection plays a significant role in the pathology of IPF [421-423]. Other studies demonstrated the anti-viral properties of itaconate using animal models of Influenza A and Zika virus infection [227, 243, 281]. In this chapter we examined the effects of 4-OI on Poly(I:C)-induced mRNA transcription of IFN-β, RANTES and RIG-I in primary human lung fibroblasts from healthy donors and IPF patients. We showed that 4-OI treatment

of healthy and IPF lung fibroblasts reduced Poly(I:C)-induced IFN-β, RANTES and RIG-I transcription (Fig. 3.6A-F), this reduction was not significant, with the exception of Poly(I:C)-induced IFN-B transcription, which was significantly decreased in healthy lung fibroblasts (Fig. 3.6A). In 2018, Mills *et al.* demonstrated 4-OI's ability to inhibit LPS and Poly(I:C)-induced production of type I IFNs in murine macrophages [195]. The downregulation of IFN-β, RANTES and RIG-I transcription can be explained by itaconate's ability to induce NRF2 [195, 230]. Activation of NRF2 leads to downregulation of STING which has been previously shown to decrease type I IFN production in response to stimulation with herpes simplex virus and in lung fibroblasts from patients suffering from STING-associated vasculopathy [231]. The close relation between itaconate and type I IFNs can also be seen in the study by Naujoks *et al.* which showed that type I IFNs positively regulated IRG-1 expression, providing the evidence for the existence of regulatory feedback loop between IRG-1 and type I IFNs [232]. Our previous data linked reduced IFN-β, RANTES ad RIG-I transcription in response to Poly(I:C) stimulation in lung fibroblast to an accelerated rate of IPF progression as well as AE-related death in IPF [161, 366]. Based on our previous data, the reduction in Poly(I:C)-induced, IRF3 driven transcription of IFN-β, RANTES and RIG-I in response to 4-OI treatment, is indicatory of potential pathogenic effects of itaconate in IPF.

A large body of data has demonstrated the detrimental effects of oxidative stress in IPF, with positive correlation between levels of ROS and the rate of the disease progression as well as life expectancy of IPF patients [382-385]. Previous studies by other authors showed that itaconate induced the activity of NRF2 in human and mouse macrophages [195]. In this study, the effects of 4-OI on the transcription of IRG-1 as well as NRF2 –driven expression of the anti-oxidants HMOX-1, GSR and NQOI were examined in primary human lung fibroblasts from healthy donors and IPF patients. We reported that Poly(I:C) treatment of healthy control lung fibroblasts had no significant effect on the transcription of IRG-1 (Fig. 3.7G). Treatment with Poly(I:C) significantly increased IRG-1 transcription in lung fibroblasts from IPF patients (Fig. 3.7H). This is the first study to report Poly(I:C)-driven, Poly(I:C)-induced IRG-1 transcription in IPF lung fibroblasts. 4-OI reduced Poly(I:C)-induced IRG-1 transcription in IPF lung fibroblasts, which is indicative of self-regulatory, negative feedback loop of IRG-1 (Fig. 3.7H). Recently, a study by Ogger *et al.* showed a reduction in the IRG-1 mRNA in alveolar macrophages derived from IPF patients [245]. The same study reported greater levels of fibrosis exhibited by IRG-$1^{-/-}$ mice in the bleomycin model of pulmonary fibrosis [245]. Moreover, itaconate reduced wound healing capacity as well as cellular proliferation in

cultured lung fibroblasts from IPF patients [245]. Additionally inhaled itaconate produced anti-fibrotic response in mice [245]. These recent findings suggest a protective role of IRG-1 in pulmonary fibrosis. Therefore, the increased Poly(I:C)-induced IRG-1 transcription in IPF lung fibroblasts observed in our study may provide a protective effect in IPF.

In this chapter, we demonstrated that treatment with 4-OI significantly increased transcription of HMOX-1 in healthy lung fibroblasts (Fig. 3.7A), as well as in HMOX-1 and GSR transcription in IPF fibroblasts (Fig. 3.7B, D). 4-OI treatment significantly increased HMOX-1 transcription compared with DMSO in healthy and IPF lung fibroblasts (Fig. 3.7A, B). 4-OI significantly upregulated GSR transcription in the presence of Poly(I:C) compared with DMSO in IPF lung fibroblasts (Fig. 3.7D). HMOX-1 mRNA was significantly increased by 4-OI in the presence of Poly(I:C) compared with Poly(I:C) in healthy and IPF lung fibroblasts (Fig. 3.7A, B). 4-OI significantly increased GSR transcription in the presence of Poly(I:C) compared with Poly(I:C) in IPF lung fibroblasts (Fig. 3.7D). The transcription of NQOI following 4-OI treatment in the presence of Poly(I:C) was reduced compared with Poly(I:C) treatment, in healthy and IPF lung fibroblasts, this reduction was not significant (Fig. 3.7E, F). These findings are in agreement with other authors who demonstrated 4-OI mediated upregulation in NRF2-dependant HMOX-1, GSR and NQOI transcription in murine macrophages [195]. The upregulation of NRF2-induced antioxidant genes, HMOX-1 and GSR by 4-OI may be explained by 4-OI-driven alkylation of cysteine residues on KEAP-1, a molecule which, under homeostatic conditions, targets NRF2 for lysosomal degradation [195]. Upon alkylation by itaconate, KEAP-1 is inhibited which results in activation of NRF2-induced genes [195]. Despite some contradictory data regarding the role of oxidative damage in IPF, the majority of studies demonstrated that increased levels of ROS as well as reduced anti-oxidant activity has detrimental effects on IPF progression Given that oxidative stress drives the development and progression of IPF, our findings regarding increased transcription of anti-oxidant genes HMOX-1, GSR and NQOI upon 4-OI treatment in the presence of Poly(I:C) are indicative of the protective role of 4-OI in terms of IPF pathology.

IPF is characterised by increased deposition of collagens and ECM proteins, which creates an imbalance between the activity of pro- and anti-fibrotic mediators, resulting in the scarring of the pulmonary tissue [3]. In this study we investigated the effects of 4-OI on Poly(I:C)-induced transcription of pro-fibrotic markers, TGF-β, α-SMA, COL3α3 and COL3α1 in healthy controls and IPF lung fibroblasts. We report that treatment of primary lung fibroblasts from IPF patients with 4-OI significantly decreased Poly(I:C)-induced transcription of pro-

fibrotic markers, α-SMA, COL3α3 and COL3α1 (Fig. 3.8B, D, F, H). We report that the 4-OI-mediated reduction in Poly(I:C)-induced TGF-β transcription in IPF lung fibroblasts was not significant (Fig. 3.8B). Our data is in agreement with the findings of Ogger *et al.* who using the bleomycin model of pulmonary fibrosis, demonstrated that IRG-$1^{-/-}$ mice presented with worsened elastance, airway resistance and compliance as well as increased collagen deposition compared with WT mice [245].

This study demonstrated that 4-OI decreased Poly(I:C)-induced transcription of pro-fibrotic markers TGF-β, α-SMA, COL3α1 and COL1α. These inhibitory effects may be explained by the anti-inflammatory properties of itaconate, exerted through inhibition of various pro-inflammatory agents, such as IL-1β as well as ROS and iNOS [195, 209, 229, 230]. Other studies have shown that IPF lung fibroblasts generate excessive contractile force, in order to induce the production of various pro-fibrotic agents, such as collagens, α-SMA and TGF-β [388-391]. Bergeron *et al.* reported increased transcription in TGF-β in lung biopsies from IPF patients, compared with healthy controls [424]. Moreover, protein production of α-SMA was significantly elevated in blood serum from patients with IPF [391]. Although promising in terms of the therapeutic outcome, further investigation into whether the downregulation in the transcription of TGF-β, α-SMA, COL3A1 and COL1A1 by 4-OI can directly translate into reduction in fibrosis in patients with IPF is required.

Other authors have shown that itaconate regulated LPS-dependant signalling in human and mouse macrophages [192, 195, 229]. In this chapter, we investigated whether the effects of 4-OI were limited to modulation of TLR3 function in healthy and IPF lung fibroblasts. We examined the effects of 4-OI on LPS-induced production and transcription of pro-inflammatory, anti-viral and pro-fibrotic agents, as well as levels of anti-oxidant activity in primary human lung fibroblasts from healthy donors and IPF patients. We report that 4-OI significantly decreased LPS-induced RANTES production (and IL-8, non-significantly) in lung fibroblasts from healthy donors (Fig. 3.10A-D). Itaconate has a number of anti-inflammatory properties of itaconate, such as SDH and glycolytic inhibition as well as induction of NRF2 and ATF3. [195, 209, 230, 400, 408]. Other authors reported that itaconate attenuated STING in NRF2- dependant manner which may explain its ability to reduce LPS-induced RANTES production [195, 231]. Our data shows that in addition to modulation of TLR3 function, 4-OI has the ability to modulate TLR4-driven production of the pro-inflammatory IL-8 and the anti-viral RANTES in lung fibroblasts from healthy donors but not in IPF lung fibroblasts.

Other authors have shown that 4-OI decreased LPS-induced IL-1β transcription in mouse BMDMs and human PBMCs, it also reduced pro-IL-1β mRNA in mouse macrophages [192, 195]. We examined the effects of 4-OI on LPS-driven, TLR4 mediated transcription of pro-inflammatory genes, IL-8, IL-1β and caspase-1 in IPF lung fibroblasts. Treatment with 4-OI decreased LPS-induced transcription of IL-8, IL-1β and caspase-1 in lung fibroblasts from IPF patients, however this decrease was not significant (Fig. 3.11B, D, F). Itaconate's ability to decrease LPS-driven IL-8, IL-1β and caspase-1 mRNA can be explained by the electrophilic nature of the metabolite, whereby via activation of ATF3, it inhibits the production of IκBζ, a known transcriptional coactivator of selected NF-κB target genes, such as IL-8, IL-1β and capsase-1 [229]. In addition, other studies have shown that itaconate induced NRF2, which decreased IL-1β expression, both indirectly through inhibition of ROS and iNOS production, and directly via inhibition of the transcriptional initiation of IL-1β gene [195, 230]. Moreover, Liao *et al.* demonstrated that 4-OI reduced the rate of glycolysis via alkylation of GAPDH, which diminished nuclear NF-κB translocation and inhibition of the expression of IL-1β, TNF, and iNOS [400]. Finally, Lampropoulou *et al.* reported that inhibition of SDH by itaconate reduced the production of IL-1β, generated upon succinate oxidation [192]. Increased transcription IL-1β has been linked to induction of exacerbation of fibrotic events in the mouse bleomycin model of pulmonary fibrosis. [285, 419]. Moreover, increased transcription of IL-8 has been linked to a worsened prognosis in IPF [414, 420, 425]. We predict that the decrease in 4-OI-mediated, TLR4-driven IL-8, IL-1β and capsase-1 transcription observed in our study may have a potential therapeutic effect in terms of the reduction in inflammation-related pathology in IPF.

Induction of TLR4 by viral and bacterial PAMPs triggers a signalling cascade which leads to activation of NF-κB and IRF3 signalling pathways [130, 373, 426-429]. RIG-I functions as a sensor of viral and bacterial RNA [430, 431]. Activation of RIG-I also leads to induction of NF-κB and IRF3 signalling which results in increased expression of pro-inflammatory cytokines and type I IFNs [130, 373, 426-431].

The role of Type I IFNs during viral infection is widely recognized, however, the importance of Type I IFN signalling during bacterial infection is lesser known [432, 433]. For example, Stanley *et al.* reported that type I IFNs signalling contributed to pathogenesis during *Mycobacterium tuberculosis* (MTB) infection in mice [432]. In this study, we investigated the effects of 4-OI on TLR4-driven mRNA transcription of IFN-β, RANTES and RIG-I in primary human lung fibroblasts from healthy donors and IPF patients (Fig. 3.11A-F). We report an

increase in the transcription of LPS-induced RANTES and RIG-I in lung fibroblasts from healthy donors (Fig. 3.11C, E) as well as IFN-β, RANTES and RIG-I in IPF lung fibroblasts (Fig. 3.11B, D, F). Treatment with 4-OI reduced LPS-induced transcription of RANTES and RIG-I in healthy lung fibroblasts (Fig. 3.11C, E). This reduction was not significant. LPS-induced transcription of IFN-β and RANTES in lung fibroblasts from IPF patients was decreased (Fig. 3.11B, D). This decrease was not significant. Our results are in agreement with findings by Mills *et al.* who have demonstrated the inhibitory activity of 4-OI on LPS-induced production of type I IFNs in mouse macrophages [195]. The reduction in the transcription of IFN-β, RANTES and RIG-I reported in our study may be explained by 4-OI-mediated, NRF2- dependent inhibition of STING, which, as has been demonstrated by other authors, resulted in decreased type I IFNs response [195, 230, 231]. Our previous data suggested a correlation between the reduction in LPS-induced IFN-β, RANTES ad RIG-I transcription in lung fibroblast as well as AE-related death in IPF [366]. In this context, the reduction in TLR4-induced transcription of IFN-β, RANTES and RIG-I in response to 4-OI treatment, is indicatory of potential pathogenic effects of itaconate in IPF.

Other authors have demonstrated that oxidative stress is a pathogenic factor in IPF [382-385]. Mills *et al.* reported that itaconate decreased TLR4-driven production of ROS in human and murine macrophages [195]. We proceeded to study the effects of 4-OI on TLR4-driven mRNA transcription of anti-oxidants, HMOX-1, GSR and NQOI in primary human lung fibroblasts from healthy donors and IPF patients. In the presence of LPS, 4-OI treatment increased transcription of GSR and HMOX-1 compared with LPS treatment alone in healthy and IPF fibroblasts (Fig. 3.13A-D). This increase was not significant. In 2018, *Mills et al.* ~~who~~ demonstrated an increased transcription of HMOX-1 upon 4-OI treatment to be true in LPS stimulated murine macrophages [195]. The group has also reported an increase in the transcription of GSR and NQOI [195]. The enhanced 4-OI-mediated LPS-induced transcription in HMOX-1 observed in our study may be explained by 4-OI's ability to alkylate cysteine residues on KEAP-1, which in turn leads to activation of the antioxidant regulator, NRF2 [195]. Considering that other groups have previously related elevated levels of ROS to IPF progression [382-385], and that induction of NRF2-activated genes such as HMOX-1 leads to decrease in ROS production, we believe that the increased LPS-induced transcription in HMOX-1 and GSR by 4-OI itaconate may be of therapeutic benefit in terms of reduction in oxidative damage in the context of IPF pathogenesis. Other studies have identified TGF-β as a pleiotropic growth factor which governs a recruitment and proliferation of fibroblasts and which functions as a potent driver of fibrosis in IPF [388-391]. We investigated the effects of

4-OI on TGF-β- induced transcription of antioxidants, HMOX-1 and NQOI in primary human lung fibroblasts from IPF patients. We showed that IPF fibroblasts co-treated with TGF-β, and 4-OI significantly increased HMOX-1 transcription compared with TGF-β treatment (Fig. 3.14A). 4-OI-induced upregulation in NQOI transcription was reduced to basal levels following LPS and 4-OI co-treatment (Fig. 3.14B). Mills *et al.* reported that 4-OI has been shown to increase the expression of HMOX-1 and NQOI in murine macrophages [195]. These effects may be explained by the ability of itaconate to induce NRF2 signalling [195]. Studies by other authors demonstrated the detrimental effects of anti-oxidative stress in IPF, as increased levels of ROS as well as impaired anti-oxidative mechanisms were found to promote fibrotic events [382-385]. We believe that the ability of 4-OI to upregulate the transcription of anti-oxidant HMOX-1 in the presence of TGF-β in lung fibroblasts from IPF patients observed in our study might be of a beneficial value in terms of slowing down of the disease progression.

King *et al.* demonstrated that an increase in TGF-β levels in IPF resulted in the differentiation of resident fibroblasts into activated myofibroblasts in the lung, thereby promoting excessive ECM deposition and excessive collagen accumulation [434]. Ogger *et al.* reported that itaconate limited TGF-β transcription in murine macrophages [245]. We investigated the effects of 4-OI on TGF-β-driven transcription of pro-fibrotic agents TGF-β, α-SMA, COL1A1 and COL3A1 in primary human lung fibroblasts from IPF patients (Fig. 3.15A-D). We reported decreased TGF-β-induced TGF-β and COL1A1 transcription following 4-OI treatment compared with TGF-β treatment alone (Fig. 3.15A, C). This decrease was not significant. 4-OI-mediated increase in TGF-β-induced COL3α1 transcription in these cells was not significant (Fig. 3.15D). Anti-fibrotic properties of itaconate have been recently shown in a study by Ogger *et al.* where in the bleomycin model of fibrosis, *IRG-1*$^{-/-}$ mice exhibited an increased collagen deposition compared with WT mice. Moreover, the study reported upregulation in the expression of fibrosis-related genes in IRG-1$^{-/-}$ tissue-resident AMs (Tr-AMs) compared to WT [245]. The reduction in 4-OI-mediated TGF-β-driven transcription of TGF-β and COL1A1 in IPF fibroblasts, is indicative of the potential therapeutic use of itaconate in the future.

Lower respiratory tracts were believed to be sterile until utilization of novel techniques based on high-throughput sequencing of the gene coding for the 16S ribosomal RNA, demonstrated that the presence of various bacterial strains is a part of a healthy lung microbiota [435-440]. In recent years, other authors have identified bacterial infection as a causative factor in IPF development and progression as patients with IPF are often

compromised with higher bacterial loads compared with healthy individuals. [83, 85, 402, 403]. In order to examine the anti-bacterial properties of itaconate in the context of IPF, we infected primary human lung fibroblasts from healthy donors and IPF patients with live *Pseudomonas aeruginosa* (*P. aeruginosa,* PAO1) in the presence of 4-OI for 8 h, and subsequently quantitated protein production of IL-6, IL-8 and RANTES. Our study showed that protein production of IL-6 and IL-8 were significantly increased in healthy donors and IPF lung fibroblasts infected with PAO1, compared with DMSO treatment (Fig. 3.16 A-D). Infection with PAO1 did not affect production of RANTES in fibroblasts from healthy controls and IPF patients at the 8h time point (Fig. 3.16E, F).

Our data in this chapter is agreement with the findings of other authors, which demonstrated that PAO1 infection significantly induced the production of IL-6 and IL-8 in human bronchial epithelial cells as well as human pulmonary fibroblasts [441, 442]. Azghani *et al.* reported that *PAO1* exploited the EGFR/ERK signalling cascades to enhance IL-8 production in the lungs via NF-κB activation [442]. In this study, we demonstrated that IL-8 and IL-6 protein production was significantly upregulated following PAO1 infection in lung fibroblasts from healthy donors and IPF patients (Fig. 3.16A-D). Treatment of PAO1-infected healthy and IPF lung fibroblasts with 4-OI did not have a significant effect on the production of IL-6, IL-8 or RANTES protein (Fig. 3.16A-F). We conclude that live infection with PAO1 induced proinflammatory response in lung fibroblasts from healthy donors and IPF patients, however at this time point, 4-OI did not modulate PAO1-induced production of IL-6, IL-8 and RANTES protein in these cells. It is possible that the 8 h infection time used in the experiment may have been too early to see full, anti-bacterial properties of itaconate. Nevertheless, the 8 h PAO1 infection duration is routinely used in order to prevent significant cell death.

Other authors have shown increased transcription of pro-inflammatory mediators IL-8 and IL-1β during PAO1 infection [441, 443]. Increased transcription of IL-1β was shown in mouse models of pulmonary fibrosis [285, 419]. Moreover, higher levels of IL-8 mRNA correlated with to a worsen disease prognosis and higher mortality in patients [414, 420, 425]. In this study, we examined the effects of 4-OI on PAO1-infected lung fibroblasts from healthy donors in terms of transcription of pro-inflammatory mediators, IL-8, IL-1β and caspase-1, which we used as readouts of NF-κB activation. Lung fibroblasts were infected with live PAO1 in the presence of 4-OI, for 8 h. We report that transcriptional levels of IL-8 and IL-1β were significantly increased in fibroblasts infected with PAO1, compared with DMSO treatment (Fig. 3.17A, B). The transcription of caspase-1 was also upregulated; however, this increase was not

significant (Fig. 3.17C). Lung fibroblasts infected with PAO1 in the presence of 4-OI showed reduced transcription of IL-8, IL-1β and caspase-1 compared with fibroblasts infected with PAO1 (Fig. 3.17A-C). One of the mechanisms in which 4-OI may have downregulated PAO1-induced IL-8, IL-1β and caspase-1 transcription observed in our studies is the ability of itaconate to inhibit acetate assimilation as well as isocitrate lyase (ICL), an essential enzyme involved in bacterial glyoxylate cycle [232, 236, 237]. Considering the emerging importance of bacterial infection as a co-factor in development and progression of IPF, we believe that the reduction in PAO1-induced transcription of IL-8, IL-1β and caspase-1 by 4-OI in IPF lung fibroblasts might be of significance in terms of novel, therapeutic strategies in IPF.

Other authors have demonstrated that Type I IFNs played a major role in the immune response against bacterial infection, as evidenced by studies done on Gram-negative bacteria, such as *Salmonella spp* [444] or *Mycobacterium tuberculosis* [432]. In order to further examine the effects of 4-OI on PAO1-driven anti-viral response in healthy human lung fibroblasts, we live infected the pulmonary fibroblasts with PAO1 in the presence of 4-OI for 8 h, then measured transcriptional levels of IFN-β, RANTES, RIG-I and IRG-1. We report that fibroblasts infected with PAO1 showed increased transcription of IFN-β, RANTES, RIG-I and IRG-1 compared with DMSO treatment (Fig. 3.18A-D). This increase was not significant, with the exception of RIG-I transcription (Fig. 3.18C). We further showed that healthy lung fibroblasts infected with PAO1 in the presence of 4-OI exhibited attenuated transcription of IFN-β, RANTES, RIG-I and IRG-1 compared with PAO1 infection only at 8 h post-treatment (Fig. 3.18A-D). These results were not of statistical significance. Recent findings reported by Pylaeva *et al.* highlighted the detrimental role of Type I IFNs during acute lung infection with PAO1, whereby higher levels of Type I IFNs were correlated with increased biofilm formation, supporting the bacterial persistence in the infected lung [445]. Other studies have reported contradictory data regarding the role of IRF3 in *P. aeruginosa* infection, as mice deficient in IRF3, infected with PAO1 exhibited an impaired bacterial clearance from the lung [446]. In terms of PAO1-induced IRG-1 transcription, recently, other authors have reported that infection with PAO1 was shown to induce itaconate production from macrophages, however, contrary to the previous accounts, the bacteria was reported to use itaconate as a fuel for growth and replication [240, 447]. Whether 4-OI-mediated reduction in the transcription of PAO1-induced IFN-β, RANTES, RIG-I and IRG-1 is of beneficial or detrimental effects in IPF requires further investigation.

Data from our previous experiments suggest a modulatory role of 4-OI on TLR3 signalling as well as RIG-I transcription. Here, we investigated the effects of 4-OI directly on TLR3 and RIG-I protein expression in primary human lung fibroblasts from healthy donors and IPF patients, using western blot. We report that 4-OI treatment decreased Poly(I:C)-driven protein expression of TLR3 and RIG-I in both healthy and IPF lung fibroblasts (Fig. 3.18A, B). Both TLR3 and RIG-I serve as cellular sensors of bacterial and viral pathogens and are responsible for initiation of the anti-viral and the pro-inflammatory response [130, 367-369, 372, 430, 431]. The observed downregulation of RIG-I and TLR3 expression may be due to anti-inflammatory effects of itaconate, such as inhibition of SDH, which translates into reduction in IL-1β and ROS production [192, 209, 228]. Additionally, other authors have reported that itaconate exerted anti-inflammatory function through induction of NRF2-associated downregulation of ROS, iNOS, IL-6, TNF and IL-1β production [195, 229, 415]; Moreover, Bambouskova *et al.* demonstrated that the metabolite was shown to induce ATF3 which led to inhibition of IκBζ protein-induction, and by extension limited the production of IL-6, as well as IL-12B [229]. Finally, *Mills et al.* showed the ability of itaconate to attenuate the production of type I IFNs in response to TLR3 and TLR4 stimulation [195]. The suppressive effect of 4-OI on TLR3 and RIG-I protein expression is indicatory of the metabolite's anti-viral and anti-inflammatory properties, which may be of beneficial value in terms IPF treatment.

In this chapter, we demonstrated that 4-OI increased Poly(I:C)-induced IL-8 protein production in lung fibroblasts from healthy donors and IPF patients. The production of Poly(I:C)-driven IL-6 and RANTES production was attenuated following 4-OI treatment in IPF lung fibroblasts. We reported that 4-OI decreased Poly(I:C)-driven, NF-κB-dependent IL-8, IL-1β and caspase-1 transcription in IPF lung fibroblasts. Our study demonstrated a reduced transcription of Poly(I:C)-mediated, IRF3-induced IFN-β, RANTES and RIG-I upon 4-OI treatment in lung fibroblasts from healthy donors and IPF patients. We showed a significant increase in IRG-1 mRNA levels in lung fibroblasts harvested from IPF patients, upon stimulation with Poly(I:C). We reported that treatment with 4-OI increased the transcription of anti-oxidant genes, HMOX-1 in healthy lung fibroblasts, as well as HMOX-1 and GSR in lung fibroblasts from IPF patients. 4-OI increased the transcription of HMOX-1, GSR and NQOI in the presence of Poly(I:C) compared with DMSO and Poly(I:C) treatments. Lung fibroblasts from IPF patients showed a decreased Poly(I:C)-induced transcription of pro-fibrotic markers, TGF-β, α-SMA, COL3α3 and COL3α1 in response to 4-OI treatment. We report that 4-OI decreased LPS-induced IL-8 and RANTES protein production in lung fibroblasts from healthy donors, but

not in IPF fibroblasts. In our study we demonstrated the ability of 4-OI to downregulate LPS-driven, TLR4-mediated transcription of pro-inflammatory genes, IL-8, IL-1β and caspase-1 in IPF fibroblasts. We reported that 4-OI decreased LPS-induced transcription in RANTES and RIG-I in healthy lung fibroblasts as well as IFN-β and RANTES transcription in lung fibroblasts from IPF patients. 4-OI treatment increased transcription of GSR and HMOX-1 in the presence of LPS, compared with DMSO and LPS treatments in healthy and IPF lung fibroblasts. We showed the ability of 4-OI to upregulate the transcription of HMOX-1 and NQOI was attenuated in the presence of TGF-β in lung fibroblasts from IPF patients. 4-OI reduced TGF-β-induced TGF-β and COL1A1 transcription and increased TGF-β-induced COL3α1 transcription in IPF lung fibroblasts. Lung fibroblasts infected with PAO1 in the presence of 4-OI showed reduced transcription of IL-8, IL-1β and caspase-1 compared with fibroblasts infected with PAO1. We further showed that healthy lung fibroblasts infected with PAO1 in the presence of 4-OI exhibited attenuated transcription of IFN-β, RANTES, RIG-I and IRG-1 compared with PAO1 infection-only at 8 h post-treatment. We reported that 4-OI decreased Poly(I:C)-induced protein expression of TLR3 and RIG-I in lung fibroblast from healthy donors and IPF patients. In this chapter we demonstrated the ability of 4-OI to downregulate TLR3 and TLR4-mediated protein production, protein expression as well as transcription of pro-inflammatory, pro-fibrotic and anti-viral agents in pulmonary fibroblasts from healthy donors and IPF patients. Furthermore, we reported upregulation in the transcription of anti-oxidant mediators, HMOX-1, GSR and NQOI in IPF lung fibroblasts. In addition, we demonstrated anti-bacterial properties of 4-OI using live *P. aeruginosa* infection.

In conclusion, itaconate (4-OI) displayed both protective and pathogenic properties in the context of modulating TLR3, TLR4, TGF-β and *P. aeruginosa* responses in primary human lung fibroblasts from IPF patients (see summary in **Figure 3.20**). Itaconate/4-OI also downregulated the expression of TLR3 following activation of TLR3 on healthy and IPF lung fibroblasts. This suggests that itaconate has the ability to dampen TLR3responses during viral infection which would not be a beneficial effect during IPF. Further investigation is needed to explore the role of itaconate in infection and TLR responses in IPF patients.

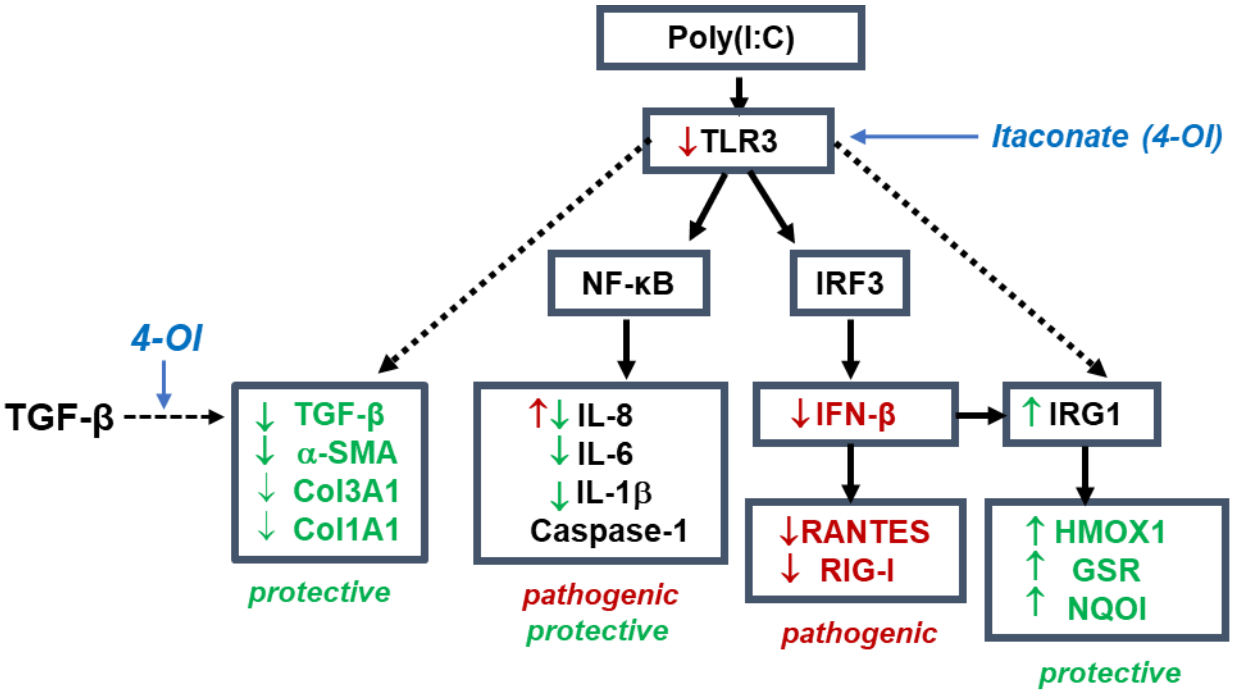

Figure 3.20. Summary of the results reported in chapter 3. This schematic summarises our findings on the effects of 4-OI on TLR3 function in primary human IPF lung fibroblasts following viral dsRNA treatment using the poly(I:C) dsRNA analogue. The putative protective or pathogenic effects of 4-OI modulation of TLR3 are shown in IPF lung fibroblasts.

Chapter 4 – Characterisation of the immunomodulatory effects of IL-17A on TLR3 function in IPF lung fibroblasts; and investigation of the role of the *IL-17A* G197A (rs2275913) promoter polymorphism in IPF development and death.

4.1 Introduction.

The IL-17 superfamily consists of six different members IL-17A-IL-17F. With 50% homology, IL-17A and IL-17F are the most closely related. Cytokines of the IL-17A family share conserved cysteine residues, and are secreted in the form of dimers, which bind their family of receptors including IL-17RA, IL-17RB, IL-17RC, IL-17RD/SEF, and IL-17RE [448]. Although IL-17A and IL-17F are primarily produced by activated T cells, a variety of cell types, including pulmonary fibroblasts, epithelial cells and endothelial cells have been shown to express the IL-17R [251, 257-259]. Signalling through the receptor activates several intracellular kinases, such as TGF-beta-activated Kinase 1 (TAK1), Extracellular Signal-regulated Kinase (ERK), Glycogen Synthase Kinase 3 beta (GSK-3 beta), p38, I-kappa B Kinase (IKK) and MAPK. This leads to induction of the NF-kappa B-, C/EBP and -AP-1- and results in the expression of pro-inflammatory cytokines, chemokines, and anti-microbial peptides [260].

IL-17A signalling leads to the induction of NF-kB activity, which results in increased expression of pro-inflammatory cytokines and chemokines [260]. Elevated levels of inflammation have been shown to be an important co-factor in the development and progression of IPF [3]. Previously, our lab demonstrated that IL-17A and IL-17E (IL-25) were increased in the BAL fluid of IPF patients [299]. In addition, other authors have also Studies have shown increased levels of IL-17A in BALF and pulmonary tissue of IPF patients [285]. Furthermore, in the bleomycin (BLM) murine model of pulmonary fibrosis, treatment with exogenous IL-17A significantly induced neutrophilia and pulmonary fibrosis [285]. In contrast, mice deficient in IL-17A challenged with BLM exhibited a significant reduction in fibrosis, compared with wild-type mice, as seen by increased collagen expression in the BAL and collagen deposition in the lung [285].

In previous studies by other authors, IL-17A has been shown to be increased in the blood, bronchoalveolar lavage (BAL) fluid and lung tissue of patients with IPF [299, 449]. In 2010, Wilson *et al*. also demonstrated that the IL-1β-induced pulmonary fibrosis observed in the bleomycin (BLM) model of IPF, was dependent on IL-17A [285]. These data suggest that IL-17A plays an important role in IPF. Although IL-17A has been demonstrated to play a critical role in anti-fungal and anti-extracellular bacterial immunity, more recently IL-17A has been shown to play an important role in viral persistence [266, 450]. In 2009, Hou *et al.* described a mechanism by which IL-17A upregulated anti-apoptotic molecules in virally infected cells in order to promote viral persistence during Theiler's murine encephalomyelitis virus (TMEV) infection in a murine demyelinating disease model [450]. In addition, previous studies have shown increased expression of anti-apoptotic proteins, Bcl-2 and Bcl-xL in murine bone marrow cells, following a combined IL-6 and IL-17A treatment. This

elevated expression of anti-apoptotic proteins led to protection of virally infected cells from apoptosis and CD8+ T cell-mediated target destruction which promoted viral persistence [266].

Our lab has previously demonstrated that IL-17A has the ability to downregulate TLR3 function in primary human lung fibroblasts from pulmonary sarcoidosis patients (Armstrong *et al.*, unpublished data). Specifically, this data demonstrates that IL-17A can act to modulate TLR3 function (NF-κB, IRF3 and apoptotic activities) in primary lung fibroblasts from pulmonary sarcoidosis patients. This data is of importance in the context of disease progression in IPF. In this chapter, we investigated the ability of IL-17A to modulate TLR3 function in primary lung fibroblasts from IPF patients in the context of pro-inflammatory, anti-viral and fibrotic responses.

In the second part of this chapter, we describe studies investigating the role of the promoter-polymorphism, *IL-17A* G197A (rs2275913), in the development and progression of IPF in a cohort of UK patients (n=161) versus healthy donors (n=140). This study aims to investigate the value of *IL-17A* G197A as a prognostic marker in IPF. The role of *IL-17A* G197A in IPF has not been reported to date. Other authors have demonstrated that the variant IL-17A A allele promotes increased binding of the NFAT transcription factor to the human IL-17A gene promoter [451] and thus, increases transcription of this gene. Therefore, here we hypothesise that *IL-17A* 197A-homozygous individuals may have increased levels of IL-17A in their BAL fluid which may promote the development of IPF. The dual aims of the studies described in this chapter are to establish the ability of IL-17A to modulate TLR3 function in IPF lung fibroblasts and to investigate the role of *IL-17A* G197A in development of IPF, in IPF-pneumonia related death and in time to death from diagnosis in IPF patients. **Figure 4.1.** outlines the experimental design implemented in this chapter.

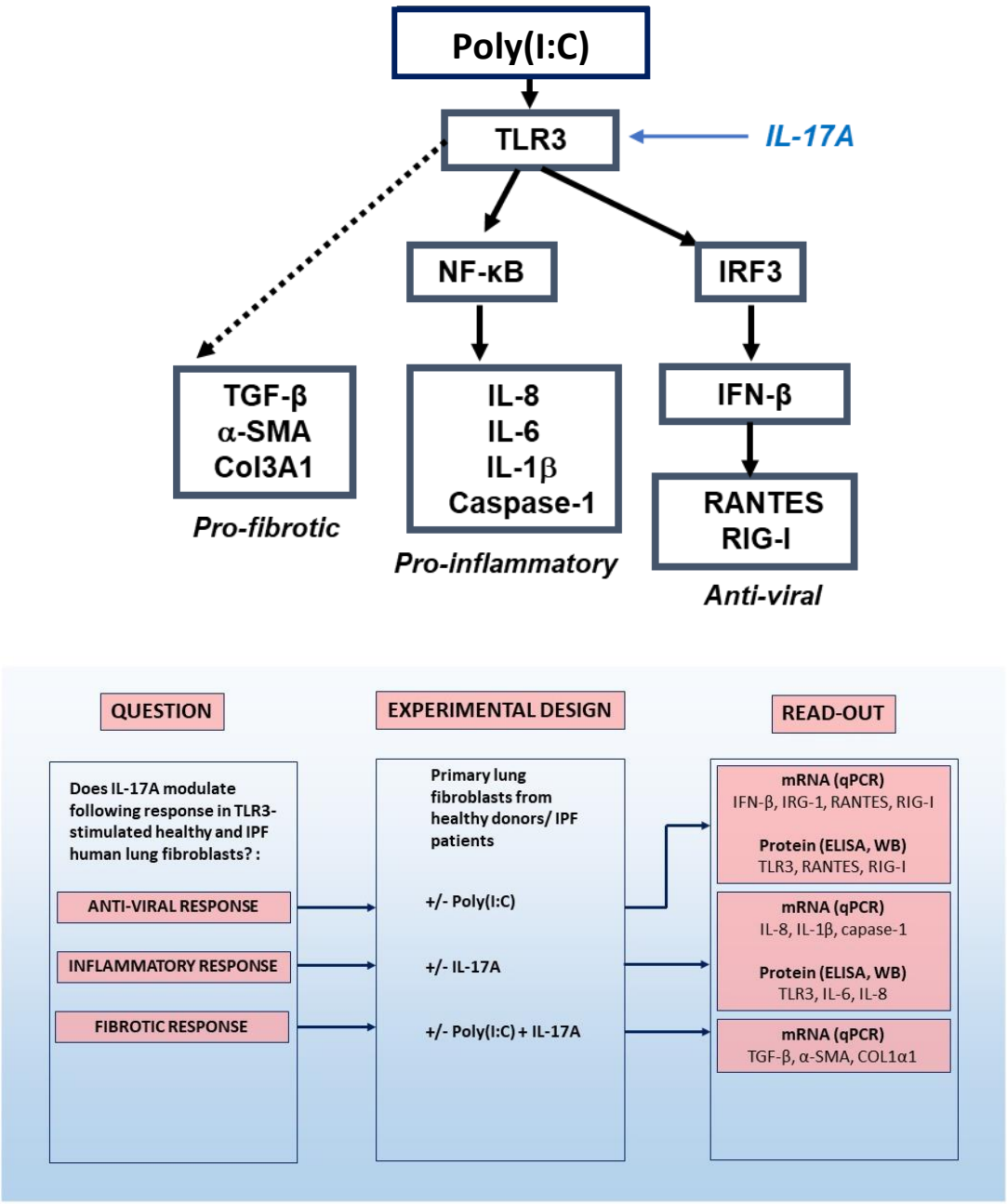

Figure 4.1. **Overview of the experimental design for chapter 4.** In this chapter we investigate the effects of IL-17A on TLR3 function and its implication in IPF pathogenicity.

4.2. Effects of IL-17A on Poly(I:C)-induced IL-6, IL-8 and RANTES protein production in primary human lung fibroblasts from healthy donors and IPF patients.

TLR3 is an important component of the host protection mechanism, adapted to recognise viral dsRNA, danger–associated molecular patterns (DAMPS), tissue necrosis as well as endogenous mRNA [130, 267, 268, 277, 372]. In this experiment, primary human lung fibroblasts from healthy donors and IPF patients were stimulated with TLR3 agonist, Poly(I:C), recombinant IL-17A or co-treated with Poly(I:C) and IL-17A for 24 hours. IL-6, IL-8 (pro-inflammatory cytokines) and RANTES (anti-viral chemokine) production was quantitated by ELISA. Poly(I:C) treatment significantly increased IL-8 and RANTES protein production from primary human lung fibroblasts from healthy donors compared with DMSO treatment only (**Fig. 4.2A, C, E; *p<0.05**). In addition, Poly(I:C) treatment significantly increased IL-6, IL-8 and RANTES production from IPF lung fibroblasts (**Fig. 4.2B, D, F; ***p<0.001**). IL-17A treatment alone (100 ng/ml) significantly increased protein production of IL-6 and IL-8 in IPF fibroblasts compared with medium only treatment (**Fig. 4.2B, D; *p<0.05).** IL-17A treatment alone had no significant effect on the production of RANTES protein in healthy and IPF fibroblasts (**Fig. 4.2E, F)**. Co-treatment of healthy (**Fig. 4.2A, C, E)** or IPF fibroblasts (**Fig. 4.2B, D, F)** with Poly(I:C) and IL-17A had no significant effect on IL-6, IL-8 or RANTES production compared with Poly(I:C) treatment only.

4.3. Effects of IL-17A on Poly(I:C)-induced protein production of IL-8, IL-6 and RANTES in primary human lung fibroblasts from healthy donors and IPF patients.

Here, we measured Poly(I:C)-induced protein production of RANTES, as well as IL-6 and IL-8 production in primary lung fibroblasts from healthy donors and IPF patients. Lung fibroblasts were stimulated with Poly(I:C), IL-17A or co-treated with Poly(I:C) and IL-17A for 24 hours. Treatment with Poly(I:C) significantly increased the production of IL-6, IL-8 and RANTES in healthy (**Fig. 4.3A, C, E; ***p<0.001**) and IPF human lung fibroblasts (**Fig. 4.3B, D, F; ***p<0.001**), respectively, compared with medium only treatment. Treatment with IL-17A alone (10 ng/ml) significantly increased IL-6 protein production in IPF fibroblasts (**Fig. 4.B; **p<0.01)** compared to medium only. Treatment with IL-17A alone had no significant effect on protein production of RANTES in fibroblasts from healthy donors and IPF patients (**Fig. 4.3E, F)**. Co-treatment with IL-17A significantly upregulated Poly(I:C)-induced production of IL-6 in IPF lung fibroblasts (**Fig. 4.3B; †p<0.05)**.

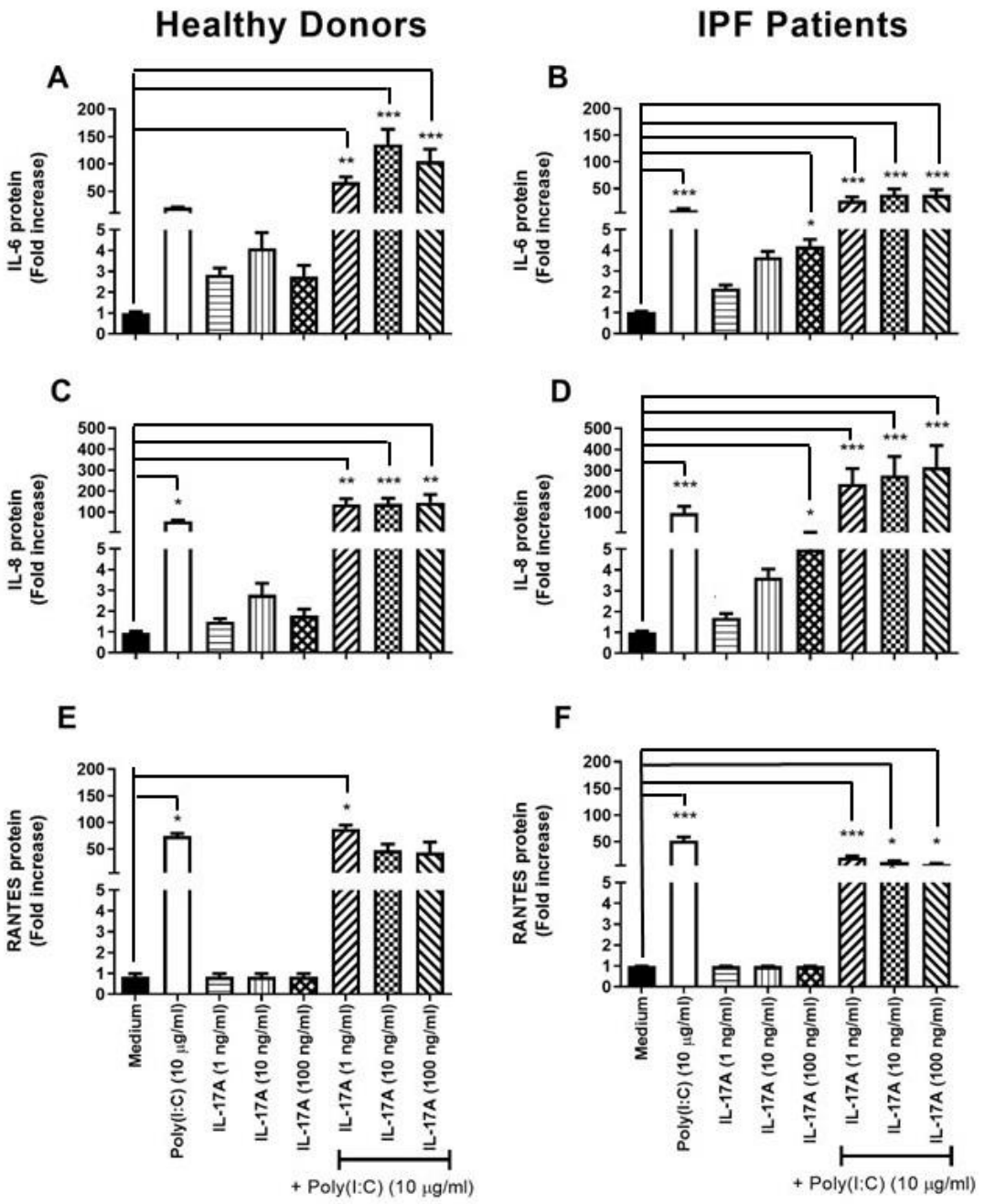

Figure 4.2. Effects of IL-17A on Poly(I:C)-induced IL-6, IL-8 and RANTES protein production in primary human lung fibroblasts from healthy donors and IPF patients. Poly(I:C) treatment significantly increased levels of IL-6, IL-8 and RANTES protein production in primary lung fibroblasts from IPF patients (**B, D, F**); Poly(I:C) treatment significantly increased levels of IL-6 and IL-8 from healthy lung fibroblasts (**A, C, E**).
Co-treatment of healthy or IPF lung fibroblasts with Poly(I:C) and IL-17A did not significantly modulate IL-6 (**A, B**), IL-8 (**C, D**) or RANTES (**E, F**) protein production compared with Poly(I:C) treated fibroblasts only. IL-6, IL-8 and RANTES protein production was quantitated by ELISA at 24 h post-treatment. A Kruskal-Wallis Test with a Dunn's multiple comparison post-hoc test was used to test for statistical differences. *p<0.05, **p<0.01, ***p<0.001: Medium compared with Poly(I:C) or Poly(I:C) & IL-17A treatment, respectively. Each graph represents data from primary lung fibroblasts from 3 healthy donors and 3 IPF patients, respectively, performed twice (n=6). Results shown represent the mean +/- S.E.M. [Poly(I:C), 10 μg/ml; IL-17A, 1, 10, 100 ng/ml].

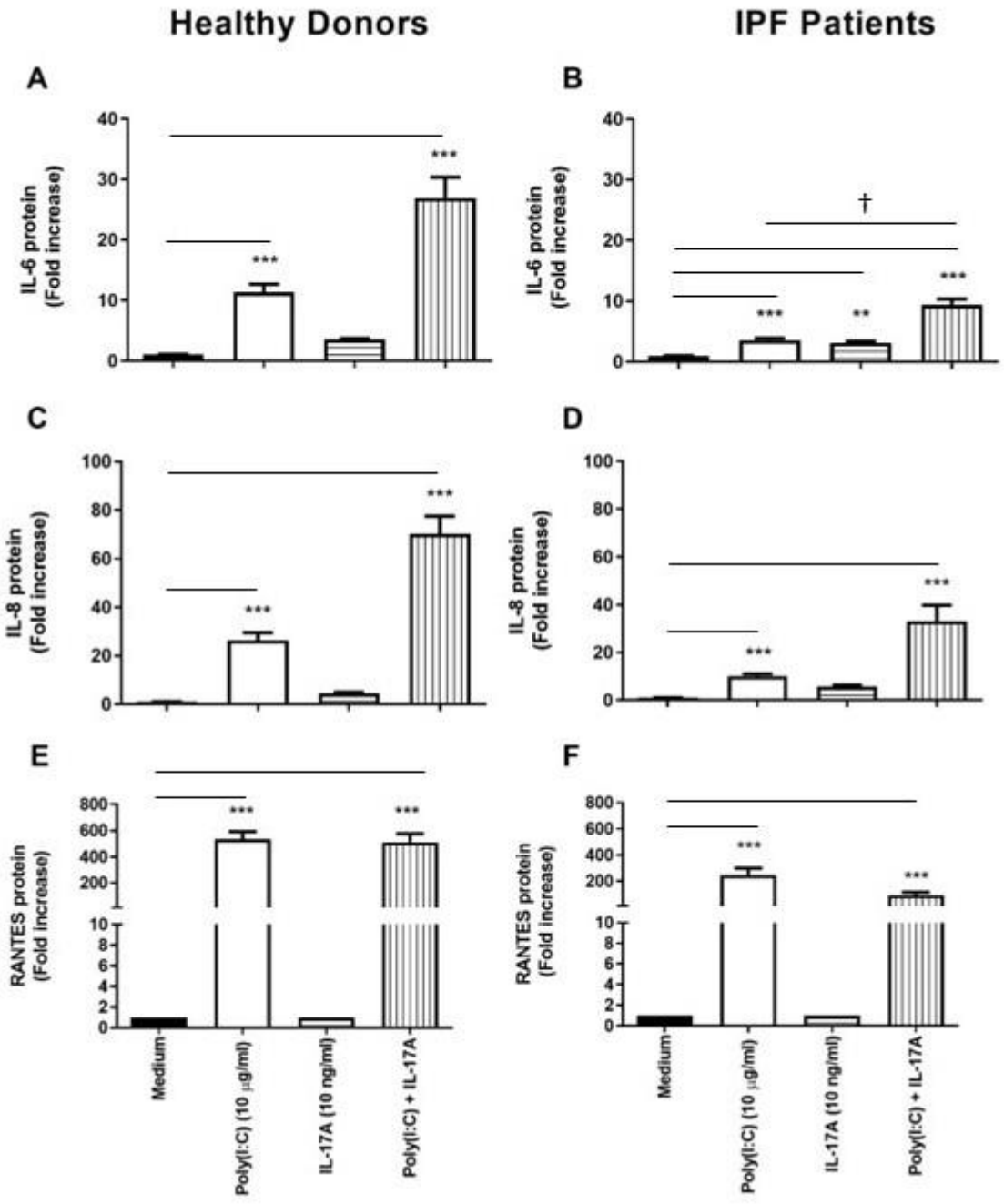

Figure 4.3. Effects of IL-17A on Poly(I:C)-induced protein production of IL-8, IL-6 and RANTES in primary human lung fibroblasts from healthy donors and IPF patients. Poly(I:C) treatment increased levels of IL-6, IL-8 and RANTES protein production in primary lung fibroblasts from healthy donors (**A, C, E**) and IPF patients (**B, D, F**). IL-17A treatment significantly induced IL-6 protein production from lung fibroblasts from IPF patients (**B**). Poly(I:C)-induced IL-6 protein was significantly increased following co-treatment with IL-17A in IPF fibroblasts (**B**) at 24 h post-treatment, as quantitated by ELISA. A Kruskal-Wallis Test with a Dunn's multiple comparison post-hoc test was used to test for statistical differences. **p<0.01, ***p<0.001: Medium only compared with Poly(I:C) or Poly(I:C) & IL-17A treatment, respectively. p<0.05: Poly(I:C) & IL-17A compared with Poly(I:C) treatment only. Each graph represents data from primary lung fibroblasts from 3 healthy donors and 3 IPF patients, respectively, performed twice (n=6). Results shown represent the mean +/- S.E.M. [Poly(I:C), 10 μg/ml; IL-17A, 10 ng/ml].

4.4. Effects of IL-17A on Poly(I:C)-induced transcription of pro-inflammatory genes IL-8, IL-1β and caspase-1 in primary human lung fibroblasts from healthy donors and IPF patients.

TLR3 and NF-κB activation are associated with elevated levels of IL-8, IL-1β and caspase-1 transcription, all implicated as drivers of inflammation, as well as fibrosis and tissue re-modelling in diseases including renal fibrosis, liver cirrhosis, asthma and most relevantly, IPF [286, 289]. In this experiment, primary human lung fibroblasts from healthy donors and IPF patients were stimulated with Poly(I:C), IL-17A or co-treated with Poly(I:C) and IL-17A for 24 hours, after which the levels of pro-inflammatory IL-8, IL-1β and caspase-1 mRNA were measured by qPCR. Treatment with Poly(I:C) significantly upregulated the transcription of IL-8, IL-1β and caspase-1 compared with medium in IPF fibroblasts (**Fig. 4.4B, ***p<0.001; Fig. 4.4D, F; **p<0.01**). Treatment with IL-17A alone (10 ng/ml) had no significant effect on IL-8, IL-1β and caspase-1 transcription in healthy **(Fig. 4.4A, C, E)** or IPF fibroblasts (**Fig. 4.4B, D, F)**. Co-treatment with IL-17A had no significant effect on Poly(I:C)-induced IL-8, IL-1β and caspase-1 transcription in healthy **(Fig. 4.4A, C, E)** or IPF fibroblasts (**Fig. 4.4B, D, F)** compared with Poly(I:C) treatment only.

4.5. Effects of IL-17A on Poly(I:C)-induced transcription of anti-viral genes IFN-β, RANTES and RIG-I in primary human lung fibroblasts from healthy donors and IPF patients.

Our lab has previously demonstrated the association between defective, Poly(I:C)-induced Type-1 IFN response and the disease progression in IPF [161]. In this experiment, primary human lung fibroblasts from healthy donors and IPF patients were stimulated with Poly(I:C), IL-17A or combined Poly(I:C) and IL-17A treatment for 24 hours, after which the levels of IFN-β, RANTES and RIG-I transcription were quantitated by qPCR. Treatment with Poly(I:C) significantly upregulated the transcription of IFN-β, RANTES and RIG-I transcription compared with medium in IPF fibroblasts (**Fig. 4.5B, **p<0.01; Fig. 4.5D, F; ***p<0.001**). Treatment with IL-17A alone (10 ng/ml) had no significant effect on IFN-β, RANTES and RIG-I transcription in healthy **(Fig. 4.5A, C, E)** or IPF fibroblasts (**Fig. 4.5B, D, F)**. Co-treatment with IL-17A had no significant effect on Poly(I:C)-induced IFN-β, RANTES and RIG-I transcription in healthy **(Fig. 4.5A, C, E)** or IPF fibroblasts (**Fig. 4.5B, D, F)** compared with Poly(I:C) treatment only.

4.6. Effects of IL-17A on Poly(I:C)-induced transcription of pro-fibrotic genes TGF-β, α-SMA and COL3α1 in primary human lung fibroblasts from healthy donors and IPF patients.

Studies have shown dysregulated production of several pro-fibrotic mediators, including TGF-β, α-SMA and collagens, due to an excessive contractile force generated by IPF lung fibroblasts [388-391]. TGF-β is a known pleiotropic growth factor associated with promotion of cellular proliferation [388-391]. In this experiment, primary human lung fibroblasts from healthy donors and IPF patients were stimulated with Poly(I:C), IL-17A and a combined Poly(I:C) and IL-17A treatment for 24 h, after which the levels of TGF-β, α-SMA and COL3α1 transcription were used as read-outs for Poly(I:C)-induced, pro-fibrotic response. Treatment with Poly(I:C) had no significant effect on TGF-β, α-SMA and COL3α1 transcription in healthy **(Fig. 4.6A, C, E)** or IPF fibroblasts (**Fig. 4.6B, D, F)** compared with medium only treatment. Treatment with IL-17A alone (10 ng/ml) had no significant effect on TGF-β, α-SMA and COL3α1 transcription in healthy **(Fig. 4.6A, C, E)** or IPF fibroblasts (**Fig. 4.6B, D, F)** compared with medium only treatment. Co-treatment with IL-17A had no significant effect on Poly(I:C)-induced TGF-β, α-SMA and COL3α1 transcription in healthy **(Fig. 4.6A, C, E)** or IPF fibroblasts (**Fig. 4.6B, D, F)** compared with Poly(I:C) treatment only.

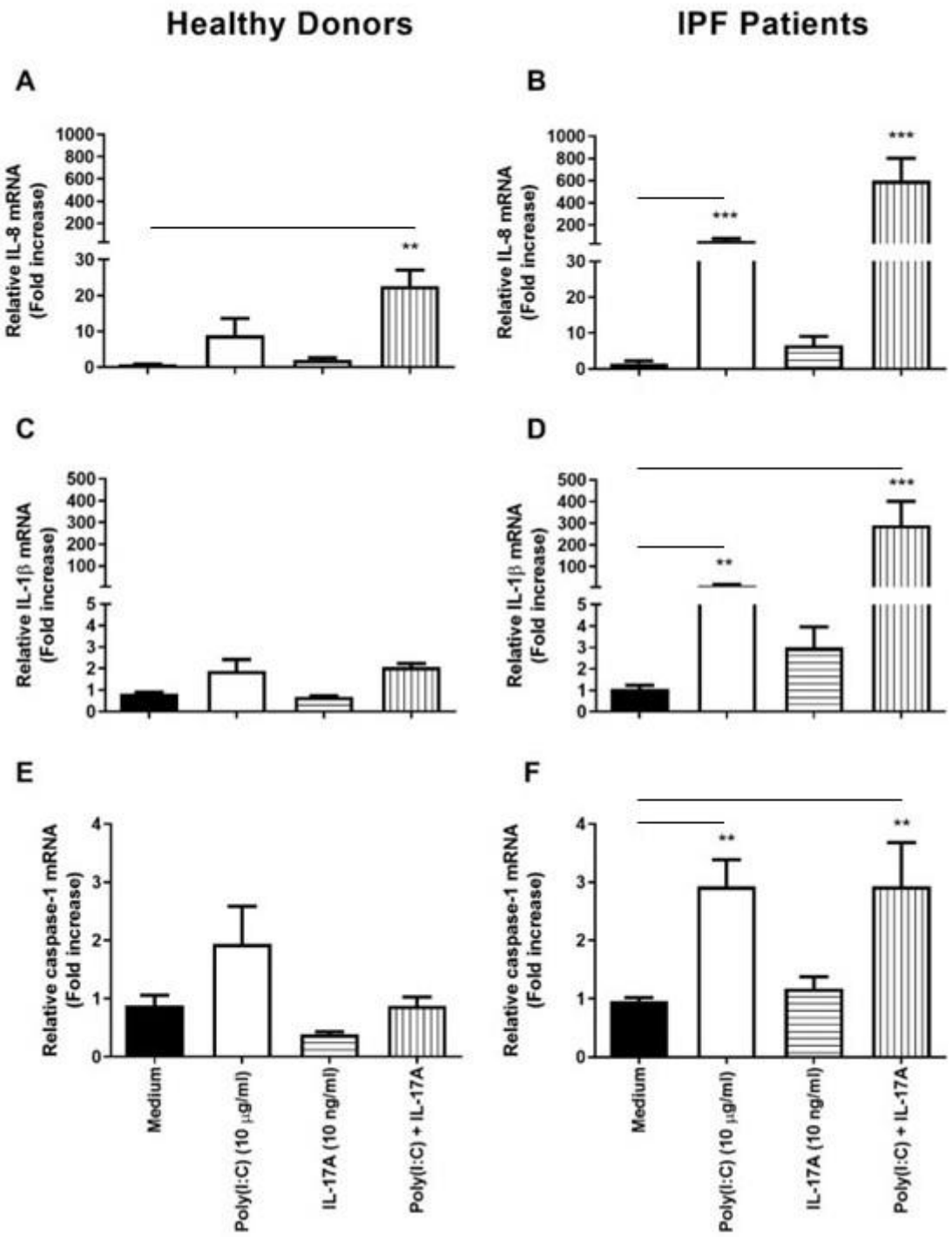

Figure 4.4. Effects of IL-17A on Poly(I:C)-induced transcription of pro-inflammatory genes IL-8, IL-1β and caspase-1 in primary human lung fibroblasts from healthy donors and IPF patients. Poly(I:C) treatment increased levels of IL-8, and IL-1β and caspase-1 transcription in IPF lung fibroblasts (**B, D, F**). IL-17A treatment had no effect on IL-8, and IL-1β and caspase-1 transcription in healthy or IPF fibroblasts (**A-F**). Co-treatment of healthy or IPF lung fibroblasts with Poly(I:C) and IL-17A did not significantly modulate IL-8 (**A, B**), IL-1β (**C, D**) or caspase-1 (**E, F**) transcription compared with Poly(I:C) treated fibroblasts only. Transcription was analysed at 24 h post-treatment and quantitated by qPCR analysis. A Kruskal-Wallis Test with a Dunn's multiple comparison post-hoc test was used to test for statistical differences. **p<0.01, ***p<0.001: Medium only compared with Poly(I:C) or Poly(I:C) & IL-17A treatment, respectively. Each graph represents data from primary lung fibroblasts from 3 healthy donors and 3 IPF patients, respectively, performed twice (n=6). Results shown represent the mean +/- S.E.M. [Poly(I:C), 10 μg/ml; IL-17A, 10 ng/ml].

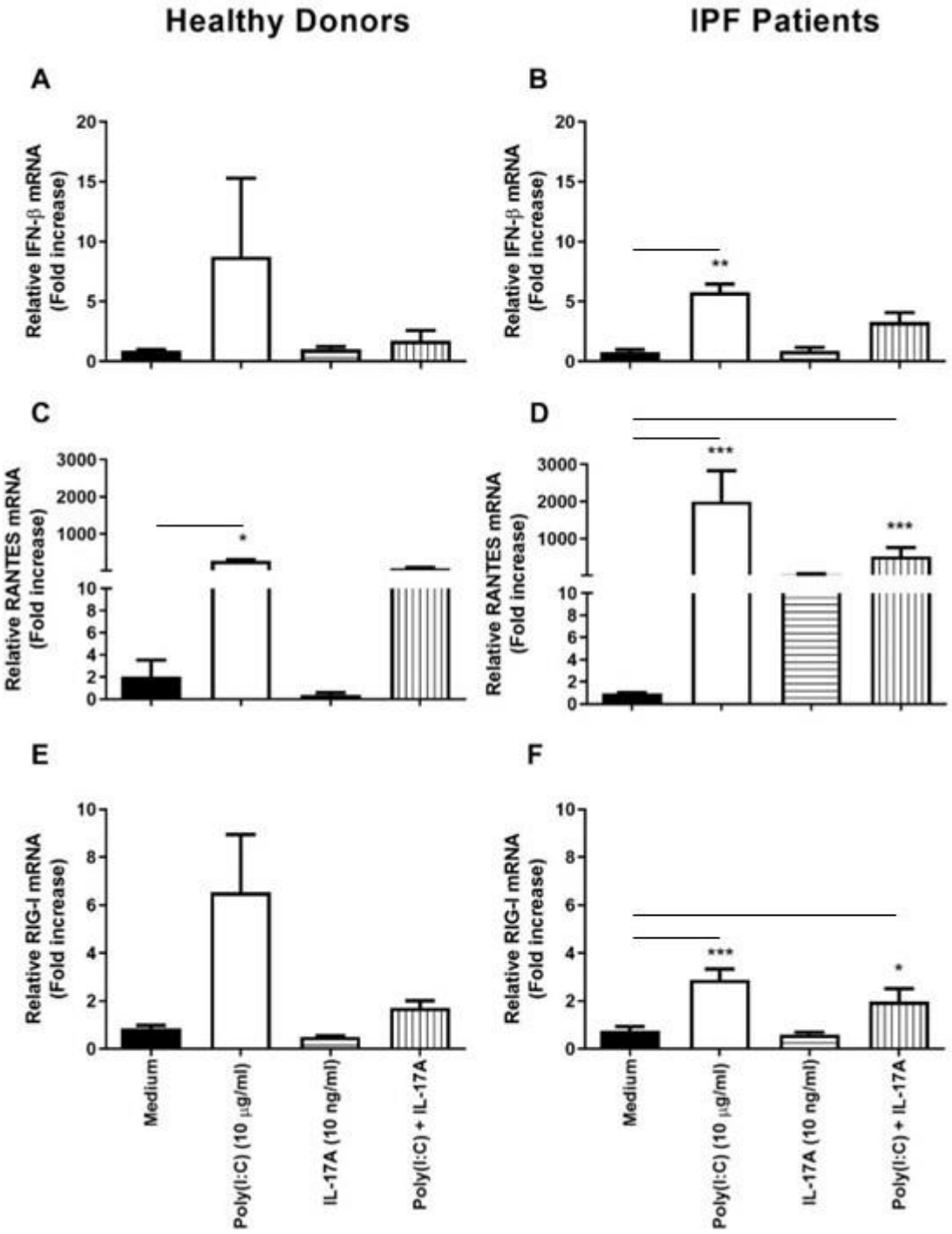

Figure 4.5. Effects of IL-17A on Poly(I:C)-induced transcription of anti-viral genes IFN-β, RANTES and RIG-I in primary human lung fibroblasts from healthy donors and IPF patients. Poly(I:C) treatment increased levels of IFN-β and RIG-I mRNA in primary human lung fibroblasts from IPF patients (**B, F**). RANTES transcription was increases in response to 24 h Poly(I:C) treatment in healthy lung fibroblasts. IL-17A treatment had no effect on IFN-β, RANTES or RIG-I transcription in healthy or IPF fibroblasts (**A-F**). Co-treatment of healthy or IPF lung fibroblasts with Poly(I:C) and IL-17A did not significantly modulate IFN-β (**A, B**), RANTES (**C, D**) or RIG-I (**E, F**) transcription compared with Poly(I:C) treated lung fibroblasts only. Transcription was analysed at 24 h post-treatment and quantitated by qPCR analysis. A Kruskal-Wallis Test with a Dunn's multiple comparison post-hoc test was used to test for statistical differences. *p<0.05, **p<0.01, ***p<0.001: Medium only compared with Poly(I:C) or Poly(I:C) & IL-17A treatment, respectively. Each graph represents data from primary lung fibroblasts from 3 healthy donors and 3 IPF patients, respectively, performed twice (n=6). Results shown represent the mean +/- S.E.M. [Poly(I:C), 10 μg/ml; IL-17A, 10 ng/ml].

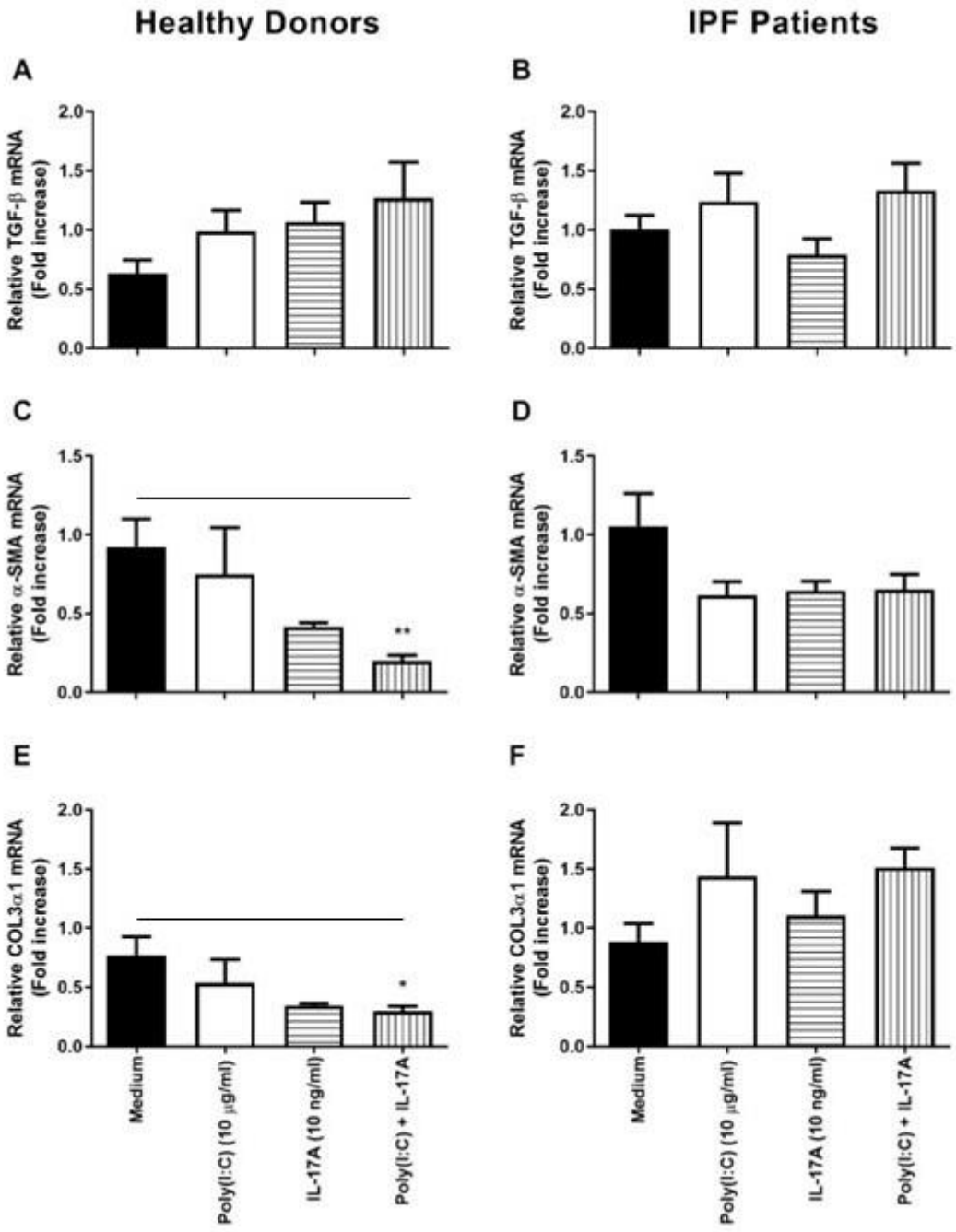

Figure 4.6. Effects of IL-17A on Poly(I:C)-induced transcription of pro-fibrotic genes TGF-β, α-SMA and COL3α1 in primary human lung fibroblasts from healthy donors and IPF patients. Healthy and IPF lung fibroblasts were treated with Poly(I:C), IL-17A or Poly(I:C) & IL-17A for 24h. TGF-β (**A, B**), α-SMA (**C, D**) and COL3α1 (**E, F**) transcription, respectively, was quantitated by qPCR analysis. A Kruskal-Wallis Test with a Dunn's multiple comparison post-hoc test was used to test for statistical differences. *p<0.05, **p<0.01: Medium only compared with Poly(I:C) & IL-17A treatment. Each graph represents data from primary lung fibroblasts from 3 healthy donors and 3 IPF patients, respectively, performed twice (n=6). Results shown represent the mean +/- S.E.M. [Poly(I:C), 10 μg/ml; IL-17A, 10 ng/ml].

4.7. Investigation of the TLR3 and RIG-I protein expression in primary human lung fibroblasts from healthy donors and IPF patients using western blot.

Here we investigated TLR3 and RIG-I protein expression in primary human lung fibroblasts from healthy donors (**Fig. 4.7A)** and IPF patients (**Fig. 4.7B)** using western blot. Primary lung fibroblasts from healthy donors and IPF patients were stimulated with Poly(I:C), IL-17A or co-treated with Poly(I:C) and IL-17A for 24 h. The protein expression of TLR3 and RIG-I was measured. Treatment with Poly(I:C) induced TLR3 and RIG-I protein expression in healthy and IPF fibroblasts. Treatment with IL-17A had no effect on Poly(I:C)-induced TLR3 and RIG-I protein expression in healthy lung fibroblasts. IL-17A treatment decreased Poly(I:C)-induced TLR3 and RIG-I protein expression in lung fibroblasts from IPF patients. Here we demonstrated, for the first time, that treatment with IL-17A modulated Poly(I:C)-induced TLR3 and RIG-I response in IPF lung fibroblasts.

4.8. Effects of 4-OI on IL-17A-induced protein production of IL-6 and IL-8 in primary human lung fibroblasts from healthy donors and IPF patients.

In this experiment, we measured IL-17A-induced protein production of IL-6 and IL-8 as read-outs for NF-κB activity in primary lung fibroblasts from healthy donors and IPF patients. Lung fibroblasts were stimulated with IL-17A, 4-OI or co-treated with IL-17A and 4-OI for 24 hours. Treatment with IL-17A significantly increased the production of IL-6and IL-8, respectively, in healthy (**Fig. 4.8A, C; *p<0.05**) and IPF human lung fibroblasts (**Fig. 4.8B, D; *p<0.05**) compared with DMSO treatment only. Treatment with 4-OI alone had no significant effect on IL-6 and IL-8 protein production in healthy (**Fig. 4.8A, C**) and IPF lung fibroblasts (**Fig. 4.8B, D)**. Treatment with 4-OI had no significant effect on IL-17A-induced IL-6 and IL-8 protein production compared with IL-17A treatment only in healthy (**Fig. 4.8A, C**) or in IPF lung fibroblasts, respectively (**Fig. 4.8B, D)**.

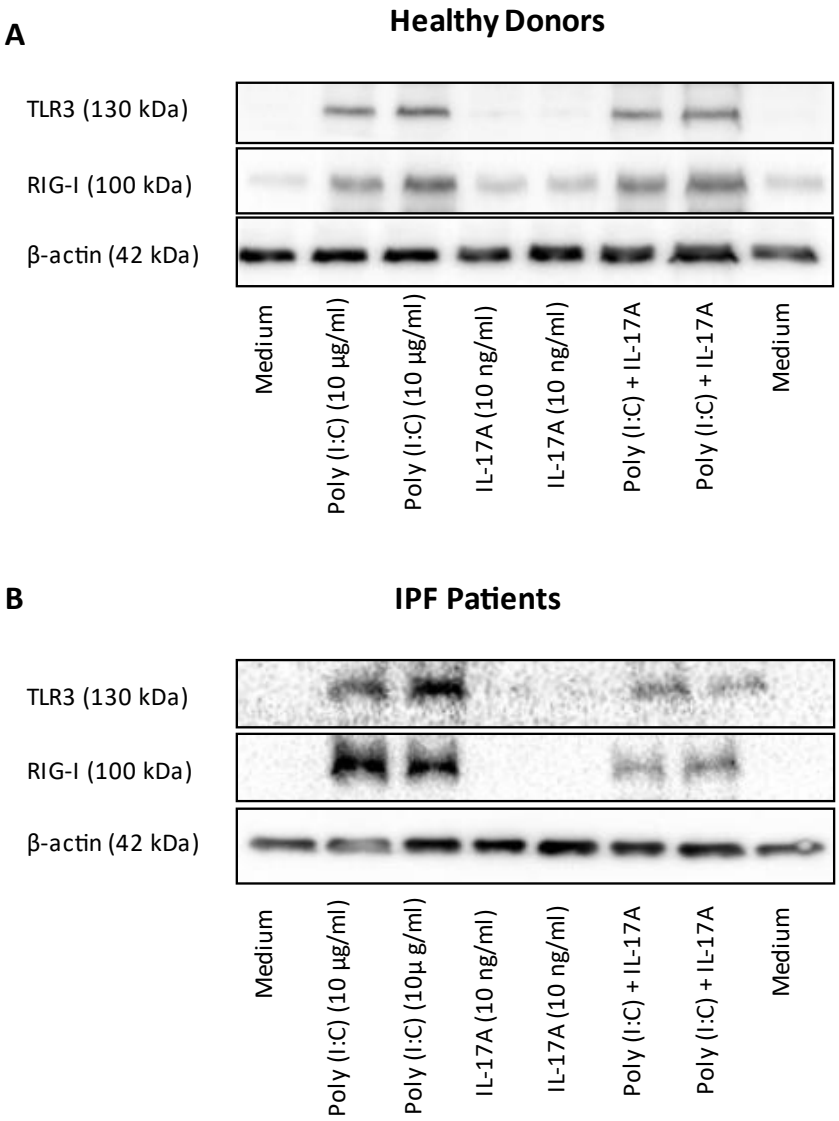

Figure 4.7. Investigation of the TLR3 and RIG-I protein expression in primary human lung fibroblasts from healthy donors and IPF patients using western blot. Treatment with Poly(I:C) increased TLR3 and RIG-I protein expression in healthy (**A**) and IPF lung fibroblasts (**B**). IL-17A treatment decreased the protein expression of Poly(I:C)-induced TLR3 and RIG-I in lung fibroblasts from IPF patients (**B**) at 24 h post-treatment with Poly(I:C) (10 µg/ml), IL-17A (10 ng/ml) or Poly(I:C) (10 µg/ml) and 4-OI (250 µM). β-actin was used as a loading control. Each Western blot represents data from primary lung fibroblasts from 3 healthy donors and 3 IPF patients, respectively, performed twice.

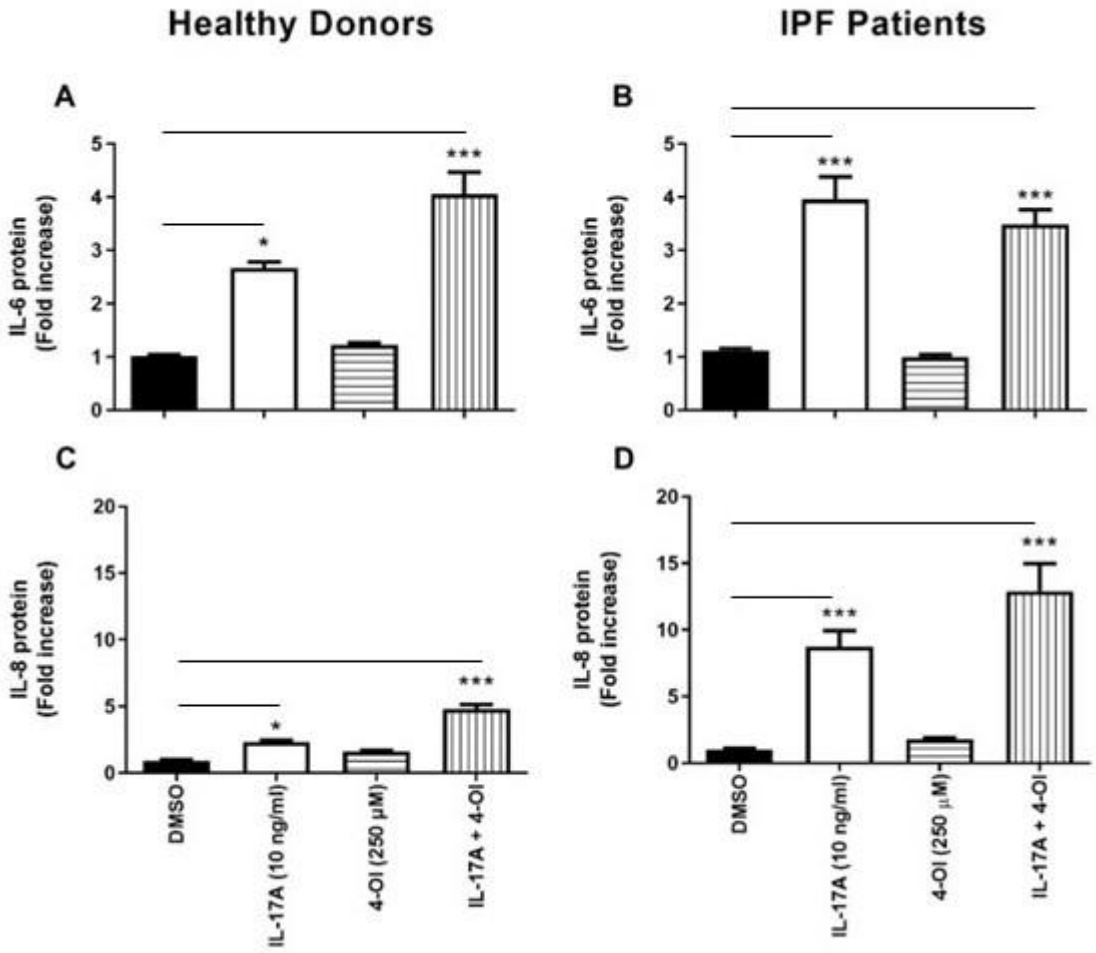

Figure 4.8. Effects of 4-OI on IL-17A-induced protein production of IL-6 and IL-8 in primary human lung fibroblasts from healthy donors and IPF patients. IL-17A treatment significantly increased levels of IL-6 and IL-8 protein production in primary lung fibroblasts from healthy donors (**A, C**) and IPF patients (**B, D**). 4-OI treatment did not significantly increase IL-6 (**A, B**) or IL-8 (**C, D**) production in healthy or IPF fibroblasts, respectively. 4-OI did not significantly modulate IL-17A-induced IL-6 or IL-8 in healthy (**A, B**) or IPF lung fibroblasts (**C, D**). Cytokines were measured at 24 h post-treatment and were quantitated by ELISA.
A Kruskal-Wallis Test with a Dunn's multiple comparison post-hoc test was used to test for statistical differences. *p<0.05, ***p<0.001: DMSO only compared with IL-17A or IL-17A & 4-OI treatment, respectively.
Each graph represents data from primary lung fibroblasts from 3 healthy donors and 3 IPF patients, respectively, performed twice (n=6). Results shown represent the mean +/- S.E.M. [IL-17A, 10 ng/ml; 4-OI, 250 µM].

4.9. *IL-17A* G197A (rs2275913) polymorphism is associated with development of IPF in UK patients.

In this project, we carried out a pilot study to test for an association between the *IL-17A* G197A (rs2275913) promoter-polymorphism and development of IPF in a case-control study of UK 140 control subjects and 161 UK IPF cases, respectively (**Tables 4.1 to 4.3).** The IPF study population employed in this analysis consisted of 161 patients diagnosed with IPF based on recommended international consensus guidelines. The baseline clinical characteristics of the population are summarised in **Table 4.1** and **4.2**. In this project, we observed a significant association between development of IPF and the *IL-17A* G197A homozygous genotype (AA) [Odds Ratio (OR): 3.504 (1.161-5.398; p=0.0200); **Table 4.3**]. Development of IPF was not significantly associated with variant allele frequency (A allele) [P=0.1183; OR: 1.319 (C.I.: 0.9355-1.859); **Table 4.3**. Future studies will involve the investigation of the role of *IL-17A* G197A in the development and the clinical progression of IPF in this larger cohort.

4.10 *IL-17A* G197A is associated with significant acute exacerbation-related death in IPF patients

Here, we investigated the association between *IL-17A* G197A and incidence of death in IPF patients (n=161) attending the Edinburgh Lung Fibrosis clinic, UK. The number of deaths in the IPF cohort was analysed at census 31/12/2016 **(Table 4.4).** A total of 115 IPF patients had died including 54 G197-wild type (G197-WT), 45 197A-heterozygous (197A-HET) and 16 197A-homozygous (197A-HOM) patients. A total of 15 IPF patients died of IPF-pneumonia including 4 G197-WT, 9 197A-HET and 2 197A-HOM patients. There was a trend towards an increase in IPF-pneumonia-related deaths in 197A-variant patients (p=0.07) compared with G197-wild type IPF patients **(Table 4.5)**. Specifically, 11 (73.3%) /15 IPF patients who died following an AE-IPF were 197A-heterozygous (CT) or -homozygous (TT) for *IL-17A* G197A **(Table 4.5).** In addition, we investigated the time to death in G197-WT and 197A-variant IPF patients. We observed an increase in the number of days to death in G197-WT IPF patients (2136.5 ± 483 days) compared to 197A-variant IPF patients (1632.5 ± 285 days) **(Table 4.6)**. This difference failed to reach statistical significance. These data suggest a role for *IL-17A* G197A in IPF-pneumonia deaths in IPF patients and warrant further investigation with a larger cohort. This effect was not due to any significant difference in pulmonary function (% predicted FVC, FEV_1 or TL_{co}) in G197A-WT compared to 197A-variant IPF patients **(Table 4.6)**.

Table 4.1. Study demographics for UK Controls and UK IPF Cases.

	UK Controls	UK IPF Cases
No.	**140**	**161**
Sex, Males (%)	56 (40)	106 (66)
Age, yrs (± S.D.)	57 (10)	73 (9)

Table 4.2. Baseline clinical characteristics for UK IPF Cases.

Baseline PFTs*	
FVC (± S.D.)	93 (20)
DLCO (± S.D.)	55 (16)
Smoking Status	
Non (%)	44 (27)
Ex (%)	101 (63)
Current (%)	16 (10)

*PFTs: pulmonary function tests; FVC: forced vital capacity; DLCO: diffusion capacity for carbon monoxide expressed as a percentage of predicted value. Results are expressed as mean ± S.D.

Table 4.3. *IL-17A* G197A (rs2275913) polymorphism frequencies in IPF: UK case-control Study

Status	GG (wild-type)	GA (heterozygous)	AA (homozygous)
Control Subjects (n=140)	67 *(0.48)*	63 *(0.45)*	10 *(0.07)*
UK IPF Cases (n=161)	72 *(0.50)*	63 *(0.39)*	26 *(0.11)*
***P* values**			
Genotype		[a]0.0200	
Trend		[b]0.0.053	
Allele		[c]0.1183	
Odds ratio (95% C.I.)			
A carrier		[d]1.135 (0.7201-1.787)	
AA homozygote		[e]2.504 (1.161-5.398)	

UK case-control Study: G197A genotype frequencies were significantly different between control subjects and IPF cases: [a] Fischer's Exact test (2 d.f.) and [b]χ2 test for trend (1 d.f.). Odds ratio (OR) and 95% confidence interval (C.I.) for [d]A carriers (GA and AA) and [e]AA homozygotes. [c]Allele frequencies were not significantly different between control subjects and IPF cases (Fischer's Exact test).

Table 4.4. *IL-17A* G197A and incidence of death in UK IPF cohort

***IL-17A* G197A Genotype**	***n* (Total)**	**Died (All cause)**	**Died (IPF-pneumonia)**
IPF, *n*	115	66	15
G197-WT, *n (%)*	54 (47.0)	32 (48.5)	4 (26.7)
197A-HET, *n (%)*	45 (39.1)	25 (37.9)	9 (60.0)
197A-HOM, *n (%)*	16 (1)	9 (13.6)	2 (13.3)

Definition of abbreviations: G197-WT: GG; 197A-HET: GA; 197A-HOM: AA.

Table 4.5. *IL-17A* G197A in IPF-pneumonia deaths in IPF UK cohort.

***IL-17A G197A* Genotype**	**Died (IPF-pneumonia)**	**Died (non-IPF-pneumonia)**	***P* value**
G197-WT, *n (%)*	4 (26.7)	28 (54.9)	0.07
197A-variant, *n (%)*	11 (73.3)	23 (45.1)	

Definition of abbreviations: G197-WT: GG; 197A-variant: GA+AA. *P* value = G197-WT versus 197A-variant using Fisher's exact test.

Table 4.6. *IL-17A* G197A in time to death and baseline characteristics in IPF-pneumonia deaths in IPF UK cohort.

***IL-17A G197A* Genotype**	***Time to death (days)**	**Baseline PFTs**		
		FVC	**FEV**	**TLco**
G197-WT (± SD)	2136.5 (483)	100.1 (10.8)	98.9 (7.7)	43.9 (19.5)
197A-variant (± SD)	1632.5 (285)	101.8 (15.2)	99.0 (13.8)	49.5 (18.0)

Definition of abbreviations: G197-WT: GG; 197A-variant: GA+AA. PFTs: pulmonary function Tests. *Time to death in days from first CT scan.

4.11 Discussion

IL-17A is a pro-inflammatory cytokine, which has been implicated in the development and progression of IPF [285, 452, 453]. Other authors reported elevated levels of IL-17A in BALF of IPF patients compared with healthy individuals [452]. In addition, other studies demonstrated a significantly increased expression of IL-17RA in fibrotic areas in IPF lung compared with areas unaffected by fibrosis [453]. Moreover, studies by other authors revealed that treatment with exogenous IL-17A resulted in exacerbation of fibrotic events in the lungs of mice in the bleomycin model of pulmonary fibrosis [285].

In this chapter, we firstly examined the effects of IL-17A on Poly(I:C) responses in the context of pro-inflammatory and anti-viral responses in the progression of IPF. We have previously shown that optimal TLR3 function is essential in maintaining lung function in IPF patients [161, 366]. Specifically, we have shown that *TLR3* 412F-variant IPF patients have defective TLR3 function and this is associated with an increased risk of mortality, accelerated IPF-disease progression and decline in FVC, dysregulation of the lung microbiome and an increased risk of AE-IPF death [161, 366]. Previously, our lab demonstrated that IL-17A could modulate TLR3 function in pulmonary sarcoidosis lung fibroblasts to promote a worsened disease phenotype (160). The *IL-17A* G197A (rs2275913) is a SNP within the promoter of the IL-17A gene, which results in altered binding of the transcription factor NFAT to the promoter region and leads to increased IL-17A transcription and secretion [451]. In this chapter, we secondly investigated the role *of IL-17A* G197A in development of IPF, in IPF-pneumonia related death and in time to death from diagnosis in IPF patients.

Previous studies reported increased levels of IL-6 in the sputum of AE-IPF patients, compared with patients with stable IPF and healthy individuals [418]. Other authors demonstrated increased IL-8 levels in the BALF, serum, plasma, and sputum of IPF patients compared with healthy controls [376, 412-414]. Moreover, IL-6 and IL-17A were reported to synergistically promote viral persistence in the mouse model of TMEV-induced multiple sclerosis [266]. In our previous study, we demonstrated that the dysregulated NF-κB-driven IL-8 response in patients homozygous for the *TLR3* L412F SNP resulted in a greater risk of mortality and an accelerated decline in FVC [161, 366]. In this study, we reported that, on its own, IL-17A significantly increased protein levels of IL-6 and IL-8 in both healthy (Fig. 4.8A, C) and IPF lung fibroblasts (Fig. 4.2B, D; Fig 4.3B; Fig. 8B, D). Our data are in agreement with findings of other authors, which reported that IL-17A induced NF-κB-dependent IL-6 and IL-8 production [312]. We predict that the increased protein production of IL-6 and IL-8 following

IL-17A treatment may have potentially negative effects on the disease progression in IPF patients. In addition, we reported that treatment of IPF lung fibroblasts with 4-OI significantly increased Poly(I:C)-driven IL-6 (Fig. 4.3B). Both Poly(I:C) and IL-17A were previously reported to activate NF-κB signalling pathway [95, 260, 454, 455]. Induction of the NF-κB leads to transcription of IL-6 and IL-8 and may provide explanation behind the increased Poly(I:C)-induced IL-6 production following IL-17A treatment reported in this study. Here, we predict that this may have potentially pathogenic effects on disease progression in IPF.

In this study, we used RANTES as a read-out for Poly(I:C)-driven, IFN-β activity. We previously demonstrated a significant correlation between decreased RANTES protein production in response to Poly(I:C) stimulation with worsened IPF prognosis as well as increased incidence of AE-related mortality in IPF patients [161, 366].

Here, we reported that treatment with IL-17A alone had no significant effect on production of RANTES protein in lung fibroblasts from healthy donors or IPF patients (Fig. 4.3E, F). Co-treatment with IL-17A had no significant effect on Poly(I:C)-induced RANTES protein production in lung fibroblasts from IPF patients (Fig. 4.3E, F). Binding of TLR3 leads to activation of IRF3, which results in induction of type I IFNs and ultimately increases RANTES transcription and secretion [154]. Neupane *et al.* demonstrated that IL-17A inhibited IRF3 transcription during Chikungunya Virus infection in mice [456]. Inhibition of IRF3 may offer a possible explanation behind the reduction in Poly(I:C)-induced RANTES protein production following IL-17A treatment observed in our study. Moreover, inhibition of anti-viral response by IL-17A has been demonstrated by Hou *et al.* who reported that the cytokine increased expression of anti-apoptotic proteins in murine bone marrow cells during Influenza infection, promoting viral persistence [266]. In addition, other studies demonstrated that Type I IFN signalling inhibited IL-17A by γδ T cells during bacterial infections in mice [457]. This suggests a possible negative feedback loop between Type I IFN signalling and IL-17A. In our previous study, we demonstrated that dysregulated Poly(I:C)-induced NF-κB responses in human lung fibroblasts from 412F-variant patients was associated with worsened clinical prognosis, greater decline in lung function, increased mortality as well as and higher incidence of AE-related death in IPF patients [161, 366].

Here, we used IL-8, IL-1β and caspase-1 transcription as a readout for Poly(I:C)-induced, pro-inflammatory activity in primary lung fibroblasts from healthy donors and IPF patients (Fig. 4.4A-F). We reported that treatment of IPF lung fibroblasts with Poly(I:C)

resulted in significantly increased IL-8, IL-1β and caspase-1 transcription (Fig. 4.4, B, D, F). In contrast, treatment with IL-17A had no of effect on IL-8, IL-1β and caspase-1 transcription in healthy lung fibroblasts (Fig. 4.4A, C, E). In this chapter, we demonstrated that the Poly(I:C)-driven increase in the transcription of IL-8, IL-1β and caspase-1 was potentiated in the presence of IL-17A in IPF fibroblasts, this did not reach significance. This increase was more pronounced in lung fibroblasts from IPF patients, relative to lung fibroblast from healthy individuals.

Research by other authors demonstrated the detrimental role of viral infection in IPF. Viruses, in particular herpesviruses, were recognised as an important causative factor underlying IPF development and disease progression. In addition, a large portion of IPF patients reported having an incidence of viral infection shortly prior to the onset of respiratory problems [7]. In a previous study, our lab demonstrated correlation between attenuated IFN-β and RANTES transcription in response to TLR3 stimulation with accelerated decline in lung function and an accelerated risk of mortality as well as higher rate of AE-related mortality in 412F-variant IPF patients [161, 366].

Here, we reported that treatment with IL-17A non-significantly decreased Poly(I:C)-driven transcription of IFN-β and RIG-I in lung fibroblasts from healthy donors (Fig. 4.5A, E). In addition, we demonstrated a non-significant reduction in Poly(I:C)-driven IFN-β, RANTES and RIG-I transcription in response to IL-17A treatment in lung fibroblasts from IPF patients (Fig. 4.5B, D, F). The reduced anti-viral response reported in our study is in agreement with findings by Hou *et al.* who reported that treatment with IL-17A increased expression of anti-apoptotic proteins, Bcl-2 and Bcl-xL in murine bone marrow cells. This resulted in protection of virally infected cells from apoptosis and CD8+ T cell-mediated target destruction which promoted viral persistence [266]. Inhibition of IRF3 by IL-17A during Chikungunya Virus infection in mice was demonstrated by Neupane *et al.* [456] and may provide a possible explanation behind the reduction in Poly(I:C)-induced IFN-β, RANTES and RIG-I transcription following IL-17A treatment observed in our study. We predict that the reduction in Poly(I:C)-driven IFN-β, RANTES and RIG-I transcription in response to IL-17A may impede resolution of viral infection and result in worsened development disease prognosis in IPF.

Other authors have demonstrated that IPF fibroblasts exhibited increased production or expression of pro-fibrotic mediators, such as TGF-β, α-SMA and collagens [388-391]. Here, we reported that co-treatment with IL-17A significantly decreased Poly(I:C)-induced transcription of α-SMA and COL3α1 in lung fibroblasts from healthy donors compared with

Poly(I:C) treatment only (Fig. 4.6C, E). IL-17A treatment had no significant effect on Poly(I:C)-induced transcription of α-SMA and COL3α1 in lung fibroblasts from IPF patients (Fig. 4.6B, D).

In this chapter, we investigated the effects of Poly(I:C)-induced TLR3 and RIG-I protein expression using western blot. TLR3 and RIG-I play a pivotal role in recognition of dsRNA of bacterial and viral pathogens [146, 458, 459]. Other authors demonstrated that induction of RIG-I led to activation of NF-κB and IRF3-driven signalling [460-464]. In this chapter, we demonstrated firstly that Poly(I:C)-treatment of healthy and IPF lung fibroblasts increased their TLR3 and RIG-I protein expression (Fig. 4.7A, B). We demonstrated that on its own treatment with IL-17A had no effect on TLR3 and RIG-I protein expression in healthy and IPF lung fibroblasts (Fig. 4.7A, B). We reported that treatment with IL-17A reduced Poly(I:C)-induced protein expression of TLR3 and RIG-I in lung fibroblasts from IPF patients (Fig. 4.7B) but not in lung fibroblasts from healthy controls (Fig. 4.7A). Other studies reported that treatment with IL-17A resulted in protection of virally infected murine bone marrow cells and led to increased viral persistence [266]. In addition, IL-17A was demonstrated to inhibit IRF3 transcription in mice infected with Chikungunya Virus [456]. Inhibition of IRF3 transcription by IL-17A may provide an explanation behind the decreased Poly(I:C)-induced TLR3 and RIG-I protein expression following IL-17A treatment reported in this study. In our previous studies, we reported that dysregulated TLR3 function was associated with accelerated decline in lung function and an accelerated risk of mortality as well as higher rate of AE-related mortality in IPF patients [161, 366].We predict that the decrease in Poly(I:C)-induced TLR3 and RIG-I protein expression following IL-17A treatment observed in IPF lung fibroblasts may have a potentially pathogenic effects in terms of IPF progression.

In the first experimental chapter, we demonstrated the modulatory effects of 4-OI on Poly(I:C)-induced production of IL-8 in lung fibroblasts from healthy donors and IPF patients. We reported that treatment with 4-OI increased Poly(I:C)-driven production of IL-8 protein in both healthy and IPF lung fibroblasts. Previously in this chapter, we demonstrated that IL-17A treatment significantly increased Poly(I:C)-induced production IL-6 protein in lung fibroblasts from IPF patients. Here, we investigated the effects of 4-OI on IL-17A-induced protein production of IL-6 and IL-8 in primary human lung fibroblasts from healthy donors and IPF patients. Our data demonstrated that treatment with 4-OI non-significantly increased IL-17A-induced protein production of IL-6 in healthy lung fibroblasts; and non-significantly decreased IL-6 protein production in IPF lung fibroblasts. In addition, 4-OI non-significantly increased IL-17A-induced IL-8 protein production in lung fibroblasts from healthy donors and IPF patients.

The ability of 4-OI to reduce IL-17A-driven IL-6 protein production may be explained by inhibition of NF-κB both directly via NRF2 activation and indirectly via induction of ATF3 [195, 229, 230]. The non-significant increase in IL-17A-induced IL-8 protein production following 4-OI treatment is in agreement with a study carried out in human monocytes, in which the authors reported increased IL-8 protein production following DI treatment; a synthetic analogue of itaconate in uninfected cells and in cells infected with Influenza virus [370]. In addition, Muri *et al.* demonstrated that at higher doses, itaconate promoted caspase-8-driven IL-1β processing in murine bone marrow-derived dendritic cells (BMDCs) [465]. Other authors reported that activation of caspase-8 resulted in induction of NF-κB pathway and therefore may provide the explanation behind the increased IL-17A-driven IL-8 protein production by 4-OI reported in this study [466]. Our lab has previously demonstrated that dysregulated Poly(I:C)-induced NF-κB response resulted in worsened clinical prognosis in patients with IPF. We predict that increased IL-17A-driven IL-8 protein production reported following 4-OI treatment may have pathogenic effects on the disease prognosis in IPF patients.

In this second part of this study, we demonstrated a significant association between the *IL-17A* G197A (rs2275913) polymorphism with development of IPF in UK patients. Here, we presented data from our case-control study in which we determined that the *IL-17A* 197A-homozygous genotype was significantly associated with development of IPF. The Odds Ratio of 3.167 obtained in this pilot study suggested that *IL-17A* 197A-homozygous individuals were three times more likely to develop IPF. In addition, we demonstrated that IPF patients who were 197A-variant had an increased risk of IPF-pneumonia death that approached statistical significance (p=0.07). Furthermore, 197A-variant IPF patients had less time to death compared to their G197-WT IPF patient counterparts. This effect was not due to a significant difference in pulmonary function in G197-WT IPF patients at diagnosis. These *IL-17A* G197A studies were carried out in an IPF cohort of modest size due to sample availability. These findings warrant further investigation into possible use of *IL-17A* G197A SNP as a prognostic biomarker for IPF patients.

In conclusion, in this chapter we demonstrated that treatment with IL-17A alone significantly increased IL-6 and IL-8 in IPF fibroblasts. Co-treatment with IL-17A significantly increased Poly(I:C)-induced IL-6 protein production in lung fibroblasts IPF patients. Our western blot data demonstrated that IL-17A reduced Poly(I:C)-driven TLR3 and RIG-I protein expression in IPF lung fibroblasts. Overall, we reported that IL-17A decreased Poly(I:C)-driven TLR3 expression in lung fibroblasts from IPF patients, which we predict may have pathogenic

effects on IPF progression. Finally, this chapter provides evidence that the *IL-17A* G197A promoter polymorphism may represent a novel prognostic marker in IPF, and further studies are required to investigate this further.

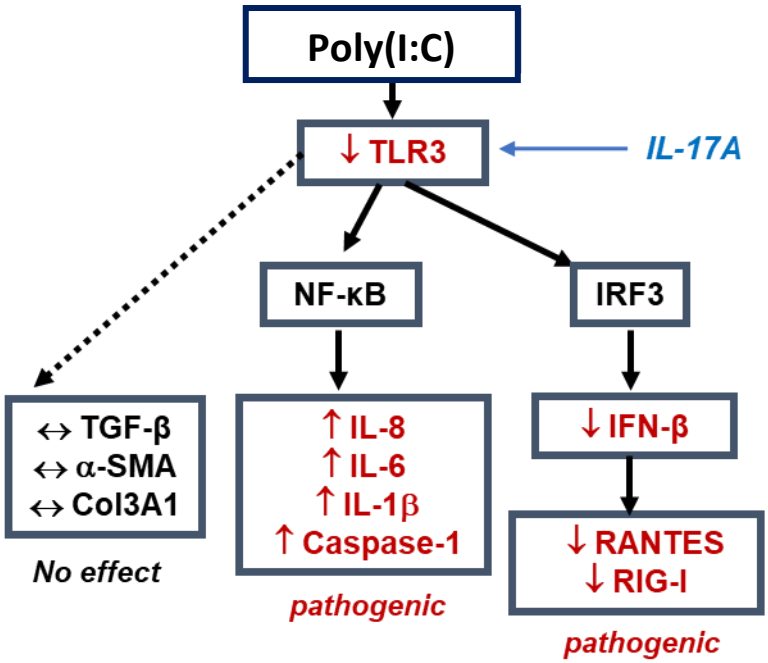

Figure. 4.9. Summary of the results reported in chapter 4. This schematic summarises our findings on the effects of IL-17A on TLR3 function in primary human IPF lung fibroblasts following viral dsRNA treatment using the poly(I:C) dsRNA analogue. The putative protective or pathogenic effects of IL-17A modulation of TLR3 are shown in IPF lung fibroblasts.

Chapter 5 – Characterisation of the effect of *TLR3* L412F (rs3775291) on the lung microbiome in IPF patients; investigation of the function of *TLR3* L413F *in vivo* in novel CRISPR/Cas 9 knock-in mice.

5.1 Introduction

Idiopathic Pulmonary Fibrosis (IPF) is a non-neoplastic form of chronic fibrosing interstitial pneumonia [1]. The origin of IPF is unknown, the disease is characterised by scarring of the lung parenchyma which ultimately results in respiratory failure [2, 3, 7]. IPF is a fatal disease which affects 13 to 20 in every 100,000 people worldwide [2, 3, 7]. With its incidence on the rise, it has been estimated that on average, one in every 100 deaths in the UK occurs due to IPF [2, 3, 7]. The median survival rate of the patients is 5 years following the diagnosis [2, 3, 7]. The progression of IPF can be divided into 3 major pathways [7]. The pathway most prevalent in IPF patients is a slow, gradual loss of respiratory function over the span of 5 years [7]. A more rapid pathway of the disease progression which results in a median lifespan of 1 year since the diagnosis manifests in approximately 15% of IPF patients [7]. Lastly, a subgroup of IPF patients experience initially a mild and steady progression in the loss of respiratory function, which rapidly worsens due to an adverse event known as an acute exacerbation (AE) [7]. On average 50% of the patients who experience AE event will die within 30 days [7].

Currently, there is no reliable method to predict which progression pathway will manifest in individual patients with IPF. Despite the fatality and the rapid progression rate of IPF, the treatment as well as diagnostic biomarkers of the disease are very limited. Pirfenidone and Nintedanib are the two FDA and EMA-approved pharmacological treatments [7]. Pirfenidone and Nintedanib significantly increase progression free survival in IPF patients, however, the majority of patients is not able to tolerate Pirfenidone or Nintedanib due to severe gastrological side effects (7).In terms of prognostic biomarkers, MUCB5 promoter polymorphism is a sole validated prognostic biomarker in IPF up to date [7]. Identification of reliable, and easily measured prognostic biomarkers is crucial for more tailored approach to patient treatment, patient prioritisation, and even early remission for lung transplantation.

TLR3 L412F (rs3775291) is a single nucleotide polymorphism (SNP) in the TLR3 gene [165]. In our previous study we reported that the presence of the SNP resulted in decreased TLR3 function in IPF patients [161]. Ranjith-Kumar *et al.* reported a high degree of homology between human and murine *TLR3* L412F polymorphism, in which the amino-acid substitution Leu412Phe in humans corresponds to that of Leu413Phe in mice [165]. We previously commissioned the generation of *TLR3* L413F-knock in mice (Taconic Biosciences Inc., Köln, Germany), using CRISPR-Cas-9 gene editing in order to investigate the effects of *TLR3* L412F SNP *in vivo*. We previously characterised the functionality of our *TLR3* L413F-knock in mice in

response to TLR3 stimulation *in vitro* using primary murine lung fibroblasts from L413F-WT, 413F-HET and 413F-HOM mice (McElroy *et al.* unpublished data). We reported that primary lung fibroblasts from 413F-HET and 413F-HOM mice presented with reduced RANTES and KC protein production compared with L413-WT mice following Poly(I:C) treatment (McElroy *et al.* unpublished data). In our previous *in vitro* study, our group have also demonstrated attenuated transcription of Poly(I:C)-induced RANTES in primary murine lung fibroblasts from 413F-HET and 413F-HOM mice compared with L413-WT mice (McElroy *et al.* unpublished data). Moreover, the *TLR3* L413F SNP resulted in decreased transcription of MIP2; a human IL-8 homologue in mice, in murine lung fibroblasts stimulated with Poly(I:C) in 413F-HET mice compared with L413-WT mic*e* (McElroy *et al.* unpublished data). In addition, we have previously determined the effects of *TLR3* L413F SNP on TLR3 and TLR4 transcription in primary murine lung fibroblasts. We reported comparable levels of TLR3 and TLR4 transcription in response to Poly(I:C) treatment in lung fibroblasts from L413-WT and 413F-HET mice. Treatment with Poly(I:C) produced most profound increase in the transcription of TLR3 and TLR4 in primary murine lung fibroblasts from 413F-HOM mice (McElroy *et al.* unpublished data). Our *in vitro* data reveal that the presence of the *TLR3* 413F SNP affected Poly(I:C)-induced, NF-κB and IRF3-mediated response in primary murine lung fibroblasts.

We have previously demonstrated the importance of Poly(I:C)-driven responses in the pathology of pulmonary fibrosis in mice [161]. In our previous study, we utilised the bleomycin model of pulmonary fibrosis to demonstrate that deletion of TLR3 led to reduced survival and greater levels of fibrosis in $TLR3^{-/-}$ mice compared to their WT counterparts [161]. The increased fibrosis was associated with enhanced production of pro-fibrotic mediators TGF-β, IL-4 and IL-13 as well as greater collagen deposition in the pulmonary tissue [161]. In addition, we have previously characterised the effects of *TLR3* L412F (rs3775291) SNP in the context of IPF in patients [161]. Although we reported no association between *TLR3* L412F and the development of IPF in two separate IPF cohorts, we determined a strong correlation between the SNP and increased hazard ratio as 412F-HET and 412F-HOM IPF patients had five times greater risk of mortality at 12 months and 24 months compared with *TLR3* L412-WT patients [161]. Moreover, patients heterozygous and homozygous for the 412F SNP presented with an accelerated rate of decline in forced vital capacity (FVC) over the period of 12 months compared with L412-WT patients [161]. We demonstrated defective Poly(I:C)-driven cytokine, type I IFN and fibroproliferative responses in primary lung fibroblasts from 412F-HET and L412F-HOM IPF patients compared with lung fibroblasts from L412F WT patients [161].

Transcription of IFN-β and RANTES, as well as protein production of RANTES was attenuated in lung fibroblasts from 412F-HET and L412F-HOM IPF patients in response to TLR3 stimulation [161]. Moreover, we reported that lung fibroblasts from L412F-HOM patients presented with decreased Poly(I:C)-driven protein production of IL-8 compared with lung fibroblasts from L412-WT IPF patients. Additionally, in our study, we determined that fibroblasts from patients with the L412F allele variant showed reduced mRNA expression of TLR3, compared with L412-WT IPF patients [161]. In a more recent study, our group has demonstrated a significant correlation between the presence of L412F variant and incidence of AE-related death in IPF patients [366]. We reported that IPF patients heterozygous for *TLR3* L412F presented with dysregulated anti-bacterial responses to LPS, Pam3CYSK4, flagellin, FSL-1 and live *Pseudomonas aeruginosa* infection compared with L412-WT IPF patients [366].

Thus, the aim of this chapter was to characterise the functionality of the TLR3 L412F SNP in vivo in IPF patients. We firstly investigated the impact of *TLR3* L412F on the lung microbiome of IPF patients. The second aim of this chapter is to determine the functionality of this TLR3 SNP *in vivo* using our novel *TLR3* L413F, CRISPR-Cas-9 knock-in mice. Here, we investigated the effect of the 413F-variant on basal production of RANTES and KC in lung, spleen, liver, and brain in 413F-HET mice. We then investigated the ability of Poly(I:C) to upregulate pro-inflammatory, anti-viral and anti-oxidant mediators in 413F-HET mice. We finally investigated the differences in the above responses in female versus male mice.

5.1.1. 412F-heterozygous IPF patients have changes in bacterial burden and specific bacterial species in their lung microbiome compared with L412-wild type patients.

Prof. Toby Maher and Prof. Phil Molyneaux recruited a separate cohort of 47 patients with IPF from the Royal Brompton Hospital, London, UK (**Table 5.1**.). Subjects underwent bronchoalveolar lavage and bacterial DNA was isolated, quantified by qPCR and the 16S rRNA gene sequenced to characterise the bacterial communities in the lower airways as described previously [83, 84]. The *TLR3* L412F genotype status was established for each IPF patient. **Fig. 5.1A** and **5.1B** illustrate the differences observed at the phylum and genus level for bacteria in the BAL from L412-wild type (WT) (**Fig. 5.1A)** compared with 412F-heterozygous IPF patients (**Fig. 5.1B)**. Here, we determined that the bacterial burden was significantly less in BAL from 412F-heterozygous (HET: 4.39 ± 0.15; Log10 16S rRNA gene copies/ml) compared with L412-wild type (WT: 4.96 ± 0.98; Log10 16S rRNA gene copies/ml) (p=0.0024; **Fig. 5.1C)**. Analysis of specific bacterial populations revealed that 412F-heterozygous patients had significantly higher prevalence of *Streptococcus spp.* **(Fig. 5.1E)** and *Staphylococcus spp.* **(Fig. 5.1F)** in their BAL samples compared with wild-type IPF patients (**Fig. 5.1E, 5.1F)**. Conversely, we demonstrated that L412-wild type IPF patients **(Fig. 5.1D)** had significantly higher levels of *Prevotella spp.* compared to 412F-heterozygous patients **(Fig. 5.1D)**. These results demonstrate the *TLR3* L412F polymorphism acts to dysregulate the lung microbiome in 412F-heterozygous IPF patients and may predispose these patients to a worsened disease phenotype and progression.

Table 5.1. Baseline characteristics of UK IPF cohort for microbiome analysis.

	All IPF	CC (L412-WT)	CT (412F-HET)	† *P* value
Patients *n (%)*	47	22 (46.8)	25 (53.2)	-
Male, *n (%)*	38 (80.8)	18 (82)	20 (80.0)	0.60
Age, yr (± SD)	65 (15.76)	62 (18.37)	67 (12.84)	0.28
Baseline PFTs*:				
FVC (± SD)	75.87 (20.14)	76.03 (24.93)	75.53 (15.2)	0.96
DLco (± SD)	44.74 (17.52)	43.20 (14.00)	46.21 (20.56	0.86
Smoking status:				
Non-smoker, *n (%)*	18 (38.3)	10 (45.5)	8 (32.0)	-
Ex-smoker, *n (%)*	25 (53.2)	11 (50)	14 (56.0)	0.50
Current smoker, *n (%)*	4 (8.5)	1 (4.5)	3 (12.0)	-

Definition of abbreviations: DL_{CO} = diffusion capacity for carbon monoxide; PFT = pulmonary function test. *FVC and DL_{CO} expressed as percentage of predicted value. Data are presented as mean (± SD) unless otherwise stated. † *P* value = CC versus CT IPF patients using Mann Whitney U or Fisher's exact test. [CC: L412-wild type (WT); CT: 412F-heterozygous (HET)].

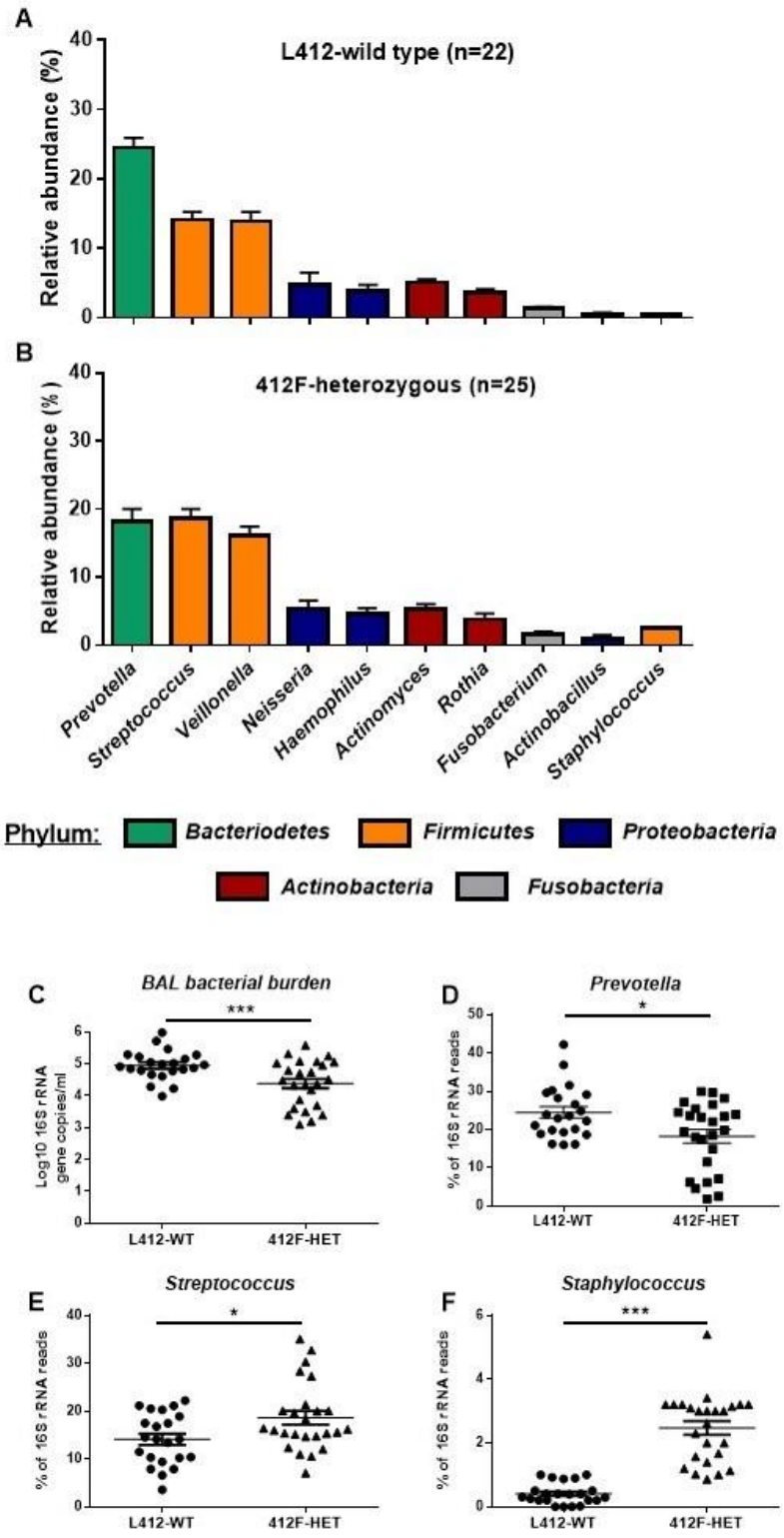

Fig. 5.1. Effects of *TLR3* L412F on taxonomic composition of bacteria in bronchoalveolar lavage (BAL) of subjects with IPF. (A, B) Representing relative abundance of bacteria at the phylum and genus levels in L412-wild type (WT) and 412F-heterozygous (HET) IPF patients. **(C)** Bacterial burden and **(D-F)** taxonomic differences were statistically tested by Mann-Whitney U test between individual bacterial genera in the BAL of L412-WT (n=22) and 412F-HET (n=25) IPF patients. Data is presented as mean ± S.E.M. *p<0.05, **p<0.001: L412-WT compared with 412F-HET IPF patients.

5.2. Effects of *TLR3* L413F on basal production of RANTES protein in the lung, spleen and brain tissue of L413-WT and 413F-HET female mice.

Our group has previously demonstrated the role of defective TLR3 in the bleomycin model of pulmonary fibrosis in mice [161]. We determined that $TLR3^{-/-}$ mice challenged with bleomycin exhibited reduced survival rates and greater levels of fibrosis compared with WT mice [161]. In consequent studies, we demonstrated significantly increased basal levels of RANTES protein production in primary lung fibroblasts from 412F-HET IPF patients compared with L412-WT IPF patients [366]. In order to examine the effects of *TLR3* L412F *in vivo*, we previously commissioned generation of novel *TLR3* 413F-HET and 413F-HOM knock-in mice. Here, we examined whether the *TLR3* L413F SNP affected basal production of RANTES protein *in vivo* in mice. RANTES is an anti-viral chemokine, induced by type I IFNs, and regulated by TLR3 activity [377]. Female mice were administered an intraperitoneal (I.P) injection of PBS. After 6 hours post-injection, mice were sacrificed, their lungs, spleens and brains harvested and homogenized. Tissue homogenates from individual organs were tested for the amount of protein present using BCA. The samples were used to quantify RANTES protein production using ELISA. Here, we reported that the basal levels of RANTES protein production was significantly increased in the spleen tissue of 413F-HET mice (**Fig. 5.2B; *p<0.05**) compared with the spleen tissue of L413-WT mice. Basal production of RANTES protein was reduced in the brain tissue of 413F-HET mice compared with the brain tissue of L413-WT mice, however, this reduction was insignificant (**Fig. 5.2C)**.

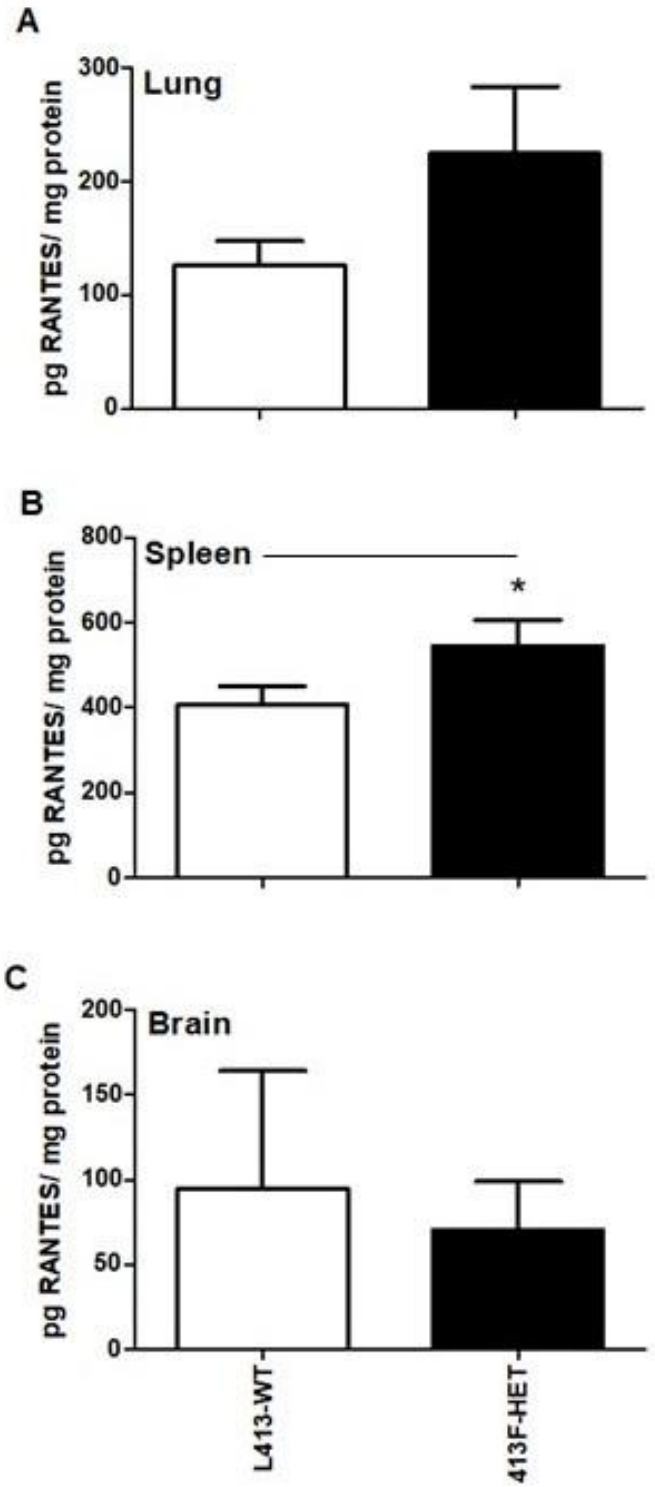

Figure 5.2. Effects of *TLR3* L413F on basal production of RANTES protein in the lung, spleen and brain tissue of L413-WT and 413F-HET female mice. Basal levels of RANTES protein production were significantly increased in the spleen tissue (**B**) of 413F-HET female mice compared with female L413-WT mice, as quantitated by ELISA. An unpaired Student's t-test was used to test for statistical differences. *p<0.05: female L413-WT compared with 413F-HET female mice. The graph represents data from lung, spleen and brain tissue from six L413-WT and six 413F-HET female mice, respectively, performed once (n=6). Results shown represent the mean ± SEM.

5.3. Effects of *TLR3* L413F on basal production of KC protein in the lung, spleen and brain tissue of L413-WT and 413F-HET female mice.

Keratinocyte-derived chemokine (KC) is the closest murine IL-8 homologue in humans [467]. KC is induced via Poly(I:C)-driven, NF-κB signalling and its role is to attract neutrophils to the stie of the infection and to drive the production of pro-inflammatory mediators [468, 469]. Our group previously demonstrated significantly increased basal levels of IL-8 protein production in primary lung fibroblasts from 412F-HET IPF patients compared with L412-WT IPF patients [366]. Here, we aimed to examine the effects of the *TLR3* L413F on the basal production of KC protein *in vivo*. In this study, we reported a significant increase in the basal KC protein production in the lung tissue of 413F-HET female mice compared with the lung tissue of L413-WT female mice (**Fig. 5.3A; *p<0.05**). Basal levels of KC protein production were increased in the brain tissue of the 413F-HET female mice compared with the brain tissue of L413-WT female mice; however, these data did not reach statistical significance (**Fig. 5.3C)**. There was no change in the basal levels of KC protein production in the spleen tissue of 413F-HET and L413-WT female mice (**Fig. 5.3B)**.

5.4. Effects of *TLR3* L413F on RANTES protein production in the lung, spleen, liver, and brain tissue of Poly(I:C)-treated L413-WT and 413F-HET female mice.

Previously, we demonstrated that lung fibroblasts from 412F-HET IPF patients presented with increased basal RANTES protein production compared with lung fibroblasts from L412-WT IPF patients [366]. We previously reported decreased RANTES protein production, as well as decreased IFN-β and RANTES mRNA in response to TLR3 stimulation in lung fibroblasts from 412F-HET IPF patients compared with L412-WT patients [161, 366]. These dysregulated responses were associated with elevated pulmonary fibrosis, accelerated rate in FVC decline, increased hazard mortality ratios as well as increased risk of AE-related mortality in IPF patients [161, 366]. Here, we investigated the effects of the *TLR3* L413F on RANTES protein production in the lung, spleen, liver, and brain tissue of Poly(I:C)-treated female mice *in vivo.* Female L413-WT and 413F-HET mice were administered with I.P injection of PBS or Poly(I:C) (50 μg/mouse in 200 μl of PBS). After 6 hours post-injection, mice were humanely killed, their lungs, spleens, livers, and brains harvested and homogenized. Tissue homogenates from individual organs were tested for the amount of protein present using BCA. The samples were used to quantify RANTES protein production using ELISA. We reported that Poly(I:C) injection resulted in a trend towards increased RANTES protein production compared with PBS in the lung (**Fig. 5.4A)**, liver

(**Fig. 5.4E)** and brain (**Fig. 5.4G)** tissue of L413-WT female mice. Treatment of L413-WT female mice with Poly(I:C) significantly increased RANTES protein production compared with PBS in the spleen tissue (**Fig. 5.4C; *p<0.05**). We demonstrated that the decrease in production of RANTES protein in 413F-HET female mice treated with Poly(I:C) in the spleen (**Fig. 5.4D)** tissue was not significant compared with PBS. Treatment of 413F-HET female mice with Poly(I:C) increased RANTES protein production in the liver tissue (**Fig. 5.4F)** compared with PBS, these data did not reach statistical significance. 413F-HET female mice injected with Poly(I:C) presented with no change in the production of RANTES protein in the lung (**Fig. 5.4B)** and brain (**Fig. 5.4H)** tissue compared with PBS.

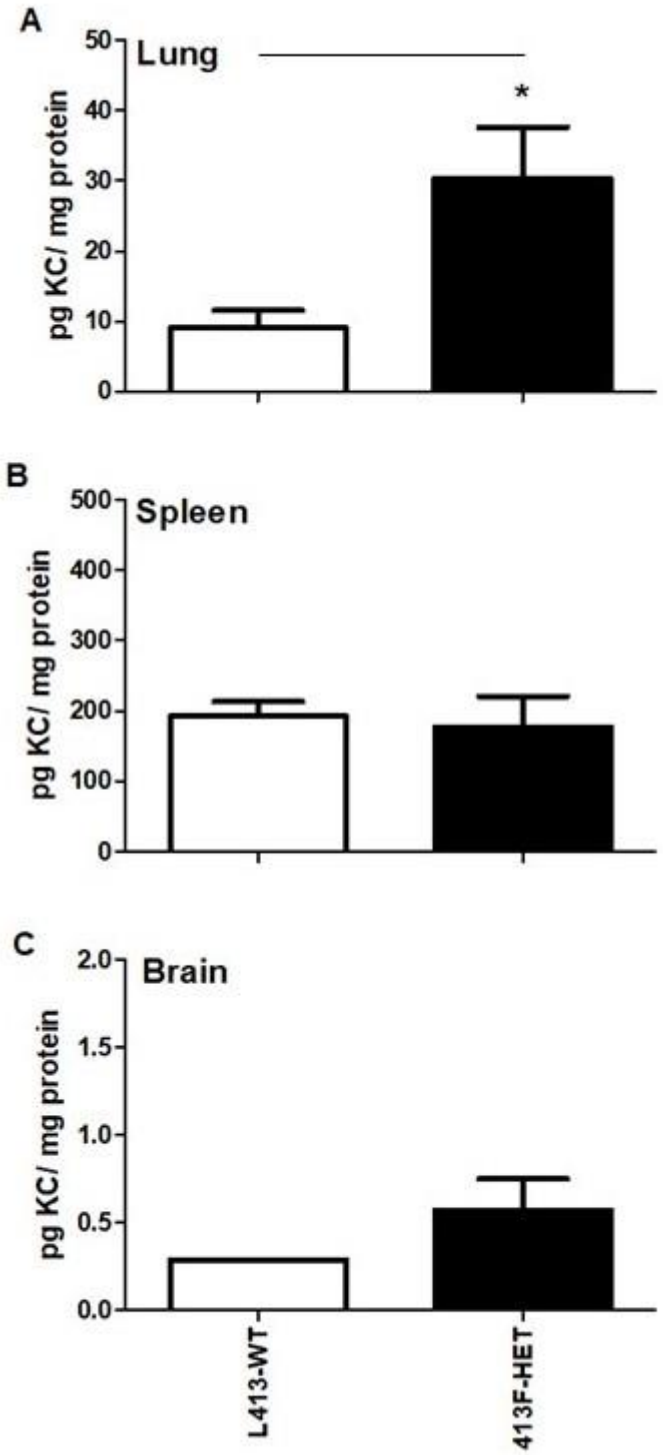

Figure 5.3. Effects of *TLR3* L413F on basal production of KC protein in the lung, spleen and brain tissue of L413-WT and 413F-HET female mice. Basal levels of KC protein production were significantly increased in the lung tissue (**A**) of 413F-HET female mice compared with the lung tissue of L413-WT female mice, as quantitated by ELISA. An unpaired Student's t-test was used to test for statistical differences. *$p<0.05$: female L413-WT compared with 413F-HET female mice. Graphs represent data from lung, spleen and brain tissue from six L413-WT and six 413F-HET female mice, respectively, performed once (n=6). Results shown represent the mean ± SEM.

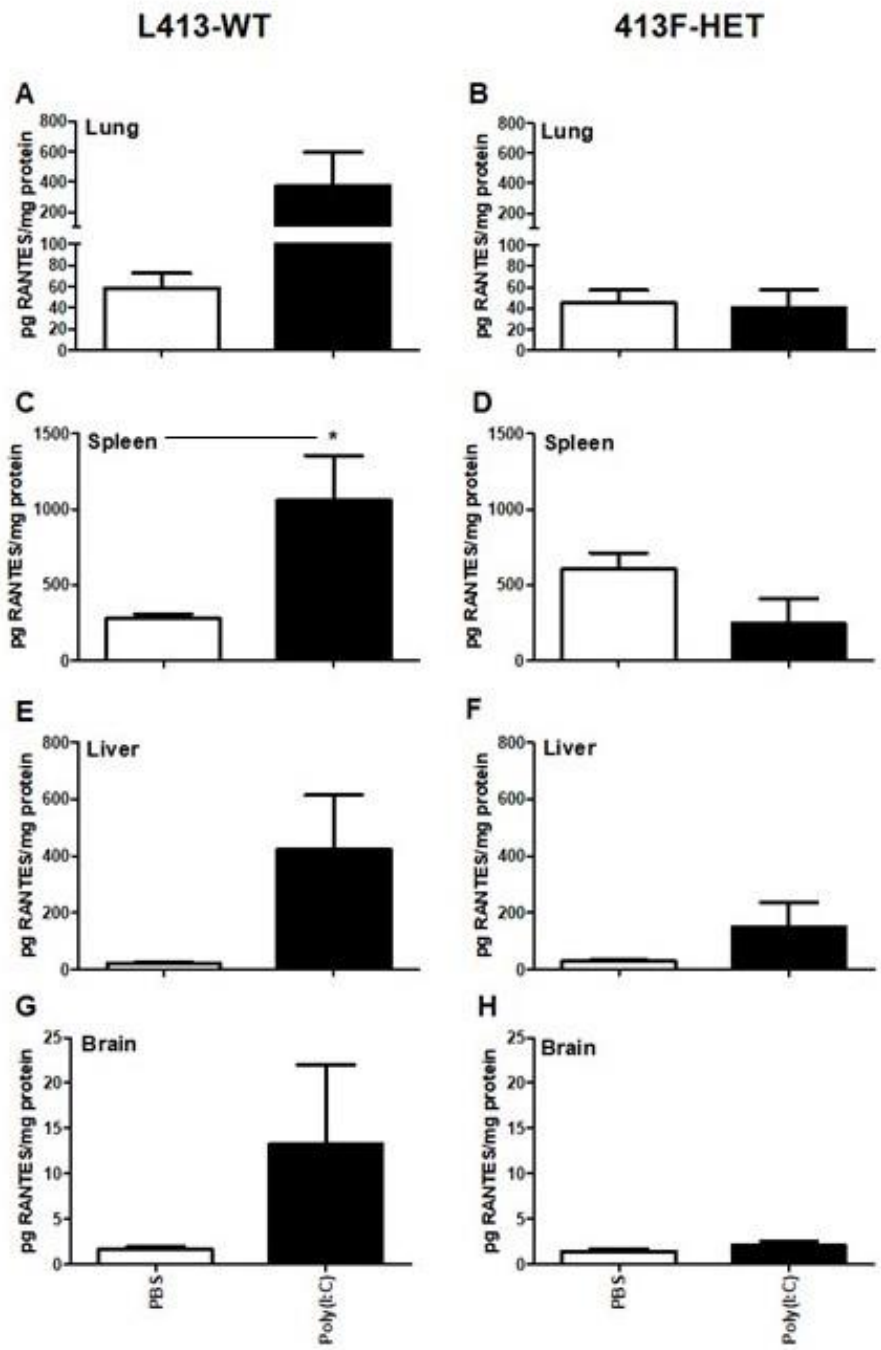

Figure 5.4. Effects of *TLR3* L413F on RANTES protein production in the lung, spleen, liver, and brain tissue of Poly(I:C)-treated L413-WT and 413F-HET female mice. RANTES protein production was significantly increased in the spleen (**C**) of Poly(I:C)-treated L413-WT female mice compared with PBS-treated female mice, as quantitated by ELISA. No significant Poly(I:C)-induced changes were quantitated in 413F-HET female mice tissues (B, D, F, H) compared with PBS-treatment. An unpaired Student's t-test was used to test for statistical differences. *$p<0.05$: Poly(I:C) treatment compared with PBS only treatment. Graphs represent data from lung, spleen, liver and brain tissue at 6h post I.P. injection with Poly(I:C) or PBS injection, respectively, from six L413-WT and six 413F-HET female mice (performed once; n=6 per group). Results shown represent the mean ± SEM. [Poly(I:C), 50 µg/mouse in 200 µl of PBS].

5.5. Effects of *TLR3* L413F on KC protein production in the lung, spleen, liver, and brain tissue of Poly(I:C)-treated L413-WT and 413F-HET female mice.

In our lab, we previously demonstrated increased basal KC protein production in lung fibroblasts from 412F-HET IPF patients compared with lung fibroblasts from L412-WT IPF patients [366]. However, we also determined that despite the increased levels of basal protein production, lung fibroblasts from IPF patients homozygous and heterozygous for *TLR3* L412F, presented with reduced IL-8 protein production in response to TLR3 stimulation [161, 366]. Our previous data from *in vitro* experiments on *TLR3* L413F knock-in mice demonstrated that primary lung fibroblasts from 413F-HET and 413F-HOM mice presented with reduced protein production of KC in response to Poly(I:C) treatment, compared with lung fibroblasts from L413-WT mice (McElroy *et al.* unpublished data). . Here, we investigated the effects of the *TLR3* L413F on KC protein production in the lung, spleen, liver, and brain tissue of Poly(I:C)-treated mice *in vivo.* We reported a trend towards increased KC protein production in the lung (**Fig 5.5A)**, spleen (**Fig. 5.5C)** and brain (**Fig. 5.5G)** tissue of Poly(I:C)-injected L413-WT female mice compared with PBS treatment. Production of KC protein was significantly increased in the liver tissue of L413-WT female mice treated with Poly(I:C), compared with female mice treated with PBS (**Fig. 5.5E; *p<0.05**). 413F-HET female mice exhibited elevated KC protein production in the lung and liver tissue in response to Poly(I:C) injection compared with PBS treatment (**Fig. 5.5B, F)** respectively, these results did not reach significance. There was no difference in the KC protein production in the spleen (**Fig. 5.5D)** and brain (**Fig. 5.5H)** tissue of Poly(I:C)-injected 413F-HET female mice compared with PBS.

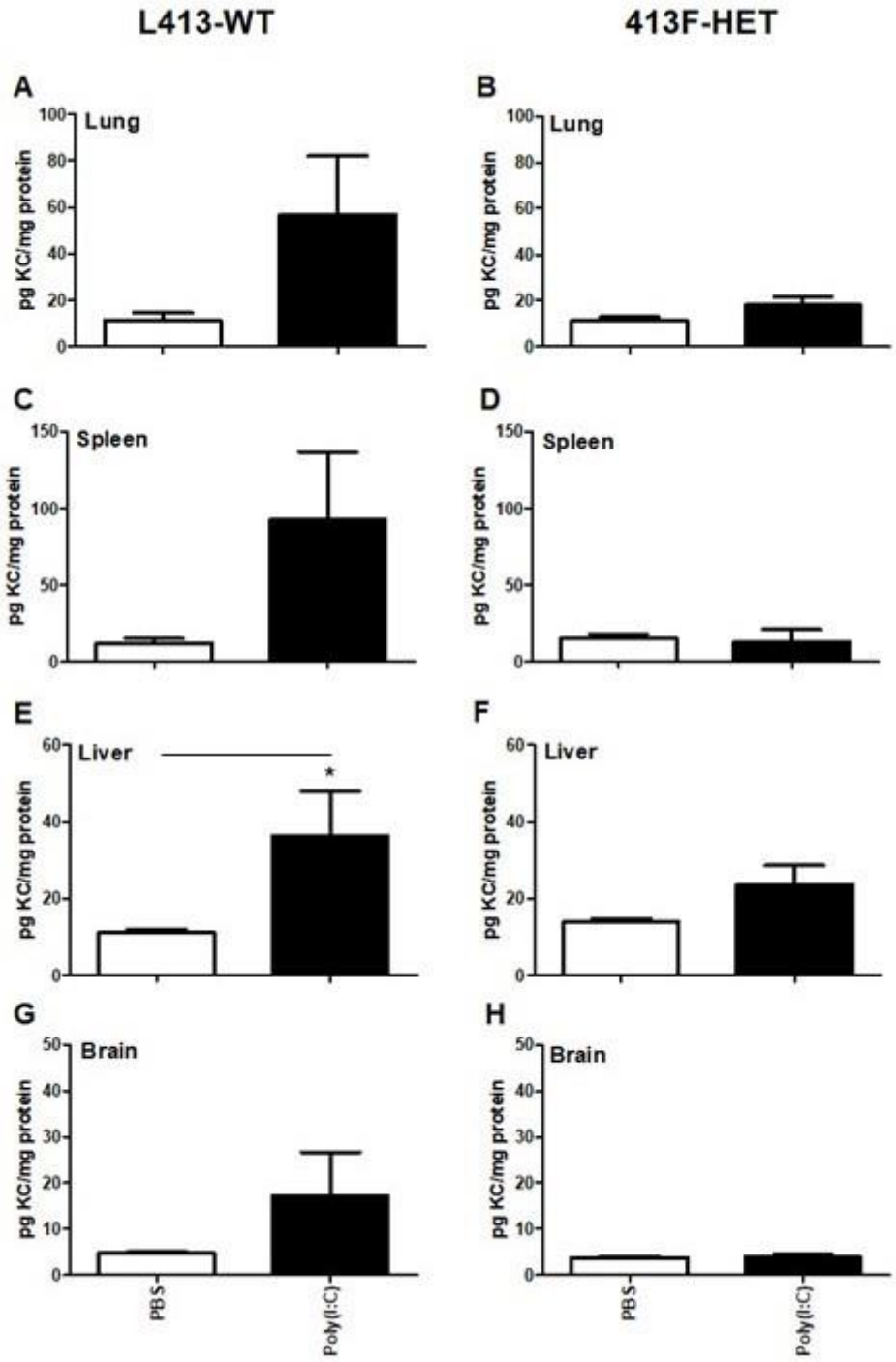

Figure 5.5. Effects of *TLR3* L413F on KC protein production in the lung, spleen, liver, and brain tissue of Poly(I:C)-treated L413-WT and 413F-HET female mice. KC protein production was significantly increased in the liver (**E**) of Poly(I:C)-treated L413-WT female mice compared with PBS-treated female mice, as quantitated by ELISA. No significant Poly(I:C)-induced changes were quantitated in 413F-HET female mice tissues (B, D, F, H) compared with PBS-treatment. An unpaired Student's t-test was used to test for statistical differences. *$p<0.05$: Poly(I:C) treatment compared with PBS only treatment. Graphs represent data from lung, spleen, liver and brain tissue at 6h post I.P. injection with Poly(I:C) or PBS injection, respectively, from six L413-WT and six 413F-HET female mice (performed once; n=6 per group). Results shown represent the mean ± SEM. [Poly(I:C), 50 µg/mouse in 200 µl of PBS].

5.6. Effects of *TLR3* L413F on IL-1β, IL-6, TNF-α and caspase-1 transcription in the lung tissue of Poly(I:C)-treated L413-WT and 413F-HET female mice.

IL-1β, IL-6, TNF-α are pro-inflammatory cytokines induced via NF-κB signalling [470-472]. caspase-1 is an enzyme which converts various pro-inflammatory cytokines, including IL-1β into their active forms [473]. Other authors have demonstrated that the transcription of the pro-inflammatory cytokines IL-1β, IL-6 and TNF-α were initially elevated in the bleomycin model of pulmonary fibrosis in mice and rats [474, 475]. Other authors have shown that AE-IPF patients presented with increased levels of IL-6 in the serum when compared to healthy controls and patients with stable IPF [418]. In their study, Papiris *et al.* demonstrated that elevated blood levels of IL-6 predicted exacerbations in IPF patients [376]. Here we investigated the effects of the *TLR3* L413F on IL-1β, IL-6, TNF-α and caspase-1 transcription in the lung tissue of Poly(I:C)-treated mice *in vivo.* Female L413-WT and 413F-HET mice were administered with I.P injection of PBS or Poly(I:C) (50 μg/mouse in 200 μl of PBS). After 6 hours post-injection, mice were sacrificed, their lungs harvested and homogenized. mRNA was extracted from the lung tissue homogenates and used to generate cDNA. Transcription of IL-1β, IL-6, TNF-α and caspase-1 was quantitated using qPCR. We reported significantly increased transcription of IL-6 (**Fig. 5.6C; *p<0.05**) and TNF-α (**Fig. 5.6E; *p<0.05**) in the lung tissue of Poly(I:C)-treated L43-WT female mice compared with PBS-treatment. In addition, we reported significantly decreased transcription in caspase-1 in the lung tissue of L413-WT female mice injected with Poly(I:C) compared with PBS-treatment only (**Fig. 5.6G; **p<0.01**). Lung tissue of 413F-HET female mice treated with Poly(I:C) had significantly increased transcription of IL-1β (**Fig. 5.6B; *p<0.05**), IL-6 (**Fig. 5.6D; **p<0.01**) and caspase-1 (**Fig. 5.6H; ***p<0.001**) compared with PBS-treated mice.

5.7. Effects of *TLR3* L413F on IFN-β, RANTES and RIG-I transcription in the lung tissue of Poly(I:C)-treated L413-WT and 413F-HET female mice.

IFN-β, RANTES and RIG-I are anti-viral IRF3-driven mediators induced in response to TLR3 activation [379-381]. In our previous studies, we demonstrated reduced Poly(I:C)-driven IFN-β, RANTES and RIG-I transcription in lung fibroblasts from 412F-HET IPF patients compared with lung fibroblasts from L412-WT IPF patients [161, 366]. These dysregulated responses were associated with greater levels of pulmonary fibrosis, increased risk of mortality as well as increased AE-related death in IPF patients heterozygous for the *TLR3* L412F allele [161, 366]. Our previous data from *in vitro* experiments on *TLR3* L413F knock-in mice demonstrated

that primary lung fibroblasts from 413F-HET and 413F-HOM mice presented with reduced RANTES transcription compared with L413-WT in response to Poly(I:C) treatment (McElroy *et al.* unpublished data). Here we investigated the effects of the *TLR3* L413F on IFN-β, RANTES and RIG-I transcription in the lung tissue of Poly(I:C)-treated mice *in vivo.* We reported significantly increased transcription of RIG-I (**Fig. 5.7E; *p<0.5**) in the lung tissue of L413-WT female mice compared with PBS. The transcription of IL-1β, RANTES and RIG-I was significantly increased in the lung tissue of 413F-HET female mice injected with Poly(I:C) compared with PBS (**Fig. 5.7B, D, F; *p<0.5**) respectively.

5.8. Effects of *TLR3* L413F on TLR3 and IRF3 transcription in the lung tissue of Poly(I:C)-treated L413-WT and 413F-HET female mice.

Binding of dsRNA to TLR3 leads to induction of IRF3 and ultimately results in increased interferon response [476]. Our group have previously reported that *TLR3* L412F SNP was associated with defective cytokine, IRF3-regulated type I IFN, and fibroproliferative responses which were associated with worsen clinical prognosis and higher risk of mortality in IPF patients [161, 366]. In our previous study, we demonstrated that pulmonary fibroblasts from *TLR3* 413F-HET and *TLR3* L413F-HOM knock in mice presented with reduced IRF3-dependent RANTES transcription compared with lung fibroblasts from L413-WT mice in response to Poly(I:C) treatment *in vitro* (McElroy *et al.* unpublished data). Here, we investigated the effects of the *TLR3* L413F on TLR3 and IRF3 transcription in the lung tissue of Poly(I:C)-treated mice *in vivo.* TLR3 transcription was significantly increased in the lung tissue of Poly(I:C)-treated L413-WT female mice with PBS-treated mice (**Fig. 5.8A, *p<0.05**). TLR3 and IRF3 transcription was significantly increased in the lung tissue of Poly(I:C)-treated 413F-HET female mice compared with PBS-treated mice (**Fig. 5.8B, D; *p<0.05, **p<0.01**).

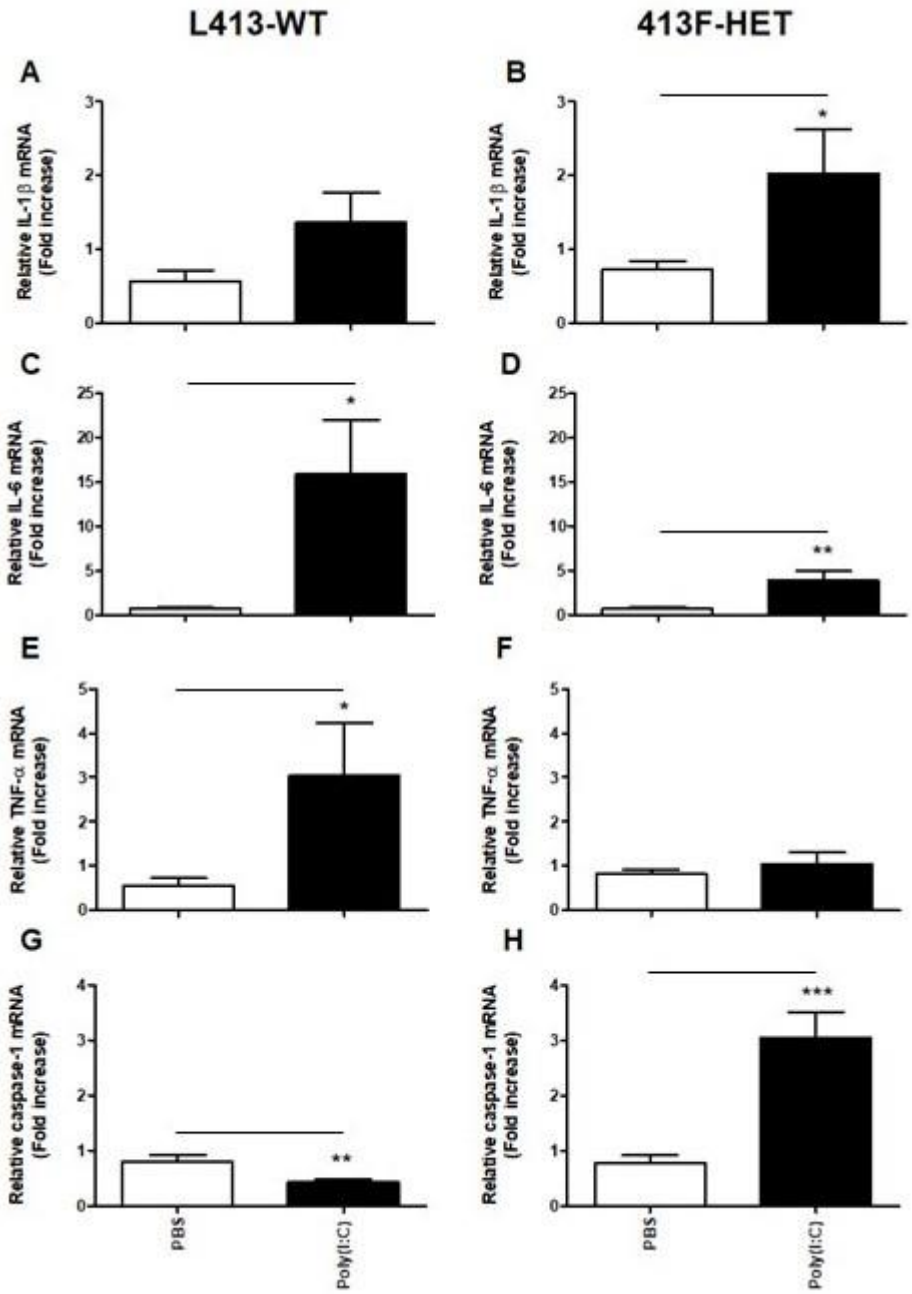

Figure 5.6. Effects of *TLR3* L413F on IL-1β, IL-6, TNF-α and caspase-1 transcription in the lung tissue of Poly(I:C)-treated L413-WT and 413F-HET female mice. IL-6 **(C)** and TNF-α **(E)** transcription was significantly increased, and caspase-1 **(G)** transcription was significantly decreased, respectively, in the lung tissue of Poly(I:C)-treated L413-WT female mice (**A, C, E**) compared with PBS-treated mice. IL-1β, IL-6 and caspase-1 transcription was significantly increased in the lung tissue of Poly(I:C)-treated 413F-HET female mice (**B, D, H**) compared with PBS-treated mice, as quantitated by qPCR analysis. An unpaired Student's t-test was used to test for statistical differences. *p<0.05, **p<0.01, ***p<0.001: Poly(I:C)-treatment compared with PBS-treatment. Graphs represent data from lung tissue at 6h post I.P. injection with Poly(I:C) or PBS injection, respectively, from six L413-WT and six 413F-HET female mice (performed once; n=6 per group). Results shown represent the mean ± SEM. [Poly(I:C), 50 μg/mouse in 200 μl of PBS].

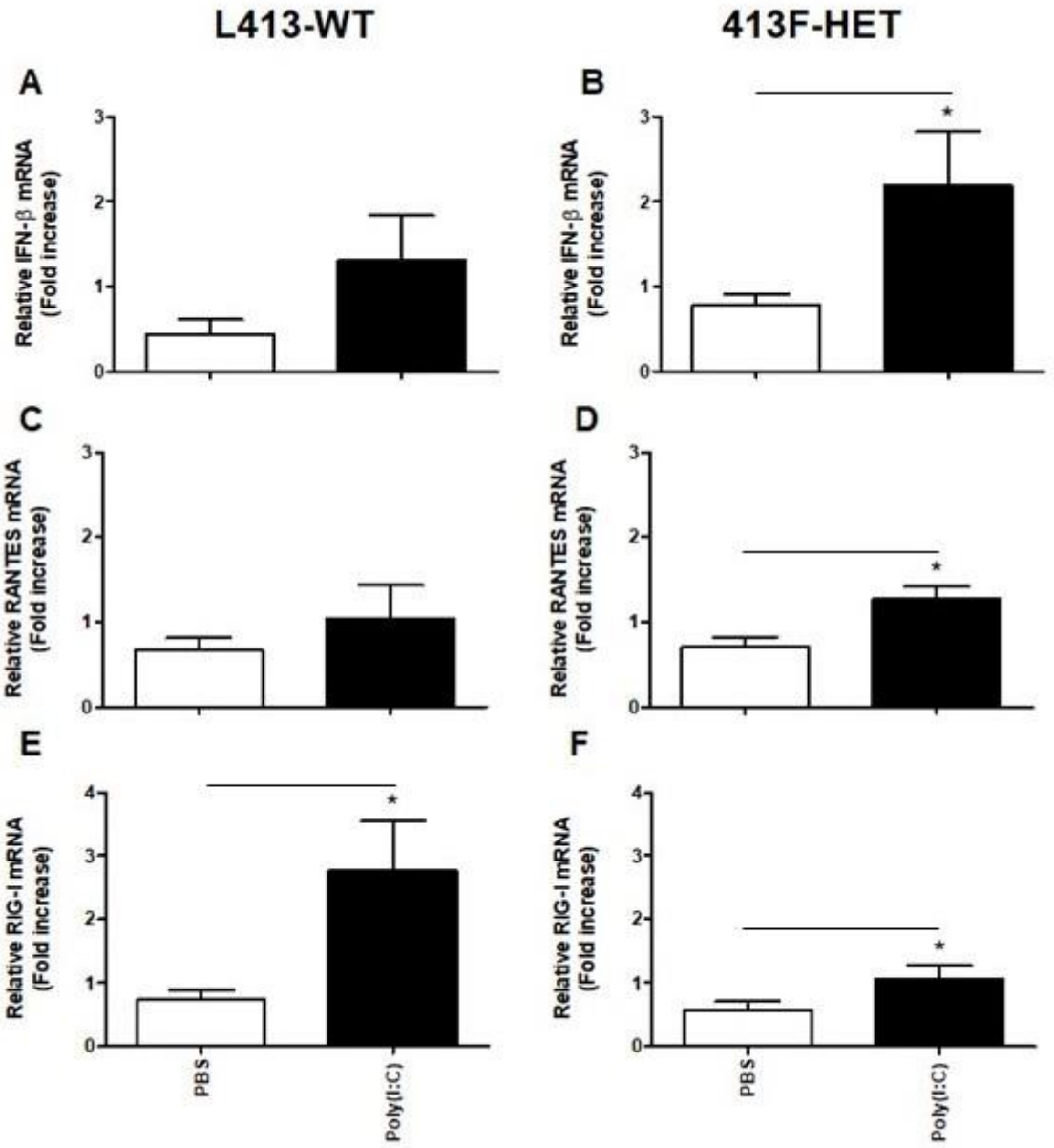

Figure 5.7. Effects of *TLR3* L413F on IFN-β, RANTES and RIG-I transcription in the lung tissue of Poly(I:C)-treated L413-WT and 413F-HET female mice. RIG-I transcription was significantly increased in the lung tissue of Poly(I:C)-treated L413-WT female mice (**A**) compared with PBS-treated mice. IFN-β, RANTES and RIG-I transcription was significantly increased in the lung tissue of Poly(I:C)-treated 413F-HET female mice (**B, D, F**) compared with PBS-treated mice, as quantitated by qPCR analysis. An unpaired Student's t-test was used to test for statistical differences. *p<0.05: Poly(I:C)-treatment compared with PBS-treatment. Graphs represent data from lung tissue at 6h post I.P. injection with Poly(I:C) or PBS injection, respectively, from six L413-WT and six 413F-HET female mice (performed once; n=6 per group). Results shown represent the mean ± SEM. [Poly(I:C), 50 µg/mouse in 200 µl of PBS].

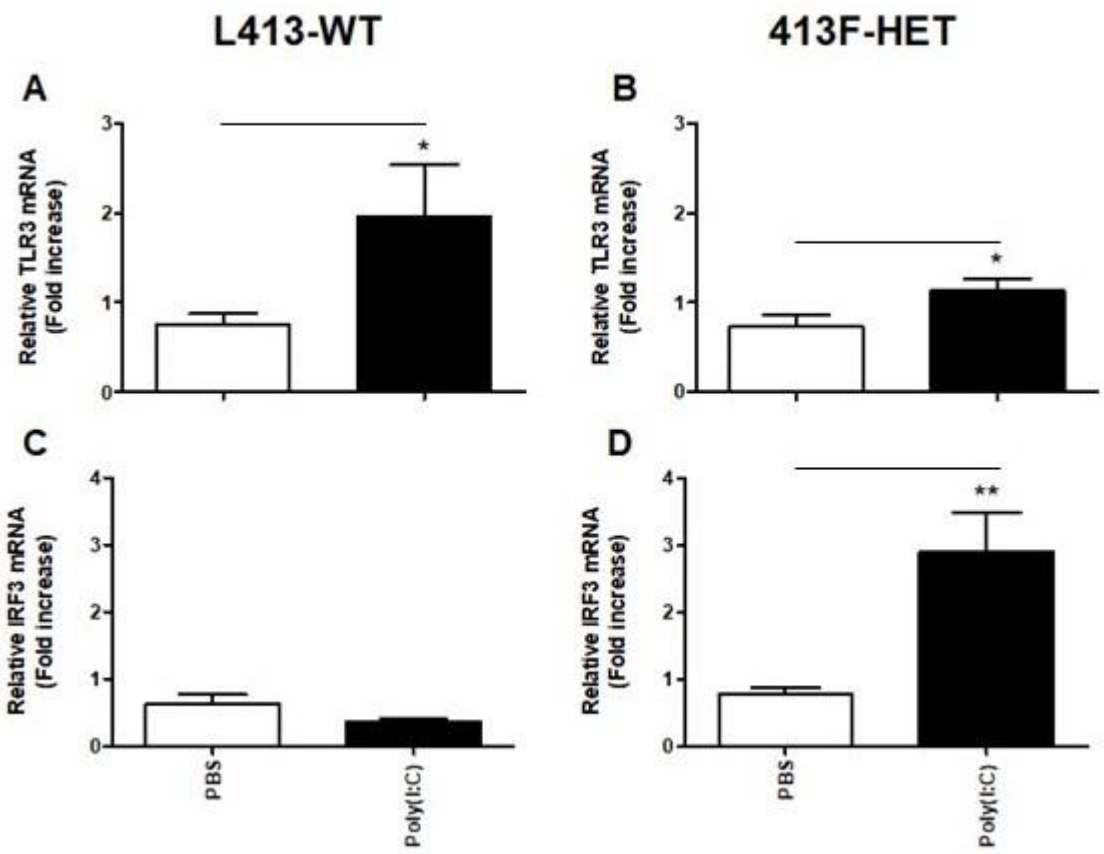

Figure 5.8. Effects of *TLR3* L413F on TLR3 and IRF3 transcription in the lung tissue of Poly(I:C)-treated L413-WT and 413F-HET female mice. TLR3 transcription was significantly increased in the lung tissue of Poly(I:C)-treated L413-WT female mice (**A**) compared with PBS-treated mice. TLR3 and IRF3 transcription was significantly increased in the lung tissue of Poly(I:C)-treated 413F-HET female mice (**B, D**) compared with PBS-treated mice, as quantitated by qPCR analysis. An unpaired Student's t-test was used to test for statistical differences. *p<0.05, **p<0.01: Poly(I:C)-treatment compared with PBS-treatment. Graphs represent data from lung tissue at 6h post I.P. injection with Poly(I:C) or PBS injection, respectively, from six L413-WT and six 413F-HET female mice (performed once; n=6 per group). Results shown represent the mean ± SEM. [Poly(I:C), 50 µg/mouse in 200 µl of PBS].

5.9. Effects of *TLR3* L413F on IRG-1, HMOX-1 and GLUT-1 transcription in the lung tissue of Poly(I:C)-treated L413-WT and 413F-HET female mice.

Other authors have identified the production of ROS and oxidative damage as pivotal co-factors in the pathophysiology of IPF [382-385]. Itaconate is a metabolite, which has recently emerged as a potent immunomodulator with anti-oxidant properties, mainly via its ability to induce NRF2-induced anti-oxidants, such as HMOX-1, as well as its limiting effect on aerobic glycolysis during infection [195, 386, 387]. IRG-1 gene encodes cis-aconitate decarboxylase, an enzyme which catalyses the synthesis of itaconate from the tricarboxylic acid (TCA) cycle [238]. The glycolytic marker GLUT-1 has been shown to drive glycolysis, oxidative stress, and fibroblast proliferation in keloid tissue [477]. Here, we investigated the effects of the *TLR3* L413F on IRG-1, HMOX-1 and GLUT-1 transcription in the lung tissue of Poly(I:C)-treated mice *in vivo.* IRG-1 transcription was significantly increased in the lung tissue of Poly(I:C)-treated L413-WT female mice compared with PBS-treated mice **(Fig. 5.9A; **p<0.01).** IRG1 transcription was significantly increased in the lung tissue of Poly(I:C)-treated 413F-HET female mice compared with PBS-treated mice **(Fig. 5.9B; **p<0.01).**

5.10. Effects of *TLR3* L413F on IL-1β, TNF-α and TLR3 transcription in the brain tissue of Poly(I:C)-treated L413-WT and 413F-HET female mice.

IL-1β and TNF-α are pro-inflammatory cytokines induced downstream of NF-κB signalling [470-472, 478]. Studies using mouse and rat models of bleomycin pulmonary fibrosis demonstrated upregulated transcription of IL-1β and TNF-α in these animals [474, 475]. Here, we investigated the effects of the *TLR3* L413F on IL-1β, TNF-α and TLR3 transcription in the brain tissue of Poly(I:C)-treated mice *in vivo.* We reported increased transcription in IL-1β, TNF-α and TLR3 (**Fig. 5.10A, C, E)** in the brain tissue of Poly(I:C)-treated L413-WT female mice compared with PBS. However, these data did not reach statistical significance. We observed a significant increase in transcription of TNF-α (**Fig. 5.10D; *p<0.05**) and TLR3 (**Fig. 5.10F; *p<0.05**) in the brain tissue of female 413F-HET mice injected with Poly(I:C) compared with PBS-treatment.

5.11. Effects of *TLR3* L413F on IRG-1 and GLUT-1 transcription in the brain tissue of Poly(I:C)-treated L413-WT and 413F-HET female mice.

Itaconate exerts its immunomodulatory effects via induction of NRF2 and well as inhibition of glycolysis, both resulting in decreased rates of oxidative damage [195, 386, 387]. GLUT-1 is a transporter used as a glycolytic marker [477]. Here, we investigated the effects of the *TLR3* L413F on IRG-1 and GLUT-1 transcription in the brain tissue of Poly(I:C)-treated mice *in vivo.* We reported a non-significant increase in IRG-1 and GLUT-1 transcription in the brain tissue of Poly(I:C)-treated female L413-WT mice compared with PBS-treatment (**Fig. 5.11A)**, respectively.

5.12. Effects of *TLR3* L413F on basal production of RANTES protein in the lung, spleen and brain tissue of L413-WT and 413F-HET male mice.

Previously, in this chapter we investigated the effects of *TLR3* L413F SNP on the transcription and production of cytokines, chemokines and IFN-β in various organs harvested from female L413F knock-in mice *in vivo*. Female mice have been used in the bleomycin model of pulmonary fibrosis which models the progression of IPF in animals [347, 474]. Recently, other authors have reported differences in the immune responses between different sexes [322, 479]. Moreover, IPF has been shown to be more pre-dominant in males than in females [3]. Therefore, in this study section, we aimed to study the effects of the *TLR3* L413F SNP on the basal or constitutive levels of RANTES production in the lung, spleen and brain tissue of L413-WT and 413F-HET male mice *in vivo*. Here, we reported no significant difference in basal protein production of RANTES in the lung and spleen tissue of 413F-HET male mice compared with L413-WT male mice **(Fig. 5.12A, B)**, respectively. We observed a trend towards a decrease in basal RANTES production in the brain tissue of male 413F-HET mice compared with L413-WT male mice **(Fig. 5.12C)**, this decrease failed to reach statistical significance.

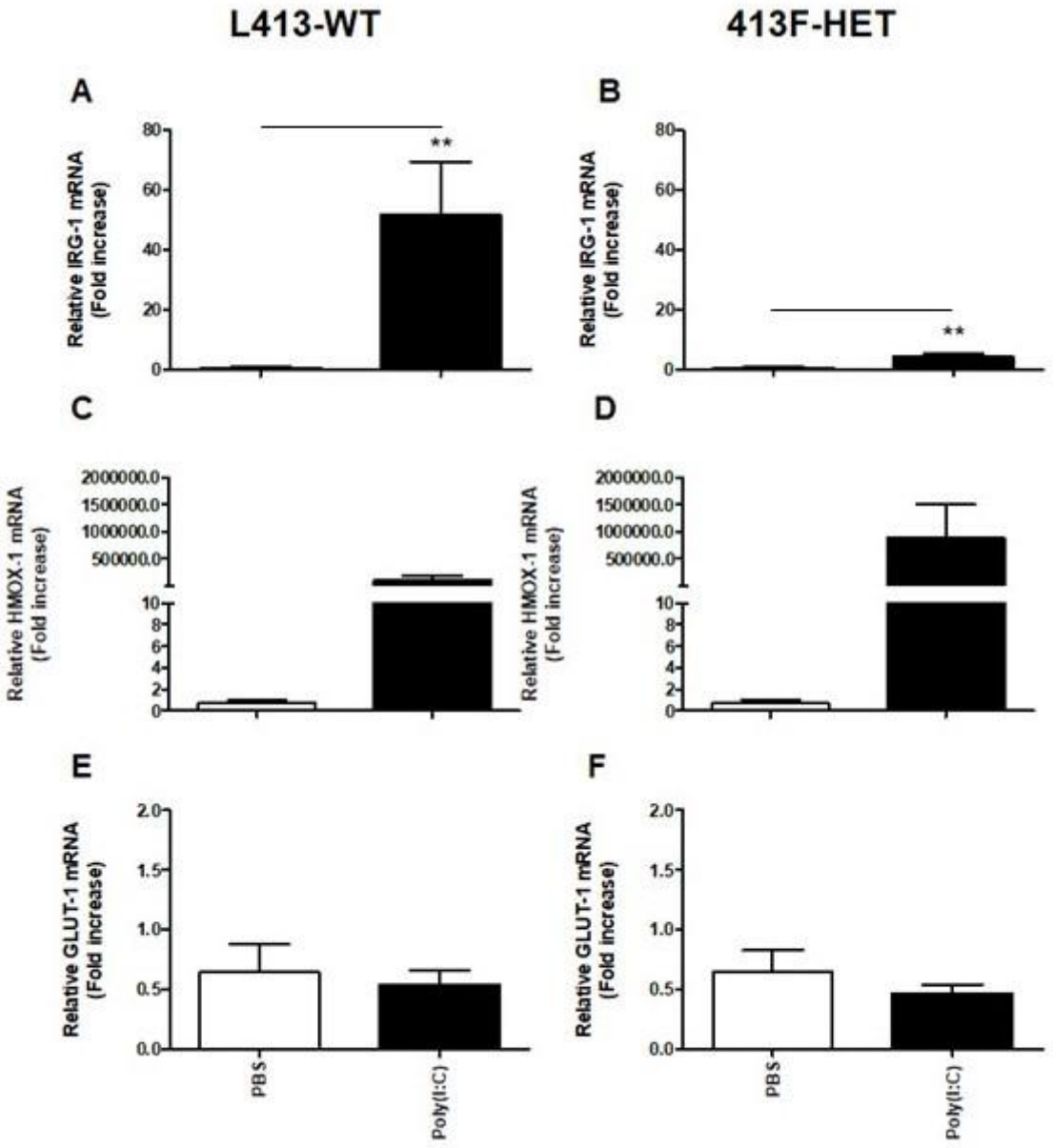

Figure 5.9. Effects of *TLR3* L413F on IRG-1, HMOX-1 and GLUT-1 transcription in the lung tissue of Poly(I:C)-treated L413-WT and 413F-HET female mice. IRG-1 transcription was significantly increased in the lung tissue of Poly(I:C)-treated L413-WT female mice (**A**) compared with PBS-treated mice. IRG1 transcription was significantly increased in the lung tissue of Poly(I:C)-treated 413F-HET female mice (**B**) compared with PBS-treated mice, as quantitated by qPCR analysis. An unpaired Student's t-test was used to test for statistical differences. **p<0.01: Poly(I:C)-treatment compared with PBS-treatment. Graphs represent data from lung tissue at 6h post I.P. injection with Poly(I:C) or PBS injection, respectively, from six L413-WT and six 413F-HET female mice (performed once; n=6 per group). Results shown represent the mean ± SEM. [Poly(I:C), 50 µg/mouse in 200 µl of PBS].

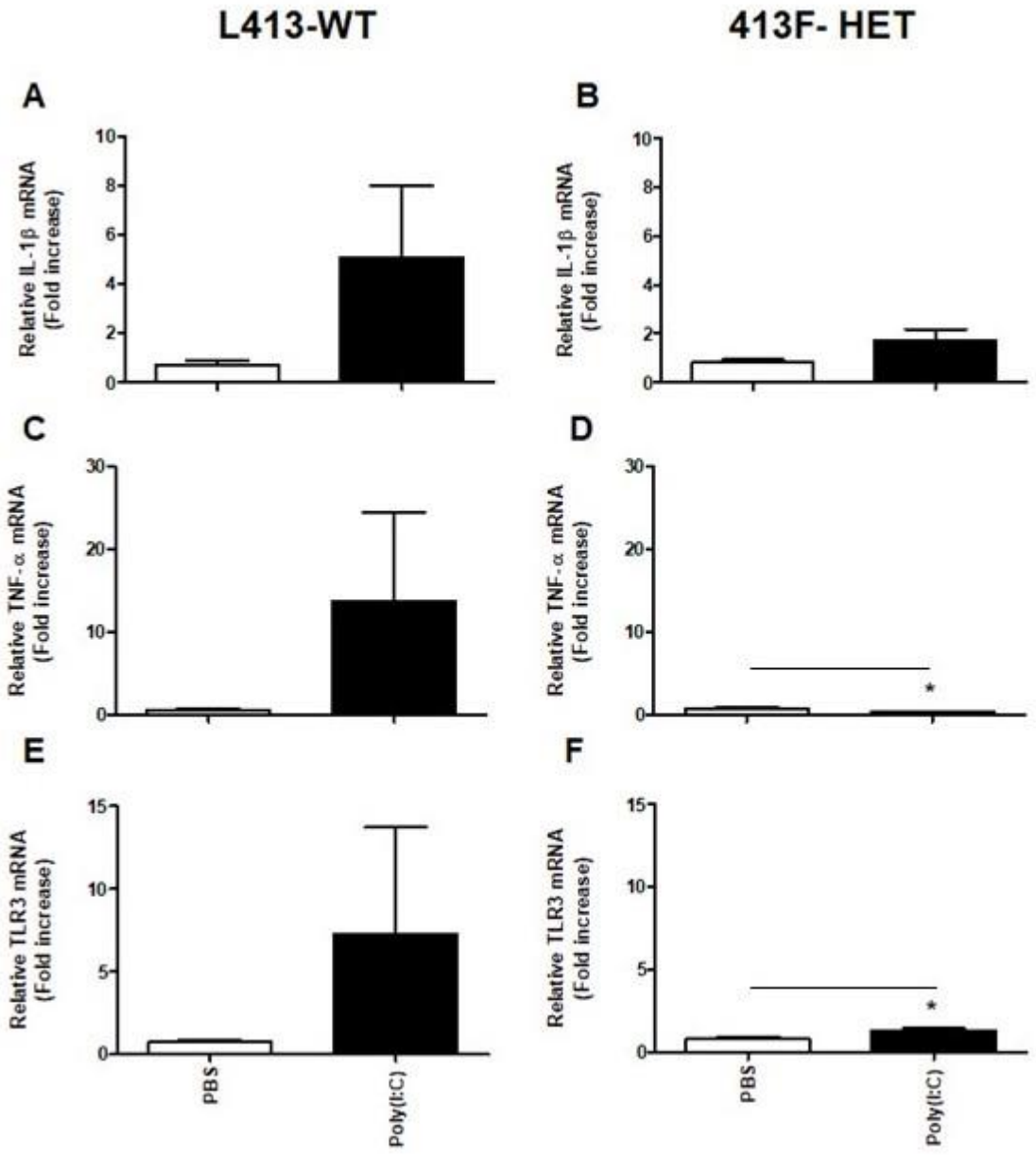

Figure 5.10. Effects of *TLR3* L413F on IL-1β, TNF-α and TLR3 transcription in the brain tissue of Poly(I:C)-treated L413-WT and 413F-HET female mice. TNF-α (**D**) and TLR3 (**F**) transcription was significantly decreased in the brain tissue of Poly(I:C)-treated 413F-HET female mice compared with PBS-treated mice, as quantitated by qPCR analysis. An unpaired Student's t-test was used to test for statistical differences. *p<0.05: Poly(I:C)-treatment compared with PBS-treatment. Graphs represent data from brain tissue at 6h post I.P. injection with Poly(I:C) or PBS injection, respectively, from six L413-WT and six 413F-HET female mice (performed once; n=6 per group). Results shown represent the mean ± SEM. [Poly(I:C), 50 μg/mouse in 200 μl of PBS].

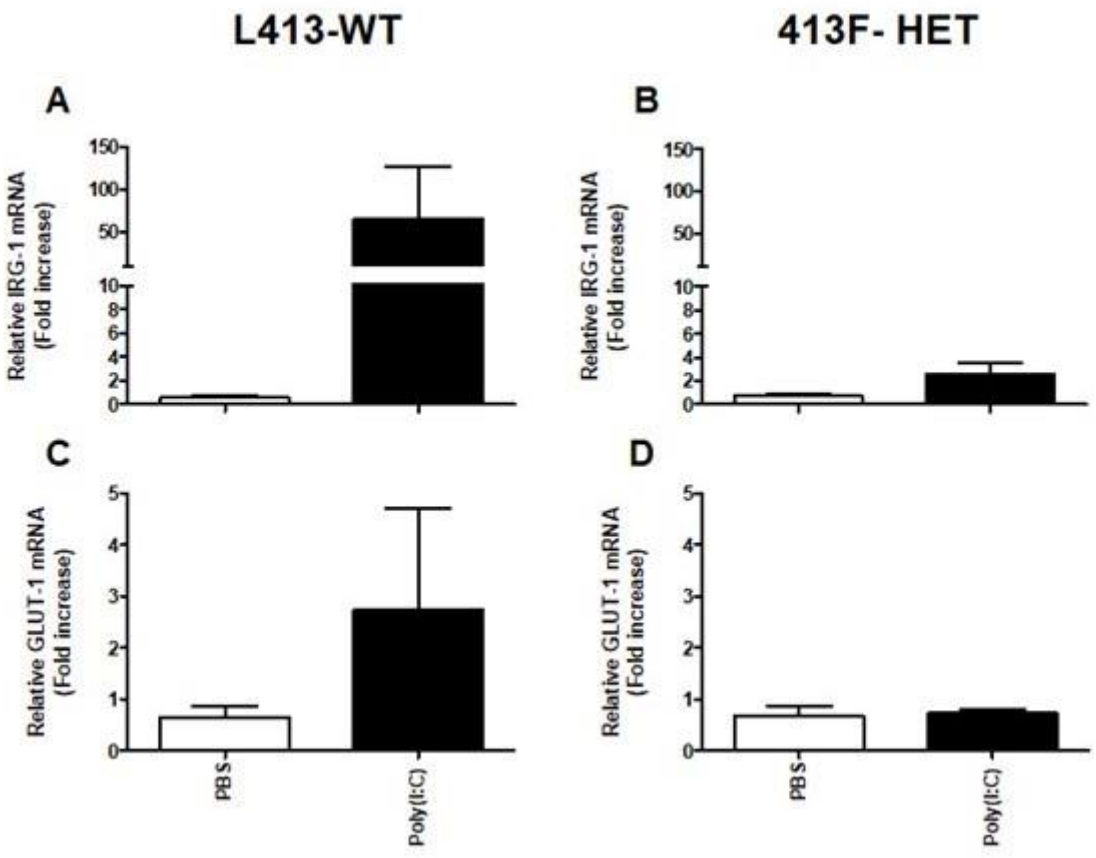

Figure 5.11. Effects of *TLR3* L413F on IRG-1 and GLUT-1 transcription in the brain tissue of Poly(I:C)-treated L413-WT and 413F-HET female mice. IRG-1 (**A**) and GLUT-1 (**C**) transcription in the brain tissue of Poly(I:C)-treated L413-WT female mice compared with PBS-treated mice. IRG-1 (**B**) and GLUT-1 (**D**) transcription in the brain tissue of Poly(I:C)-treated 413F-HET female mice compared with PBS-treated mice, as quantitated by qPCR analysis. An unpaired Student's t-test was used to test for statistical differences. Graphs represent data from brain tissue at 6h post I.P. injection with Poly(I:C) or PBS injection, respectively, from six L413-WT and six 413F-HET female mice (performed once; n=6 per group). Results shown represent the mean ± SEM. [Poly(I:C), 50 µg/mouse in 200 µl of PBS].

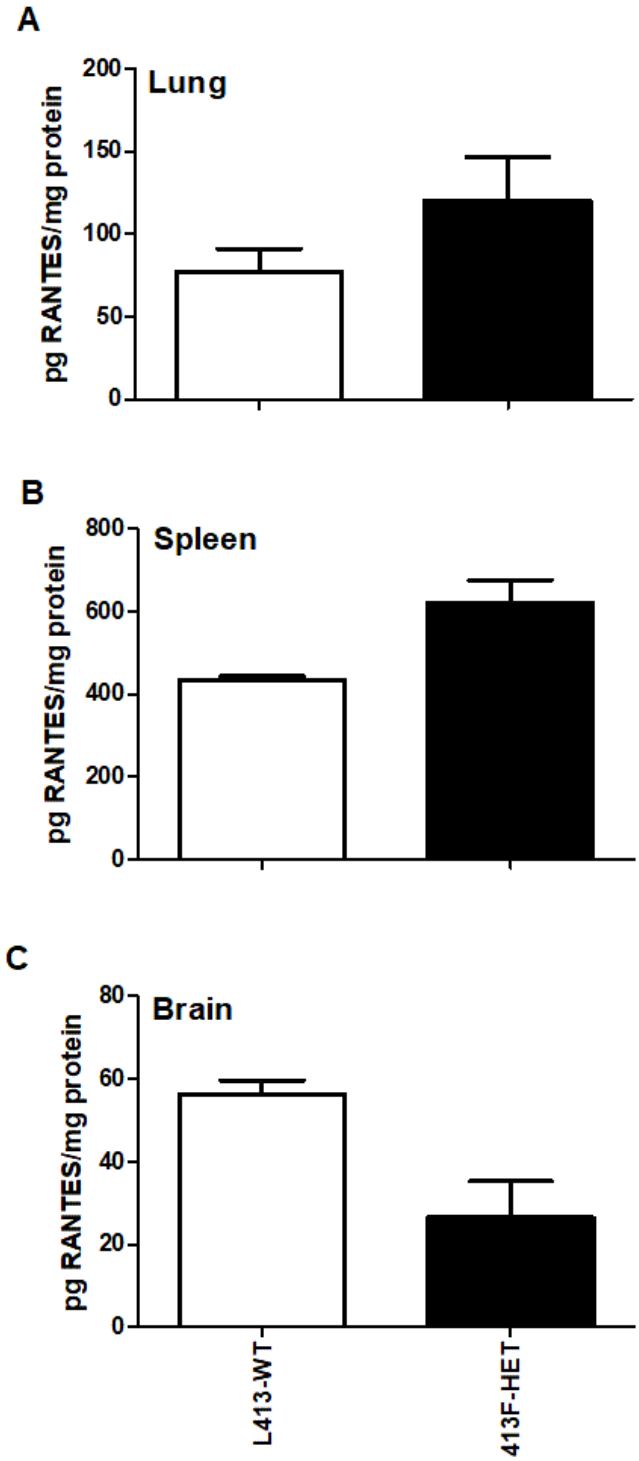

Figure 5.12. Effects of *TLR3* L413F on basal production of RANTES protein in the lung, spleen and brain tissue of L413-WT and 413F-HET male mice. Basal levels of RANTES protein production in the lung (**A**), spleen **(B)** and brain **(C)** tissue of L413-WT male mice compared with the lung tissue of 413F-HET male mice, as quantitated by ELISA. An unpaired Student's t-test was used to test for statistical differences. Graphs represent data from lung, spleen and brain tissue from two L413-WT and seven 413F-HET male mice, respectively, performed once (n=2, L413-WT; n=7, 413F-HET). Results shown represent the mean ± SEM. [Poly(I:C), 50 µg/mouse in 200 µl of PBS].

5.13. Effects of *TLR3* L413F on basal production of KC protein in the lung and spleen tissue of L413-WT and 413F-HET male mice.

In our previous studies, we determined that lung fibroblasts from 412F-HET IPF patients produced significantly increased basal levels of IL-8 protein compared with L412-WT patients [366]. Here, we aimed to examine the effects of the *TLR3* L413F SNP on the basal production of KC protein *in vivo*. We reported that the basal levels of KC protein production were not-significantly different in the lung (**Fig. 5.13A)** and spleen (**Fig. 5.13B)** tissue of 413F-HET male mice compared with the lung and spleen tissue of L413-WT male mice, respectively.

5.14. Effects of *TLR3* L413F on RANTES protein production in the lung, spleen, liver, and brain tissue of Poly(I:C)-treated L413-WT and 413F-HET male mice.

Findings by other authors demonstrate that gender is as an important factor in the immune response and susceptibility to various infections, moreover, IPF has been found to be more predominant in male patients than in female [3, 322, 479]. In this section, we aimed to characterise the effects of Poly(I:C) treatment *in vivo* on the production of RANTES protein in the lung, spleen, liver and brain tissue of L413-WT and 413F-HET male mice. Here, we reported that RANTES protein production was significantly increased in the lung (**A**) and brain tissue **(G)** of Poly(I:C)-treated L413-WT male mice compared with PBS-treated male mice **(Fig. 5.14A, G; *p<0.05, **p<0.01).** RANTES protein production was significantly increased in the lung and brain tissue of Poly(I:C)-treated 413F-HET male mice compared with PBS-treated male mice **(Fig. 5.14B, H; *p<0.01, **p<0.05).**

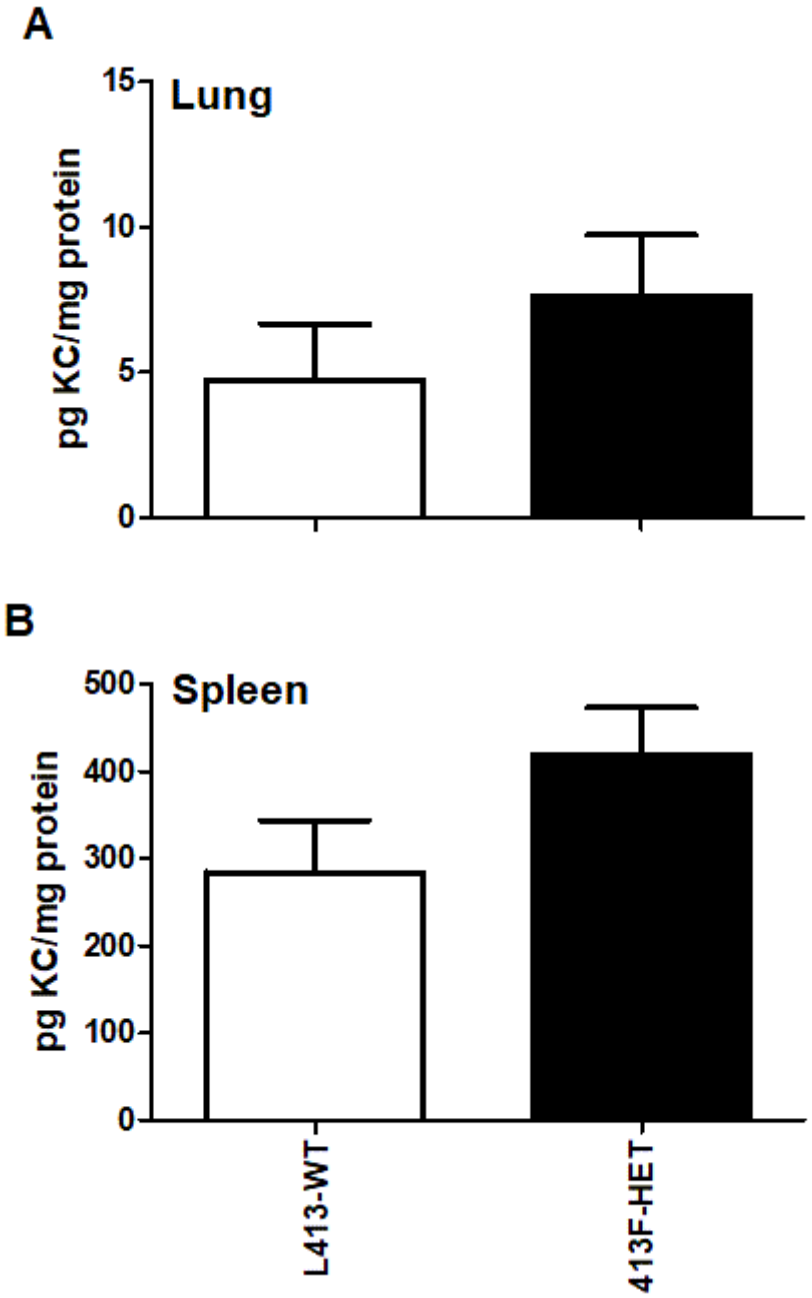

Figure 5.13. Effects of *TLR3* L413F on basal production of KC protein in the lung and spleen tissue of L413-WT and 413F-HET male mice. Basal levels of KC protein production in the lung (**A**) and spleen **(B)** tissue of L413-WT male mice compared with the lung tissue of 413F-HET male mice, as quantitated by ELISA. An unpaired Student's t-test was used to test for statistical differences. Graphs represent data from lung and spleen tissue from two L413-WT and seven 413F-HET male mice, respectively, performed once (n=2, L413-WT; n=7, 413F-HET). Results shown represent the mean ± SEM. [Poly(I:C), 50 µg/mouse in 200 µl of PBS].

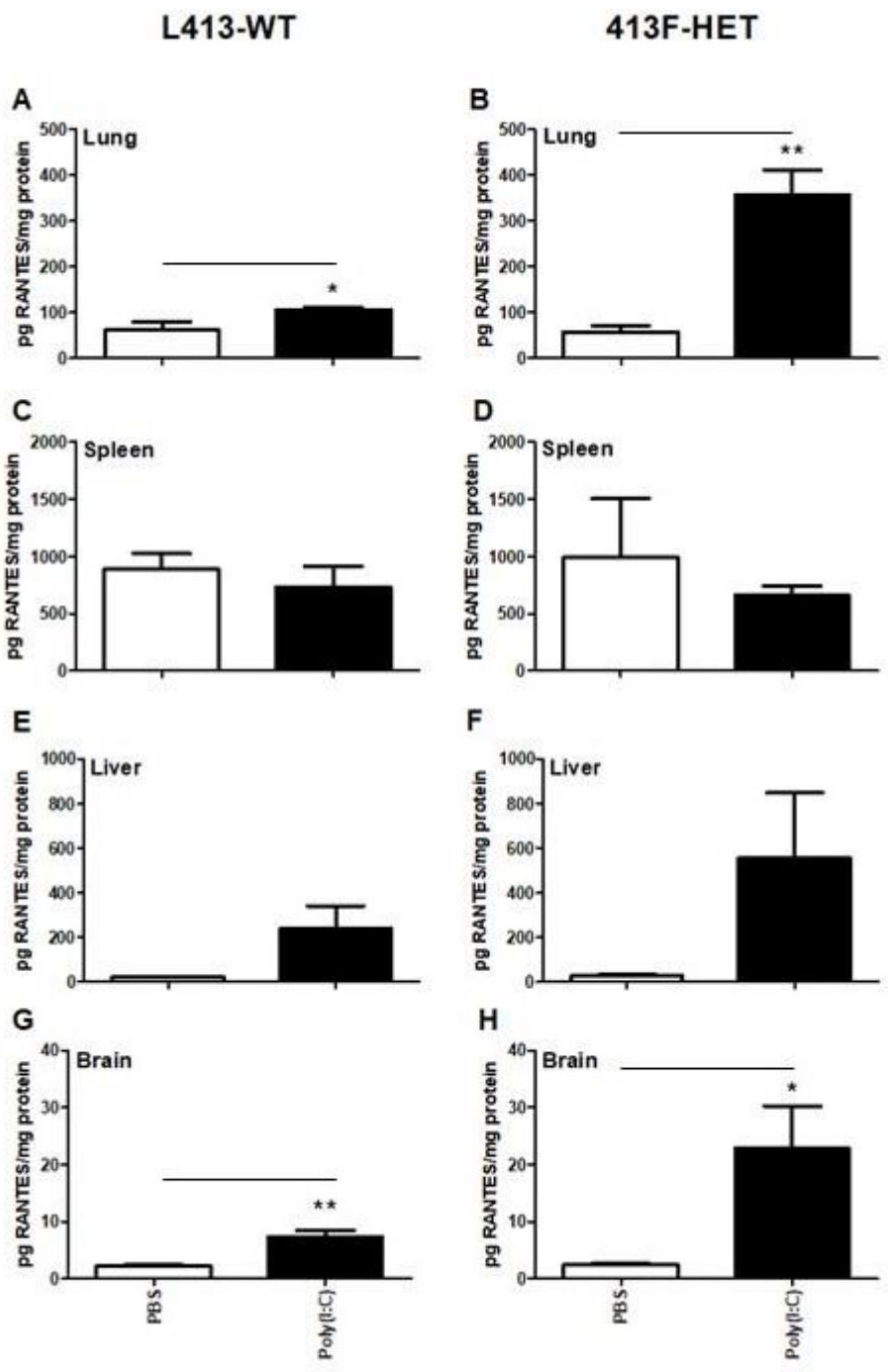

Figure 5.14. Effects of *TLR3* L413F on RANTES protein production in the lung, spleen, liver and brain tissue of Poly(I:C)-treated L413-WT and 413F-HET male mice. RANTES protein production was significantly increased in the lung (**A**) and brain tissue **(G)** of Poly(I:C)-treated L413-WT male mice compared with PBS-treated male mice. RANTES protein production was significantly increased in the lung (**B**) and brain tissue **(H)** of Poly(I:C)-treated 413F-HET male mice compared with PBS-treated male mice, as quantitated by ELISA. An unpaired Student's t-test was used to test for statistical differences. *p<0.05, **p<0.01: Poly(I:C) treatment compared with PBS only treatment. Graphs represent data from lung, spleen, liver and brain tissue at 6h post I.P. injection with Poly(I:C) or PBS injection, respectively, from six L413-WT and six 413F-HET male mice (performed once; n=6 per group). Results shown represent the mean ± SEM. [Poly(I:C), 50 µg/mouse in 200 µl of PBS].

5.15. Effects of *TLR3* L413F on KC protein production in the lung, spleen, liver, and brain tissue of Poly(I:C)-treated L413-WT and 413F-HET male mice.

Here, we aimed to characterise the effects of Poly(I:C) treatment *in vivo* on the production of KC protein in the lung, spleen, liver and brain tissue of L413-WT and 413F-HET male mice. We reported significantly increased KC protein production in the spleen (**Fig. 5.15C; *p<0.05**) of Poly(I:C)-treated L413-WT male mice compared with PBS-treatment. Poly(I:C)-induced KC protein was significantly increased in the liver (**Fig. 5.15F; **p<0.01**) and brain (**Fig. 5.15H; ***p<0.001**) tissue of 413F-HET male mice treated with Poly(I:C) compared with PBS-treatment.

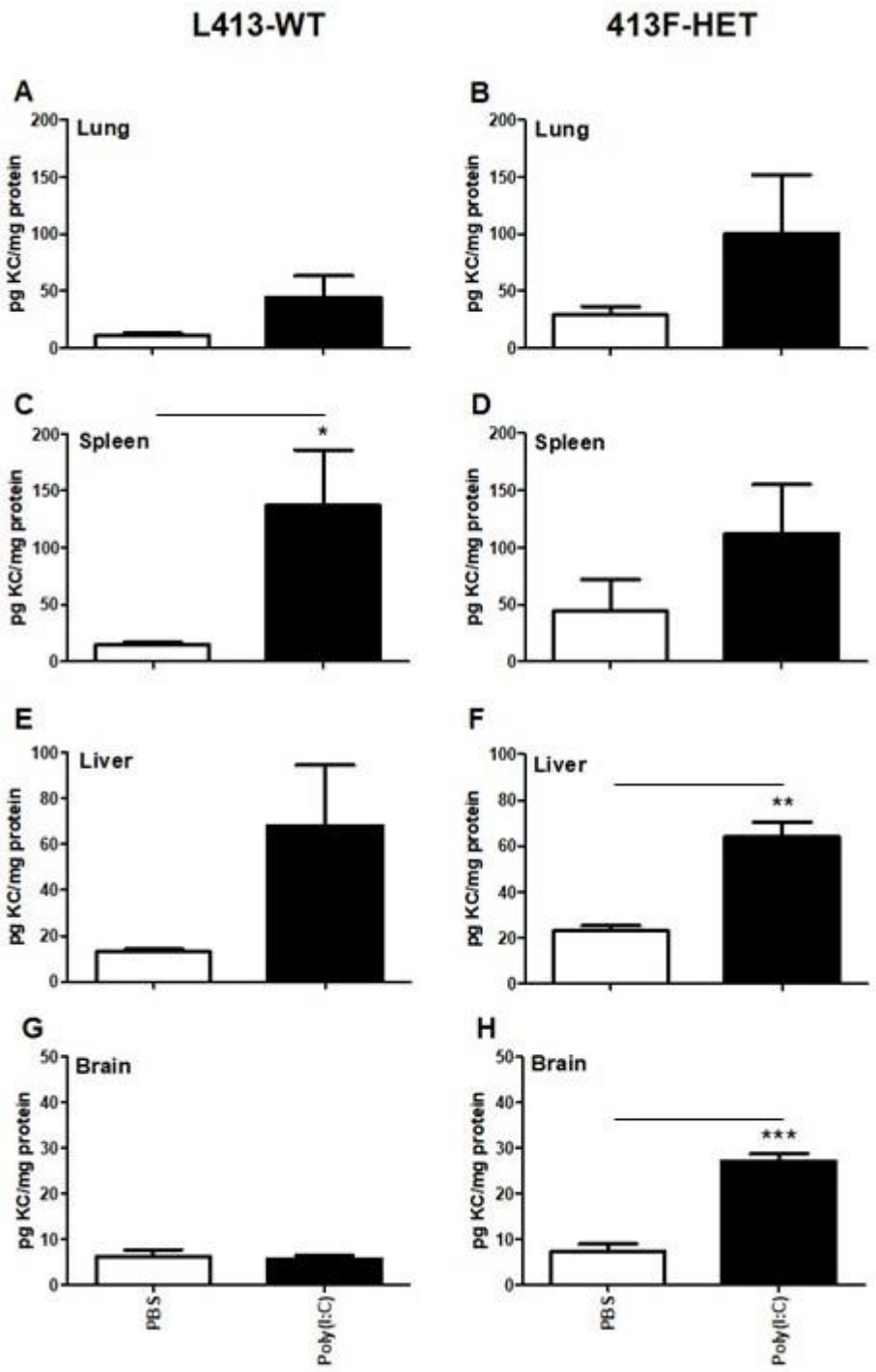

Figure 5.15. Effects of *TLR3* L413F on KC protein production in the lung, spleen, liver and brain tissue of Poly(I:C)-treated L413-WT and 413F-HET male mice. KC protein production was significantly increased in the spleen tissue (**B**) of Poly(I:C)-treated L413-WT male mice compared with PBS-treated male mice. KC protein production was significantly increased in the liver (**F**) and brain tissue **(H)** of Poly(I:C)-treated 413F-HET male mice compared with PBS-treated male mice, as quantitated by ELISA. An unpaired Student's t-test was used to test for statistical differences. *p<0.05, **p<0.01, ***p<0.001: Poly(I:C) treatment compared with PBS only treatment. Graphs represent data from lung, spleen, liver and brain tissue at 6h post I.P. injection with Poly(I:C) or PBS injection, respectively, from six L413-WT and six 413F-HET male mice (performed once; n=6 per group). Results shown represent the mean ± SEM. [Poly(I:C), 50 µg/mouse in 200 µl of PBS].

5 .16 Discussion

The aim of this chapter was to determine the functionality of our novel *TLR3 L413F* CRISPR/Cas 9 knock-in mice. Specifically, we wished to determine if the *TLR3* L412F SNP conferred functional effects *in vivo* in these mice, following TLR3-activation using a 6 h intraperitoneal injection with the synthetic viral dsRNA analogue, Poly(I:C). We previously demonstrated that 412F-variant IPF patients have an increased risk of mortality, an accelerated decline in lung function and an increased incidence of AE-IPF death. In this chapter, we firstly investigated the impact of *TLR3* L412F on the lung microbiome of IPF patients. The second aim of this chapter is to determine the functionality of this TLR3 SNP *in vivo* using our novel *TLR3* L413F, CRISPR-Cas-9 knock-in mice. Here, we investigated the effect of the 413F-variant on basal production of RANTES and KC in lung, spleen, liver and brain in 413F-HET mice. We then investigated the ability of Poly(I:C) to upregulate pro-inflammatory, anti-viral and anti-oxidant mediators in 413F-HET mice. We finally investigated the differences in the above responses in female versus male mice. The aim of this chapter is to determine if our novel L413F knock-in mice are a functional model to study the effects of the *TLR3* L412F SNP in patients with IPF, and whether it could be utilised to elucidate the mechanisms underlying the disease progression and lung fibrosis in IPF patients.

Previously, we characterised the effect of *TLR3* L413F *in vitro* in lung fibroblasts from L413-WT, 413F-HET and 413F-HOM mice *in vitro* (McElroy *et al.* unpublished data). This *in vitro* data demonstrated that the *TLR3* L413F SNP attenuated Poly(I:C)-driven RANTES and KC protein production as well as RANTES transcription in lung fibroblasts from 413F-HET and 413F-HOM mice compared with L413-WT mice (McElroy *et al.* unpublished data). Moreover, lung fibroblasts treated with Poly(I:C) presented with decreased MIP2 transcription in 413F-HET mice compared with lung fibroblasts from L413-WT mice (McElroy *et al.* unpublished data). Our *in vitro* results revealed that the *TLR3* L413F SNP affected TRL3-driven, NF-κB and IRF3-induced protein production and transcription in primary murine lung fibroblasts.

In this chapter we utilised our novel CRISPR/Cas9 *TLR3* L413F knock-in mice to study the effects of the *TLR,3* L413F SNP *in vivo* on the immune response in the lung, spleen and brain tissue of L413-WT and 413F-HET female and male mice.

Previously, our lab determined the pivotal role Poly(I:C)-driven responses in lung fibrosis in mice [161]. In our previous study, our group used the bleomycin model of pulmonary fibrosis to demonstrate that complete deletion of TLR3 led to reduced survival and greater levels of fibrosis in $TLR3^{-/-}$ mice compared to their WT counterparts [161]. The

enhanced fibrosis reported in these animals was associated with elevated production of pro-fibrotic mediators TGF-β, IL-4 and IL-13 as well as greater collagen deposition in the pulmonary tissue [161]. In addition, our group has previously determined a significant correlation between the *TLR3* L412F SNP and worsen clinical prognosis as well as higher mortality hazard ratios and AE-related death in patients positive for the 412F allele [161, 366]. To our knowledge, we are the only research group with access to our novel *TLR3* L413F, CRISPR-Cas-9 knock-in mice. Therefore, these mice provide a unique tool in which to investigate the role of the *TLR3* L412F SNP *in vivo.*

In the first part of this study, we investigated the effect of *TLR3* L412F on bacterial load and composition of the lung microbiome in IPF patients. It is well recognized that hospitalized individuals suffering from influenza pneumonia are at a significantly increased risk of secondary bacterial infection with in particular *Staphylococcus* [480]. We sought to investigate whether there was an association in IPF between patients expressing *TLR3* L412F and evidence for specific bacterial pathogens within the lung microbiome of these patients. We determined that 412F-heterozygous IPF patients had a significantly reduced bacterial burden but had an increased frequency of *Streptococcus* and *Staphylococcus spp* in their BAL samples compared with L412-wild type IPF patients (Fig. 5.1A). These results demonstrated that *TLR3* L412F alters the lung microbiome in IPF patients. Furthermore, these divergent results may suggest that defective TLR3 function resulted in an increased frequency of bacteria in the host for which TLR3 function is necessary. Previously, Spelmink *et al.* demonstrated that TLR3 was a critical factor in cellular responses to *Streptococcus pneumoniae* [368]. IL-12p70 is an interleukin crucial to clearance of Streptococcus pneumonia infection. TLR3 is required to induce full IL-12p70 secretion. Influenza A virus (IAV) infection in human lung DCs (367). Further investigation is required in order to determine the specific mechanism underlying the reduced bacterial load in the 412F-heterozygous IPF patients' BAL fluid."

In the second part of this chapter, we employ our novel *TLR3* L413F CRISPR/Cas9 *TLR3* L413F knock-in mice to characterise the functionality of this TLR3 SNP *in vivo.* Firstly, we characterised the effects of *TLR3* L413F on the basal production of RANTES protein in the lung, spleen and brain tissue of L413-WT and 413F-HET female mice. We reported that the basal production of RANTES protein was increased in the lung tissue of 413F-HET female mice and significantly increased in the spleen tissue of 413F-HET female mice compared with the lung and spleen tissue of L413-WT female mice (Fig. 5.2A, B). Interestingly, in our previous *in vitro* studies, we demonstrated a significantly increased basal production of RANTES protein in

primary lung fibroblasts from 412F-HET IPF patients compared with L412-WT IPF patients [366]. Here, we reported that 413F-HET mice presented with reduced basal production of RANTES protein in the brain tissue compared with the brain tissue of L413-WT mice (Fig. 5.2C), however, this reduction did not reach statistical significance. Our results demonstrated that the *TLR3* L413F SNP affected constitutive production of RANTES protein in the lung, spleen, and brain tissue of female mice. We predict that the increased basal RANTES protein production in the lung tissue of 413F-HET female mice observed in this study may have pathogenic effects in terms of IPF disease progression.

In this *in vivo*, we examined the effects of the *TLR3* L413F SNP on the basal production of KC protein in the lung, spleen and brain tissue of L413-WT and 413F-HET female mice. KC is a chemokine induced via NF-κB activation and is the closest murine IL-8 homologue in humans [467-469]. Here, we reported that the basal production of KC protein was significantly increased in the lung tissue of 413F-HET female mice (Fig. 5.3A) and non-significantly increased in the brain tissue of 413F-HET female mice compared with the lung and brain tissue of L413-WT female mice (Fig. 5.3C). Interestingly, our previous *in vitro* studies, we demonstrated a significantly increased basal levels of IL-8 protein production in primary lung fibroblasts from 412F-HET IPF patients compared with L412-WT IPF patients [366]. Here, we reported that the *TLR3* L413F SNP had no effect on the basal production of KC protein in the spleen tissue of 413F-HET and L413-WT female mice (Fig. 5.3B). Our results demonstrated that the *TLR3* L413F SNP affected constitutive production of KC protein in the lung and brain tissue of female mice. A number of studies reported that overproduction of IL-8 drives the pro-inflammatory response, which plays a pivotal role in the development and progression of IPF [3, 408-410] In addition, increased levels of IL-8 protein were found in the BALF serum, plasma, and sputum of IPF patients compared with healthy controls [376, 411-414]. Based on the information in the current literature, as well as findings from our own previous studies, we predict that the increased basal KC protein production observed in the lung and the brain tissue of female 413F-HET mice may have pathogenic effect in terms of IPF prognosis.

Next, we investigated whether the *TLR3* L413F SNP affected RANTES protein production in the lung, spleen, liver and brain tissue of L413-WT and 413F-HET female mice treated with Poly(I:C). We reported that L413-WT female mice, treated with Poly(I:C), presented with increased RANTES protein production compared with L413-WT mice injected with PBS in the lung, liver, and brain tissue, however, these data did not reach statistical significance (Fig. 5.4A, C, E, G). Moreover, L413-WT female mice injected with Poly(I:C) exhibited significantly

increased production in RANTES protein in the spleen tissue compared with the spleen tissue of PBS-injected L413-WT female mice (Fig. 5.4C). The decreased production in RANTES protein in the spleen tissue of female 413F-HET mice reported in this study was not significant compared with PBS (Fig. 5.4D). 413F-HET female mice treated with Poly(I:C) presented with increased RANTES protein production in the liver tissue compared with 413F-HET female mice injected with PBS, these data did not reach statistical significance (Fig. 5.4F). 413F-HET female mice injected with Poly(I:C) presented with no change in the production of RANTES protein in the lung and brain tissue compared with PBS (Fig. 5.4B, H). Interestingly, our previous *in vitro* data using novel *TLR3* L413F knock in mice demonstrated reduced protein production of RANTES in response to Poly(I:C) treatment in primary murine lung fibroblasts from 413F-HET and 413F-HOM mice compared with lung fibroblasts from L413-WT mice (McElroy *et al.* unpublished data). In addition, our group have previously demonstrated that primary lung fibroblasts from 412F-HET IPF patients presented with reduced Poly(I:C)-driven production in RANTES protein compared with lung fibroblasts from L412-WT IPF patients [161, 366]. The attenuated production of RANTES protein in IPF patients positive for the 412F allele was associated with elevated pulmonary fibrosis, accelerated rate in FVC decline, higher hazard mortality ratios as well as increased risk of AE-related mortality [161, 366]. Therefore, these data suggest that our novel L413F knock-in mouse may provide a good model to investigate the effects of L413F in IPF patients and may provide further insight into the mechanism behind the fibrotic processes associated with the disease progression in the lung. To date, our group has the exclusive access to the novel L413F knock-in mice, however, previous experiments on $TLR3^{-/-}$ mice demonstrated that TLR3 knock-out resulted in significantly reduced levels of IFN-α and IFN-β mRNA expression in mouse macrophages treated with Poly(I:C), compared with macrophages from wild-type mice [367]. Therefore, the data obtained in our novel L413F knock-in mice in response to Poly(I:C) stimulation reiterates the defective IFN function observed in the $TLR3^{-/-}$ mice in the lung. Our results presented in this chapter demonstrated that Poly(I:C) treatment affected production of RANTES protein in the lung, spleen, liver, and brain tissue of L413-WT female mice, as well as the spleen and liver tissue of 413F-HET female mice. We predict that the less robust RANTES protein production in the lung, spleen and brain tissue of female 413F-HET mice treated with Poly(I:C) compared with PBS may indicate more severe outcome in terms of IPF prognosis.

In this chapter, we characterised the effects of the *TLR3* L413F on KC protein production in the lung, spleen, liver, and brain tissue of Poly(I:C)-treated L413-WT and 413F-HET female

mice. Here, we reported that injection of Poly(I:C) resulted in increased KC protein production in the lung, spleen, and brain tissue (Fig. 5.5A, C, G), as well as significantly increased KC production in the liver tissue of L413-WT female mice compared with PBS (Fig. 5.5E). Poly(I:C)-treated 413F-HET female mice presented with elevated KC protein production in the lung and liver tissue compared with PBS, however, these data did not reach statistical significance (Fig. 5.5B, E). Injection with Poly(I:C) had no effect on KC protein production in the spleen and brain tissue of 413F-HET female mice compared with PBS (Fig. 5.5H). Interestingly, in our previous *in vitro* study, we demonstrated that primary lung fibroblasts from 413F-HET and 413F-HOM mice presented with reduced Poly(I:C)-driven KC protein production compared with lung fibroblasts from L413-WT mice (McElroy *et al.* unpublished data). Moreover, we previously reported that lung fibroblasts from 412F-HET and 412F-HOM IPF patients exhibited decreased IL-8 protein production in response to TLR3 stimulation [161, 366]. Therefore, our data suggest that our novel L413F knock-in mouse may provide a good model to investigate the effects of L413F in IPF patients. Studies by other authors demonstrated that macrophages from $TLR3^{-/-}$ mice presented with significantly impaired protein production of Poly(I:C)-induced, NF-κB-driven IL-6, IL-12 and TNF-α, compared with wild-type mice [367]. Moreover, using the electrophoretic mobility shift assay, the authors demonstrated significantly reduced, Poly(I:C)-driven NF-κB binding activity in macrophages from $TLR3^{-/-}$ mice, compared with their wild-type counterparts [367]. Therefore, the impaired NF-kB-driven protein responses following Poly(I:C) stimulation reported in our novel L413F knock-in mice mimic the results observed in the $TLR3^{-/-}$ mice. Our results presented in this study demonstrated that Poly(I:C) treatment affected KC protein production in the lung, spleen, liver, and brain tissue of L413-WT female mice, as well as lung and liver tissue of 413F-HET female mice. The less pronounced KC protein production reported in the lung, spleen and brain tissue of female 413F-HET mice injected with Poly(I:C) compared with PBS may indicate pathogenic effect in terms of IPF disease prognosis.

In this *in vivo* study, we investigated the effects of *TLR3* L413F on IL-1β, IL-6, TNF-α and caspase-1 transcription in the lung tissue of Poly(I:C)-treated L413-WT and 413F-HET female mice. Studies by other authors demonstrated that mRNA levels of cytokines IL-1β, IL-6 and TNF-α were initially elevated in the bleomycin model of pulmonary fibrosis in rodents [474, 475]. Here, we reported that treatment of L413-WT female mice with Poly(I:C) increased IL-1β transcription (Fig. 5.6A) and significantly increased the transcription of IL-6 and TNF-α in the lung tissue compared with PBS (Fig. 5.6C, E). In contrast, caspase-1 transcription was

significantly decreased in the lung tissue of L413-WT female mice injected with Poly(I:C) compared with PBS (Fig. 5.6G) female 413F-HET mice treated with Poly(I:C) presented with increased TNF-α transcription, and significantly increased transcription of IL-1β, IL-6 and caspase-1 in the lung tissue compared with PBS (Fig. 5.6A, C, E, G:). Treatment with Poly(I:C) induced a more robust response in IL-6 and TNF-α transcription in the lung tissue of L413-WT mice, whereas the upregulation in IL-6 and TNF-α mRNA in response to Poly(I:C) injection was more subtle in the lung tissue of female 413F-HET mice. Interestingly, in our previous *in vitro* data we reported that lung fibroblasts from 413F-HET mice presented with attenuated transcription in MIP2; NF-κB-driven human IL-8 homologue in mice (McElroy *et al.* unpublished data). In addition, our group have previously demonstrated dysregulated NF-κB-mediated responses in lung fibroblasts from 412-HET and 412-HOM IPF patients compared with L412-WT IPF patients [161, 366]. We have previously reported decreased Poly(I:C)-driven transcription in IL-8, RIG-I and TLR3 in 412F-HET IPF patients compared with L412-WT IPF patients [366].

Other authors demonstrated that macrophages from TLR3$^{-/-}$ mice presented with significantly reduced IL-6 and TNF-α protein production in response to Poly(I:C) stimulation, compared with wild-type mice [367]. Our data using the novel L413F knock-in mice reiterates the effects reported in the TLR3 $^{-/-}$ mice. Overall, our data demonstrated that Poly(I:C) treatment induced IL-1β, IL-6 and TNF-α transcription in the lung tissue of L413-WT and 413F-HET female mice compared with PBS. Caspase-1 transcription was increased in the lung tissue of 413F-HET female mice injected with Poly(I:C) compared with PBS in contrast to the lung tissue of L413-WT female mice, in which Poly(I:C) treatment reduced caspase-1 transcription compared with PBS. We predict that the less pronounced IL-6 and TNF-α transcription in the lung tissue of Poly(I:C)-treated 413F-HET mice reported in this study might have pathogenic effect in terms of IPF disease progression. In contrast, the induction in caspase-1 transcription in Poly(I:C)-treated 413F-HET female mice compared with PBS observed in this study may be of therapeutic benefit.

Next, we investigated *in vivo* effects of *TLR3* L413F on IFN-β, RANTES and RIG-I transcription in the lung tissue of Poly(I:C)-treated L413-WT and 413F-HET female mice. Our group have previously demonstrated dysregulated IRF3-driven IFN-β, RANTES and RIG-I transcription to TLR3 activation in lung fibroblasts from IPF patients homozygous and heterozygous for the *TLR3* L412F SNP [161, 366]. These aberrant responses were associated with a higher decline in FVC, worsen clinical prognosis, increased hazard mortality risk ratios

as well as increased AE-related patient death [161, 366]. In addition, our previous *in vitro* study demonstrated dysregulated Poly(I:C)-driven IRF3-induced RANTES transcription in lung fibroblasts harvested from the novel *TLR3* L413F knock-in mice (McElroy *et al.* unpublished data). Here we demonstrated increased transcription of IFN-β (Fig. 5.7A) and RANTES (Fig. 5.7C) as well as significantly increased RIG-I transcription in the lung tissue of female L413-WT mice injected with Poly(I:C) compared with PBS (Fig. 5.7E). In this *in vivo*, we reported that the lung tissue of 413F-HET female mice treated with Poly(I:C) presented with significantly increased transcription of IFN-β, RANTES and RIG-I compared with PBS (Fig. 5.7B, D, F). Previous studies by other authors demonstrated significantly reduced IFN-α and IFN-β transcription in response to Poly(I:C) stimulation in macrophages from TLR3$^{-/-}$ mice compared with wild-type mice [367]. Contrary to this data, in our *in vivo* we did not report dysregulated IFN-β transcription in 413F-HET mice treated with Poly(I:C).

In this chapter, we investigated the effects of the *TLR3* L413F on TLR3 and IRF3 transcription in the lung tissue of Poly(I:C)-treated L413-WT and 413F-HET female mice *in vivo*. Our group have previously demonstrated reduced TLR3 transcription, as well as reduced transcription of IRF3-driven IFN-β, RIG-I and RANTES in response to TLR3 activation in the lung fibroblasts of 412F-HET IPF patients compared with L412-WT IPF patients [161, 366]. These attenuated responses were associated with worsen clinical prognosis, increased levels of fibroproliferation, higher mortality hazard risks ratios as well as increased AE-related patient death [161, 366]. Moreover, we have previously demonstrated dysregulated Poly(I:C)-driven IRF3-meiated RANTES transcription in lung fibroblasts of 413F-HET and 413-HOM mice *in vitro* (McElroy *et al.* unpublished data). Here, we reported that the transcription of TLR3 was significantly induced in the lung tissue of Poly(I:C)-treated female L413-WT and 413F-HET mice compared with PBS (Fig. 5.8A, B). Our data demonstrated reduced IRF3 transcription in the lung tissue of Poly(I:C)-treated L413-WT female mice (Fig. 5.8C) and significantly increased in the lung tissue of Poly(I:C)-treated 413F-HET female mice compared with PBS (Fig. 5.8D). The levels of induction of TLR3 transcription in the lung tissue of Poly(I:C) treated mice were similar between L413-WT and 413F-HET female mice. Interestingly, these results are contrary to what we observed in human IPF fibroblasts, where we previously reported attenuated TLR3 transcription in response to Poly(I:C) stimulation in lung fibroblasts from 412F-HET IPF patients compared with L412-WT IPF patients [161, 366]. Furthermore, in our previous studies, we demonstrated that the *TLR3* L413F SNP attenuated Poly(I:C)-driven IRF3 responses in lung fibroblasts from both IPF patients [161, 366] as well as murine lung fibroblasts (McElroy *et al.*

unpublished data). We predict that the increased IRF3 transcription in the lung tissue of 413F-HET female mice treated with Poly(I:C) compared with mice treated with PBS may have protective effect in terms of IPF progression.

Here, we investigated the effects of the *TLR3* L413F on IRG-1, HMOX-1 and GLUT-1 transcription in the lung tissue of Poly(I:C)-treated female mice. Here, we reported that IRG-1 transcription was significantly induced in the lung tissue of female L413-WT and 413F-HET mice treated with Poly(I:C) compared with PBS (Fig. 5.9A, B:). The transcription of HMOX-1 was also increased in the lung tissue of Poly(I:C)-treated female L413-WT and 413F-HET mice compared with PBS, however, this increase was not statistically significant (Fig. 5.9C, D). We reported that Poly(I:C) injection had no effect on the transcription of GLUT-1 in the lung tissue of female L413-WT and 413F-HET mice compared with PBS (Fig. 5.9E, F). In this chapter we demonstrated that Poly(I:C) treatment induced IRG-1 and HMOX-1 transcription in the lung tissue of both L413-WT and 413F-HET female mice. Our data indicated that the transcription of IRG-1 was more pronounced in the lung tissue of L413-WT mice treated with Poly(I:C) compared with 413F-HET following Poly(I:C) injection. Here, we predict that the induction of IRG-1 and HMOX-1 transcription in the lung tissue of L413-WT and 413F-HET female mice treated with Poly(I:C) compared with PBS reported in this study may have protective effect in IPF disease progression.

In this chapter, we investigated the effects of the *TLR3* L413F SNP on IL-1β, TNF-α and TLR3 transcription in the brain tissue of Poly(I:C)-treated L413-WT and 413F-HET female mice. Our group has previously demonstrated dysregulated Poly(I:C)-induced, NF-κB-driven cytokine responses in lung fibroblasts of 413F-HET and 413F-HOM mice *in vitro* (McElroy *et al.* unpublished data), as well attenuated responses in lung fibroblasts from 412F-HET and 412F-HOM IPF patients compared with L312-WT IPF patients [161, 366]. Here, we reported induction in the IL-1β, TNF-α and TLR3 transcription in the brain tissue of female L413-WT mice injected with Poly(I:C) compared with PBS, however, these results did not reach statistical significance (Fig. 5.10A, C, E). In this *in vivo,* we demonstrated increased IL-1β transcription (Fig. 5.10B) and a significantly increased TNF-α and TLR3 transcription in the brain tissue of Poly(I:C)-treated female 413F-HET mice compared with PBS (Fig. 5.10D, F). The increased transcription in IL-1β (Fig. 5.10A, B), TNF-α (Fig. 5.10C, D) and TLR3 (Fig. 5.10E, F) reported in the brain tissue of Poly(I:C)-treated L413-WT and 413F-HET mice is in agreement with our data on the effects of Poly(I:C) on IL-1β (Fig. 5.6A, B), TNF-α (Fig. 5.6E, F) and TLR3 (Fig. 5.8A, B) transcription in the lung tissue of L413-WT and 413F-HET female mice presented

earlier in this chapter. Treatment with Poly(I:C) induced a more robust response in IL-1β, TNF-α and TLR3 transcription in the lung tissue of L413-WTmice (Fig. 5.10A, C, E), whereas the upregulation in IL-1β, TNF-α and TLR3 mRNA in response to Poly(I:C) injection was more subtle in the lung tissue of female 413F-HET mice (Fig. 5.10B, D, F). Interestingly, we previously reported that lung fibroblasts from 413F-HET mice presented with attenuated NF-κB-driven MIP2 transcription in mice *in vitro* (McElroy *et al.* unpublished data). In addition, our group have previously demonstrated decreased NF-κB-driven responses in lung fibroblasts from 412F-HET and 412F-HOM IPF patients compared with L412-WT IPF patients [161, 366]. These dysregulated NF-κB-induced responses to TLR3 activation resulted in worsen clinical prognosis, higher mortality hazard risk ratios as well as increased AE-related patient death [161, 366]. We predict that the induction in IL-1β, TNF-α and TLR3 transcription in the brain tissue of Poly(I:C)-treated female L413-WT and 413F-HET mice may be of therapeutic benefit in terms of fibrosis in these animals.

In this chapter, we have previously characterised IRG-1 and GLUT-1 transcriptional response in the lung tissue of L413-WT and 413F-HET female mice treated with Poly(I:C) *in vivo*. Here, we investigated the effects of the *TLR3* L413F SNP on IRG-1 and GLUT-1 transcription in the brain tissue of Poly(I:C)-treated L413-WT and 413F-HET female mice. In this *in vivo*, we reported that the increase in the IRG-1 transcription in the brain tissue of Poly(I:C)-treated female L413-WT and 413F-HET mice was statistically not significant compared with PBS (Fig. 5.11A, B). We demonstrated induction in GLUT-1 transcription in the brain tissue of female L413-WT mice injected with Poly(I:C) compared with PBS (Fig. 5.11C). In contrast, we reported no induction in the transcription of GLUT-1 in the brain tissue of 413F-HET female mice treated with Poly(I:C) compared with PBS (Fig. 5.11D). The transcription of IRG-1 in the brain tissue of Poly(I:C)-injected female L413-WT mice was more pronounced than the IRG-1 induction observed in the brain tissue of female 413F-HET mice treated with Poly(I:C) compared with PBS (Fig. 5.11 A, B). The induction of IRG-1 transcription reported in the brain tissue of Poly(I:C)-treated female L413-WT and 413F-HET mice follows the same pattern as the transcriptional induction of IRG-1 in the lung tissue of female L413-WT and 413F-HET mice injected with Poly(I:C) reported earlier on in this chapter (Fig. 5.9A, B) . In contrast to the induction of GLUT-1 transcription in the brain tissue of Poly(I:C)-treated female L413-WT mice, where the transcription of GLUT-1 was reduced in the lung tissue of female L413-WT mice treated with Poly(I:C) compared with PBS (Fig. 5.9E, F). Other authors have demonstrated the protective role of IRG-1 in pulmonary fibrosis in mice [245], we predict that

the induction in IRG-1 transcription in the brain tissue of Poly(I:C)-treated female L413-WT and 413F-HET mice reported in this study may be of therapeutic effect in terms of fibrosis. Other studies reported that GLU-1 promoted fibrosis in keloid tissue. We predict that the induction in GLUT-1 transcription in the brain tissue of female L413-WT mice observed in this study may have a potentially pathogenic effect in terms of IPF progression.

In this *in vivo* study, we characterised the effects of the *TLR3* L413F SNP on the basal production of RANTES protein in the lung, spleen and brain tissue of L413-WT and 413F-HET male mice. Here, we reported that 413F-HET male mice presented with increased basal production of RANTES protein in the lung and spleen tissue compared with L413-WT male mice (Fig. 5.12A, B). Interestingly, results from our previous *in vitro* study, demonstrated significantly increased basal production of RANTES protein in primary lung fibroblasts from 412F-HET IPF patients compared with L412-WT IPF patients [366]. These results are also in keeping with the data previously presented in this chapter, where the *TLR3* L413F SNP increased basal production of RANTES protein in the lung and spleen tissue of 413F-HET female mice compared with L413-WT female mice (Fig. 5.4A, B) Here, we reported that basal protein production of RANTES was reduced in the brain tissue of male 413F-HET mice compared with L413-WT male mice (Fig. 5.12C). This data in agreement with the effects of the *TLR3* L413F SNP on the basal production of RANTES protein in the brain tissue of L413-WT and 413F-HET female mice, presented earlier on in this chapter (Fig. 5.2C). Our results demonstrated that the *TLR3* L413F SNP affected constitutive production of RANTES protein in the lung, spleen, and brain tissue of male mice. We predict that the increased basal RANTES protein production reported in the lung and spleen tissue of male 413F-HET mice may have pathogenic effects in terms of the fibrosis and worsen prognosis in IPF.

In this chapter, we have investigated the effects of the *TLR3* L413F SNP on the basal production of KC protein in the lung, spleen and brain tissue of L413-WT and 413F-HET male mice. Here, we reported that 413F-HET male mice presented with increased basal production of KC protein in the lung and spleen tissue, however, these data did not reach statistical significance (Fig. 5.13A, B). Interestingly, we previously demonstrated significantly increased basal levels of IL-8 protein production in primary lung fibroblasts from 412F-HET IPF patients compared with L412-WT IPF patients [366]. The increased production in KC protein observed in 413F-HET male mice compared with L413-WT male mice reported in this study is in agreement with the data previously presented in the chapter, where we demonstrated increased basal production of KC protein in the lung tissue of 413F-HET female mice compared

with L413-WT mice (Fig. 5.3A) However, unlike the absence of the effects of the *TLR3* L413F SNP on the basal production of KC protein in the spleen tissue of female mice (Fig. 5.3B), we reported an increase in the basal KC protein production in the spleen tissue of 413F-HET male mice compared with L413-WT male mice (Fig. 5.13B). We predict that the increased basal KC protein production observed in the lung and the spleen tissue of 413F-HET male mice may indicate pathogenic effects in terms of fibrosis in these animals. We predict that the higher basal production of KC protein observed in the spleen tissue of 413F-HET male mice compared with L413-WT mice, in contrast to the lack of KC upregulation in the 413F-HET female mice compared with L413-WT female mice, may indicate pathogenic effects in terms of fibrosis in the male 413F-HET mice.

Next, we investigated the effects of the *TLR3* L413F on RANTES protein production in the lung, spleen, liver, and brain tissue of Poly(I:C)-treated L413-WT and 413F-HET male mice. Here, we reported that the injection with Poly(I:C) increased RANTES protein production in the liver (Fig. 5.14E, F) as well as significantly increased RANTES production in the lung (Fig. 5.14A, B) and brain tissue of male L413-WT and male 413F-HET mice compared with PBS (Fig. 5.14G, H). We reported decreased production in RANTES protein in the spleen tissue of Poly(I:C)-treated male L413-WT and male 413F-HET mice compared with PBS, this decrease did not reach statistical significance (Fig. 5.14C, D). In this *in vivo*, we reported that treatment with Poly(I:C) induced a similar trend in RANTES protein production in the lung, spleen, liver and brain tissue of L413-WT and 43F-HET male mice. Compared with our data on the effects of Poly(I:C) treatment on RANTES protein production in the lung, spleen, liver and brain tissue of L413-WT and 413F-HET female mice presented earlier on in this chapter, we reported that in contrast to male L413-WT mice treated with Poly(I:C), RANTES protein production in the spleen tissue of the L314-WT female mice injected with Poly(I:C) was increased compared with PBS (Fig. 5.4C). Moreover, RANTES protein production following Poly(I:C) treatment was more pronounced in the lung tissue female L413-WT mice (F, whereas the lung tissue of Poly(I:C)-treated male L413-WT mice presented with a less pronounced increase in RANTES protein production (Fig. 5.14A). In contrast to the lung and brain tissue of female 413F-HET mice treated with poly(I:C), in which we reported no upregulation in RANTES protein production compared with PBS (Fig. 5.4B, H), the brain and lung tissue of Poly(I:C)-treated 413F-HET male mice presented with significantly upregulated RANTES protein production (Fig. 5.14B, H).

In this chapter, we investigated the effects of the *TLR3* L413F on KC protein production in the lung, spleen, liver, and brain tissue of Poly(I:C)-treated L413-WT and 413F-HET male

mice. Here, we reported that that the injection with Poly(I:C) resulted in increased KC protein production in the lung and liver tissue as well as a significantly increased production of KC protein in the spleen tissue of L413-WT male mice compared with PBS (Fig. 5.15A, D). Poly(I:C) treatment did not affect KC protein production in the brain tissue of L413-WT male mice compared with PBS (Fig. 5.15G). In this *in vivo*, KC protein production was increased in the lung (Fig. 5.15B) and spleen (Fig. 5.15D) tissue as well as significantly increased in the liver (Fig. 5.15F) and brain (Fig. 5.15H) tissue of 413F-HET male mice compared with PBS. We reported a similar trend in the effects of Poly(I:C)-treatment on the induction of KC protein production in the lung, spleen and liver in both L413-WT and 413F-HET male mice, with the exception of the brain tissue, where L413-WT male mice injected with Poly(I:C) exhibited no change in the KC protein production compared with PBS in contrast to Poly(:C)-injected 413F-HET male mice which presented with elevated KC protein production in the brain issue. Compared with our data on the effects of Poly(I:C) treatment on KC protein production in the lung, spleen, liver and brain tissue of L413-WT and 413F-HET female mice presented earlier on in this chapter, we reported that female L413-WT mice treated with Poly(I:C) presented with increased KC protein production compared with PBS in the brain tissue(Fig. 5.5G), in contrast to Poly(I:C)-treated male L413-WT mice, which presented with no change in the production of KC protein in the brain tissue (Fig. 5.15G). Moreover, treatment with Poly(I:C) of male 413F-HET male induced KC protein production in the spleen and the brain tissue compared with PBS (Fig. 5.15D, H), in contrast to female 413F-HET mice, which presented with no change in KC protein production in the spleen and the brain tissue compared with PBS following Poly(I:C) injection (Fig. 5.5D, H). In addition, the production of KC protein was more robust in the lung and liver tissue of Poly(I:C)-treated male 413F-HET mice (Fig. 5.15B, F), in contrast to the more subtle upregulation in the KC protein production in the lung and liver tissue of 413F-HET female mice injected with Poly(I:C) (Fig. 5.5B, F). Our results presented in this chapter demonstrated that Poly(I:C) treatment affected production of KC protein in the lung, spleen, and liver tissue of L413-WT male mice, as well as the lung, spleen, liver and brain tissue of the 413F-HET male mice.

In this study, we examined RANTES and KC protein production both basally and in female and male mice injected with Poly(I:C) *in vivo*. Here, we reported distinct differences in the RANTES and KC protein production between the two sexes. Discrepancies in the severity and progression of lung fibrosis between males and females have been previously reported by other authors. Recent publications highlighted the role of estrogen signalling in lung fibrosis

in mice, rats, and humans [344, 345]. Authors of these publications reported estrogen to be a crucial factor in the development and progression of chronic lung diseases [344, 345]. Increased protein expression of Erα was found in lung tissue and lung fibroblasts of IPF patients, compared with healthy controls [346]. IPF lung fibroblasts were more responsive to estrogen compared with healthy lung fibroblasts, this responsiveness was decreased following estrogen blockage [345]. In addition, Erα and Erβ inhibition reduced fibrosis in the bleomycin mouse model of pulmonary fibrosis [345]. The impact of sex on pulmonary fibrosis was investigated in vivo using rat model of pulmonary fibrosis [347]. In their study endotracheal injection of bleomycin was administered to male and female rats. The authors reported increased death rates and more profound fibrosis in female rats compared to male rats, as evidenced by elevated lung collagen deposition and higher expression of pro-fibrotic cytokines in the lung [347]. Ovariectomized rats were administered with either estradiol or bleomycin. The ovariectomized rats treated with bleomycin, without hormone replacement presented with reduced levels of fibrosis compared with rats treated with estradiol [347]. In summary, due to differences in sex hormones, in the rat model of pulmonary fibrosis, female rats presented with a more pronounced response to pulmonary injury compared with male rats [347]. In contrast, the effects of sex differences in IPF in humans demonstrated that the disease is more pre-dominant and severe in males than it is in females [7]. Nevertheless, the current available data on the differences in IPF manifestation and IPF comorbidities between the sexes is very limited and requires further investigation [7].

In conclusion, in this chapter we have reported findings that demonstrate the functionality of the *TLR3* L412F polymorphism in vivo. Firstly, in IPF patients who are 412F-variant we see dysregulation of their lung microbiome, a reduction in overall pulmonary bacterial load and increased frequencies of the bacteria, *Streptococcus and S. aureus*, in BAL cell pellets from 412F-variant IPF patients. Secondly, we provide evidence in this chapter of the functionality of the *TLR3* L413F *in vivo* in our novel CRISPR-Cas-9 knock-in mice. There also is evidence of sex difference in immune responses in these mice but further investigation is required. Female 413F-HET mice have higher constitutive lung production of RANTES and KC compared to L413-WT mice. In contrast, female L413-WT mice have increased Poly(I:C)-induced pro-inflammatory and anti-viral responses in the lung compared to 413F-HET mice. In the lungs of male 413F-HET mice we observed increased basal production of RANTES and KC compared to 413-WT mice; we observed this effect in females. In contrast to females, male 413F-HET mice have increased levels of Poly(I:C)-induced RANTES and KC protein production

in their lungs compared to 413-WT female mice. These data highlight the need to consider sex in mice when using murine models to recapitulate disease.

Chapter 6 – General Discussion

Idiopathic pulmonary fibrosis (IPF) is a fast progressing and chronic interstitial pneumonia of unknown cause (1). It is still considered to be fatal, with few biomarkers and limited treatment options available for the patients (1). The disease affects 13 to 20 in every 100,000 people worldwide (3). It is estimated that one in every 100 deaths in the UK occurs due to IPF (3). The disease is difficult to diagnose, treat and its incidence is on its rise (1, 3). The fast-progressing rate of the disease translates to a median survival rate of 5 years' time following the initial diagnosis, which highlights the urgency of acquiring an effective and rapid diagnostic method. Unfortunately, IPF is mostly diagnosed via means of exclusion. The hallmark characteristics of IPF include the formation of "honeycombing" as well as other features which histological appearance overlap with other forms of usual interstitial pneumoniae (UIP). Up until recently, a surgical lung biopsy specimen provided the sole method of distinguishing UIPs from other idiopathic interstitial pneumonias. This method posed a danger to the patients and often exacerbated the symptoms of the disease (1, 3). Recently, a conditional recommendation was made to regard transbronchial lung cryobiopsy as an acceptable alternative to surgical lung biopsy in centres with appropriate expertise, with hopes to provide a safer means of diagnosis for the patients (1). Despite extensive research into the aetiology of the disease, the only established method of therapy involves lung transplantation, a process with significant associated morbidity and mortality (1, 4, 5).

The exact mechanisms behind the development of IPF remain unknown, however, previous studies by other authors demonstrated that IPF development and progression are strongly associated with heightened pro-inflammatory state, often caused by bacterial or viral infection. The increased inflammation of the pulmonary tissue leads to aberrant wound healing of the pulmonary tissue, epithelial cell damage, excessive rate of fibroproliferation, myofibroblast differentiation and increased deposition of collagens and extracellular matrix (ECM) proteins, creating imbalance between pro-and anti-fibrotic mediators (4, 5). This altered state of homeostasis promotes scarring of the pulmonary tissue, which ultimately impairs gas exchange and leads to respiratory failure (4, 5).

IPF can be familial or sporadic, with the former demonstrating more severe clinical prognosis (1, 4, 5). IPF patients can be further divided into 3 major clinical phenotypes (1, 4, 5). Most patients experience a slow, gradual loss of lung function over time (1, 4, 5). Circa 15% of patients experience a more rapid progression of the disease which leads to a life expectancy of about a year following the initial diagnosis (1, 4, 5). The last group of patients undergoes an adverse event known as an acute exacerbation (AE), which results in highly accelerated

decline in disease prognosis (1, 4, 5). It is estimated that half of the patients who experience AE event will die within 30 days (1, 4, 5). Currently, MUCB5 promoter polymorphism is a sole validated prognostic biomarker in IPF up to date (4, 5). There is a dire need for fast, more accessible method of stratifying patients according to the different clinical phenotypes at the early stages of the disease. The ability to determine a relatively accurate prognosis will be invaluable for lung transplant prioritisation of the patients, as well as an appropriate clinical decision making and palliation where necessary (1, 4, 5).

Our group has previously characterised the effects of *TLR3* L412F (rs3775291) SNP in the context of disease development and progression in two separate IPF patient cohorts (11, 12). We reported a significant correlation between the SNP and increased hazard ratio as IPF patients homozygous and heterozygous for the L412 SNP demonstrated five times greater risk of mortality at 12 months and 24 months compared with *TLR3* L412-WT patients (11). In addition, 412F-HET and L412-HOM patients presented with an accelerated rate of decline in forced vital capacity (FVC) over the period of 12 months compared with L412-WT patients (11). Primary lung fibroblasts from IPF patients positive for the L412 SNP exhibited dysregulated Poly(I:C)-driven cytokine, type I IFN and fibroproliferative properties compared with lung fibroblasts from L412-WT patients (11). In a more recent study, our group has demonstrated a significant correlation between the presence of L412F variant and incidence of AE-related death in IPF patients (12). We reported that IPF patients heterozygous for *TLR3* L412F presented with dysregulated anti-bacterial responses to LPS, Pam3CYSK4, flagellin, FSL-1 and live *Pseudomonas aeruginosa* infection compared with L412-WT IPF patients (12). In addition to aberrant anti-microbial responses, 16S RNA sequencing revealed dysregulated lung microbiome in 412F-HET IPF patients compared with 412F-WT patients with increased frequencies of *Streptococcus* and *Staphylococcus spp* (12). Our findings led us to propose the role of defective TLR3 function in the progression of IPF.

In this PhD thesis, we addressed the urgent need for both novel therapeutic solution and identifications of biomarkers for IPF. Firstly, we investigated the effects of a metabolite, itaconate in terms of its effects on Poly(I:C)-driven pro-inflammatory, anti-viral and fibrotic responses in primary human lung fibroblasts from healthy donors andIPF patients. In the second experimental chapter, we conducted a case-control study for the role of *IL-17A* G197A (rs2275913), a SNP within the promoter region of the pro-inflammatory cytokine, IL-17A and its association with disease development in IPF. We also investigated the role of *IL-17A* G197A in IPF-pneumonia related death in our cohort of IPF patients. Expanding on the role of IL-17A

in the disease development and progression in IPF, we investigated the effects of IL-17A on Poly(I:C)-driven inflammatory and anti-viral responses in lung fibroblasts from healthy donors and IPF patients. Finally, in the third experimental chapter of this thesis, we investigated the association of the *TLR3* L412F SNP *in vivo* on the lung microbiome in IPF patients. We also characterised the effects of TLR3 L412F *in vivo* using a novel *TLR3* L413F-knock in mice (Taconic Biosciences Inc., Köln, Germany) – which we commissioned the generation of using CRISPR-Cas-9 gene editing.

Itaconate is a metabolite, generated as a by-product of the Krebs cycle. In recent years, itaconate has been gaining popularity for its potent anti-inflammatory and anti-oxidant properties (6, 7). In the first experimental chapter, we investigated the effects of a 4-OI, a synthetic analogue of itaconate on TLR3 activity. We reported that on its own, 4-OI did not induce IL-8, IL-6 and RANTES protein production, used as read-outs for NF-κB and IRF3 activity respectively, in both healthy and IPF fibroblasts. Poly(I:C)-driven transcription of NF-κB-induced IL-8, IL-1β and caspase-1, as well as IRF3-induced IFN-β, RANTES and RIG-I was also unaffected by 4-OI treatment in both healthy and IPF lung fibroblasts. These results demonstrated that treatment with 4-OI alone did not modulate TLR3 function in lung fibroblast from both healthy donors and IPF patients. Here, we reported that that 4-OI increased Poly(I:C)-driven production of IL-8 protein in both healthy and IPF fibroblasts. Our results are supported by other authors, who demonstrated DI, a synthetic analogue of itaconate-mediated increase in IL-8 protein production in human monocytes infected with influenza A virus (8). In their study, Muri *et al.* reported that higher doses of itaconate promoted caspase-8-induced processing of IL-1β in murine bone marrow dendric cells (BMDCs) (9). Other authors demonstrated that caspase-8 induction led to activation of NF-κB signalling, which may be mechanisms behind the increased 4-OI-mediated, Poly(I:C)-driven production of IL-8 protein observed in our study (10). In our previous study, we demonstrated that dysregulated Poly(I:C)-driven IL-8 production in IPF patients homozygous for L412 SNP led to accelerated decline if FVC and worsen clinical prognosis, therefore we predict that the increased Poly(I:C)-driven IL-8 protein production mediated by 4-OI may have pathogenic effects in terms of IPF progression (11).

Here, we reported that treatment of lung fibroblasts from IPF patients with 4-OI decreased Poly(I:C)-driven production of IL-6 protein. Our results are supported by other authors, who demonstrated reduced itaconate-mediate production of IL-6 protein in in LPS-stimulated murine BMDMs, human chondrocytes and human lung fibroblasts (13-16).

Previous studies reported that 4-OI reduced production of IL-6 protein both directly via activation of NRF2, and indirectly via activation of ATF3, as increased ATF3 expression led to inhibition of NF-κB inhibitor zeta (IκBζ) protein-induction, which limited IL-6 transcription (14, 17, 18). Increased IL-6 protein has been shown in the blood serum from IPF patents as well as supernatants derived from IPF primary human lung fibroblasts, hence, we predict that the decreased Poly(I:C)-driven IL-6 production mediated by 4-OI reported in our study may have potential therapeutic effect on disease progression in IPF (19-21).

In addition to evaluating the effects of 4-OI on NF-kB-driven protein production, we also investigated the effects of the metabolite on NF-κB-induced transcription in lung fibroblasts from healthy donors and IPF patients. We reported, that despite reduced Poly(I:C)-driven IL-8 protein production following 4-OI treatment, 4-OI decreased Poly(I:C)-induced IL-8, IL-1β and significantly reduced caspase-1 transcription IPF lung fibroblasts. The proposed mechanisms for 4-OI-mediated reduction of pro-inflammatory IL-1β and caspase-1 transcription has been described in the above paragraph (14, 7, 18).

Additionally, we reported that 4-OI decreased TLR4-driven, LPS-induced transcription of IL-8, IL-1β and caspase-1 transcription in lung fibroblasts from IPF patients. Our data is supported by other studies in which 4-OI reduced nuclear translocation of NF-κB as well the expression of IL-1β in LPS-activated, murine macrophages (22). In addition, in their study Tannahill *et al.* reported that itaconate inhibited SDH resulting in decreased production of IL-1β, generated upon succinate oxidation (23). In summary, we demonstrated the ability of 4-OI to modulate TLR3 -driven NF-κB response in lung fibroblasts from a heathy donor and IPF patients. Increased IL-1β transcription was demonstrated in the murine bleomycin model of fibrosis and was associated with adverse fibrotic events (24, 25). We predict that the 4-OI-mediated, Poly(I:C)-induced decrease in IL-6 protein production as well as IL-1β ad caspase-1 transcription reported in IPF lung fibroblasts may reduce the tissue inflammation and have a positive effect on the disease progression in IPF patients.

Among other risk factors such as genetic predisposition, and cigarette smoking, the role of viral infection, as a causative factor behind the development and progression of IPF has been studied extensively by various authors in recent years (5, 26). In addition, a large majority of PF patients reported having an incidence of viral infection shortly prior to the onset of respiratory problems (5). Despite gaining a valuable insight into the effects of viral infection in IPF, the exact pathogenetic relationship between viral infection and IPF remains the subject of ongoing investigation (27-31).

In this chapter, we investigated the effects of 4-OI on Poly(I:C)-driven, IRF3-mediated anti-viral response in lung fibroblasts form healthy donors and IPF patients. Using RANTES protein production as a read-out for IRF3-driven activity, we reported that 4-OI significantly decreased Poly(I:C)-induced RANTES in IPF lung fibroblasts. Our data was supported by findings by other authors, who reported 4-OI-mediated reduction in IFN responses in IAV-infected human macrophages, as well as 4-OI-mediated viral inhibition in human PBMCs (8). Previous studies demonstrated the ability of itaconate to inhibit stimulator of interferon genes (STING), via activation of NRF2, which translated into reduced type I IFN response and could explain the mechanism behind the anti-viral properties of itaconate (17, 32). In our previous study, we reported attenuated type I IFN response to TLR3 stimulation in IPF patients positive for the L412 SNP, which correlated with accelerated decline in FVC, worsen clinical prognosis and higher mortality rates (11). Moreover, we demonstrated that dysregulated Poly(I:C)-driven Type I IFNS responses were associated with increased rate of AE-related patient mortality (12). Therefore, we predict that the reduced anti-viral response to Poly(I:C)-stimulation, mediated by 4-OI may result in issues with resolution of viral infection and ultimately have pathogenic effects on IPF development and progression. In addition to evaluating the effects of 4-OI on IRF3-driven protein production, we also investigated the effects of the metabolite of IRF3-induced transcription in lung fibroblasts from healthy donors and IPF patients. We reported that treatment with 4-OI decreased IRF3-driven transcription of RANTES and RIG-I, and significantly reduced IRF3-induced IFN-β transcription. Our results were supported by other authors, who demonstrated that 4-OI inhibited LPS and Poly(I:C)-driven transcription of Type I IFN in murine macrophages (17). The possible explanation behind the reduction in Poly(I:C)-driven anti-viral response by 4-OI may be linked to the metabolite's ability to inhibit STING (17, 32). In summary, in this chapter we demonstrated that 4-OI downregulated Poly(I:C)-induced, IRF3-driven anti-viral response in terms of protein production and genetic transcription. Considering data from our previous study, in which we reported association between dysregulated anti-viral Type I IFN response to TLR3 stimulation in patients variant for L412 SNP and worsened clinical prognosis in IPF patients, we predict that 4-OI may have pathogenic effects in terms of the disease progression (11, 12).

Previous studies have determined oxidative stress to be a major driver behind IPF disease progression, researched shows a significant correlation between increased ROS production and life expectancy of patients with IPF (33-36). Mills *et al.* demonstrated that itaconate exhibited anti-oxidant function in both human and murine macrophages (17). Ogger

et al. reported reduced IRG-1 transcription in alveolar macrophages of patients with IPF compared with healthy individuals (37). Moreover, the group determined that $IRG^{-/-}$ mice challenged with bleomycin presented with increased levels of fibrosis, compared with their wild-type counterparts (37). Moreover, itaconate reduced wound healing capacity as well as cellular proliferation in cultured lung fibroblasts from IPF patients (37). We are the first group to report that treatment with Poly(I:C) significantly increased IRG-1 transcription in lung fibroblasts from IPF patients. Our findings suggest the importance of itaconate during TLR3 activation. In addition, in this chapter, we reported that 4-OI increased transcription of anti-oxidants HMOX-1 and GSR in IPF fibroblasts. 4-OI also increased HMOX-1 and GSR transcription in the presence of Poly(I:C) compared with Poly(I:C) treatment alone in lung fibroblasts from healthy donors and IPF patients. The upregulation of NRF2-induced antioxidant genes, HMOX-1 and GSR by 4-OI may be explained by alkylation of cysteine residues on KEAP-1 by 4-OI, a molecule which, under homeostatic conditions, targets NRF2 for lysosomal degradation (17). Upon alkylation by itaconate, KEAP-1 is inhibited which results in activation of NRF2-induced genes (17). Considering our own findings and data currently available on the therapeutic effects of itaconate in IPF patients as well as in mice in the bleomycin model of lung fibrosis, we predict that the data presented in this chapter may have possible positive effects in terms of IPF progression and warrants a more in-depth research into the role of itaconate as a potential therapeutic in IPF.

To further evaluate the effects of 4-OI on TLR3 function in IPF lung fibroblasts, we investigated 4-OI-mediated, Poly(I:C)-driven transcription of pro-fibrotic markers. We reported that treatment with 4-OI significantly decreased Poly(I:C)-induced α-SMA, COL3α3 and COL3α1 transcription in lung fibroblasts from IPF patients. We predict that the observed reduction in Poly(I:C)-driven pro-fibrotic marker transcription may be explained by anti-inflammatory and anti-oxidant function of the metabolite described in this study previously (14, 17, 18, 23). Studies by other authors demonstrated that IPF fibroblasts generate excessive contractile force, which resulted in increased production and transcription of collagens, α-SMA and TGF-β (38-41). Increased transcription of TGF-β has been reported in in lung biopsies from IPF patients, compared with healthy controls (50). In addition, protein production of α-SMA was significantly elevated in blood serum from patients with IPF compared with healthy individuals (41). We predict that the reduction of the Poly(I:C)-induced transcription of pro-fibrotic markers α-SMA, COL3α3 and COL3α1 and TGF-β by 4-OI described in our study may have potentially therapeutic benefits in terms of the disease progression in IPF. Previous

studies demonstrated that increased in TGF-β levels in IPF promoted differentiation of resident fibroblasts into activated myofibroblasts in the lung, promoting excessive ECM and collagen deposition (37). To further evaluate the effects of 4-OI on the transcription of pro-fibrotic markers in IPF lung fibroblasts, , we investigated the effects of 4-OI on TGF-β-driven transcription of pro-fibrotic agents TGF-β, α-SMA, COL1α1 and COL3α1 in primary human lung fibroblasts from IPF patients. We reported that 4-OI decreased TGF-β-driven transcription of TGF-β and COL1α1. Our data is in agreement with findings by Ogger *et al.* who demonstrated that itaconate limited TGF-β transcription in mouse macrophages (37). Moreover, in their study, the group reported that *IRG-1*$^{-/-}$ mice presented with increased collagen deposition compared with wild-type mice (37). The reduction in 4-OI-mediated Poly(I:C)-driven and TGF-β-driven transcription of pro-fibrotic markers in IPF fibroblasts presented in our study, is indicative of the potential therapeutic use of itaconate in the future.

Bacterial infection has been previously determined to be one of the major drivers behind IPF development and progression. Other authors reported increased bacterial loads in the BALF of IPF patients compared with healthy individuals (43-47). Previously, we established that 412F-heterozygous IPF lung fibroblasts have reduced antibacterial TLR responses to LPS (TLR4), Pam3CYSK4 (TLR1/2), flagellin (TLR5), and FSL-1 (TLR6/1), In addition, we reported that 412F-HET IPF patients had decreased responses to live Pseudomonas aeruginosa infection compared with L412-WT IPF patients in terms of IL-6 and IL-8 protein production. These data demonstrated that during Pseudomonas aeruginosa infection, 412F-HET IPF patients did not mount an appropriate anti-bacterial response, which may result in failure to resolve the ongoing infection and drive further inflammation and fibrosis in IPF (12).

To investigate the anti-bacterial properties of itaconate in the context of IPF, we infected primary human lung fibroblasts from healthy donors and IPF patients with live *Pseudomonas aeruginosa* (*P. aeruginosa,* PAO1) in the presence of 4-OI for 8 h, and subsequently quantitated protein production of IL-6, IL-8 and RANTES. We determined that protein production of IL-6 and IL-8 was significantly increased in lung fibroblasts from healthy donors and IPF patients infected with PAO1, compared with DMSO treatment only. We reported that PAO1 inaction did not affect production of RANTES in fibroblasts from healthy controls and IPF patients at the 8h time point. Our data is supported by findings by other authors which demonstrated that increased serum levels of both IL-6 and IL-8 are markers of bacterial infection, whereas upregulation of RANTES is predominantly associated during the immune response to viral infection (49). Our data are in agreement with the publication

presented by Azghani *et al.* who demonstrated that PAO1 enhanced IL-8 protein production via induction of the EGFR/ERK signalling cascade, which ultimately led to NF-kB activation, and thus may provide a possible mechanism behind the increased IL-8 and IL-6 protein production by PAO1 observed in our study (50). Despite previous accounts of itaconate as an anti-bacterial agent, in this study, we reported that treatment with 4-OI of PAO1-infected healthy and IPF lung fibroblasts had no effect on the IL-6, IL-8 and RANTES protein production. Recent findings by other authors determined that Pseudomonas aeruginosa exploits host-derived itaconate in order to alter its metabolism and promote biofilm formation, which aids in the multiplication and survival of the bacteria (51). This could explain why we did not observe any effect of 4-OI on IL-6, IL-8 or RANTES protein production in PAO1-infected fibroblasts from healthy individual and IPF patients. It is also possible that the 8 h infection time used in the experiment may have been too early to see full, anti-bacterial properties of itaconate. Nevertheless, the 8 h PAO1 infection duration is routinely used in order to prevent significant cell death.

In order to further our understanding on the anti-bacterial function of 4-OI in healthy lung fibroblasts during PAO1 infection, we examined the effects of 4-OI on PAO1-infected lung fibroblasts from healthy donors in terms of IL-8, IL-1β and caspase-1 transcription, used as read-outs for NF-kB activation. In our study, we reported increased IL-8, IL-1β and caspase-2 transcription in PAO1-infected healthy lung fibroblasts. Our data correlated with studies by other authors which reported upregulated IL-8 and IL-1β transcription during PAO1 infection in in human bronchial epithelial cells (52, 53). We demonstrated that treatment with 4-OI decreased PAO1-driven transcription of IL-8, IL-1β and caspase-1 in lung fibroblasts from healthy donors. Downregulation of PAO1-driven IL-8, IL-1β and caspase-1 reported in our study may be explained by itaconate's ability to inhibit acetate assimilation as well as isocitrate lyase (ICL), an essential enzyme involved in bacterial glyoxylate cycle (54-56). Bacterial infection has been determined to be a major driver behind IPF development and progression, we predict that the decrease in in PAO1-induced transcription of IL-8, IL-1β and caspase-1 by 4-OI in IPF lung fibroblasts might be of significance in terms of novel, therapeutic strategies in IPF.

As mentioned previously in this chapter, viral infection has been emerging as an important co-factor in the development and progression of IPF, although the mechanisms employed during viral infection to catalyse the pathological changes in the disease are not completely understood and requires further research. To further investigate the anti-viral

effects of 4-OI on PAO1-driven anti-viral response in healthy human lung fibroblasts, we infected the pulmonary fibroblasts with live PAO1 in the presence of 4-OI for 8 h, then measured transcriptional levels of IFN-β, RANTES, RIG-I and IRG-1. In our study, we determined that infection of healthy lung fibroblasts with PAO1 increased IFN-β, RANTES, RIG-I and IRG-1 transcription compared with DMSO treatment only. Furthermore, we reported that treatment with 4-OI attenuated PAO1-driven transcription of IFN-β, RANTES, RIG-I and IRG-1 in healthy lung fibroblasts. In a recent study, Type I IFNS were demonstrated to play pivotal role during acute lung infection with PAO1, as increased levels of Type I IFNS were associated with increased biofilm formation which led to increased bacterial persistence in the infected lungs (57). On the contrary certain authors have reported that mice infected with PAO1, and deficient in IRF3 presented with dysregulated bacterial clearance from the lung (89. In terms of PAO1-induced transcription of IRG-1, previous studies determined that infection with PAO1 to induce itaconate production from macrophages, however, contrary to the previous accounts, the bacteria was reported to use itaconate as a fuel for growth and replication (58, 59). Whether 4-OI-mediated reduction in the transcription of PAO1-induced IFN-β, RANTES, RIG-I and IRG-1 is of beneficial or detrimental effects in IPF requires further investigation.

In summary, in our itaconate studies have established for the first time that IRG-1 expression can be induced in IPF lung fibroblasts following Poly(I:C)-activation. In this study, itaconate (4-OI) displayed both protective and pathogenic properties in the context of modulating TLR3, TLR4, TGF-β and *P. aeruginosa* responses in primary human lung fibroblasts from IPF patients. Itaconate/4-OI also downregulated the expression of TLR3 following activation of TLR3 on healthy and IPF lung fibroblasts. This suggests that itaconate has the ability to dampen Poly(I:C)-responses during viral infection which would not be a beneficial effect during IPF. Further investigation is needed to explore the role of itaconate in infection and TLR responses in IPF patients.

In chapter 4, in our IL-17A and *IL-17A* G197A studies, we demonstrated that treatment with IL-17A on its own increased IL-8 and significantly increased IL-6 protein production in lung fibroblasts from IPF patients. In addition, IL-17A increased Poly(I:C)-induced IL-8 and IL-6 protein production in healthy and IPF lung fibroblasts. In contrast, the anti-viral response associated with Poly(I:C)-driven RANTES protein production was decreased in lung fibroblasts from IPF patients. The downregulation of Poly(I:C)-induced, IRF3-driven response by IL-17A in IPF lung fibroblasts was also evident in the decreased Poly(I:C)-driven IFN-β, RANTES and RIG-

I transcription. Moreover, our western blot data demonstrated that IL-17A reduced Poly(I:C)-driven TLR3 and RIG-I protein expression in IPF lung fibroblasts. Overall, we reported that IL-17A decreased Poly(I:C)-driven IRF3 response in lung fibroblasts from IPF patients, which we predict may have pathogenic effects on IPF progression. Finally, this chapter provides evidence that the *IL-17A* G197A promoter polymorphism may represent a novel prognostic marker in IPF, and further studies are required to investigate this further. [Figure 6.1 illustrates the interplay between IL-17A, itaconate and TLR3 in primary human lung fibroblasts from IPF patients].

In our final experimental chapter, we have reported findings that demonstrate the functionality of the *TLR3* L412F polymorphism in vivo. Firstly, in IPF patients who are 412F-variant we see dysregulation of their lung microbiome, a reduction in overall pulmonary bacterial load and increased frequencies of the bacteria, *Streptococcus and S. aureus*, in BAL cell pellets from 412F-variant IPF patients. Secondly, we provide evidence in this chapter of the functionality of the *TLR3* L413F *in vivo* in our novel CRISPR-Cas-9 knock-in mice. There also is evidence of sex difference in immune responses in these mice but further investigation is required. Female 413F-HET mice have higher constitutive lung production of RANTES and KC compared to L413-WT mice. In contrast, female L413-WT mice have increased Poly(I:C)-induced pro-inflammatory and anti-viral responses in the lung compared to 413F-HET mice. In the lungs of male 413F-HET mice we observed increased basal production of RANTES and KC compared to 413-WT mice; we observed this effect in females. In contrast to females, male 413F-HET mice have increased levels of Poly(I:C)-induced RANTES and KC protein production in their lungs compared to 413-WT female mice. These data highlight the need to consider sex in mice when using murine models to recapitulate disease.

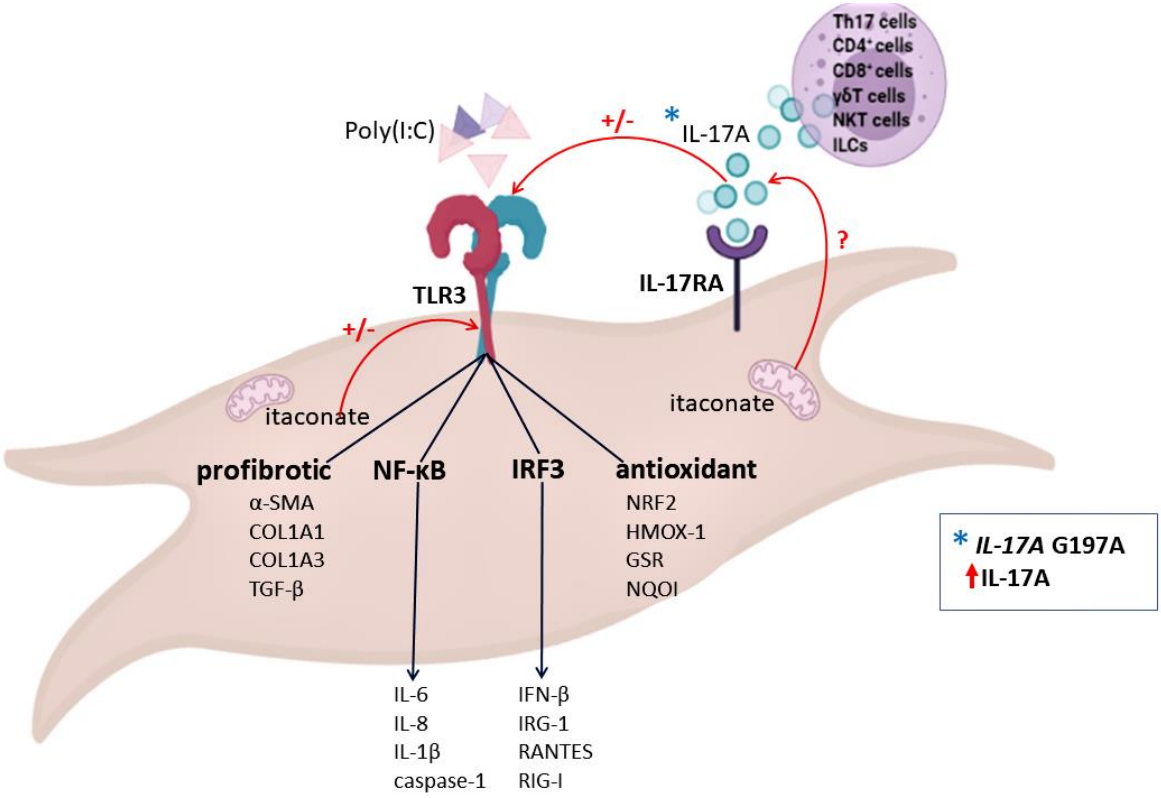

Figure 6.1 Schematic of the interplay between IL-17A, itaconate and TLR3 in primary human lung fibroblasts from IPF patients.

Chapter 7 – References

1. Chapman, S., et al., *Oxford Handbook of Respiratory Medicine*. 2014: Oxford University Press.
2. Strongman, H., I. Kausar, and T.M. Maher, *Incidence, Prevalence, and Survival of Patients with Idiopathic Pulmonary Fibrosis in the UK.* Advances in Therapy, 2018. **35**(5): p. 724-736.
3. Meltzer, E.B. and P.W. Noble, *Idiopathic pulmonary fibrosis.* Orphanet Journal of Rare Diseases, 2008. **3**(1): p. 8.
4. Rockey, D.C., P.D. Bell, and J.A. Hill, *Fibrosis--a common pathway to organ injury and failure.* N Engl J Med, 2015. **372**(12): p. 1138-49.
5. Gaffen, S.L., *Structure and signalling in the IL-17 receptor family.* Nature Reviews Immunology, 2009. **9**(8): p. 556-567.
6. Jani, M., et al., *The safety of biologic therapies in RA-associated interstitial lung disease.* Nat Rev Rheumatol, 2014. **10**(5): p. 284-94.
7. Raghu, G., et al., *An official ATS/ERS/JRS/ALAT statement: idiopathic pulmonary fibrosis: evidence-based guidelines for diagnosis and management.* American journal of respiratory and critical care medicine, 2011. **183**(6): p. 788-824.
8. Seibold, M.A., et al., *A CommonMUC5BPromoter Polymorphism and Pulmonary Fibrosis.* New England Journal of Medicine, 2011. **364**(16): p. 1503-1512.
9. Baumgartner, K.B., et al., *Cigarette smoking: a risk factor for idiopathic pulmonary fibrosis.* Am J Respir Crit Care Med, 1997. **155**(1): p. 242-8.
10. MIYAKE, Y., et al., *Occupational and Environmental Factors and Idiopathic Pulmonary Fibrosis in Japan.* The Annals of Occupational Hygiene, 2005. **49**(3): p. 259-265.
11. Raghu, G., et al., *High prevalence of abnormal acid gastro-oesophageal reflux in idiopathic pulmonary fibrosis.* Eur Respir J, 2006. **27**(1): p. 136-42.
12. Patti, M.G., et al., *Idiopathic pulmonary fibrosis: how often is it really idiopathic?* J Gastrointest Surg, 2005. **9**(8): p. 1053-6; discussion 1056-8.
13. Lee, J.S., et al., *Anti-acid treatment and disease progression in idiopathic pulmonary fibrosis: an analysis of data from three randomised controlled trials.* The Lancet Respiratory Medicine, 2013. **1**(5): p. 369-376.
14. Hubbard, R., et al., *Occupational exposure to metal or wood dust and aetiology of cryptogenic fibrosing alveolitis.* Lancet, 1996. **347**(8997): p. 284-9.
15. Hubbard, R., et al., *Risk of cryptogenic fibrosing alveolitis in metal workers.* Lancet, 2000. **355**(9202): p. 466-7.
16. Gustafson, T., et al., *Occupational exposure and severe pulmonary fibrosis.* Respir Med, 2007. **101**(10): p. 2207-12.
17. Kitamura, H., et al., *Inhalation of inorganic particles as a risk factor for idiopathic pulmonary fibrosis--elemental microanalysis of pulmonary lymph nodes obtained at autopsy cases.* Pathol Res Pract, 2007. **203**(8): p. 575-85.
18. Lopez-Otin, C., et al., *The hallmarks of aging.* Cell, 2013. **153**(6): p. 1194-217.
19. Schafer, M.J., et al., *Cellular senescence mediates fibrotic pulmonary disease.* Nat Commun, 2017. **8**: p. 14532.
20. Romero, Y., et al., *mTORC1 activation decreases autophagy in aging and idiopathic pulmonary fibrosis and contributes to apoptosis resistance in IPF fibroblasts.* Aging Cell, 2016. **15**(6): p. 1103-1112.
21. Alder, J.K., et al., *Short telomeres are a risk factor for idiopathic pulmonary fibrosis.* Proc Natl Acad Sci U S A, 2008. **105**(35): p. 13051-6.
22. Bueno, M., et al., *PINK1 deficiency impairs mitochondrial homeostasis and promotes lung fibrosis.* Journal of Clinical Investigation, 2015. **125**(2): p. 521-538.
23. Seibold, M.A., et al., *A common MUC5B promoter polymorphism and pulmonary fibrosis.* N Engl J Med, 2011. **364**(16): p. 1503-12.
24. Pulkkinen, V., et al., *ELMOD2, a candidate gene for idiopathic pulmonary fibrosis, regulates antiviral responses.* FASEB J, 2010. **24**(4): p. 1167-77.
25. Zhang, G. and S. Ghosh, *Negative regulation of toll-like receptor-mediated signaling by Tollip.* J Biol Chem, 2002. **277**(9): p. 7059-65.

26. Noth, I., et al., *Genetic variants associated with idiopathic pulmonary fibrosis susceptibility and mortality: a genome-wide association study.* The Lancet Respiratory Medicine, 2013. **1**(4): p. 309-317.
27. Zhu, L., et al., *Tollip, an intracellular trafficking protein, is a novel modulator of the transforming growth factor-beta signaling pathway.* J Biol Chem, 2012. **287**(47): p. 39653-63.
28. Allen, R.J., et al., *Genetic variants associated with susceptibility to idiopathic pulmonary fibrosis in people of European ancestry: a genome-wide association study.* Lancet Respir Med, 2017. **5**(11): p. 869-880.
29. Armanios, M.Y., et al., *Telomerase mutations in families with idiopathic pulmonary fibrosis.* N Engl J Med, 2007. **356**(13): p. 1317-26.
30. Tsakiri, K.D., et al., *Adult-onset pulmonary fibrosis caused by mutations in telomerase.* Proc Natl Acad Sci U S A, 2007. **104**(18): p. 7552-7.
31. Petrovski, S., et al., *An Exome Sequencing Study to Assess the Role of Rare Genetic Variation in Pulmonary Fibrosis.* American Journal of Respiratory and Critical Care Medicine, 2017. **196**(1): p. 82-93.
32. Kropski, J.A., et al., *A Novel Dyskerin (DKC1) Mutation Is Associated With Familial Interstitial Pneumonia.* Chest, 2014. **146**(1): p. e1-e7.
33. Gunther, A., et al., *Unravelling the progressive pathophysiology of idiopathic pulmonary fibrosis.* European Respiratory Review, 2012. **21**(124): p. 152-160.
34. Mulugeta, S., S. Nureki, and M.F. Beers, *Lost after translation: insights from pulmonary surfactant for understanding the role of alveolar epithelial dysfunction and cellular quality control in fibrotic lung disease.* Am J Physiol Lung Cell Mol Physiol, 2015. **309**(6): p. L507-25.
35. Lawson, W.E., et al., *Endoplasmic reticulum stress in alveolar epithelial cells is prominent in IPF: association with altered surfactant protein processing and herpesvirus infection.* Am J Physiol Lung Cell Mol Physiol, 2008. **294**(6): p. L1119-26.
36. Tanjore, H., T.S. Blackwell, and W.E. Lawson, *Emerging evidence for endoplasmic reticulum stress in the pathogenesis of idiopathic pulmonary fibrosis.* Am J Physiol Lung Cell Mol Physiol, 2012. **302**(8): p. L721-9.
37. Korfei, M., et al., *Epithelial Endoplasmic Reticulum Stress and Apoptosis in Sporadic Idiopathic Pulmonary Fibrosis.* American Journal of Respiratory and Critical Care Medicine, 2008. **178**(8): p. 838-846.
38. Honda, Y., et al., *Pulmonary surfactant protein D in sera and bronchoalveolar lavage fluids.* Am J Respir Crit Care Med, 1995. **152**(6 Pt 1): p. 1860-6.
39. Kuroki, Y., et al., *Elevated levels of lung surfactant protein A in sera from patients with idiopathic pulmonary fibrosis and pulmonary alveolar proteinosis.* Am Rev Respir Dis, 1993. **147**(3): p. 723-9.
40. Greene, K.E., et al., *Serum surfactant proteins-A and -D as biomarkers in idiopathic pulmonary fibrosis.* Eur Respir J, 2002. **19**(3): p. 439-46.
41. Günther, A., et al., *Surfactant abnormalities in idiopathic pulmonary fibrosis, hypersensitivity pneumonitis and sarcoidosis.* European Respiratory Journal, 1999. **14**(3): p. 565.
42. Collard, H.R., et al., *Plasma biomarker profiles in acute exacerbation of idiopathic pulmonary fibrosis.* Am J Physiol Lung Cell Mol Physiol, 2010. **299**(1): p. L3-7.
43. Gnanapandithan, K., et al., *Gastroesophageal reflux and idiopathic pulmonary fibrosis: A long term relationship.* Respir Med Case Rep, 2016. **17**: p. 40-3.
44. Nakayama, S., et al., *Pirfenidone inhibits the expression of HSP47 in TGF-beta1-stimulated human lung fibroblasts.* Life Sci, 2008. **82**(3-4): p. 210-7.
45. Conte, E., et al., *Effect of pirfenidone on proliferation, TGF-β-induced myofibroblast differentiation and fibrogenic activity of primary human lung fibroblasts.* Eur J Pharm Sci, 2014. **58**: p. 13-9.
46. Nakazato, H., et al., *A novel anti-fibrotic agent pirfenidone suppresses tumor necrosis factor-alpha at the translational level.* Eur J Pharmacol, 2002. **446**(1-3): p. 177-85.
47. Oku, H., et al., *Pirfenidone suppresses tumor necrosis factor-alpha, enhances interleukin-10 and protects mice from endotoxic shock.* Eur J Pharmacol, 2002. **446**(1-3): p. 167-76.

48. Cain, W.C., et al., *Inhibition of tumor necrosis factor and subsequent endotoxin shock by pirfenidone.* Int J Immunopharmacol, 1998. **20**(12): p. 685-95.
49. Iyer, S.N., G. Gurujeyalakshmi, and S.N. Giri, *Effects of pirfenidone on transforming growth factor-beta gene expression at the transcriptional level in bleomycin hamster model of lung fibrosis.* J Pharmacol Exp Ther, 1999. **291**(1): p. 367-73.
50. Quan, T.E., S.E. Cowper, and R. Bucala, *The role of circulating fibrocytes in fibrosis.* Curr Rheumatol Rep, 2006. **8**(2): p. 145-50.
51. Inomata, M., et al., *Pirfenidone inhibits fibrocyte accumulation in the lungs in bleomycin-induced murine pulmonary fibrosis.* Respir Res, 2014. **15**: p. 16.
52. Giri, S.N., et al., *Effects of pirfenidone on the generation of reactive oxygen species in vitro.* J Environ Pathol Toxicol Oncol, 1999. **18**(3): p. 169-77.
53. Misra, H.P. and C. Rabideau, *Pirfenidone inhibits NADPH-dependent microsomal lipid peroxidation and scavenges hydroxyl radicals.* Mol Cell Biochem, 2000. **204**(1-2): p. 119-26.
54. Taniguchi, H., et al., *Pirfenidone in idiopathic pulmonary fibrosis.* European Respiratory Journal, 2010. **35**(4): p. 821-829.
55. Noble, P.W., et al., *Pirfenidone in patients with idiopathic pulmonary fibrosis (CAPACITY): two randomised trials.* Lancet, 2011. **377**(9779): p. 1760-9.
56. King, T.E., et al., *A Phase 3 Trial of Pirfenidone in Patients with Idiopathic Pulmonary Fibrosis.* New England Journal of Medicine, 2014. **370**(22): p. 2083-2092.
57. Hilberg, F., et al., *BIBF 1120: triple angiokinase inhibitor with sustained receptor blockade and good antitumor efficacy.* Cancer Res, 2008. **68**(12): p. 4774-82.
58. Wollin, L., et al., *Antifibrotic and anti-inflammatory activity of the tyrosine kinase inhibitor nintedanib in experimental models of lung fibrosis.* J Pharmacol Exp Ther, 2014. **349**(2): p. 209-20.
59. Wollin, L., et al., *Mode of action of nintedanib in the treatment of idiopathic pulmonary fibrosis.* Eur Respir J, 2015. **45**(5): p. 1434-45.
60. Richeldi, L., et al., *Efficacy of a Tyrosine Kinase Inhibitor in Idiopathic Pulmonary Fibrosis.* New England Journal of Medicine, 2011. **365**(12): p. 1079-1087.
61. Richeldi, L., et al., *Efficacy and safety of nintedanib in idiopathic pulmonary fibrosis.* N Engl J Med, 2014. **370**(22): p. 2071-82.
62. Khalil, N., et al., *Phase 2 clinical trial of PBI-4050 in patients with idiopathic pulmonary fibrosis.* European Respiratory Journal, 2019. **53**(3): p. 1800663.
63. Richeldi, L., et al., *Pamrevlumab, an anti-connective tissue growth factor therapy, for idiopathic pulmonary fibrosis (PRAISE): a phase 2, randomised, double-blind, placebo-controlled trial.* Lancet Respir Med, 2020. **8**(1): p. 25-33.
64. Raghu, G., et al., *Effect of Recombinant Human Pentraxin 2 vs Placebo on Change in Forced Vital Capacity in Patients With Idiopathic Pulmonary Fibrosis.* JAMA, 2018. **319**(22): p. 2299.
65. Maher, T.M., et al., *Safety, tolerability, pharmacokinetics, and pharmacodynamics of GLPG1690, a novel autotaxin inhibitor, to treat idiopathic pulmonary fibrosis (FLORA): a phase 2a randomised placebo-controlled trial.* Lancet Respir Med, 2018. **6**(8): p. 627-635.
66. *A Clinical Study to Test How Effective and Safe GLPG1690 is for Participants With Idiopathic Pulmonary Fibrosis (IPF) When Used Together With Standard of Care*. https://ClinicalTrials.gov/show/NCT03733444.
67. McCormack, F.X., et al., *Surfactant protein A predicts survival in idiopathic pulmonary fibrosis.* Am J Respir Crit Care Med, 1995. **152**(2): p. 751-9.
68. Manolio, T.A., et al., *Finding the missing heritability of complex diseases.* Nature, 2009. **461**(7265): p. 747-53.
69. Whitley, R.J., *Herpesviruses*, in *Medical Microbiology*, th and S. Baron, Editors. 1996: Galveston (TX).
70. Lok, S.S., et al., *Murine gammaherpes virus as a cofactor in the development of pulmonary fibrosis in bleomycin resistant mice.* Eur Respir J, 2002. **20**(5): p. 1228-32.
71. McMillan, T.R., et al., *Exacerbation of established pulmonary fibrosis in a murine model by gammaherpesvirus.* Am J Respir Crit Care Med, 2008. **177**(7): p. 771-80.

72. Yonemaru, M., et al., *Elevation of antibodies to cytomegalovirus and other herpes viruses in pulmonary fibrosis.* Eur Respir J, 1997. **10**(9): p. 2040-5.
73. Tang, Y.-W., et al., *Herpesvirus DNA Is Consistently Detected in Lungs of Patients with Idiopathic Pulmonary Fibrosis.* Journal of Clinical Microbiology, 2003. **41**(6): p. 2633-2640.
74. Stewart, J.P., et al., *The detection of Epstein-Barr virus DNA in lung tissue from patients with idiopathic pulmonary fibrosis.* Am J Respir Crit Care Med, 1999. **159**(4 Pt 1): p. 1336-41.
75. Lasithiotaki, I., et al., *Detection of Herpes Simplex Virus Type-1 in Patients with Fibrotic Lung Diseases.* PLoS ONE, 2011. **6**(12): p. e27800.
76. Toshikuni, N., *Hepatitis C-related liver cirrhosis - strategies for the prevention of hepatic decompensation, hepatocarcinogenesis, and mortality.* World Journal of Gastroenterology, 2014. **20**(11): p. 2876.
77. Ueda, T., et al., *Idiopathic pulmonary fibrosis and high prevalence of serum antibodies to hepatitis C virus.* Am Rev Respir Dis, 1992. **146**(1): p. 266-8.
78. Arase, Y., et al., *Hepatitis C virus enhances incidence of idiopathic pulmonary fibrosis.* World Journal of Gastroenterology, 2008. **14**(38): p. 5880.
79. Bando, M., et al., *Infection of TT virus in patients with idiopathic pulmonary fibrosis.* Respir Med, 2001. **95**(12): p. 935-42.
80. Wootton, S.C., et al., *Viral infection in acute exacerbation of idiopathic pulmonary fibrosis.* American journal of respiratory and critical care medicine, 2011. **183**(12): p. 1698-1702.
81. Fujino, N., et al., *Increased severity of 2009 pandemic influenza A virus subtype H1N1 infection in alveolar type II cells from patients with pulmonary fibrosis.* J Infect Dis, 2013. **207**(4): p. 692-3.
82. Jolly, L., et al., *Influenza promotes collagen deposition via alphavbeta6 integrin-mediated transforming growth factor beta activation.* J Biol Chem, 2014. **289**(51): p. 35246-63.
83. Molyneaux, P.L., et al., *The role of bacteria in the pathogenesis and progression of idiopathic pulmonary fibrosis.* American journal of respiratory and critical care medicine, 2014. **190**(8): p. 906-913.
84. Molyneaux, P.L., et al., *Changes in the respiratory microbiome during acute exacerbations of idiopathic pulmonary fibrosis.* Respir Res, 2017. **18**(1): p. 29.
85. Han, M.K., et al., *Lung microbiome and disease progression in idiopathic pulmonary fibrosis: an analysis of the COMET study.* The Lancet Respiratory Medicine, 2014. **2**(7): p. 548-556.
86. Takahashi, Y., et al., *Impaired diversity of the lung microbiome predicts progression of idiopathic pulmonary fibrosis.* Respir Res, 2018. **19**(1): p. 34.
87. Kosmidis, C. and D.W. Denning, *The clinical spectrum of pulmonary aspergillosis.* Thorax, 2015. **70**(3): p. 270-7.
88. Kurosaki, F., et al., *Clinical features of pulmonary aspergillosis associated with interstitial pneumonia.* Intern Med, 2014. **53**(12): p. 1299-306.
89. Oda, K., et al., *Autopsy analyses in acute exacerbation of idiopathic pulmonary fibrosis.* Respir Res, 2014. **15**: p. 109.
90. Kosmidis, C., et al., *Chronic fibrosing pulmonary aspergillosis: a cause of 'destroyed lung' syndrome.* Infectious Diseases, 2017. **49**(4): p. 296-301.
91. Franco, L., et al., *Experimental pulmonary fibrosis induced by Paracoccidioides brasiliensis conidia: measurement of local host responses.* Am J Trop Med Hyg, 1998. **58**(4): p. 424-30.
92. González, A., A. Restrepo, and L.E. Cano, *Pulmonary immune responses induced in BALB/c mice by Paracoccidioides brasiliensis conidia.* Mycopathologia, 2008. **165**(4-5): p. 313-330.
93. Naranjo, T.W., et al., *Combined itraconazole-pentoxifylline treatment promptly reduces lung fibrosis induced by chronic pulmonary paracoccidioidomycosis in mice.* Pulm Pharmacol Ther, 2011. **24**(1): p. 81-91.
94. Akira, S., *Pathogen recognition by innate immunity and its signaling.* Proceedings of the Japan Academy, Series B, 2009. **85**(4): p. 143-156.
95. Akira, S. and K. Takeda, *Toll-like receptor signalling.* Nat Rev Immunol, 2004. **4**(7): p. 499-511.
96. Akira, S., S. Uematsu, and O. Takeuchi, *Pathogen recognition and innate immunity.* Cell, 2006. **124**(4): p. 783-801.
97. Beutler, B., *Innate immunity: an overview.* Mol Immunol, 2004. **40**(12): p. 845-59.

98. Chaplin, D.D., *Overview of the immune response.* Journal of Allergy and Clinical Immunology, 2010. **125**(2): p. S3-S23.
99. Bonilla, F.A. and H.C. Oettgen, *Adaptive immunity.* Journal of Allergy and Clinical Immunology, 2010. **125**(2): p. S33-S40.
100. Dranoff, G., *Cytokines in cancer pathogenesis and cancer therapy.* Nature Reviews Cancer, 2004. **4**(1): p. 11-22.
101. Hartl, D., et al., *Innate Immunity of the Lung: From Basic Mechanisms to Translational Medicine.* Journal of Innate Immunity, 2018. **10**(5-6): p. 487-501.
102. Hussell, T. and T.J. Bell, *Alveolar macrophages: plasticity in a tissue-specific context.* Nature Reviews Immunology, 2014. **14**(2): p. 81-93.
103. Kolahian, S., et al., *Immune Mechanisms in Pulmonary Fibrosis.* Am J Respir Cell Mol Biol, 2016. **55**(3): p. 309-22.
104. Liegeois, M., et al., *The interstitial macrophage: A long-neglected piece in the puzzle of lung immunity.* Cell Immunol, 2018. **330**: p. 91-96.
105. Holt, P.G., et al., *Preparation of interstitial lung cells by enzymatic digestion of tissue slices: preliminary characterization by morphology and performance in functional assays.* Immunology, 1985. **54**(1): p. 139-47.
106. Bedoret, D., et al., *Lung interstitial macrophages alter dendritic cell functions to prevent airway allergy in mice.* Journal of Clinical Investigation, 2009. **119**(12): p. 3723-3738.
107. Hoppstädter, J., et al., *Differential cell reaction upon Toll-like receptor 4 and 9 activation in human alveolar and lung interstitial macrophages.* Respiratory Research, 2010. **11**(1): p. 124.
108. Gibbings, S.L., et al., *Three Unique Interstitial Macrophages in the Murine Lung at Steady State.* American Journal of Respiratory Cell and Molecular Biology, 2017. **57**(1): p. 66-76.
109. Franke-Ullmann, G., et al., *Characterization of murine lung interstitial macrophages in comparison with alveolar macrophages in vitro.* J Immunol, 1996. **157**(7): p. 3097-104.
110. Fathi, M., et al., *Functional and morphological differences between human alveolar and interstitial macrophages.* Exp Mol Pathol, 2001. **70**(2): p. 77-82.
111. Sabatel, C., et al., *Exposure to Bacterial CpG DNA Protects from Airway Allergic Inflammation by Expanding Regulatory Lung Interstitial Macrophages.* Immunity, 2017. **46**(3): p. 457-473.
112. Kawano, H., et al., *IL-10-producing lung interstitial macrophages prevent neutrophilic asthma.* Int Immunol, 2016. **28**(10): p. 489-501.
113. Lehnert, B.E., Y.E. Valdez, and L.M. Holland, *Pulmonary macrophages: alveolar and interstitial populations.* Exp Lung Res, 1985. **9**(3-4): p. 177-90.
114. Toussaint, M., et al., *Myeloid hypoxia-inducible factor 1α prevents airway allergy in mice through macrophage-mediated immunoregulation.* Mucosal Immunology, 2013. **6**(3): p. 485-497.
115. Johansson, A., et al., *Functional, morphological, and phenotypical differences between rat alveolar and interstitial macrophages.* Am J Respir Cell Mol Biol, 1997. **16**(5): p. 582-8.
116. Holtzman, M.J., et al., *The role of airway epithelial cells and innate immune cells in chronic respiratory disease.* Nature Reviews Immunology, 2014. **14**(10): p. 686-698.
117. Whitsett, J.A., *Airway Epithelial Differentiation and Mucociliary Clearance.* Annals of the American Thoracic Society, 2018. **15**(Supplement_3): p. S143-S148.
118. Holtzman, M.J., et al., *Control of epithelial immune-response genes and implications for airway immunity and inflammation.* Proc Assoc Am Physicians, 1998. **110**(1): p. 1-11.
119. Holgate, S.T., et al., *Epithelial-mesenchymal interactions in the pathogenesis of asthma.* J Allergy Clin Immunol, 2000. **105**(2 Pt 1): p. 193-204.
120. Lambrecht, B.N. and H. Hammad, *The airway epithelium in asthma.* Nature Medicine, 2012. **18**(5): p. 684-692.
121. Van Linthout, S., K. Miteva, and C. Tschöpe, *Crosstalk between fibroblasts and inflammatory cells.* Cardiovasc Res, 2014. **102**(2): p. 258-69.
122. Buckley, C.D., et al., *Fibroblasts regulate the switch from acute resolving to chronic persistent inflammation.* Trends Immunol, 2001. **22**(4): p. 199-204.
123. Meneghin, A. and C.M. Hogaboam, *Infectious disease, the innate immune response, and fibrosis.* J Clin Invest, 2007. **117**(3): p. 530-8.

124. Otte, J.M., I.M. Rosenberg, and D.K. Podolsky, *Intestinal myofibroblasts in innate immune responses of the intestine.* Gastroenterology, 2003. **124**(7): p. 1866-78.
125. Parsonage, G., et al., *A stromal address code defined by fibroblasts.* Trends in Immunology, 2005. **26**(3): p. 150-156.
126. Nash, G.B., C.D. Buckley, and G. Ed Rainger, *The local physicochemical environment conditions the proinflammatory response of endothelial cells and thus modulates leukocyte recruitment.* FEBS Letters, 2004. **569**(1-3): p. 13-17.
127. Rainger, G.E., et al., *A novel system for investigating the ability of smooth muscle cells and fibroblasts to regulate adhesion of flowing leukocytes to endothelial cells.* J Immunol Methods, 2001. **255**(1-2): p. 73-82.
128. Lukacs, N.W., et al., *Production of monocyte chemoattractant protein-1 and macrophage inflammatory protein-1 alpha by inflammatory granuloma fibroblasts.* Am J Pathol, 1994. **144**(4): p. 711-8.
129. Wu, B., L. Tang, and M. Kapoor, *Fibroblasts and their responses to chronic injury in pulmonary fibrosis.* Semin Arthritis Rheum, 2021. **51**(1): p. 310-317.
130. Kawai, T. and S. Akira, *The role of pattern-recognition receptors in innate immunity: update on Toll-like receptors.* Nature Immunology, 2010. **11**(5): p. 373-384.
131. *How invaders are recognized*. Innate immnutity: The recognition of invaders 2016 [cited 2022; Available from: https://veteriankey.com/innate-immunity-the-recognition-of-invaders/.
132. O'Neill, L.A.J., D. Golenbock, and A.G. Bowie, *The history of Toll-like receptors — redefining innate immunity.* Nature Reviews Immunology, 2013. **13**: p. 453.
133. Rock, F.L., et al., *A family of human receptors structurally related to Drosophila Toll.* Proceedings of the National Academy of Sciences, 1998. **95**(2): p. 588-593.
134. Medzhitov, R., P. Preston-Hurlburt, and C.A. Janeway, *A human homologue of the Drosophila Toll protein signals activation of adaptive immunity.* Nature, 1997. **388**(6640): p. 394-397.
135. Takeuchi, O., et al., *TLR6: A novel member of an expanding Toll-like receptor family.* Gene, 1999. **231**(1): p. 59-65.
136. Chuang, T.H. and R.J. Ulevitch, *Cloning and characterization of a sub-family of human toll-like receptors: hTLR7, hTLR8 and hTLR9.* Eur Cytokine Netw, 2000. **11**(3): p. 372-8.
137. Chuang, T. and R.J. Ulevitch, *Identification of hTLR10: a novel human Toll-like receptor preferentially expressed in immune cells.* Biochim Biophys Acta, 2001. **1518**(1-2): p. 157-61.
138. Zhang, D., et al., *A toll-like receptor that prevents infection by uropathogenic bacteria.* Science, 2004. **303**(5663): p. 1522-6.
139. Raetz, M., et al., *Cooperation of TLR12 and TLR11 in the IRF8-Dependent IL-12 Response toToxoplasma gondiiProfilin.* The Journal of Immunology, 2013. **191**(9): p. 4818-4827.
140. Oldenburg, M., et al., *TLR13 recognizes bacterial 23S rRNA devoid of erythromycin resistance-forming modification.* Science, 2012. **337**(6098): p. 1111-5.
141. West, A.P., A.A. Koblansky, and S. Ghosh, *Recognition and signaling by toll-like receptors.* Annu Rev Cell Dev Biol, 2006. **22**: p. 409-37.
142. Jin, M.S. and J.O. Lee, *Structures of the toll-like receptor family and its ligand complexes.* Immunity, 2008. **29**(2): p. 182-91.
143. Bell, J.K., et al., *Leucine-rich repeats and pathogen recognition in Toll-like receptors.* Trends Immunol, 2003. **24**(10): p. 528-33.
144. Slack, J.L., et al., *Identification of Two Major Sites in the Type I Interleukin-1 Receptor Cytoplasmic Region Responsible for Coupling to Pro-inflammatory Signaling Pathways.* Journal of Biological Chemistry, 2000. **275**(7): p. 4670-4678.
145. Vercammen, E., J. Staal, and R. Beyaert, *Sensing of viral infection and activation of innate immunity by toll-like receptor 3.* Clin Microbiol Rev, 2008. **21**(1): p. 13-25.
146. Pandey, S., T. Kawai, and S. Akira, *Microbial sensing by Toll-like receptors and intracellular nucleic acid sensors.* Cold Spring Harb Perspect Biol, 2014. **7**(1): p. a016246.
147. Collins, B. and I.A. Wilson, *Crystal structure of the C-terminal domain of mouse TLR9.* Proteins: Structure, Function, and Bioinformatics, 2014. **82**(10): p. 2874-2878.
148. Fitzgerald, K.A., et al., *Mal (MyD88-adapter-like) is required for Toll-like receptor-4 signal transduction.* Nature, 2001. **413**(6851): p. 78-83.

149. Sarkar, S.N., et al., *Two tyrosine residues of Toll-like receptor 3 trigger different steps of NF-kappa B activation.* J Biol Chem, 2007. **282**(6): p. 3423-7.
150. Tissari, J., et al., *IFN-alpha enhances TLR3-mediated antiviral cytokine expression in human endothelial and epithelial cells by up-regulating TLR3 expression.* J Immunol, 2005. **174**(7): p. 4289-94.
151. Mayer, A.K., et al., *Differential recognition of TLR-dependent microbial ligands in human bronchial epithelial cells.* J Immunol, 2007. **178**(5): p. 3134-42.
152. Project, T.H.A. *TLR3* [cited 2018 09.04.18]; Available from: https://www.proteinatlas.org/ENSG00000164342-TLR3/tissue#gene_information.
153. Fagerberg, L., et al., *Analysis of the human tissue-specific expression by genome-wide integration of transcriptomics and antibody-based proteomics.* Mol Cell Proteomics, 2014. **13**(2): p. 397-406.
154. Kawasaki, T. and T. Kawai, *Toll-like receptor signaling pathways.* Front Immunol, 2014. **5**: p. 461.
155. Oshiumi, H., et al., *TICAM-1, an adaptor molecule that participates in Toll-like receptor 3-mediated interferon-beta induction.* Nat Immunol, 2003. **4**(2): p. 161-7.
156. Yamamoto, M., et al., *Role of adaptor TRIF in the MyD88-independent toll-like receptor signaling pathway.* Science, 2003. **301**(5633): p. 640-3.
157. Cusson-Hermance, N., et al., *Rip1 Mediates the Trif-dependent Toll-like Receptor 3- and 4-induced NF-κB Activation but Does Not Contribute to Interferon Regulatory Factor 3 Activation.* Journal of Biological Chemistry, 2005. **280**(44): p. 36560-36566.
158. Meylan, E., et al., *RIP1 is an essential mediator of Toll-like receptor 3-induced NF-kappa B activation.* Nat Immunol, 2004. **5**(5): p. 503-7.
159. Shim, J.H., et al., *TAK1, but not TAB1 or TAB2, plays an essential role in multiple signaling pathways in vivo.* Genes Dev, 2005. **19**(22): p. 2668-81.
160. Joshi, A.D., et al., *TLR3 modulates immunopathology during a Schistosoma mansoni egg-driven Th2 response in the lung.* European Journal of Immunology, 2008. **38**(12): p. 3436-3449.
161. O'Dwyer, D.N., et al., *The Toll-like receptor 3 L412F polymorphism and disease progression in idiopathic pulmonary fibrosis.* Am J Respir Crit Care Med, 2013. **188**(12): p. 1442-50.
162. Takahashi, T., et al., *Amelioration of tissue fibrosis by toll-like receptor 4 knockout in murine models of systemic sclerosis.* Arthritis Rheumatol, 2015. **67**(1): p. 254-65.
163. Meneghin, A., et al., *TLR9 is expressed in idiopathic interstitial pneumonia and its activation promotes in vitro myofibroblast differentiation.* Histochemistry and Cell Biology, 2008. **130**(5): p. 979-992.
164. Trujillo, G., et al., *TLR9 differentiates rapidly from slowly progressing forms of idiopathic pulmonary fibrosis.* Sci Transl Med, 2010. **2**(57): p. 57ra82.
165. Ranjith-Kumar, C.T., et al., *Effects of single nucleotide polymorphisms on Toll-like receptor 3 activity and expression in cultured cells.* J Biol Chem, 2007. **282**(24): p. 17696-705.
166. Assmann, T.S., et al., *Polymorphisms in the TLR3 gene are associated with risk for type 1 diabetes mellitus.* Eur J Endocrinol, 2014. **170**(4): p. 519-27.
167. Studzinska, M., et al., *Association of TLR3 L412F Polymorphism with Cytomegalovirus Infection in Children.* PLoS One, 2017. **12**(1): p. e0169420.
168. Laska, M.J., et al., *Polymorphisms within Toll-like receptors are associated with systemic lupus erythematosus in a cohort of Danish females.* Rheumatology (Oxford), 2014. **53**(1): p. 48-55.
169. Fischer, J., et al., *Polymorphisms in the Toll-like receptor 3 (TLR3) gene are associated with the natural course of hepatitis B virus infection in Caucasian population.* Sci Rep, 2018. **8**(1): p. 12737.
170. Gorbea, C., et al., *A role for Toll-like receptor 3 variants in host susceptibility to enteroviral myocarditis and dilated cardiomyopathy.* J Biol Chem, 2010. **285**(30): p. 23208-23.
171. Kindberg, E., et al., *A functional Toll-like receptor 3 gene (TLR3) may be a risk factor for tick-borne encephalitis virus (TBEV) infection.* J Infect Dis, 2011. **203**(4): p. 523-8.
172. Mickiene, A., et al., *Polymorphisms in chemokine receptor 5 and Toll-like receptor 3 genes are risk factors for clinical tick-borne encephalitis in the Lithuanian population.* PLoS One, 2014. **9**(9): p. e106798.

173. Barkhash, A.V., M.I. Voevoda, and A.G. Romaschenko, *Association of single nucleotide polymorphism rs3775291 in the coding region of the TLR3 gene with predisposition to tick-borne encephalitis in a Russian population.* Antiviral Res, 2013. **99**(2): p. 136-8.
174. Sironi, M., et al., *A common polymorphism in TLR3 confers natural resistance to HIV-1 infection.* J Immunol, 2012. **188**(2): p. 818-23.
175. Svensson, A., et al., *Polymorphisms in Toll-like receptor 3 confer natural resistance to human herpes simplex virus type 2 infection.* J Gen Virol, 2012. **93**(Pt 8): p. 1717-24.
176. Wang, A., H.H. Luan, and R. Medzhitov, *An evolutionary perspective on immunometabolism.* Science, 2019. **363**(6423).
177. Ryan, D.G. and L.A.J. O'Neill, *Krebs Cycle Reborn in Macrophage Immunometabolism.* Annu Rev Immunol, 2020. **38**: p. 289-313.
178. Lunt, S.Y. and M.G. Vander Heiden, *Aerobic glycolysis: meeting the metabolic requirements of cell proliferation.* Annu Rev Cell Dev Biol, 2011. **27**: p. 441-64.
179. Li, X.B., J.D. Gu, and Q.H. Zhou, *Review of aerobic glycolysis and its key enzymes - new targets for lung cancer therapy.* Thorac Cancer, 2015. **6**(1): p. 17-24.
180. O'Neill, L.A.J., R.J. Kishton, and J. Rathmell, *A guide to immunometabolism for immunologists.* Nature Reviews Immunology, 2016. **16**(9): p. 553-565.
181. Feher, J., *Quantitative Human Physiology*. Biomedical Engineering. 2012.
182. Alabduladhem, T.O. and B. Bordoni, *Physiology, Krebs Cycle*, in *StatPearls*. 2022, StatPearls Publishing

Copyright © 2022, StatPearls Publishing LLC.: Treasure Island (FL).

183. Martínez-Reyes, I. and N.S. Chandel, *Mitochondrial TCA cycle metabolites control physiology and disease.* Nature Communications, 2020. **11**(1).
184. Remington, S.J., *Structure and mechanism of citrate synthase.* Curr Top Cell Regul, 1992. **33**: p. 209-29.
185. Lloyd, S.J., et al., *The mechanism of aconitase: 1.8 A resolution crystal structure of the S642a:citrate complex.* Protein Sci, 1999. **8**(12): p. 2655-62.
186. Ma, T., et al., *The β and γ subunits play distinct functional roles in the α2βγ heterotetramer of human NAD-dependent isocitrate dehydrogenase.* Scientific Reports, 2017. **7**(1): p. 41882.
187. Sheu, K.F. and J.P. Blass, *The alpha-ketoglutarate dehydrogenase complex.* Ann N Y Acad Sci, 1999. **893**: p. 61-78.
188. Johnson, J.D., W.W. Muhonen, and D.O. Lambeth, *Characterization of the ATP- and GTP-specific succinyl-CoA synthetases in pigeon. The enzymes incorporate the same alpha-subunit.* J Biol Chem, 1998. **273**(42): p. 27573-9.
189. Rose, I.A., *How Fumarase Recycles after the Malate → Fumarate Reaction. Insights into the Reaction Mechanism.* Biochemistry, 1998. **37**(51): p. 17651-17658.
190. Chapman, A.D., et al., *Structural basis of substrate specificity in malate dehydrogenases: crystal structure of a ternary complex of porcine cytoplasmic malate dehydrogenase, alpha-ketomalonate and tetrahydoNAD.* J Mol Biol, 1999. **285**(2): p. 703-12.
191. Mills, E.L., et al., *Succinate Dehydrogenase Supports Metabolic Repurposing of Mitochondria to Drive Inflammatory Macrophages.* Cell, 2016. **167**(2): p. 457-470.e13.
192. Lampropoulou, V., et al., *Itaconate Links Inhibition of Succinate Dehydrogenase with Macrophage Metabolic Remodeling and Regulation of Inflammation.* Cell Metab, 2016. **24**(1): p. 158-66.
193. Jha, A.K., et al., *Network integration of parallel metabolic and transcriptional data reveals metabolic modules that regulate macrophage polarization.* Immunity, 2015. **42**(3): p. 419-30.
194. Everts, B., et al., *TLR-driven early glycolytic reprogramming via the kinases TBK1-IKKε supports the anabolic demands of dendritic cell activation.* Nat Immunol, 2014. **15**(4): p. 323-32.
195. Mills, E.L., et al., *Itaconate is an anti-inflammatory metabolite that activates Nrf2 via alkylation of KEAP1.* Nature, 2018. **556**(7699): p. 113-117.
196. Galván-Peña, S. and L.A. O'Neill, *Metabolic reprograming in macrophage polarization.* Front Immunol, 2014. **5**: p. 420.
197. Wynn, T.A. and K.M. Vannella, *Macrophages in Tissue Repair, Regeneration, and Fibrosis.* Immunity, 2016. **44**(3): p. 450-462.

198. Russell, D.G., L. Huang, and B.C. VanderVen, *Immunometabolism at the interface between macrophages and pathogens.* Nat Rev Immunol, 2019. **19**(5): p. 291-304.
199. Rodríguez-Prados, J.C., et al., *Substrate fate in activated macrophages: a comparison between innate, classic, and alternative activation.* J Immunol, 2010. **185**(1): p. 605-14.
200. Krawczyk, C.M., et al., *Toll-like receptor-induced changes in glycolytic metabolism regulate dendritic cell activation.* Blood, 2010. **115**(23): p. 4742-9.
201. Donnelly, R.P., et al., *mTORC1-dependent metabolic reprogramming is a prerequisite for NK cell effector function.* J Immunol, 2014. **193**(9): p. 4477-84.
202. Michalek, R.D., et al., *Cutting edge: distinct glycolytic and lipid oxidative metabolic programs are essential for effector and regulatory CD4+ T cell subsets.* J Immunol, 2011. **186**(6): p. 3299-303.
203. Warburg, O., F. Wind, and E. Negelein, *THE METABOLISM OF TUMORS IN THE BODY.* J Gen Physiol, 1927. **8**(6): p. 519-30.
204. Nagy, C. and A. Haschemi, *Time and Demand are Two Critical Dimensions of Immunometabolism: The Process of Macrophage Activation and the Pentose Phosphate Pathway.* Front Immunol, 2015. **6**: p. 164.
205. Halligan, D.N., S.J. Murphy, and C.T. Taylor, *The hypoxia-inducible factor (HIF) couples immunity with metabolism.* Semin Immunol, 2016. **28**(5): p. 469-477.
206. van Uden, P., N.S. Kenneth, and S. Rocha, *Regulation of hypoxia-inducible factor-1alpha by NF-kappaB.* Biochem J, 2008. **412**(3): p. 477-84.
207. Van Uden, P., et al., *Evolutionary Conserved Regulation of HIF-1β by NF-κB.* PLoS Genetics, 2011. **7**(1): p. e1001285.
208. Semenza, G.L., et al., *Transcriptional regulation of genes encoding glycolytic enzymes by hypoxia-inducible factor 1.* J Biol Chem, 1994. **269**(38): p. 23757-63.
209. Tannahill, G.M., et al., *Succinate is an inflammatory signal that induces IL-1β through HIF-1α.* Nature, 2013. **496**(7444): p. 238-42.
210. Selak, M.A., et al., *Succinate links TCA cycle dysfunction to oncogenesis by inhibiting HIF-alpha prolyl hydroxylase.* Cancer cell, 2005. **7**(1): p. 77-85.
211. Blouin, C.C., et al., *Hypoxic gene activation by lipopolysaccharide in macrophages: implication of hypoxia-inducible factor 1alpha.* Blood, 2004. **103**(3): p. 1124-30.
212. Nishi, K., et al., *LPS induces hypoxia-inducible factor 1 activation in macrophage-differentiated cells in a reactive oxygen species-dependent manner.* Antioxid Redox Signal, 2008. **10**(5): p. 983-95.
213. Cramer, T., et al., *HIF-1alpha is essential for myeloid cell-mediated inflammation.* Cell, 2003. **112**(5): p. 645-57.
214. Kim, J.W., et al., *HIF-1-mediated expression of pyruvate dehydrogenase kinase: a metabolic switch required for cellular adaptation to hypoxia.* Cell Metab, 2006. **3**(3): p. 177-85.
215. Luke, *A Broken Krebs Cycle in Macrophages.* Immunity, 2015. **42**(3): p. 393-394.
216. Owen, O.E., S.C. Kalhan, and R.W. Hanson, *The key role of anaplerosis and cataplerosis for citric acid cycle function.* J Biol Chem, 2002. **277**(34): p. 30409-12.
217. Infantino, V., et al., *The mitochondrial citrate carrier: a new player in inflammation.* Biochem J, 2011. **438**(3): p. 433-6.
218. Kelly, B. and L.A. O'Neill, *Metabolic reprogramming in macrophages and dendritic cells in innate immunity.* Cell Res, 2015. **25**(7): p. 771-84.
219. Kurtz, R., M.F. Anderman, and B.D. Shepard, *GPCRs get fatty: the role of G protein-coupled receptor signaling in the development and progression of nonalcoholic fatty liver disease.* Am J Physiol Gastrointest Liver Physiol, 2021. **320**(3): p. G304-g318.
220. Chouchani, E.T., et al., *Ischaemic accumulation of succinate controls reperfusion injury through mitochondrial ROS.* Nature, 2014. **515**(7527): p. 431-435.
221. Berlin, N.I., *Hans Krebs: Architect of Intermediary Metabolism 1933-1937.* JAMA, 1994. **271**(14): p. 1137-1138.
222. Shin, J.H., et al., *(1)H NMR-based metabolomic profiling in mice infected with Mycobacterium tuberculosis.* J Proteome Res, 2011. **10**(5): p. 2238-47.

223. Strelko, C.L., et al., *Itaconic acid is a mammalian metabolite induced during macrophage activation.* J Am Chem Soc, 2011. **133**(41): p. 16386-9.
224. Sugimoto, M., et al., *Non-targeted metabolite profiling in activated macrophage secretion.* Metabolomics, 2012. **8**(4): p. 624-633.
225. Ganta, V.C., et al., *A MicroRNA93-Interferon Regulatory Factor-9-Immunoresponsive Gene-1-Itaconic Acid Pathway Modulates M2-Like Macrophage Polarization to Revascularize Ischemic Muscle.* Circulation, 2017. **135**(24): p. 2403-2425.
226. Nair, S., et al., *Irg1 expression in myeloid cells prevents immunopathology during M. tuberculosis infection.* J Exp Med, 2018. **215**(4): p. 1035-1045.
227. Preusse, M., et al., *Infection- and procedure-dependent effects on pulmonary gene expression in the early phase of influenza A virus infection in mice.* BMC Microbiol, 2013. **13**: p. 293.
228. Ackermann, W.W. and V.R. Potter, *Enzyme inhibition in relation to chemotherapy.* Proc Soc Exp Biol Med, 1949. **72**(1): p. 1-9.
229. Bambouskova, M., et al., *Electrophilic properties of itaconate and derivatives regulate the IκBζ-ATF3 inflammatory axis.* Nature, 2018. **556**(7702): p. 501-504.
230. Kobayashi, E.H., et al., *Nrf2 suppresses macrophage inflammatory response by blocking proinflammatory cytokine transcription.* Nature Communications, 2016. **7**(1): p. 11624.
231. Olagnier, D., et al., *Nrf2 negatively regulates STING indicating a link between antiviral sensing and metabolic reprogramming.* Nat Commun, 2018. **9**(1): p. 3506.
232. Naujoks, J., et al., *IFNs Modify the Proteome of Legionella-Containing Vacuoles and Restrict Infection Via IRG1-Derived Itaconic Acid.* PLoS Pathog, 2016. **12**(2): p. e1005408.
233. O'Neill, L.A.J. and M.N. Artyomov, *Itaconate: the poster child of metabolic reprogramming in macrophage function.* Nat Rev Immunol, 2019. **19**(5): p. 273-281.
234. Levonen, A.L., et al., *Redox regulation of antioxidants, autophagy, and the response to stress: implications for electrophile therapeutics.* Free Radic Biol Med, 2014. **71**: p. 196-207.
235. Tsoi, L.C., et al., *Enhanced meta-analysis and replication studies identify five new psoriasis susceptibility loci.* Nature Communications, 2015. **6**(1): p. 7001.
236. Williams, J.O., T.E. Roche, and B.A. McFadden, *Mechanism of action of isocitrate lyase from Pseudomonas indigofera.* Biochemistry, 1971. **10**(8): p. 1384-90.
237. Berg, I.A., L.V. Filatova, and R.N. Ivanovsky, *Inhibition of acetate and propionate assimilation by itaconate via propionyl-CoA carboxylase in isocitrate lyase-negative purple bacterium Rhodospirillum rubrum.* FEMS Microbiology Letters, 2002. **216**(1): p. 49-54.
238. Michelucci, A., et al., *Immune-responsive gene 1 protein links metabolism to immunity by catalyzing itaconic acid production.* Proc Natl Acad Sci U S A, 2013. **110**(19): p. 7820-5.
239. Hammerer, F., et al., *Small Molecule Restores Itaconate Sensitivity in Salmonella enterica: A Potential New Approach to Treating Bacterial Infections.* Chembiochem, 2016. **17**(16): p. 1513-7.
240. Riquelme, S.A., et al., *Pseudomonas aeruginosa Utilizes Host-Derived Itaconate to Redirect Its Metabolism to Promote Biofilm Formation.* Cell Metab, 2020. **31**(6): p. 1091-1106.e6.
241. Rittenhouse, J.W. and B.A. McFadden, *Inhibition of isocitrate lyase from Pseudomonas indigofera by itaconate.* Arch Biochem Biophys, 1974. **163**(1): p. 79-86.
242. Lin, J., et al., *The Emerging Application of Itaconate: Promising Molecular Targets and Therapeutic Opportunities.* Frontiers in Chemistry, 2021. **9**.
243. Daniels, B.P., et al., *The Nucleotide Sensor ZBP1 and Kinase RIPK3 Induce the Enzyme IRG1 to Promote an Antiviral Metabolic State in Neurons.* Immunity, 2019. **50**(1): p. 64-76.e4.
244. Cho, H., et al., *Differential innate immune response programs in neuronal subtypes determine susceptibility to infection in the brain by positive-stranded RNA viruses.* Nat Med, 2013. **19**(4): p. 458-64.
245. Ogger, P.P., et al., *Itaconate controls the severity of pulmonary fibrosis.* Sci Immunol, 2020. **5**(52).
246. Hu, L., F. Kong, and Y. Pan, *Association between IL-17A G197A polymorphism and gastric cancer risk: an updated meta-analysis based on 6,624 cases and 7,631 controls.* Onco Targets Ther, 2018. **11**: p. 703-710.

247. Feng, B., et al., *IL-17A G197A and C1249T polymorphisms in gastric carcinogenesis.* Tumour Biol, 2014. **35**(10): p. 9977-85.
248. Dai, Z.M., et al., *Role of IL-17A rs2275913 and IL-17F rs763780 polymorphisms in risk of cancer development: an updated meta-analysis.* Sci Rep, 2016. **6**: p. 20439.
249. Rafiei, A., et al., *Polymorphism in the interleukin-17A promoter contributes to gastric cancer.* World journal of gastroenterology, 2013. **19**(34): p. 5693-5699.
250. Samiei, G., et al., *Association between polymorphisms of interleukin-17A G197A and interleukin-17F A7488G and risk of colorectal cancer.* J Cancer Res Ther, 2018. **14**(Supplement): p. S299-s305.
251. Yao, Z., et al., *Human IL-17: a novel cytokine derived from T cells.* Journal of immunology (Baltimore, Md. : 1950), 1995. **155**(12): p. 5483-5486.
252. Damsker, J.M., A.M. Hansen, and R.R. Caspi, *Th1 and Th17 cells: adversaries and collaborators.* Ann N Y Acad Sci, 2010. **1183**: p. 211-21.
253. Chang, S.H. and C. Dong, *A novel heterodimeric cytokine consisting of IL-17 and IL-17F regulates inflammatory responses.* Cell Res, 2007. **17**(5): p. 435-40.
254. Grieco, F.A., et al., *IL-17A increases the expression of proinflammatory chemokines in human pancreatic islets.* Diabetologia, 2014. **57**(3): p. 502-511.
255. Bettelli, E., T. Korn, and V.K. Kuchroo, *Th17: the third member of the effector T cell trilogy.* Curr Opin Immunol, 2007. **19**(6): p. 652-7.
256. Gaffen, S.L., *Recent advances in the IL-17 cytokine family.* Curr Opin Immunol, 2011. **23**(5): p. 613-9.
257. Fossiez, F., et al., *T cell interleukin-17 induces stromal cells to produce proinflammatory and hematopoietic cytokines.* J Exp Med, 1996. **183**(6): p. 2593-603.
258. Yao, Z., et al., *Herpesvirus Saimiri encodes a new cytokine, IL-17, which binds to a novel cytokine receptor.* Immunity, 1995. **3**(6): p. 811-21.
259. Chen, K., et al., *IL-17 Receptor Signaling in the Lung Epithelium Is Required for Mucosal Chemokine Gradients and Pulmonary Host Defense against K. pneumoniae.* Cell Host Microbe, 2016. **20**(5): p. 596-605.
260. Li, X., et al., *IL-17 receptor-based signaling and implications for disease.* Nat Immunol, 2019. **20**(12): p. 1594-1602.
261. *IL-17 Family Signaling Pathways*. Available from: https://www.rndsystems.com/pathways/il17-family-signaling-pathways.
262. Ye, P., et al., *Requirement of interleukin 17 receptor signaling for lung CXC chemokine and granulocyte colony-stimulating factor expression, neutrophil recruitment, and host defense.* J Exp Med, 2001. **194**(4): p. 519-27.
263. Huang, W., et al., *Requirement of interleukin-17A for systemic anti-Candida albicans host defense in mice.* J Infect Dis, 2004. **190**(3): p. 624-31.
264. Infante-Duarte, C., et al., *Microbial lipopeptides induce the production of IL-17 in Th cells.* J Immunol, 2000. **165**(11): p. 6107-15.
265. Chung, D.R., et al., *CD4+T Cells Mediate Abscess Formation in Intra-abdominal Sepsis by an IL-17-Dependent Mechanism.* The Journal of Immunology, 2003. **170**(4): p. 1958-1963.
266. Hou, W., et al., *Interleukin-6 (IL-6) and IL-17 synergistically promote viral persistence by inhibiting cellular apoptosis and cytotoxic T cell function.* J Virol, 2014. **88**(15): p. 8479-89.
267. Maek, A.N.W., et al., *Increased interleukin-17 production both in helper T cell subset Th17 and CD4-negative T cells in human immunodeficiency virus infection.* Viral Immunol, 2007. **20**(1): p. 66-75.
268. Molesworth-Kenyon, S.J., et al., *IL-17 receptor signaling influences virus-induced corneal inflammation.* J Leukoc Biol, 2008. **83**(2): p. 401-8.
269. Brand, S., *Crohn's disease: Th1, Th17 or both? The change of a paradigm: new immunological and genetic insights implicate Th17 cells in the pathogenesis of Crohn's disease.* Gut, 2009. **58**(8): p. 1152-67.
270. Komatsu, N., et al., *Pathogenic conversion of Foxp3+ T cells into TH17 cells in autoimmune arthritis.* Nat Med, 2014. **20**(1): p. 62-8.

271. Marinoni, B., et al., *The Th17 axis in psoriatic disease: pathogenetic and therapeutic implications.* Auto Immun Highlights, 2014. **5**(1): p. 9-19.
272. Zhou, T., et al., *Associations between Th17-related inflammatory cytokines and asthma in adults: A Case-Control Study.* Sci Rep, 2017. **7**(1): p. 15502.
273. Steinman, L., *A brief history of T(H)17, the first major revision in the T(H)1/T(H)2 hypothesis of T cell-mediated tissue damage.* Nat Med, 2007. **13**(2): p. 139-45.
274. Nakae, S., et al., *Suppression of immune induction of collagen-induced arthritis in IL-17-deficient mice.* J Immunol, 2003. **171**(11): p. 6173-7.
275. Bush, K.A., et al., *Reduction of joint inflammation and bone erosion in rat adjuvant arthritis by treatment with interleukin-17 receptor IgG1 Fc fusion protein.* Arthritis Rheum, 2002. **46**(3): p. 802-5.
276. Komiyama, Y., et al., *IL-17 plays an important role in the development of experimental autoimmune encephalomyelitis.* J Immunol, 2006. **177**(1): p. 566-73.
277. Happel, K.I., et al., *Divergent roles of IL-23 and IL-12 in host defense against Klebsiella pneumoniae.* J Exp Med, 2005. **202**(6): p. 761-9.
278. Ritchie, N.D., et al., *IL-17 can be protective or deleterious in murine pneumococcal pneumonia.* PLoS Pathog, 2018. **14**(5): p. e1007099.
279. Bayes, H.K., N.D. Ritchie, and T.J. Evans, *Interleukin-17 Is Required for Control of Chronic Lung Infection Caused by Pseudomonas aeruginosa.* Infect Immun, 2016. **84**(12): p. 3507-3516.
280. Robinson, K.M., et al., *Influenza A virus exacerbates Staphylococcus aureus pneumonia in mice by attenuating antimicrobial peptide production.* J Infect Dis, 2014. **209**(6): p. 865-75.
281. Pociask, D.A., et al., *IL-22 is essential for lung epithelial repair following influenza infection.* Am J Pathol, 2013. **182**(4): p. 1286-96.
282. Li, Q., et al., *Blockade of Interleukin-17 Restrains the Development of Acute Lung Injury.* Scand J Immunol, 2016. **83**(3): p. 203-11.
283. Yan, Z., et al., *Rapamycin attenuates acute lung injury induced by LPS through inhibition of Th17 cell proliferation in mice.* Scientific Reports, 2016. **6**(1): p. 20156.
284. Decraene, A., et al., *Elevated expression of both mRNA and protein levels of IL-17A in sputum of stable Cystic Fibrosis patients.* Respir Res, 2010. **11**(1): p. 177.
285. Wilson, M.S., et al., *Bleomycin and IL-1beta-mediated pulmonary fibrosis is IL-17A dependent.* J Exp Med, 2010. **207**(3): p. 535-52.
286. Lee, J., et al., *IL-17E, a novel proinflammatory ligand for the IL-17 receptor homolog IL-17Rh1.* J Biol Chem, 2001. **276**(2): p. 1660-4.
287. Rickel, E.A., et al., *Identification of functional roles for both IL-17RB and IL-17RA in mediating IL-25-induced activities.* J Immunol, 2008. **181**(6): p. 4299-310.
288. Reynolds, J.M., et al., *Interleukin-17B Antagonizes Interleukin-25-Mediated Mucosal Inflammation.* Immunity, 2015. **42**(4): p. 692-703.
289. Iwakura, Y., et al., *Functional specialization of interleukin-17 family members.* Immunity, 2011. **34**(2): p. 149-62.
290. Song, X. and Y. Qian, *IL-17 family cytokines mediated signaling in the pathogenesis of inflammatory diseases.* Cell Signal, 2013. **25**(12): p. 2335-47.
291. Valizadeh, A., et al., *Role of IL-25 in Immunity.* J Clin Diagn Res, 2015. **9**(4): p. Oe01-4.
292. Cheng, D., et al., *Epithelial interleukin-25 is a key mediator in Th2-high, corticosteroid-responsive asthma.* Am J Respir Crit Care Med, 2014. **190**(6): p. 639-48.
293. Morita, H., et al., *IL-25 and IL-33 Contribute to Development of Eosinophilic Airway Inflammation in Epicutaneously Antigen-Sensitized Mice.* PLOS ONE, 2015. **10**(7): p. e0134226.
294. Angkasekwinai, P., et al., *Interleukin 25 promotes the initiation of proallergic type 2 responses.* J Exp Med, 2007. **204**(7): p. 1509-17.
295. Kouzaki, H., et al., *Transcription of interleukin-25 and extracellular release of the protein is regulated by allergen proteases in airway epithelial cells.* Am J Respir Cell Mol Biol, 2013. **49**(5): p. 741-50.
296. Corrigan, C.J., et al., *Allergen-induced expression of IL-25 and IL-25 receptor in atopic asthmatic airways and late-phase cutaneous responses.* J Allergy Clin Immunol, 2011. **128**(1): p. 116-24.

297. Wang, Y.H., et al., *IL-25 augments type 2 immune responses by enhancing the expansion and functions of TSLP-DC-activated Th2 memory cells.* J Exp Med, 2007. **204**(8): p. 1837-47.
298. Fort, M.M., et al., *IL-25 induces IL-4, IL-5, and IL-13 and Th2-associated pathologies in vivo.* Immunity, 2001. **15**(6): p. 985-95.
299. Hams, E., et al., *IL-25 and type 2 innate lymphoid cells induce pulmonary fibrosis.* Proc Natl Acad Sci U S A, 2014. **111**(1): p. 367-72.
300. *IL17A Gene - Interleukin 17A*. Available from: https://www.genecards.org/cgi-bin/carddisp.pl?gene=IL17A.
301. Liu, X.K., X. Lin, and S.L. Gaffen, *Crucial role for nuclear factor of activated T cells in T cell receptor-mediated regulation of human interleukin-17.* J Biol Chem, 2004. **279**(50): p. 52762-71.
302. Zacarias, J.M., et al., *The Influence of Interleukin 17A and IL17F Polymorphisms on Chronic Periodontitis Disease in Brazilian Patients.* Mediators Inflamm, 2015. **2015**: p. 147056.
303. Ge, J., et al., *IL-17A G197A gene polymorphism contributes to susceptibility for liver cirrhosis development from patients with chronic hepatitis B infection in Chinese population.* Int J Clin Exp Med, 2015. **8**(6): p. 9793-8.
304. Lee, S.Y., et al., *Interleukin-17 increases the expression of Toll-like receptor 3 via the STAT3 pathway in rheumatoid arthritis fibroblast-like synoviocytes.* Immunology, 2014. **141**(3): p. 353-61.
305. Liu, S., et al., *IL-17A synergistically enhances TLR3-mediated IL-36γ production by keratinocytes: A potential role in injury-amplified psoriatic inflammation.* Exp Dermatol, 2019. **28**(3): p. 233-239.
306. Xu, W.L., et al., *[The Relationship of Polymorphisms in Interleukin 17A Gene, Interleukin 17F Gene and the Pulmonary Inflammation Risk in Dust Exposed Workers in a Chinese Population].* Sichuan Da Xue Xue Bao Yi Xue Ban, 2017. **48**(1): p. 86-90.
307. Zhai, C., et al., *Association of interleukin-17a rs2275913 gene polymorphism and asthma risk: a meta-analysis.* Arch Med Sci, 2018. **14**(6): p. 1204-1211.
308. Al Obeed, O.A., et al., *IL-17 and colorectal cancer risk in the Middle East: gene polymorphisms and expression.* Cancer Manag Res, 2018. **10**: p. 2653-2661.
309. Omrane, I., et al., *Significant association between interleukin-17A polymorphism and colorectal cancer.* Tumour Biol, 2014. **35**(7): p. 6627-32.
310. MA, E.L., G. Abd El Fatah, and H. Zaghla, *IL17A gene polymorphism, serum IL17 and total IgE in Egyptian population with chronic HCV and hepatocellular carcinoma.* Immunol Lett, 2015. **168**(2): p. 240-5.
311. Han, L., et al., *Association of IL-17A and IL-17F single nucleotide polymorphisms with susceptibility to osteoarthritis in a Korean population.* Gene, 2014. **533**(1): p. 119-22.
312. Ghaznavi, H. and M.S. Soltanpour, *Association study between rs2275913 genetic polymorphism and serum levels of IL-17A with risk of coronary artery disease.* Mol Biol Res Commun, 2020. **9**(1): p. 35-40.
313. Gueiros, L.A., et al., *IL17A polymorphism and elevated IL17A serum levels are associated with oral lichen planus.* Oral Dis, 2018. **24**(3): p. 377-383.
314. Corrêa, J.D., et al., *Brain-derived neurotrophic factor in chronic periodontitis.* Mediators Inflamm, 2014. **2014**: p. 373765.
315. Hejr, S., et al., *Association of IL-17, IL-21, and IL-23R gene polymorphisms with HBV infection in kidney transplant patients.* Viral Immunol, 2013. **26**(3): p. 201-6.
316. Aquino, J.S., et al., *IL8 and IL17A polymorphisms associated with multibacillary leprosy and reaction type 1 in a mixed population from southern Brazil.* Ann Hum Genet, 2019. **83**(2): p. 110-114.
317. Reis, P.G., et al., *Genetic Polymorphisms ofIL17and Chagas Disease in the South and Southeast of Brazil.* Journal of Immunology Research, 2017. **2017**: p. 1-7.
318. Arisawa, T., et al., *The influence of polymorphisms of interleukin-17A and interleukin-17F genes on the susceptibility to ulcerative colitis.* J Clin Immunol, 2008. **28**(1): p. 44-9.

319. Zhang, X., et al., *Genetic polymorphisms of interleukin 17A and interleukin 17F and their association with inflammatory bowel disease in a Chinese Han population.* Inflamm Res, 2013. **62**(8): p. 743-50.
320. Wang, J., et al., *Association of IL-17A and IL-17F gene polymorphisms with chronic hepatitis B and hepatitis B virus-related liver cirrhosis in a Chinese population: A case-control study.* Clin Res Hepatol Gastroenterol, 2016. **40**(3): p. 288-296.
321. Sun, B., et al., *The interleukin-17 G-197A polymorphism is associated with cyclosporine metabolism and transplant rejection in liver transplant recipients.* Pharmacogenomics, 2019. **20**(6): p. 447-456.
322. Klein, S.L. and K.L. Flanagan, *Sex differences in immune responses.* Nat Rev Immunol, 2016. **16**(10): p. 626-38.
323. Pisitkun, P., et al., *Autoreactive B cell responses to RNA-related antigens due to TLR7 gene duplication.* Science, 2006. **312**(5780): p. 1669-72.
324. Berghöfer, B., et al., *TLR7 ligands induce higher IFN-alpha production in females.* J Immunol, 2006. **177**(4): p. 2088-96.
325. Griesbeck, M., et al., *Sex Differences in Plasmacytoid Dendritic Cell Levels of IRF5 Drive Higher IFN-α Production in Women.* J Immunol, 2015. **195**(11): p. 5327-36.
326. Klein, S.L., A. Jedlicka, and A. Pekosz, *The Xs and Y of immune responses to viral vaccines.* Lancet Infect Dis, 2010. **10**(5): p. 338-49.
327. Hannah, M.F., V.B. Bajic, and S.L. Klein, *Sex differences in the recognition of and innate antiviral responses to Seoul virus in Norway rats.* Brain Behav Immun, 2008. **22**(4): p. 503-16.
328. Torcia, M.G., et al., *Sex differences in the response to viral infections: TLR8 and TLR9 ligand stimulation induce higher IL10 production in males.* PLoS One, 2012. **7**(6): p. e39853.
329. Moxley, G., et al., *Sexual dimorphism in innate immunity.* Arthritis Rheum, 2002. **46**(1): p. 250-8.
330. Asai, K., et al., *GENDER DIFFERENCES IN CYTOKINE SECRETION BY HUMAN PERIPHERAL BLOOD MONONUCLEAR CELLS: ROLE OF ESTROGEN IN MODULATING LPS-INDUCED CYTOKINE SECRETION IN AN EX VIVO SEPTIC MODEL.* Shock, 2001. **16**(5).
331. Rettew, J.A., Y.M. Huet-Hudson, and I. Marriott, *Testosterone reduces macrophage expression in the mouse of toll-like receptor 4, a trigger for inflammation and innate immunity.* Biol Reprod, 2008. **78**(3): p. 432-7.
332. Lesmeister, M.J., et al., *17beta-estradiol suppresses TLR3-induced cytokine and chemokine production in endometrial epithelial cells.* Reproductive Biology and Endocrinology, 2005. **3**(1): p. 74.
333. Svenson, J., et al., *Estrogen receptor alpha modulates mesangial cell responses to toll-like receptor ligands.* Am J Med Sci, 2014. **348**(6): p. 492-500.
334. Zandieh, Z., et al., *Sex hormones alter the response of Toll-like receptor 3 to its specific ligand in fallopian tube epithelial cells.* Clin Exp Reprod Med, 2018. **45**(4): p. 154-162.
335. Gambara, G., et al., *TLR3 engagement induces IRF-3-dependent apoptosis in androgen-sensitive prostate cancer cells and inhibits tumour growth in vivo.* J Cell Mol Med, 2015. **19**(2): p. 327-39.
336. Carey, M.A., et al., *The impact of sex and sex hormones on lung physiology and disease: lessons from animal studies.* Am J Physiol Lung Cell Mol Physiol, 2007. **293**(2): p. L272-8.
337. Han, M.K., et al., *Female Sex and Gender in Lung/Sleep Health and Disease. Increased Understanding of Basic Biological, Pathophysiological, and Behavioral Mechanisms Leading to Better Health for Female Patients with Lung Disease.* Am J Respir Crit Care Med, 2018. **198**(7): p. 850-858.
338. Tsiligianni, I., et al., *Call to action: improving primary care for women with COPD.* NPJ Prim Care Respir Med, 2017. **27**(1): p. 11.
339. Isla, D., et al., *A consensus statement on the gender perspective in lung cancer.* Clin Transl Oncol, 2017. **19**(5): p. 527-535.
340. Gleicher, N. and D.H. Barad, *Gender as risk factor for autoimmune diseases.* J Autoimmun, 2007. **28**(1): p. 1-6.

341. Humbert, M., et al., *Survival in patients with idiopathic, familial, and anorexigen-associated pulmonary arterial hypertension in the modern management era.* Circulation, 2010. **122**(2): p. 156-63.
342. Silveyra, P., N. Fuentes, and D.E. Rodriguez Bauza, *Sex and Gender Differences in Lung Disease.* Adv Exp Med Biol, 2021. **1304**: p. 227-258.
343. Hemnes, A.R., *Gender, Sex Hormones and Respiratory Disease: A Comprehensive Guide*. 2015: Springer.
344. Kim, H.K., et al., *Induction of RANTES and CCR5 through NF-kappaB activation via MAPK pathway in aged rat gingival tissues.* Biotechnol Lett, 2006. **28**(1): p. 17-23.
345. Elliot, S., et al., *MicroRNA let-7 Downregulates Ligand-Independent Estrogen Receptor-mediated Male-Predominant Pulmonary Fibrosis.* Am J Respir Crit Care Med, 2019. **200**(10): p. 1246-1257.
346. Gupta, N., et al., *Lymphangioleiomyomatosis Diagnosis and Management: High-Resolution Chest Computed Tomography, Transbronchial Lung Biopsy, and Pleural Disease Management. An Official American Thoracic Society/Japanese Respiratory Society Clinical Practice Guideline.* Am J Respir Crit Care Med, 2017. **196**(10): p. 1337-1348.
347. Gharaee-Kermani, M., et al., *Gender-based differences in bleomycin-induced pulmonary fibrosis.* Am J Pathol, 2005. **166**(6): p. 1593-606.
348. Ley, B., et al., *A multidimensional index and staging system for idiopathic pulmonary fibrosis.* Ann Intern Med, 2012. **156**(10): p. 684-91.
349. Kalafatis, D., et al., *Gender differences at presentation of idiopathic pulmonary fibrosis in Sweden.* BMC Pulmonary Medicine, 2019. **19**(1).
350. Zaman, T., et al., *Differences in Clinical Characteristics and Outcomes Between Men and Women With Idiopathic Pulmonary Fibrosis: A Multicenter Retrospective Cohort Study.* Chest, 2020. **158**(1): p. 245-251.
351. Sesé, L., et al., *Gender Differences in Idiopathic Pulmonary Fibrosis: Are Men and Women Equal?* Front Med (Lausanne), 2021. **8**: p. 713698.
352. Caminati, A., et al., *The natural history of idiopathic pulmonary fibrosis in a large European population: the role of age, sex and comorbidities.* Intern Emerg Med, 2021. **16**(7): p. 1793-1802.
353. Palomäki, A., et al., *Lifetime risk of rheumatoid arthritis-associated interstitial lung disease in MUC5B mutation carriers.* Ann Rheum Dis, 2021. **80**(12): p. 1530-1536.
354. Yang, I.V., et al., *MUC5B and Idiopathic Pulmonary Fibrosis.* Ann Am Thorac Soc, 2015. **12 Suppl 2**(Suppl 2): p. S193-9.
355. Qi, S., et al., *Sex differences in the immune response to acute COVID-19 respiratory tract infection.* Biology of Sex Differences, 2021. **12**(1).
356. Gómez, J., et al., *Angiotensin-converting enzymes (ACE, ACE2) gene variants and COVID-19 outcome.* Gene, 2020. **762**: p. 145102.
357. Gagliardi, M.C., et al., *ACE2 expression and sex disparity in COVID-19.* Cell Death Discov, 2020. **6**: p. 37.
358. Xie, X., et al., *Age- and gender-related difference of ACE2 expression in rat lung.* Life Sci, 2006. **78**(19): p. 2166-71.
359. Bukowska, A., et al., *Protective regulation of the ACE2/ACE gene expression by estrogen in human atrial tissue from elderly men.* Exp Biol Med (Maywood), 2017. **242**(14): p. 1412-1423.
360. Channappanavar, R., et al., *Sex-Based Differences in Susceptibility to Severe Acute Respiratory Syndrome Coronavirus Infection.* J Immunol, 2017. **198**(10): p. 4046-4053.
361. Aloufi, N., et al., *Angiotensin-converting enzyme 2 expression in COPD and IPF fibroblasts: the forgotten cell in COVID-19.* Am J Physiol Lung Cell Mol Physiol, 2021. **320**(1): p. L152-l157.
362. Okwan-Duodu, D., et al., *TMPRSS2 activity may mediate sex differences in COVID-19 severity.* Signal Transduction and Targeted Therapy, 2021. **6**(1).
363. Hoffmann, M., et al., *SARS-CoV-2 Cell Entry Depends on ACE2 and TMPRSS2 and Is Blocked by a Clinically Proven Protease Inhibitor.* Cell, 2020. **181**(2): p. 271-280.e8.
364. Asselta, R., et al., *ACE2 and TMPRSS2 variants and expression as candidates to sex and country differences in COVID-19 severity in Italy.* Aging (Albany NY), 2020. **12**(11): p. 10087-10098.

365. Li, H.H., et al., *Upregulation of ACE2 and TMPRSS2 by particulate matter and idiopathic pulmonary fibrosis: a potential role in severe COVID-19.* Part Fibre Toxicol, 2021. **18**(1): p. 11.
366. McElroy, A.N., et al., *Candidate Role for Toll-like Receptor 3 L412F Polymorphism and Infection in Acute Exacerbation of Idiopathic Pulmonary Fibrosis.* American journal of respiratory and critical care medicine, 2022. **205**(5): p. 550-562.
367. Alexopoulou, L., et al., *Recognition of double-stranded RNA and activation of NF-kappaB by Toll-like receptor 3.* Nature, 2001. **413**(6857): p. 732-8.
368. Spelmink, L., et al., *Toll-Like Receptor 3/TRIF-Dependent IL-12p70 Secretion Mediated by Streptococcus pneumoniae RNA and Its Priming by Influenza A Virus Coinfection in Human Dendritic Cells.* mBio, 2016. **7**(2): p. e00168-16.
369. Aksoy, E., et al., *Double-stranded RNAs from the helminth parasite Schistosoma activate TLR3 in dendritic cells.* The Journal of biological chemistry, 2005. **280**(1): p. 277-283.
370. Sohail, A., et al., *Itaconate and derivatives reduce interferon responses and inflammation in influenza A virus infection.* PLOS Pathogens, 2022. **18**(1): p. e1010219.
371. Daniels, B.P., et al., *RIPK3 Restricts Viral Pathogenesis via Cell Death-Independent Neuroinflammation.* Cell, 2017. **169**(2): p. 301-313.e11.
372. Cavassani, K.A., et al., *TLR3 is an endogenous sensor of tissue necrosis during acute inflammatory events.* J Exp Med, 2008. **205**(11): p. 2609-21.
373. Honda, K. and T. Taniguchi, *IRFs: master regulators of signalling by Toll-like receptors and cytosolic pattern-recognition receptors.* Nat Rev Immunol, 2006. **6**(9): p. 644-58.
374. Kagan, J.C. and R. Medzhitov, *Phosphoinositide-mediated adaptor recruitment controls Toll-like receptor signaling.* Cell, 2006. **125**(5): p. 943-55.
375. Pantelidis, P., et al., *Analysis of tumor necrosis factor-alpha, lymphotoxin-alpha, tumor necrosis factor receptor II, and interleukin-6 polymorphisms in patients with idiopathic pulmonary fibrosis.* Am J Respir Crit Care Med, 2001. **163**(6): p. 1432-6.
376. Papiris, S.A., et al., *High levels of IL-6 and IL-8 characterize early-on idiopathic pulmonary fibrosis acute exacerbations.* Cytokine, 2018. **102**: p. 168-172.
377. Karikó, K., et al., *mRNA is an endogenous ligand for Toll-like receptor 3.* J Biol Chem, 2004. **279**(13): p. 12542-50.
378. Kolb, M., et al., *Transient expression of IL-1beta induces acute lung injury and chronic repair leading to pulmonary fibrosis.* J Clin Invest, 2001. **107**(12): p. 1529-36.
379. Doyle, S., et al., *IRF3 mediates a TLR3/TLR4-specific antiviral gene program.* Immunity, 2002. **17**(3): p. 251-63.
380. Matsumoto, M. and T. Seya, *TLR3: interferon induction by double-stranded RNA including poly(I:C).* Adv Drug Deliv Rev, 2008. **60**(7): p. 805-12.
381. Lin, R., et al., *Essential role of interferon regulatory factor 3 in direct activation of RANTES chemokine transcription.* Mol Cell Biol, 1999. **19**(2): p. 959-66.
382. Cheresh, P., et al., *Oxidative stress and pulmonary fibrosis.* Biochim Biophys Acta, 2013. **1832**(7): p. 1028-40.
383. He, C., et al., *Mitochondrial Cu,Zn-superoxide dismutase mediates pulmonary fibrosis by augmenting H2O2 generation.* J Biol Chem, 2011. **286**(17): p. 15597-607.
384. Kliment, C.R. and T.D. Oury, *Oxidative stress, extracellular matrix targets, and idiopathic pulmonary fibrosis.* Free Radic Biol Med, 2010. **49**(5): p. 707-17.
385. Osborn-Heaford, H.L., et al., *Mitochondrial Rac1 GTPase import and electron transfer from cytochrome c are required for pulmonary fibrosis.* J Biol Chem, 2012. **287**(5): p. 3301-12.
386. Cho, H.-Y., S. Reddy, and S. Kleeberger, *Nrf2 Defends the Lung from Oxidative Stress.* Antioxidants & redox signaling, 2006. **8**: p. 76-87.
387. Liu, Q., Y. Gao, and X. Ci, *Role of Nrf2 and Its Activators in Respiratory Diseases.* Oxid Med Cell Longev, 2019. **2019**: p. 7090534.
388. Fernandez, I.E. and O. Eickelberg, *The impact of TGF-β on lung fibrosis: from targeting to biomarkers.* Proc Am Thorac Soc, 2012. **9**(3): p. 111-6.
389. Tatler, A.L. and G. Jenkins, *TGF-β activation and lung fibrosis.* Proc Am Thorac Soc, 2012. **9**(3): p. 130-6.

390. Sun, K.H., et al., *α-Smooth muscle actin is an inconsistent marker of fibroblasts responsible for force-dependent TGFβ activation or collagen production across multiple models of organ fibrosis.* Am J Physiol Lung Cell Mol Physiol, 2016. **310**(9): p. L824-36.
391. Holm Nielsen, S., et al., *Serological Assessment of Activated Fibroblasts by alpha-Smooth Muscle Actin (α-SMA): A Noninvasive Biomarker of Activated Fibroblasts in Lung Disorders.* Transl Oncol, 2019. **12**(2): p. 368-374.
392. Johnson, A.G., *Molecular adjuvants and immunomodulators: new approaches to immunization.* Clin Microbiol Rev, 1994. **7**(3): p. 277-89.
393. Yao, C., et al., *Toll-like receptor family members in skin fibroblasts are functional and have a higher expression compared to skin keratinocytes.* Int J Mol Med, 2015. **35**(5): p. 1443-50.
394. Okayasu, K., et al., *RANTES expression induced by Toll-like receptor 4 ligand in rat airway smooth muscle cells.* J Med Dent Sci, 2010. **57**(4): p. 193-201.
395. Wang, J., et al., *Toll-like receptors expressed by dermal fibroblasts contribute to hypertrophic scarring.* Journal of Cellular Physiology, 2011. **226**(5): p. 1265-1273.
396. Horváth, I., et al., *Raised levels of exhaled carbon monoxide are associated with an increased expression of heme oxygenase-1 in airway macrophages in asthma: a new marker of oxidative stress.* Thorax, 1998. **53**(8): p. 668-72.
397. Yamada, N., et al., *Microsatellite polymorphism in the heme oxygenase-1 gene promoter is associated with susceptibility to emphysema.* Am J Hum Genet, 2000. **66**(1): p. 187-95.
398. Lee, P.J., et al., *Overexpression of heme oxygenase-1 in human pulmonary epithelial cells results in cell growth arrest and increased resistance to hyperoxia.* Proc Natl Acad Sci U S A, 1996. **93**(19): p. 10393-8.
399. Kodama, N., et al., *Expression of RANTES by bronchoalveolar lavage cells in nonsmoking patients with interstitial lung diseases.* Am J Respir Cell Mol Biol, 1998. **18**(4): p. 526-31.
400. Liao, S.T., et al., *4-Octyl itaconate inhibits aerobic glycolysis by targeting GAPDH to exert anti-inflammatory effects.* Nat Commun, 2019. **10**(1): p. 5091.
401. Dickson, R.P., J.R. Erb-Downward, and G.B. Huffnagle, *The role of the bacterial microbiome in lung disease.* Expert Rev Respir Med, 2013. **7**(3): p. 245-57.
402. Kiley, J.P. and E.V. Caler, *The lung microbiome. A new frontier in pulmonary medicine.* Ann Am Thorac Soc, 2014. **11 Suppl 1**(Suppl 1): p. S66-70.
403. Molyneaux, P.L. and T.M. Maher, *Respiratory microbiome in IPF: cause, effect, or biomarker?* Lancet Respir Med, 2014. **2**(7): p. 511-3.
404. Lorenz, M.C. and G.R. Fink, *Life and death in a macrophage: role of the glyoxylate cycle in virulence.* Eukaryot Cell, 2002. **1**(5): p. 657-62.
405. Mai, C., et al., *Thin-Section CT Features of Idiopathic Pulmonary Fibrosis Correlated with Micro-CT and Histologic Analysis.* Radiology, 2017. **283**(1): p. 252-263.
406. Peace, C.G. and L.A. O'Neill, *The role of itaconate in host defense and inflammation.* J Clin Invest, 2022. **132**(2).
407. *IPF: Statistics, Facts, and You*. 2022; Available from: https://www.healthline.com/health/managing-idiopathic-pulmonary-fibrosis/ipf-facts.
408. Mukaida, N., M. Shiroo, and K. Matsushima, *Genomic structure of the human monocyte-derived neutrophil chemotactic factor IL-8.* J Immunol, 1989. **143**(4): p. 1366-71.
409. Thiel, G., et al., *Resveratrol stimulation induces interleukin-8 gene transcription via NF-κB.* Pharmacol Res, 2018. **134**: p. 238-245.
410. Liu, T., et al., *NF-κB signaling in inflammation.* Signal Transduct Target Ther, 2017. **2**: p. 17023-.
411. Ley, B., H.R. Collard, and T.E. King, Jr., *Clinical course and prediction of survival in idiopathic pulmonary fibrosis.* Am J Respir Crit Care Med, 2011. **183**(4): p. 431-40.
412. Ziegenhagen, M.W., et al., *Serum Level of Interleukin 8 Is Elevated in Idiopathic Pulmonary Fibrosis and Indicates Disease Activity.* American journal of respiratory and critical care medicine, 1998. **157**: p. 762-8.
413. Yang, L., et al., *IL-8 mediates idiopathic pulmonary fibrosis mesenchymal progenitor cell fibrogenicity.* Am J Physiol Lung Cell Mol Physiol, 2018. **314**(1): p. L127-l136.

414. Guiot, J., et al., *Sputum biomarkers in IPF: Evidence for raised gene expression and protein level of IGFBP-2, IL-8 and MMP-7.* PLoS One, 2017. **12**(2): p. e0171344.
415. Zhang, Q., et al., *4-octyl Itaconate inhibits lipopolysaccharide (LPS)-induced osteoarthritis via activating Nrf2 signalling pathway.* Journal of Cellular and Molecular Medicine, 2022. **26**(5): p. 1515-1529.
416. He, R., et al., *Itaconate inhibits ferroptosis of macrophage via Nrf2 pathways against sepsis-induced acute lung injury.* Cell Death Discov, 2022. **8**(1): p. 43.
417. Epstein Shochet, G., et al., *TGF-β pathway activation by idiopathic pulmonary fibrosis (IPF) fibroblast derived soluble factors is mediated by IL-6 trans-signaling.* Respiratory Research, 2020. **21**(1).
418. Weng, D., et al., *The Role of Infection in Acute Exacerbation of Idiopathic Pulmonary Fibrosis.* Mediators Inflamm, 2019. **2019**: p. 5160694.
419. Hoshino, T., et al., *Role of proinflammatory cytokines IL-18 and IL-1beta in bleomycin-induced lung injury in humans and mice.* Am J Respir Cell Mol Biol, 2009. **41**(6): p. 661-70.
420. Carré, P.C., et al., *Increased expression of the interleukin-8 gene by alveolar macrophages in idiopathic pulmonary fibrosis. A potential mechanism for the recruitment and activation of neutrophils in lung fibrosis.* J Clin Invest, 1991. **88**(6): p. 1802-10.
421. Naik, P.K. and B.B. Moore, *Viral infection and aging as cofactors for the development of pulmonary fibrosis.* Expert Rev Respir Med, 2010. **4**(6): p. 759-71.
422. Kottmann, R.M., et al., *Determinants of initiation and progression of idiopathic pulmonary fibrosis.* Respirology, 2009. **14**(7): p. 917-33.
423. Vannella, K.M. and B.B. Moore, *Viruses as co-factors for the initiation or exacerbation of lung fibrosis.* Fibrogenesis & Tissue Repair, 2008. **1**(1): p. 2.
424. Bergeron, A., et al., *Cytokine profiles in idiopathic pulmonary fibrosis suggest an important role for TGF-beta and IL-10.* Eur Respir J, 2003. **22**(1): p. 69-76.
425. Tomos, I., et al., *IL-6 and IL-8 in stable and exacerbated IPF patients and their association to outcome.* European Respiratory Journal, 2016. **48**(suppl 60): p. PA3890.
426. Kawai, T. and S. Akira, *Signaling to NF-kappaB by Toll-like receptors.* Trends Mol Med, 2007. **13**(11): p. 460-9.
427. Yamamoto, M., et al., *Essential role for TIRAP in activation of the signalling cascade shared by TLR2 and TLR4.* Nature, 2002. **420**(6913): p. 324-9.
428. Tanimura, N., et al., *Roles for LPS-dependent interaction and relocation of TLR4 and TRAM in TRIF-signaling.* Biochem Biophys Res Commun, 2008. **368**(1): p. 94-9.
429. Kagan, J.C., et al., *TRAM couples endocytosis of Toll-like receptor 4 to the induction of interferon-beta.* Nat Immunol, 2008. **9**(4): p. 361-8.
430. Monroe, K.M., S.M. McWhirter, and R.E. Vance, *Identification of host cytosolic sensors and bacterial factors regulating the type I interferon response to Legionella pneumophila.* PLoS Pathog, 2009. **5**(11): p. e1000665.
431. Dixit, E. and J.C. Kagan, *Intracellular pathogen detection by RIG-I-like receptors.* Adv Immunol, 2013. **117**: p. 99-125.
432. Stanley, S.A., et al., *The Type I IFN response to infection with Mycobacterium tuberculosis requires ESX-1-mediated secretion and contributes to pathogenesis.* J Immunol, 2007. **178**(5): p. 3143-52.
433. Decker, T., M. Müller, and S. Stockinger, *The yin and yang of type I interferon activity in bacterial infection.* Nat Rev Immunol, 2005. **5**(9): p. 675-87.
434. King, T.E., Jr., et al., *Predicting survival in idiopathic pulmonary fibrosis: scoring system and survival model.* Am J Respir Crit Care Med, 2001. **164**(7): p. 1171-81.
435. Baughman, R.P., et al., *Use of the protected specimen brush in patients with endotracheal or tracheostomy tubes.* Chest, 1987. **91 2**: p. 233-6.
436. Monsó, E., et al., *Bacterial infection in chronic obstructive pulmonary disease. A study of stable and exacerbated outpatients using the protected specimen brush.* Am J Respir Crit Care Med, 1995. **152**(4 Pt 1): p. 1316-20.
437. Erb-Downward, J.R., et al., *Analysis of the Lung Microbiome in the "Healthy" Smoker and in COPD.* PLoS ONE, 2011. **6**(2): p. e16384.

438. Goddard, A.F., et al., *Direct sampling of cystic fibrosis lungs indicates that DNA-based analyses of upper-airway specimens can misrepresent lung microbiota.* Proceedings of the National Academy of Sciences, 2012. **109**(34): p. 13769-13774.
439. Rudkjøbing, V.B., et al., *True microbiota involved in chronic lung infection of cystic fibrosis patients found by culturing and 16S rRNA gene analysis.* J Clin Microbiol, 2011. **49**(12): p. 4352-5.
440. Cabrera-Rubio, R., et al., *Microbiome diversity in the bronchial tracts of patients with chronic obstructive pulmonary disease.* J Clin Microbiol, 2012. **50**(11): p. 3562-8.
441. Nakamoto, K., et al., *Pseudomonas aeruginosa-derived flagellin stimulates IL-6 and IL-8 production in human bronchial epithelial cells: A potential mechanism for progression and exacerbation of COPD.* Exp Lung Res, 2019. **45**(8): p. 255-266.
442. Azghani, A.O., et al., *Mechanism of fibroblast inflammatory responses to Pseudomonas aeruginosa elastase.* Microbiology (Reading), 2014. **160**(Pt 3): p. 547-555.
443. Sun, J., et al., *The Pseudomonas aeruginosa protease LasB directly activates IL-1β.* EBioMedicine, 2020. **60**: p. 102984.
444. Frendéus, B., et al., *Escherichia coli P fimbriae utilize the Toll-like receptor 4 pathway for cell activation.* Mol Microbiol, 2001. **40**(1): p. 37-51.
445. Pylaeva, E., et al., *Detrimental Effect of Type I IFNs During Acute Lung Infection With Pseudomonas aeruginosa Is Mediated Through the Stimulation of Neutrophil NETosis.* Front Immunol, 2019. **10**: p. 2190.
446. Carrigan, S.O., et al., *IFN Regulatory Factor 3 Contributes to the Host Response duringPseudomonas aeruginosaLung Infection in Mice.* The Journal of Immunology, 2010. **185**(6): p. 3602-3609.
447. Riquelme, S.A., et al., *CFTR-PTEN-dependent mitochondrial metabolic dysfunction promotes Pseudomonas aeruginosa airway infection.* Sci Transl Med, 2019. **11**(499).
448. Gaffen, S.L., et al., *The IL-23-IL-17 immune axis: from mechanisms to therapeutic testing.* Nat Rev Immunol, 2014. **14**(9): p. 585-600.
449. Choe, J., M.S. Kelker, and I.A. Wilson, *Crystal structure of human toll-like receptor 3 (TLR3) ectodomain.* Science, 2005. **309**(5734): p. 581-5.
450. Hou, W., H.S. Kang, and B.S. Kim, *Th17 cells enhance viral persistence and inhibit T cell cytotoxicity in a model of chronic virus infection.* J Exp Med, 2009. **206**(2): p. 313-28.
451. Espinoza, J.L., et al., *A genetic variant in the IL-17 promoter is functionally associated with acute graft-versus-host disease after unrelated bone marrow transplantation.* PLoS One, 2011. **6**(10): p. e26229.
452. Tiringer, K., et al., *A Th17- and Th2-skewed cytokine profile in cystic fibrosis lungs represents a potential risk factor for Pseudomonas aeruginosa infection.* Am J Respir Crit Care Med, 2013. **187**(6): p. 621-9.
453. Zhang, J., et al., *Profibrotic effect of IL-17A and elevated IL-17RA in idiopathic pulmonary fibrosis and rheumatoid arthritis-associated lung disease support a direct role for IL-17A/IL-17RA in human fibrotic interstitial lung disease.* Am J Physiol Lung Cell Mol Physiol, 2019. **316**(3): p. L487-l497.
454. Omagari, D., et al., *Nuclear factor kappa B plays a pivotal role in polyinosinic-polycytidylic acid-induced expression of human β-defensin 2 in intestinal epithelial cells.* Clin Exp Immunol, 2011. **165**(1): p. 85-93.
455. Reimer, T., et al., *poly(I:C) and LPS induce distinct IRF3 and NF-kappaB signaling during type-I IFN and TNF responses in human macrophages.* J Leukoc Biol, 2008. **83**(5): p. 1249-57.
456. Neupane, B., et al., *Interleukin-17A Facilitates Chikungunya Virus Infection by Inhibiting IFN-α2 Expression.* Front Immunol, 2020. **11**: p. 588382.
457. Henry, T., et al., *Type I IFN signaling constrains IL-17A/F secretion by gammadelta T cells during bacterial infections.* J Immunol, 2010. **184**(7): p. 3755-67.
458. Chattopadhyay, S. and G.C. Sen, *dsRNA-activation of TLR3 and RLR signaling: gene induction-dependent and independent effects.* J Interferon Cytokine Res, 2014. **34**(6): p. 427-36.
459. Rehwinkel, J. and M.U. Gack, *RIG-I-like receptors: their regulation and roles in RNA sensing.* Nature Reviews Immunology, 2020. **20**(9): p. 537-551.

460. Yoneyama, M., et al., *The RNA helicase RIG-I has an essential function in double-stranded RNA-induced innate antiviral responses.* Nat Immunol, 2004. **5**(7): p. 730-7.
461. Kawai, T., et al., *IPS-1, an adaptor triggering RIG-I- and Mda5-mediated type I interferon induction.* Nat Immunol, 2005. **6**(10): p. 981-8.
462. Meylan, E., et al., *Cardif is an adaptor protein in the RIG-I antiviral pathway and is targeted by hepatitis C virus.* Nature, 2005. **437**(7062): p. 1167-72.
463. Seth, R.B., et al., *Identification and characterization of MAVS, a mitochondrial antiviral signaling protein that activates NF-kappaB and IRF 3.* Cell, 2005. **122**(5): p. 669-82.
464. Xu, L.G., et al., *VISA is an adapter protein required for virus-triggered IFN-beta signaling.* Mol Cell, 2005. **19**(6): p. 727-40.
465. Muri, J., et al., *Electrophilic Nrf2 activators and itaconate inhibit inflammation at low dose and promote IL-1β production and inflammatory apoptosis at high dose.* Redox Biol, 2020. **36**: p. 101647.
466. Chaudhary, P.M., et al., *Activation of the NF-kappaB pathway by caspase 8 and its homologs.* Oncogene, 2000. **19**(39): p. 4451-60.
467. Tekamp-Olson, P., et al., *Cloning and characterization of cDNAs for murine macrophage inflammatory protein 2 and its human homologues.* J Exp Med, 1990. **172**(3): p. 911-9.
468. Manjavachi, M.N., et al., *The role of keratinocyte-derived chemokine (KC) on hyperalgesia caused by peripheral nerve injury in mice.* Neuropharmacology, 2014. **79**: p. 17-27.
469. Ohmori, Y., S. Fukumoto, and T.A. Hamilton, *Two structurally distinct kappa B sequence motifs cooperatively control LPS-induced KC gene transcription in mouse macrophages.* J Immunol, 1995. **155**(7): p. 3593-600.
470. Son, Y.H., et al., *Roles of MAPK and NF-kappaB in interleukin-6 induction by lipopolysaccharide in vascular smooth muscle cells.* J Cardiovasc Pharmacol, 2008. **51**(1): p. 71-7.
471. Hiscott, J., et al., *Characterization of a functional NF-kappa B site in the human interleukin 1 beta promoter: evidence for a positive autoregulatory loop.* Mol Cell Biol, 1993. **13**(10): p. 6231-40.
472. Collart, M.A., P. Baeuerle, and P. Vassalli, *Regulation of tumor necrosis factor alpha transcription in macrophages: involvement of four kappa B-like motifs and of constitutive and inducible forms of NF-kappa B.* Mol Cell Biol, 1990. **10**(4): p. 1498-506.
473. Thornberry, N.A., et al., *A novel heterodimeric cysteine protease is required for interleukin-1 beta processing in monocytes.* Nature, 1992. **356**(6372): p. 768-74.
474. Moeller, A., et al., *The bleomycin animal model: a useful tool to investigate treatment options for idiopathic pulmonary fibrosis?* Int J Biochem Cell Biol, 2008. **40**(3): p. 362-82.
475. Chaudhary, N.I., A. Schnapp, and J.E. Park, *Pharmacologic differentiation of inflammation and fibrosis in the rat bleomycin model.* Am J Respir Crit Care Med, 2006. **173**(7): p. 769-76.
476. Hemmi, H., et al., *The roles of two IkappaB kinase-related kinases in lipopolysaccharide and double stranded RNA signaling and viral infection.* J Exp Med, 2004. **199**(12): p. 1641-50.
477. Lu, Y.Y., et al., *GLUT-1 Enhances Glycolysis, Oxidative Stress, and Fibroblast Proliferation in Keloid.* Life (Basel), 2021. **11**(6).
478. Libermann, T.A. and D. Baltimore, *Activation of interleukin-6 gene expression through the NF-kappa B transcription factor.* Mol Cell Biol, 1990. **10**(5): p. 2327-34.
479. Jacobsen, H. and S.L. Klein, *Sex Differences in Immunity to Viral Infections.* Frontiers in Immunology, 2021. **12**.
480. Morens, D.M., J.K. Taubenberger, and A.S. Fauci, *Predominant role of bacterial pneumonia as a cause of death in pandemic influenza: implications for pandemic influenza preparedness.* J Infect Dis, 2008. **198**(7): p. 962-70.